Synthesis and Biological Evaluation of Inhibitors of the Shikimate Pathway Enzyme 3-Dehydroquinate Dehydratase

A thesis
submitted in partial fulfilment
of the requirements for the Degree of

Doctor of Philosophy in Chemistry

at the University of Canterbury
Christchurch
New Zealand

Mary Amanda Gower

January 2006

Contents

Acknowledgements

First and foremost I wish to thank my supervisor Prof. Andrew Abell for his guidance and support throughout this lengthy undertaking.

Thank you also to Prof. Chris Abell and Dr Olivier Kerbarh of Cambridge University for supplying the DHQase samples. Thanks to Chris also for his valuable collaboration during this work, in particular for helping to get the Canterbury branch of the shikimate pathway project off the ground.

Many thanks to Martin Lee for inspiring and helping to set up the NMR assay, and to Prof. John Blunt, without whose contined advice and assistance, the assay would have died a slow and painful death.

My thanks go out to all the technical staff, in particular Bruce Clark for mass spec and LCMS, Rewi Thompson for NMR, Rob McGregor for making/fixing my various items of glassware and Wayne Mackay for fixing everything else that broke.

I am grateful to the Royal Society of New Zealand Marsen Fund for my Ph.D. scholarship. The contributions of the Royal Society, the New Zealand Institute of Chemistry and the Evans Fund towards conference expenses are also gratefully acknowledged.

Thank you to past and present members of the chemistry department and the Abell group in particular, for their various advice, assistance, entertainment, and for creating a great working environment.

Finally, thanks to my family and friends, for their love, support and forbearance.

Abstract

The shikimate pathway is responsible for the biosynthesis of essential aromatic metabolites and, as such, its enzymes are targets for the design of potential antimicrobial and herbicidal agents. The enzyme 3-dehydroquinate dehydratase (dehydroquinase, DHQase) catalyses the conversion of 3-dehydroquinate **1** to 3-dehydroshikimate **2**, the third step of the shikimate pathway. There are two types of DHQase, unrelated structurally and mechanistically. Type I DHQase catalyses the rection by *via* a covalently attached imine intermediate. Type II DHQase catalyses the reaction by way of an enolate intermediate.

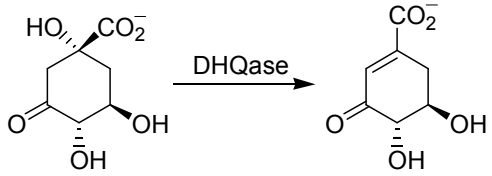

1 **2**

This thesis describes the synthesis of a series of potential inhibitors of type II DHQase. Inhibitors with C and N at C-3 and with both sp^2 and sp^3 character at this position were prepared, with general structures **3**-**5**. The potential type I DHQase inhibitor **6** was also prepared.

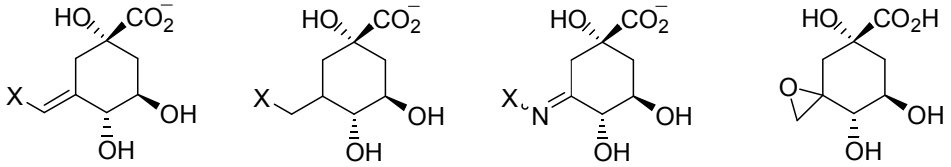

3 **4** **5** **6**

The biological evaluation of these inhibitors against type II DHQases from *Mycobacterium tuberculosis* and *Streptomyces coelicolor* and (in the case of **6**) type I DHQase from *Salmonella typhi* is described. Inhibitors were evaluated by spectrophotometric assay. However, this proved inappropriate for some inhibitors with the *S. coelicolor* enzyme. The development of an alternative ^{1}H NMR assay and its application to the evaluation of *S.*

coelicolor DHQase inhibitors is therefore also described. Some insights into the structure activity relationships of type II DHQases, obtained from the results of these studies, are discussed.

1 Introduction

1.1 Antibiotics and Antibiotic Resistance

The discovery of penicillin by Alexander Fleming in 1928 heralded a new era in the treatment of infectious disease. The drug was initially reserved for military use during WWII and this led eventually to the mass production of penicillin for public use by 1944.[1] Penicillin was hailed as a "miracle drug". There followed over the next couple of decades the development of a plethora of antimicrobial weapons, so called "magic bullets", including a variety of new and improved β-lactam antibiotics along with new classes such as the tetracyclines, aminoglycasides, macrolides and polypeptides (e.g. vancomycin). Previously fatal infections could now be easily cured. Infectious disease appeared to be on its way out. For good.

1.1.1 Antibiotic resistance

Unfortunately, claims that the war against infectious disease had been won were premature. The excessive use and abuse of antibiotics has led, inevitably, to the development of antibiotic resistance. Antibiotics are taken for ailments against which they have no power, they are fed to livestock to enhance growth, sprayed on crops, and added to soaps and household cleaners.[2] The saturation of the environment with antibiotics has created a selection pressure for the evolution and spread of antibiotic resistance. Antibiotic resistant microbes that now plague hospital wards and communities include methicillin-resistant *Staphylococcus aureus* (MRSA), vancomycin-resistant *Enterococcus faecalis* (VRE), and multi drug resistant *Mycobacterium tuberculosis* (MDR-TB).

Alexander Fleming himself warned about the consequences of the misuse of penicillin:[3]

> "The greatest possibility of evil in self-medication is the use of too small doses, so that, instead of clearing up the infection, the microbes are educated to resist penicillin and a host of penicillin-fast organisms is bred out which can be passed on to other individuals and perhaps from there to others until they reach someone who gets a septicemia or a pneumonia which penicillin cannot save. In such a case the thoughtless person playing with penicillin treatment is morally responsible for the death of the man who finally succumbs to infection with the penicillin-resistant organism. I hope this evil can be averted."

His words were prophetic. The misuse of antibiotics has lead to microbial resistance on a scale that is surely far beyond what Fleming imagined. He could not have forseen the tendency of microorganisms to share their resistance traits amongst themselves. Although organisms may have a natural resistance to a drug or may develop a spontaneous mutation which confers a certain degree of resistance, the most significant threat to the viability of existing antibiotics is the ability of organisms to acquire whole sets of resistance genes, in the form of plasmids, from other microorganisms. The passing on of resistance genes from one organism to another ("horizontal evolution") can occur by viral delivery (transduction), cell-to-cell contact (conjugation), or by the scavenging of DNA from the environment (transformation).[1]

Proteins coded for by resistance genes protect microbes from the actions of antibiotics in three main ways: by preventing accumulation of the antibiotic within the cell (e.g. by active efflux in *Pseudomonas aeruginosa*), by altering the target of the antibiotic so it is no longer susceptible (e.g. modified peptidoglycan in VRE), or by inactivating the antibiotic itself (e.g. hydrolysis of β-lactam antibiotics by β-lactamase enzymes).

1.1.2 Combating Antibiotic Resistance

There are three main chemical strategies for combating antibiotic resistance.[4] The primary strategy employed by the pharmaceuticals industry for the past 30 years is the modification and improvement of existing classes of antibiotics in order to circumvent the microbial resistance mechanisms. Another approach is the administration of drugs designed to inhibit the resistance mechanism, such as the synergistic administration of the β-lactam antibiotic

amoxicillin with the β-lactamase inhibitor clavulanate. The third strategy is the production of new classes of drugs, with novel targets, such that there is no established resistance amongst the microbial population.

Although antibiotic resistance was observed almost from the beginning of the antibiotic era, it was not at first thought to be a serious problem. It could be overcome by coming up with slight variations in the antibiotic and the bacterial resistance could be evaded. In this way it was possible to stay one step ahead of the development of resistance. However, as resistant bacteria proliferate and acquire resistance not only to whole classes of antibiotics, but to several classes at once, the need for new antibiotics, with new targets becomes increasingly apparent.

The genomics revolution is a driving force behind the search for novel antimicrobial targets.[5,6] With genome sequence information for many pathogens now available and more coming, a plethora of potential antibiotic targets has become available. New technologies enable the determination of whether a gene is essential to growth or survival under the conditions of the infection and whether transcription is induced during infection. Homology provides clues to a protein's function and *in silico* analysis can identify highly conserved (broad spectrum) or unique (narrow spectrum) targets. Human genome sequence information provides a basis for assessing the selectivity of a potential target relative to mammalian proteins.

1.2 The Shikimate Pathway as a Target for Antibiotic Development

In plants and microorganisms key aromatic compounds are synthesized *via* the shikimate pathway (Scheme 1.1). The shikimate pathway consists of seven enzymes catalysing the conversion of erythrose 4-phosphate **1.1** and phosphoenol pyruvate (PEP) **1.2** to chorismate, the precursor of the aromatic amino acids and other aromatic metabolites including *p*-aminobenzoic acid (precursor to folate, essential for neucleotide biosynthesis) ubiquinone (co-enzyme Q), the vitamins K, flavonoids, lignans and some alkaloids.[7] The seven enzymes, 3-

deoxy-D-*arabino*-heptulosonate 7-phosphate (DAHP) synthase, dehydroquinate synthase, 3-dehydroquinate dehydratase (dehydroquinase, DHQase), shikimate dehydrogenase, shikimate kinase, 5-enolpyruvylshikimate 3-phosphate (EPSP) synthase and chorismate synthase catalyse the formation of DAHP **1.3**, dehydroquinate **1.4**, dehydroshikimate **1.5**, shikimate **1.6**, shikimate 3-phosphate **1.7**, EPSP **1.8** and chorismate **1.9** respectively. The pathway occurs in plants, fungi and microorganisms but not in mammals, making the enzymes of the pathway appealing targets for the design of potentially highly selective antimicrobial and herbicidal compounds.

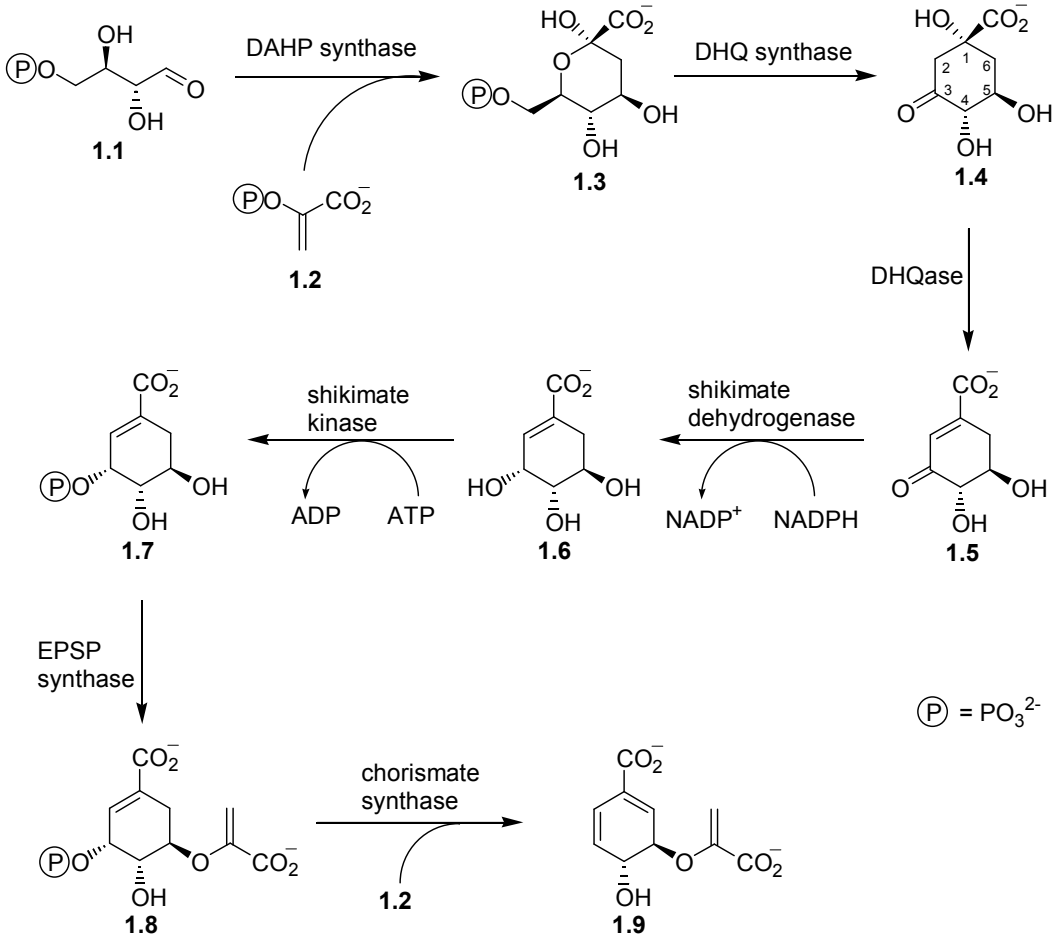

Scheme 1.1 The Shikimate Pathway.

Recent genomic research has confirmed that the shikimate pathway is indeed present in many important mammalian pathogens, such as the malaria parasite *Plasmodium falciparum*[8] and *M. tuberculosis*.[9] Inactivation of shikimate pathway genes has been shown to lead to

attenuation of virulence and loss of viability in a range of bacterial species including *M. tuberculosis*[9] and *Salmonella typhimurium*,[10] validating the shikimate pathway as a target for antimicrobial design.

Inhibition of aromatic biosynthesis as a route to novel antimicrobials has been validated by the work of Abell *et al.* on 6-fluoro- analogues of shikimate pathway substrates.[11] The 6-fluoro analogues of shikimic acid **1.10** and **1.11** were found to act as substrates for shikimate kinase, being converted first into (6*R*)- and (6*S*)-6-fluoroshikimate-3-phosphate (**1.12** and **1.13**) and then into (6*R*)- and (6*S*)-6-fluoro-EPSP (**1.14** and **1.15**) by EPSP synthase (Scheme 1.2). (6*S*)-6-Fluoro-EPSP was found to inhibit *Neurospora crassa* chorismate synthase,[11] the succeeding enzyme on the pathway, but not the corresponding *E. coli* enzyme, for which it is a substrate.[12] (6*S*)-6-Fluoroshikimic acid was, however, found to inhibit the growth of an *E. coli* strain on minimal medium (MIC = 0.25μg mL^{-1}) and protected mice infected with the same organism (50% protective dose, 0.06mg per kg body weight).[13] It was subsequently shown that (6*S*)-6-fluoroshikimate is converted by the shikimate pathway enzymes to 6-fluorochorismate, which irreversibly inhibits 4-amino-4-deoxychorismate synthase (ADCS), the succeeding enzyme *en route* to folate biosynthesis.[14] Spontaneous resistance to the inhibitor was found to occur at high frequency. The resistance mechanism is thought to be specific to 6-fluoroshikimic acid however, and should not be a general problem for inhibitors of shikimate pathway enzymes.[15]

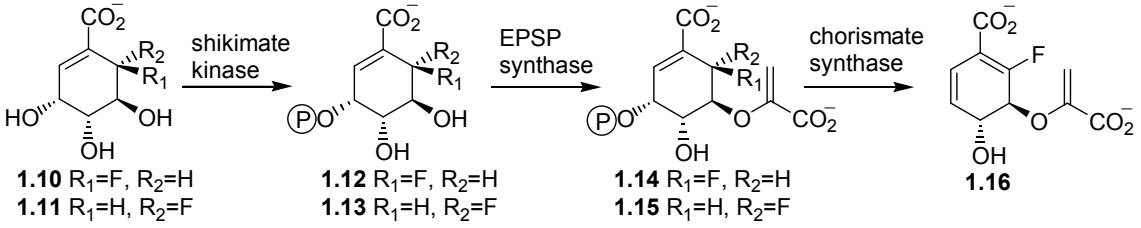

Scheme 1.2 Enzymatic conversion of (6*R*)- and (6*S*)-6-fluoroshikimate (**1.10** and **1.11**) into 6-fluorochorismate **1.16**.

An excellent example of the selective toxicity of a commercial shikimate pathway inhibitor is the herbicide *N*-phosphonomethyl glycine (glyphosate) **1.17**, marketed as Roundup® (Scheme 1.3). It has also been shown to inhibit the growth of several clinically important parasitic

pathogens.[8] Glyphosate inhibits the shikimate pathway enzyme EPSP synthase.[16] Glyphosate is extremely specific for EPSP synthase and is not known to appreciatively inhibit any other enzyme, making it a safe and effective means of weed control.[17] Binding of glyphosate is competitive with respect to PEP **1.2** and occurs only after the binding of shikimate 3-phosphate **1.7**. The step-wise binding leads to a dead-end ternary complex **1.18** which mimics the tetrahedral intermediate **1.19** of the enzymatic reaction, but does not lead to the formation of the product EPSP **1.8**.[18]

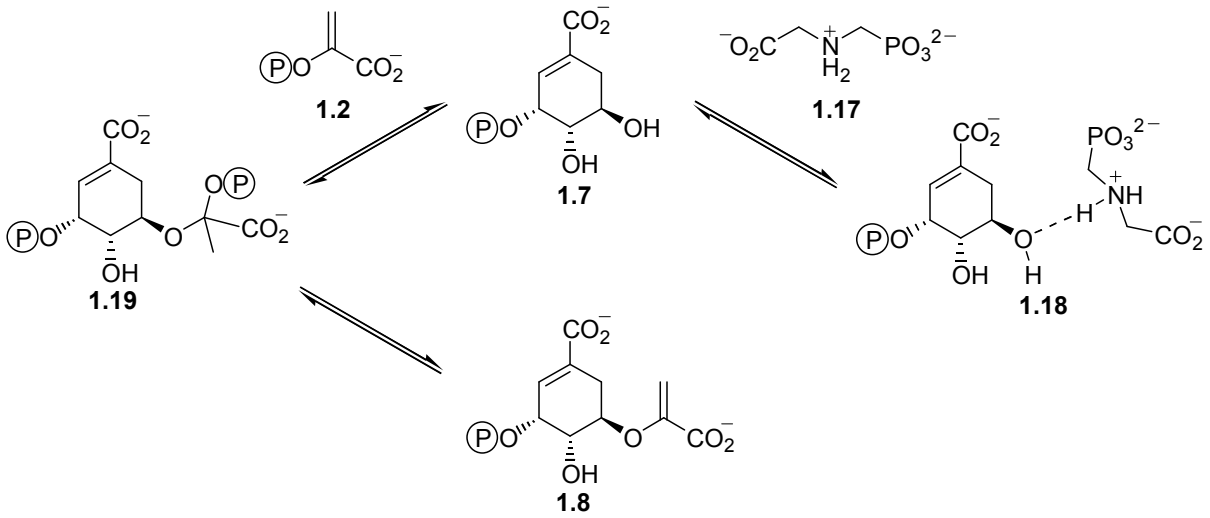

Scheme 1.3 Inhibition of EPSP synthase by glyphosate **1.17.**

1.3 DEHYDROQUINASE

Dehydroquinase is the third enzyme of the shikimate pathway, catalyzing the conversion of 3-dehydroquinate (DHQ) **1.4** to 3-dehydroshikimate (DHS) **1.5**. There are two structurally distinct classes of DHQase, known as type I and type II, that catalyse the elimination of H_2O by completely different mechanisms.[7] The two types of DHQase are unrelated in an evolutionary sense, having completely different three dimensional structures[19] and exhibiting little or no sequence homology.[20]

Type I DHQase has been reported only as a part of the biosynthetic shikimate pathway. In plants and fungi it is a part of larger multifunctional proteins such as the pentafunctional *arom* complex of *Aspergillus nidulans* and *Neurospora crassa* which catalyses steps two to six of the shikimate pathway.[20-22] In prokaryotes such as *Escherichia coli* and *Salmonella typhi* however, type I DHQases are distinct, monofunctional enzymes which are dimeric, with a 26-28 kDa subunit.[22-25]

Type II DHQases occur as a biosynthetic enzyme of the shikimate pathway, as is the case for the *M. tuberculosis* and *Streptomyces coelicolor* enzymes.[26,27] However, they also occur as a part of the catabolic quinate pathway in fungi, in which quinic acid is utilised as a carbon source *via* the β-ketoadipate pathway.[7] Fungi such as *A. nidulans* and *N. crassa* have both types of DHQase, with type I DHQase playing a biosynthetic role as a part of the *arom* protein and type II DHQase involved in quinate catabolism.[22] Type II DHQases are dodecamers with 12-18 kDa subunits.[22,28,29]

1.3.1 Mechanism of Type I dehydroquinase

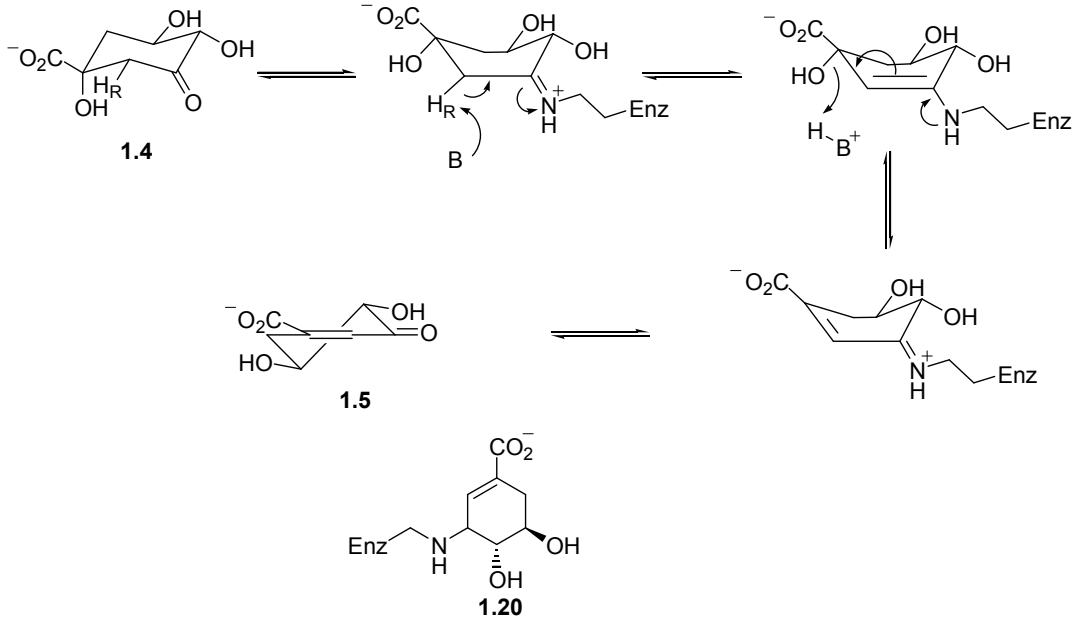

Scheme 1.4 Catalytic mechanism of type I DHQase.

The elimination catalysed by type I DHQase proceeds *via* imine formation with a highly conserved active site lysine residue (Lys-170 in *E. coli* DHQase) (Scheme 1.4).[30] Evidence for an imine intermediate comes from enzyme inactivation by borohydride trapping of the imine in the presence of an equilibrium mixture of substrate and product.[31] The reduced enzyme-product adduct **1.20** has been observed by electrospray mass spectrometry[25] and the crystal structure of the complex solved for the *S. typhi* enzyme.[19]

The elimination of water has been shown by deuterium labelling experiments to occur with *syn*-stereochemistry, involving the loss of the less acidic *pro*-R proton.[32] Substrate binding by type I DHQase induces a conformational change from the preferred chair form, resulting in a co-planar orientation of the *pro-R* hydrogen with the π-acceptor orbital of the imine, promoting the *syn*-stereo chemistry of the elimination.[32,33] Experimental evidence supports a skew-boat for the reactive conformation, in which the C-4 and C-5 hydroxyls remain in the equatorial positions throughout the reaction, while the orientation of the C-1 carboxyl becomes more axial.[33] When the C-1 carboxyl of the substrate **1.4** was masked by a methyl ester, it lost all activity, acting as neither a substrate nor an inhibitor. This supports the hypothesis that the carboxylate is necessary for substrate reactivity and that it is the carboxylate, together with the ketone that engages the enzyme and initiates the conformational change which results in the *syn*-elimination.

His-143 was initially proposed to be the active site general base responsible for abstraction of the *pro-R* proton by *E. coli* DHQase,[34] due to resulting enzyme inactivation from modification of His-143 by diethyl pyrocarbonate as well as the highly conserved nature of this residue in type I DHQases. Further studies suggested that His-143 is involved in imine formation and hydrolysis, as replacement of His-143 with alanine results in a reduced rate of catalysis and accumulation of Schiff base-bound product.[35] Crystallographic data shows His-143 at the centre of a hydrogen-bonded triad involving Lys-170 and Glu-86, which is consistent with a role in Schiff base formation, but not as the general base responsible for proton abstraction at C-2.[36] A logical role for His-143 might then be deprotonation of the ε-NH_2 of Lys 170. Chemical modification experiments with phenylglyoxal have also identified an essential hyper-reactive active site arginine (Arg-213 in *E. coli*) that may be involved in carboxylate recognition.[37]

1.3.2 Mechanism of Type II Dehydroquinase

In contrast to the type I enzyme, the conversion of DHQ **1.4** to DHS **1.5** by type II DHQase does not involve a Schiff-base intermediate. This is indicated by the lack of a conserved lysine residue[26] and the lack of enzyme inactivation observed upon treatment with sodium borohydride in the presence of an equilibrium mixture of substrate and product.[22] Another notable mechanistic difference between the two types of dehydroquinase is that, in contrast to the elimination catalysed by the type I enzyme, the type II dehydroquinase catalysed reaction proceeds with *anti*-stereochemistry and loss of the more acidic axial *pro-S* proton, as confirmed by deuterium labelling experiments.[38,39] It was proposed that type II DHQase, by analogy with type II aldolases, might require bivalent metal ions for catalysis, however, experiments employing metal analysis, chelation, and denaturation/renaturation experiments failed to show any evidence of metal ion dependence in the mechanism of *A. nidulans* type II DHQase.[40]

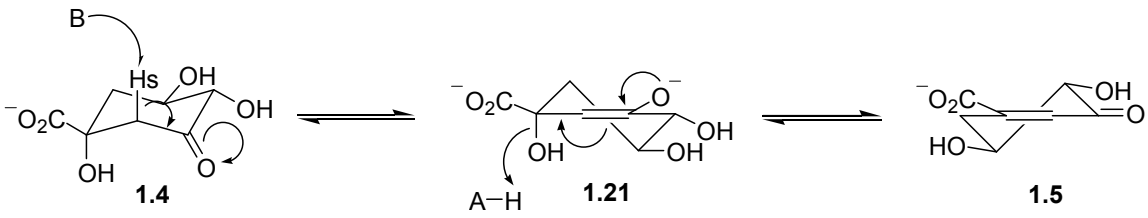

Scheme 1.5 Catalytic mechanism of type II DHQase.

The highly conserved Tyr-28 has been implicated in a catalytic role in *S. coelicolor* DHQase by inactivation of the enzyme following tetranitromethane modification of Tyr-28.[37] A conserved hyper-reactive active site arginine residue (Arg-23 in *S. coelicolor* DHQase) has been identified by phenylglyoxal modification and electrospray mass spectrometry.[29] Both chemical modification and site-directed mutagenesis of Arg-23 led to loss of activity.[37] The crystal structure of *S. coelicolor* with phosphate bound in a position analogous to that of the C-1 carboxyl and hydroxyl of the substrate indicates that recognition of the C-1 carboxylate and hydroxyl is important for *S. coelicolor* DHQase activity.[41]

A stepwise E_1CB mechanism involving an enolate intermediate **1.21** was proposed, supported by kinetic isotope experiments, to explain the stereochemistry of the elimination (Scheme

1.5).[42] The subsequent crystallographic identification of a conserved active site water molecule in *S. coelicolor* DHQase, along with the absence of any suitable residue to stabilise an enolate intermediate, suggested that an enol rather than an enolate may be a more likely intermediate for this enzyme.[43] The conserved Tyr-28 was proposed to be the general base responsible for proton abstraction, with His-106 acting as the general acid in the hydroxyl elimination step.

1.4 DEHYDROQUINASE AS A TARGET FOR INHIBITOR DESIGN

Various dehydroquinate analogues have been synthesised and tested for inhibitory activity against types I and II DHQase. The synthesis of such compounds has progressed from preparation of analogues for the purpose of mechanistic studies, to the rational design of type-specific DHQase inhibitors. Some inhibitors have also been identified by library screening.

Compounds possessing an active methylene group at C-3 (**1.22** and **1.23**) were proposed by Gorrichon *et al.* to act as inhibitors of type I DHQase. No time-dependent inhibition of *E. coli* DHQase was observed for compounds **1.22** and **1.23** however. The lack of activity was proposed to be due to the lack of the C-3 carbonyl, or steric constraints of the C-3 functional group and active site residues.[44]

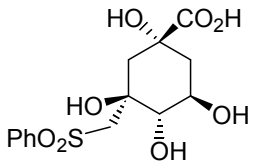

1.22

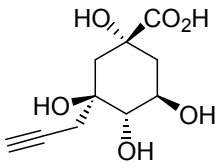

1.23

A series of affinity labels was designed by Abell and co-workers to investigate the structure of the active site of type I DHQase from *E. coli*.[45] Epoxide **1.24** showed rapid active site directed irreversible inhibition, with an inhibition constant of 400 μM and a maximal rate of inactivation k_i of 2.5 x 10^{-3} s^{-1}. Chloromethyl ketone **1.25** also demonstrated irreversible inhibition with a K_i of 680 μM and a k_i of 5.6 x 10^{-4} s^{-1}. Azide **1.26** acted as a photoaffinity

label, presumably via the generation of a reactive nitrene diradical. The inhibition constant for this inhibitor was 1.1 mM, with a maximal rate of inactivation, k_i, of 3.9 x 10^{-4} s^{-1}. All three compounds were shown to be competitive inhibitors by prevention or reduction of inhibition on addition of substrate.

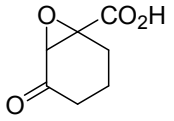

1.24

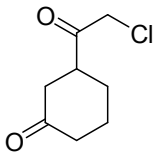

1.25

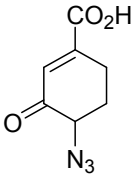

1.26

The 5-deoxy- and 4,5-dideoxy- analogues of DHQ (**1.27** and **1.28** respectively) were synthesized by Abell and coworkers to study the substrate specificity of types I and II DHQase.[46] 5-Deoxydehydroquinic acid **1.27** was found to be a modest substrate for type I DHQase from *E. coli* with a reduction in specificity constant k_{cat}/K_M of 10^3 L mol^{-1} s^{-1} relative to the natural substrate. Although the enzyme tolerates the absence of the C-5 hydroxyl, the loss of specificity suggests that the group forms an important binding interaction with the enzyme and may be hydrogen bonded to a charged acceptor such as a lysine or arginine sidechain. 4,5-Dideoxydehydroquinic acid **1.28** however, was not a substrate, but a reversible competitive inhibitor with K_i = 10 ± 1 mM. This is an indication that the C-4 hydroxyl, unlike the C-5 hydroxyl, is necessary for substrate turnover and may be involved in imine formation.

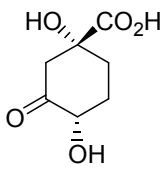

1.27

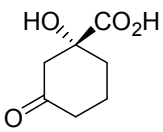

1.28

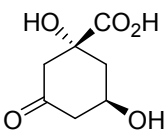

1.29

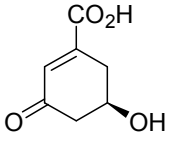

1.30

In contrast both compounds were found to be poor substrates for type II DHQase from *M. tuberculosis* (with specificities approximately 10^{-5} that of the natural substrate). The dideoxy analogue **1.28** was also a weak competitive inhibitor with a K_i of 1.0 ± 0.2 mM. That the absence of the C-5 hydroxyl results in such a loss of specificity suggests that it is involved in some important enzyme-substrate interaction(s). The removal of the C-4 hydroxyl did not seem to have any further effect on the binding affinity suggesting either that the group does not form any significant binding interactions with the enzyme, or that the removal of either C-

4 or C-5 hydroxyl group results in a breakdown of important enzyme-substrate binding interactions. Subsequent attempts to prepare 4-deoxydehydroquinic acid **1.29** in order to further investigate the contribution of the C-4 hydroxyl to substrate binding were unsuccessful due to the propensity of the β-hydroxy ketone to eliminate and aromatise.[47] No formation of 4-deoxydehydroquinic acid was observed on incubation of 4-deoxydehydroshikimic acid **1.30** with either type I DHQase from *E. coli* or type II DHQase from *M. tuberculosis*, however this may be due to an unfavourable equilibrium between the species.

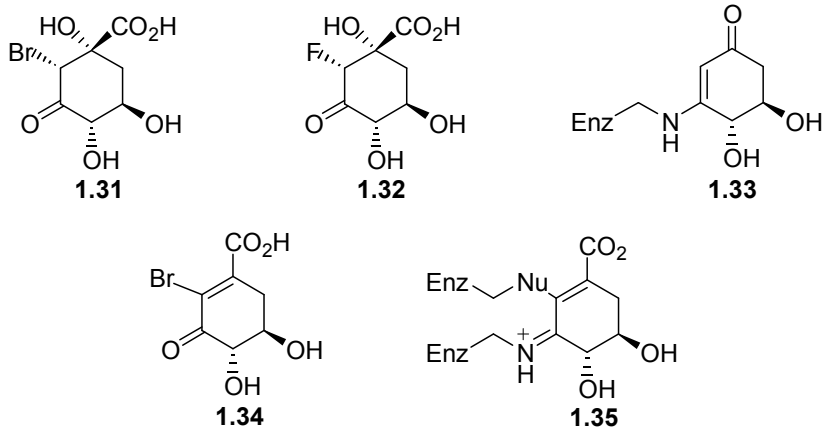

Halogenated DHQ analogues, substrates for type II DHQase,[48] were shown to be mechanism based inhibitors of type I DHQase from *E. coli*.[49] (2*R*)-2-Bromo-3-dehydroquinic acid **1.31** proved to be a weak competitive inhibitor of type I DHQase (K_i = 3.7 mM) that slowly inactivated the enzyme irreversibly (70% inactivation after 24h at 10 mM). The mass spectrum of a partially inactivated sample of enzyme showed a peak for modified enzyme corresponding to an additional mass of 126 ± 5 Da. The corresponding fluoro-analogue **1.32** was shown to be a moderate competitive inhibitor with a K_i of 80 μM and also slowly inactivated the enzyme irreversibly (45% inactivation after 22h at 2.4 mM). The mass spectrum in this case also showed a new peak for modified enzyme corresponding to an additional mass of 126 ± 5 Da. This suggests the formation of a common adduct in which the halogen substituent has been lost to form **1.33**. A possible mechanistic rationale is depicted in Scheme 1.6. Binding of the C-2 halo-analogues **1.31** and **1.32** and formation of the imine intermediate is proposed to initiate a conformational change which brings the C-2 halogen bond closer to an antiperiplanar orientation with respect to the C-1–carboxyl bond. This may trigger a decarboxylative elimination reaction. Subsequent tautomerisation of the enol

iminium adduct would form the vinylogous amide **1.33**, which is irreversibly bound to the enzyme, preventing further catalysis.

Incubation of type I DHQase with 2-bromo-3-dehydroshikimate **1.34** also resulted in slow irreversible inactivation (60% after 24h at10 mM), with the enzyme-inhibitor adduct observed by electrospray mass spectrometry now corresponding to and additional mass of 154 ± 5 Da. This may be due to the formation of the adduct **1.35** *via* imine formation, followed by conjugate attack at C-2 and subsequent elimination of bromide.

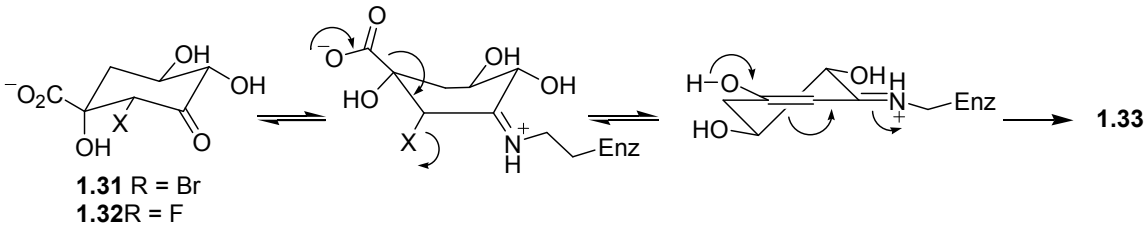

Scheme 1.6 Proposed mechanism of inhibition of type I DHQase by 2-bromo- and 2-fluorodehydroquinic acids (**1.32** and **1.32**).

Investigation into the mechanism of type II dehydroquinase by Abell *et al*. prompted the synthesis of **1.36** and **1.37** as analogues of the enolate intermediate **1.21** (Scheme 1.5).[50] Compounds **1.38** and **1.39** were also prepared as controls lacking the hydrogen bonding potential of the oxime functionality and the partial ring flattening due to the C-2–C-3 double bond respectively. The results of the biological studies are shown in Table 1.1. Oxime **1.36** was found to be much more potent an inhibitor than **1.38**, indicating the importance of hydrogen bonding interactions in both the stabilization of the enolate intermediate and inhibitor binding. 2,3-Anhydroquinic acid **1.37** was found to be more potent than the saturated analogue **1.39**. This is consistent with stabilisation by the enzyme of a transition state with some degree of ring flattening as would be expected to occur in enolate intermediate **1.21**. The inhibitors showed high selectivity for type II DHQase over the type I enzyme. The inhibitors also demonstrated unexpected selectivity between different species of type II enzyme, with the oxime **1.36** being more potent against *M. tuberculosis* DHQase and 2,3-anhydroquinic acid **1.37** being more potent against the S. *coelicolor* enzyme.

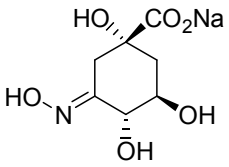
1.36

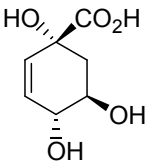
1.37

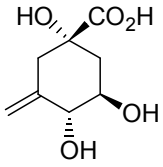
1.38

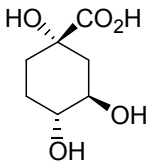
1.39

The selectivity of inhibitors **1.36-1.39** for different species of type II DHQase may be explained in part by subsequent studies of the binding of phosphate and sulphate anions by *S. coelicolor*, *M. tuberculosis* and *Helicobacter pylori* DHQases.[41] Phosphate and sulphate anions were both found to be weak competitive inhibitors of *S. coelicolor* DHQase, with inhibition constants of 7 mM and 11 mM respectively. They were also found to inhibit *H. pylori* DHQase with K_i values of 9 mM for both anions. Phosphate has also previously been shown to be a competitive inhibitor of *A. nidulans* type II DHQase.[22] The anions also appeared to inhibit *M. tuberculosis* DHQase but the kinetics were more complex than the simple competitive inhibition observed for the other enzymes, suggesting that the anions may bind to more than one site. The crystal structure of *S. coelicolor* with phosphate shows a single anion bound in the active site, occupying a position analogous to the carboxylate and C-1 hydroxyl of the substrate. This was also observed to be the case for the crystal structure of *S. coelicolor* DHQase with sulphate bound.[43] This suggests that C-1 hydroxyl and carboxylate recognition is important for binding by *S. coelicolor* DHQase.

Table 1.1 Inhibition constants, K_i (μM) for inhibitors **1.36** – **1.41** against Types I and II dehydroquinase

Inhibitor	**K_i (μM)**		
	Type I *S. typhi*	Type II *M. tuberculosis*	Type II *S. coelicolor*
1.36	> 25000	20 ± 2	500 ± 200
1.37	3000 ± 1000	200 ± 20	30 ± 10
1.38	> 25000	700 ± 200	2500 ± 200
1.39	4500 ± 500	1200 ± 20	600 ± 20
1.40	1500 ± 500	10 ± 2	15 ± 2
1.41	8000 ± 1000	700 ± 100	700 ± 100

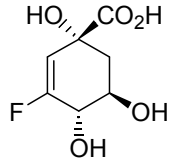
1.40

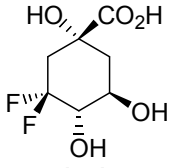
1.41

In the case of *M. tuberculosis* DHQase however, the presence of two sulphate ions was observed in the active site.[41] One of the sulphate ions was bound in a position near but not identical to the C-1 hydroxyl/carboxylate binding site, but lacking some of the interactions

observed for the phosphate ion in the *S. coelicolor* structure. It was, however, seen to interact with Arg-19, a residue shown to be important for catalysis.[37] The second sulphate ion also interacts with Arg-19 and with residues of the flexible lid domain. These results, along with the lack of potency observed for inhibitors **1.37**-**1.39** against *M. tuberculosis* DHQase relative to *S. coelicolor* DHQase and the increased activity of **1.36** relative to **1.37**-**1.39** against *M. tuberculosis* DHQase, suggest that although C-1 carboxylate/hydroxyl recognition is necessary for specific binding by *S. coelicolor* DHQase, the C-3 carbonyl is more important for binding by *M. tuberculosis* DHQase, possibly by interacting with Arg-19.

Inhibitor **1.40** was prepared by Frederickson *et al*., incorporating the vinyl fluoride moiety as an isoelectronic and isosteric replacement for the enolate anion of **1.21**.[51,52] It was shown to be highly selective for type II DHQase over type I, and was equally active against type II DHQases from both *M. tuberculosis* and *S. coelicolor*.[52] Although fluoro- analogue **1.40** showed only a small improvement in activity over **1.36** and **1.37** with the enzymes against which they were most potent, it shows a 20-30 fold increase in activity with the enzymes against which they were less potent (Table 1.1). This makes it the most effective "broad-spectrum" inhibitor of type II DHQases reported to date. 3,3-Difluoro analogue **1.41** was also a competitive reversible inhibitor, selective for type II DHQase, but was much less potent than enolate analogue **1.40**.

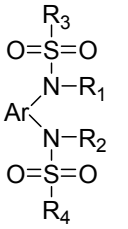

Ar = aryl or heteroaryl
R_1 = H, alkyl or R_1 and R_2 together form a C_1 - C_3 alkylene group, CO or CS
R_2 = H, alkyl or R_1 and R_2 together form a C_1 - C_3 alkylene group, CO or CS
R_3 = aryl, heteroaryl, alkyl-aryl, alkyl-heteroaryl, alkenyl-aryl, alkenyl-heteroaryl, alkynyl-aryl, or alkynyl-heteroaryl
R_4 = aryl, heteroaryl, alkyl-aryl, alkyl-heteroaryl, alkenyl-aryl, alkenyl-heteroaryl, alkynyl-aryl, or alkynyl-heteroaryl

1.42

Library screening has unearthed a completely different class of DHQase inhibitors. Bissulfonamide derivatives of general structure **1.42** were assayed against shikimate pathway enzymes and some were found to be moderate inhibitors of type II dehydroquinase from *M. tuberculosis* with IC_{50} values in the micromolar range.[53,54] Several of the compounds were demonstrated to have inhibitory activity against bacterial cell growth with minimum inhibitory concentrations (MIC) in the low micromolar range. The mode of action of the compounds was not described.

Table 1.2 Inhibition constants, K_i (μM) for inhibitors **1.43**-**1.50** against types I and II DHQase

Inhibitor	K_i (μM)	
	Type I DHQase *S. typhi*	Type II DHQase *S. coelicolor*
K_M[a]	16	250
1.37[b]	3000 ± 1000	30 ± 10
1.39[b]	4500 ± 500	600 ± 200
1.43[a]	> 20000	420 ± 50
1.44[a]	> 20000	> 20000
1.45[a]	> 20000	180 ± 20
1.46[a]	> 20000	3000 ± 500
1.47[a]	> 20000	1200 ± 150
1.48[a]	> 20000	530 ± 50
1.49[a]	> 20000	> 20000
1.50[a]	> 20000	3500 ± 400

[a] Ref. 55. [b] Ref. 50.

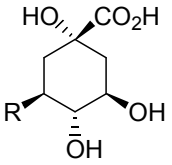

1.43 R = $CH_2CH{=}CH_2$
1.44 R = $CH_2CH(OH)CH_3$
1.45 R = $CH_2CH_2CH_2OH$
1.46 R = $CH_2CH(OH)CH_2OH$
1.47 R = $OCH_2CH{=}CH_2$
1.48 R = $OCH_2CH(OH)CH_2OH$

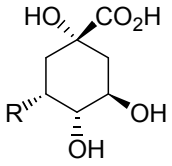

1.49 R = $OCH_2CH{=}CH_2$
1.50 R = $OCH_2CH(OH)CH_2OH$

The crystal structure of *S. coelicolor* dehydroquinase has been reported with inhibitor **1.37** bound in the active site.[43] The structure also shows a molecule of glycerol bound 3.7Å from the inhibitor. A new series of inhibitors was designed by Abell *et al*. intended to fill both binding sites by incorporating both inhibitor and glycerol components in the structure.[55] Compounds **1.43**-**1.50** were prepared and assayed against type I DHQase from *S. typhi* and type II DHQase from *S. coelicolor* (Table 1.2). None of the compounds showed any measurable inhibition against the type I enzyme. Compounds **1.43**, **1.45** and **1.48** were found to be more potent than compound **1.37** against type II dehydroquinase but none of the inhibitors were as potent as 2,3-anhydroquinic acid **1.37**.

Another series of analogues of inhibitor **1.37** has been prepared on solid-phase and assayed against type II DHQase from *S. coelicolor*.[56] The inhibition results for compounds **1.51a-i** and **1.52a-i** are given in Table 1.3. All of the compounds were found to be reversible competitive inhibitors of *S. coelicolor* DHQase, the 4-substituted series **1.52a-i** being generally more potent than the 1-substituted series **1.51a-i**. 2-Nitrobenzyl derivative **1.52i** was particularly potent showing almost a four-fold improvement over the parent inhibitor **1.37**, making it the most potent inhibitor of *S. coelicolor* type II DHQase reported to date. Docking studies indicated that most of the inhibitors bind in a similar mode to inhibitor **1.37**, with the benzyl substituent in the pocket previously occupied by the glycerol molecule.

However, in the case of inhibitor **1.52i**, the nitrobenzyl group is bound in the pocket normally occupied by the anhydro ring, with the nitro group in the carboxylate binding site, while the cyclohexene ring is bound in the glycerol binding pocket. However, this may be an artefact of the way the active site was prepared for docking, as when more water molecules were retained, docking similar to that for the other inhibitors was observed.

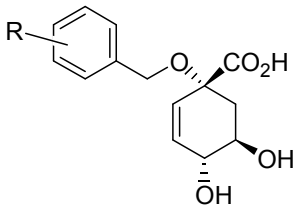

1.51
a R = H
b R = 4-F
c R = 3-F
d R = 2-F
e R = 4-CO_2H
f R = 4-CO_2OH
g R = 4-CN
h R = 4-NO_2
i R = 2-NO_2

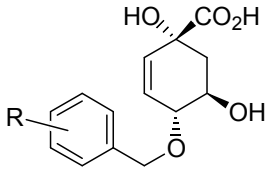

1.52
a R = H
b R = 4-F
c R = 3-F
d R = 2-F
e R = 4-CO_2H
f R = 4-CO_2OH
g R = 4-CN
h R = 4-NO_2
i R = 2-NO_2

Table 1.3 Reported inhibition constants for inhibitors **1.51** and **1.52 a-i** against *S. coelicolor* DHQase.

	K_i (μM) *S. coelicolor* type II DHQase	
	1.51	**1.52**
a	380 ± 30	200 ± 20
b	375 ± 30	70 ± 5
c	425 ± 40	140 ± 10
d	260 ± 20	130 ± 10
e	170 ± 15	100 ± 10
f	1330 ± 100	>2000
g	430 ± 40	330 ± 30
h	980 ± 90	200 ± 20
i	45 ± 5	8 ± 2

A recent paper from the Abell group describes the rational design of new DHQase inhibitors combining the strategies of having a glycerol mimic as a C-3 side-chain as seen in compounds **1.43**-**1.50** and using a phenyl ring to fill the glycerol binding pocket as seen in compounds

1.51a-i and **1.52a-i**.[57] Inhibitors **1.53-1.55** were prepared and assayed against type I DHQase from *S. typhi* and type II DHQase from *S. coelicolor*. None of the inhibitors were active against type I DHQase. The results of the assays against type II DHQase are shown in Table 1.4. Compound **1.53** was found to be almost as good an inhibitor of *S. coelicolor* DHQase as anhydroquinic acid **1.37**, though **1.54** and **1.55** were less potent, showing a decrease in potency with increasing hydrophilicity of the *ortho*-substituent.

Molecular docking studies suggested ring stacking between the aromatic rings of **1.53-1.55** and Tyr-28 as well as a possible interaction of any *ortho*-substituent with Arg-23. The crystal structure of *S. coelicolor* DHQase with **1.53** bound in the active site shows the quinate ring in the main binding pocket and the phenyl ring in the glycerol binding-pocket, with ring stacking between the benzyl ring and the side chain of Tyr-28 as predicted. However, the decreasing trend in activity with increasing hydrophilicity of the *ortho*-substituent suggests that there is no favourable interaction with Arg-23.

Table 1.4 Inhibition constants for inhibitors **1.53-1.55** against type II DHQase.

Inhibitor	K_i **(μM)** *S. coelicolor* Type II DHQase
1.53	33 ± 5.4
1.54	84 ± 13
1.55	220 ± 50

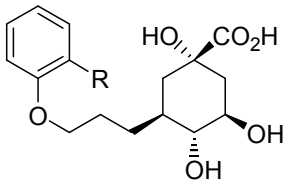

1.53 R = H
1.54 R = NO_2
1.55 R = CO_2H

Inhibition studies with DHQase have progressed from employing inhibitors as tools for elucidating structural and mechanistic details to the rational design of type-specific inhibitors. The most potent inhibitors of both types of DHQase to date have inhibition constants (K_i) in the low micromolar range. These inhibition studies have yielded information to be exploited in the rational design of future generations of inhibitors. For example, the C-4 and C-5 hydroxyl groups are important for binding by both enzyme types, the presence of hydrogen bonding substituents at C-3, and a C-2–C-3 double bond yield inhibitors specific for type II DHQases, and 2-halo analogues of DHQ are specific for type I DHQases. *S. coelicolor* DHQase also has an additional "glycerol" binding pocket which can be exploited.

1.5 OUTLINE OF THIS THESIS

The object of this work was to prepare new potential DHQase inhibitors and evaluate their biological activities. This would provide information about structure-activity relationships for DHQases, which could then be incorporated into the design of future generations of inhibitors. Work carried out by others in this area (described above), and the insights gained from this into the structure and mechanism of DHQase, were used as the basis for the design of a series of new inhibitors intended to further explore the structure activity relationships of type II DHQases.

Chapter 2 describes the preparation of a number of new potential type II DHQase inhibitors. The preparation of an inhibitor expected to be both a competitive inhibitor of type II DHQase and an irreversible inhibitor of type I DHQase is also described. The evaluation of the activities of theses inhibitors against the type II DHQases from *M. tuberculosis* and *S. coelicolor* using the standard spectrophotometric assay for DHQase is described in Chapter 3. The investigation of the irreversible inhibition of type I DHQase from *S. typhi* by one inhibitor is also described. Some of the inhibitors however, were UV active and were unable to be assayed against *S. coelicolor* DHQase by this method. An alternative ^{1}H NMR based assay was developed to evaluate these inhibitors against *S. coelicolor* DHQase. The development of this method and the results obtained are described in Chapter 4. Some insights into the structure-activity relationships for the two species of type II DHQase, obtained from the evaluation of the new inhibitors and by comparison with published results, are also discussed in Chapters 3 and 4.

1.6 REFERENCES FOR CHAPTER 1

(1) Levy, S. B. *The Antibiotic Paradox: How Miracle Drugs are Destroying the Miracle*; Plenum Press: New York, 1992.

(2) "World Health Organisation Infectious Disease Report," World Health Organisation, 2000.

(3) In *New York Times* New York, 1945, p 21.

(4) Wright, D. G. *Chem. Biol.* **2000**, *7*, R127-132.

(5) McDevitt, D.; Rosenberg, M. *TRENDS in Microbiol.* **2001**, *9*, 611-617.

(6) Nicolaou, K. C.; Boddy, N. C. In *Sci. Am.* 2001, p 47-53.

(7) Abell, C. In *Comprehensive Natural Product Chemistry*; Sankawa, U., Ed.; Elsevier: Amsterdam, 1999; Vol. 1, p 573-607.

(8) Roberts, F.; Roberts, C. W.; Johnson, J. J.; Kyle, D. E.; Krell, T.; Coggins, J. R.; Coombs, G. H.; Milhous, W. K.; Tzipori, S.; Ferguson, D. J. P.; Chakrabarti, D.; McLeod, R. *Nature* **1998**, *393*, 801.

(9) Parish, T.; Stoker, N. G. *Microbiology* **2002**, *148*, 3069-3077.

(10) Günel-Özcan, A.; Brown, K. A.; Allen, A. G.; Maskell, D. J. *Microb. Pathog.* **1997**, *23*, 311-316.

(11) Balasubramanian, S.; Davies, G. M.; Coggins, J. R.; Abell, C. *J. Am. Chem. Soc.* **1991**, *113*, 8945-8946.

(12) Bornemann, S.; Ramjee, M. K.; Balasubramanian, S.; Abell, C.; Coggins, J. R.; Lowe, D. J.; Thorneley, R. N. F. *J. Biol. Chem.* **1995**, *270*, 22811-22815.

(13) Davies, G. M.; Barrett-Bee, K. J.; Jude, D. A.; Nichols, W. W.; Pinder, P. E.; Thain, J. L.; Watkins, W. J.; Wilson, R. G. *Antimicrob. Agents Chemother.* **1994**, *38*, 403-406.

(14) Bulloch, E. M. M.; Jones, M. A.; Parker, E. J.; Osborne, A. P.; Stephens, E.; Davies, G. M.; Coggins, J. R.; Abell, C. *J. Am. Chem. Soc.* **2004**, *126*, 9912-9913.

(15) Coggins, J. R.; Abell, C.; Evans, L. B.; Frederickson, M.; Robinson, D. A.; Roszak, A. W.; Lapthorn, A. J. *Biochem. Soc. Trans.* **2003**, *31*, 548-552.

(16) Steinrucken, H. C.; Amrhein, N. *Biochem. Biophys. Res. Commun.* **1980**, *94*, 1207-12.

(17) Alibhai, M. F.; Stallings, W. C. *PNAS* **2001**, *98*, 2944-2946.

(18) Boocock, M. R.; Coggins, J. R. *FEBS Lett.* **1983**, *154*, 127-133.

(19) Gourley, D. G.; Shrive, A. K.; Polikarpov, I.; Krell, T.; Coggins, J. R.; Hawkins, A. R.; Isaacs, N. W.; Sawyer, L. *Nature* **1999**, *6*, 521.

(20) Charles, I. G.; Keyte, J. W.; Brammar, W. J.; Hawkins, A. R. *Nucleic Acids Res.* **1985**, *13*, 8119-8128.

(21) Lumsden, J.; Coggins, J. R. *Biochem. J.* **1977**, *161*, 599-607.

(22) Kleanthous, C. D., R.; Davis, K.; Kelly, S. M.; Cooper, A.; Harding, S. E.; Price, N. C.; Hawkins, A. R.; Coggins, J. R. *Biochem. J.* **1992**, *282*, 687-695.

(23) Chaudhuri, S.; Lambert, J. M.; McColl, L. A.; Coggins, J. R. *Biochem. J.* **1986**, *239*, 699-704.

(24) Moore, J. D.; Hawkins, A. R.; Charles, I. G.; Deka, R.; Coggins, J. R.; Cooper, A.; Kelly, S. M.; Price, N. C. *Biochem. J.* **1993**, *295*, 277-285.

(25) Shneier, A., Kleanthous, C., Deka, R., Coggins, J. R., Abell, C. *J. Am. Chem. Soc.* **1991**, *113*, 9416-9418.

(26) Garbe, T.; Servos, S.; Hawkins, A.; Dimitriadis, G.; Young, D.; Dougan, G.; Charles, I. *Mol. Gen. Genet.* **1991**, *228*, 385-392.

(27) White, P. J.; Young, J.; Hunter, I. S.; Nimmo, H. G.; Coggins, J. R. *Biochem. J.* **1990**, *265*, 735-738.

(28) Da Silva, A. J.; Whittington, H.; Clements, J.; Roberts, C.; Hawkins, A. R. *Biochem. J.* **1986**, *240*, 481-488.

(29) Krell, T.; Pitt, A. R.; Coggins, J. R. *FEBS Lett.* **1995**, *360*, 93-96.

(30) Chaudhuri, S., Duncan, K., Graham, L. D., Coggins, J. R. *Biochem. J.* **1991**, *275*, 1-6.

(31) Butler, J. R., Alworth, W. L., Nugent, M. J. *J. Am. Chem. Soc.* **1974**, *96*, 1617-1618.

(32) Turner, M. J., Smith, B. W., Haslam, E. *J. C. S. Perkin I* **1975**, 52-55.

(33) Vaz, A. D. N.; Butler, J. R.; Nugent, M. J. *J. Am. Chem. Soc.* **1975**, *97*, 5914-5915.

(34) Deka, R. K.; Kleanthous, C.; Coggins, J. R. *J. Biol. Chem.* **1992**, *267*, 22237-22242.

(35) Leech, A. P.; James, R.; Coggins, J. R.; Kleanthous, C. *J. Biol. Chem.* **1995**, *270*, 25827-25863.

(36) Leech, A. P.; Boetzel, R.; McDonald, C.; Shrive, A. K.; Moore, G. R.; Coggins, J. R.; Sawyer, L.; Kleanthous, C. *J. Biol. Chem.* **1998**, *273*, 9602-9607.

(37) Krell, T.; Horsburgh, M. J.; Cooper, A.; Kelly, S. M.; Coggins, J. R. *J. Biol. Chem.* **1996**, *271*, 24492-24497.

(38) Harris, J., ; Kleanthous, C.; Coggins, J. R.; Hawkins, A. R.; Abell, C. *J. Chem. Soc., Chem. Commun.* **1993**, 1080-1081.

(39) Shneier, A.; Harris, J.; Kleanthous, C.; Coggins, J. R.; Hawkins, A. R.; Abell, C. *Bioorg. Med. Chem. Lett.* **1993**, *3*, 1399-1402.

(40) Bottomley, J. R. H., A. R.; Kleanthous, C. *Biochem. J.* **1996**, *319*, 259-278.

(41) Evans, L. D. B.; Roszak, A. W.; Noble, L. J.; Robinson, D. A.; Chalk, P. A.; Matthews, J. L.; Coggins, J. R.; Price, N. C.; Lapthorn, A. J. *FEBS Lett.* **2002**, *530*, 24-30.

(42) Harris, J. M.; Gonzales-Bello, C.; Kleanthous, C.; Hawkins, A. R.; Coggins, J. R.; Abell, C. *Biochem. J.* **1996**, *319*, 333.

(43) Roszak, A. W. R., D. A.; Krell, T.; Hunter, I. S.; Frederickson, M.; Abell, C.; Coggins, J. R.; Lapthorn, A. J. *Structure* **2002**, *10*, 493-503.

(44) Despeyroux, P.; Baltas, M.; Gorrichon, L. *Bull. Soc. Chim. Fr* **1997**, *134*, 777-784.

(45) Bugg, T. D. H.; Abell, C.; Coggins, J. R. *Tetrahedron Lett.* **1988**, *29*, 6783.

(46) Harris, J. M.; Watkins, W. J.; Hawkins, A. R.; Coggins, J. R.; Abell, C. *J. Chem. Soc., Perkin Trans. 1* **1996**, 2371-2377.

(47) González-Bello, C.; Coggins, J. R.; Hawkins, A. R.; Abell, C. *J. Chem. Soc., Perkin Trans. 1* **1999**, 849-854.

(48) González-Bello, C.; Manthey, M. K.; Harris, J.; Hawkins, A. R.; Coggins, J. R.; Abell, C. *J. Org. Chem* **1998**, *63*, 1591-1597.

(49) González-Bello, C.; Harris, J. M.; Manthey, M. K.; Coggins, J. R.; Abell, C. *Bioorg. Med. Chem. Lett.* **2000**, *10*, 407.

(50) Frederickson, M.; Parker, E. J.; Hawkins, A. R.; Coggins, J. R.; Abell, C. *J. Org. Chem.* **1999**, *64*, 2612.

(51) Frederickson, M.; Coggins, J. R.; Abell, C. *Chem. Commun.* **2002**, 1886-1887.

(52) Frederickson, M.; Roszak, A. W.; Coggins, J. R.; Lapthorn, A. J.; Abell, C. *Org. Biomol. Chem.* **2004**, *2*, 1592-1596.

(53) *Expert Opin. Ther. Patents* **2001**, *11*, 1797-1799.

(54) Chana, S. S.; Cockerill, G. S.; Madge, D. In *PCT Int. Appl.*; Arrow Therapoeutics Limited: UK, 2002, p pp56.

(55) Toscano, M. D.; Frederickson, M.; Evans, D. P.; Coggins, J. R.; Abell, C.; González-Bello, C. *Org. Biomol. Chem.* **2003**, *1*, 2075-2083.

(56) González-Bello, C.; E., L.; Toscano, M. D.; Catedo, L.; Coggins, J. R.; Abell, C. *J. Med. Chem.* **2003**, *46*, 5735-5744.

(57) Toscano, M. D.; Stewart, K. A.; Coggins, J. R.; Lapthorn, A. J.; Abell, C. *Org. Biomol. Chem.* **2005**, *3*, 3102-3104.

2 Synthesis of Potential Dehydroquinase Inhibitors

2.1 INTRODUCTION

The design of new potential inhibitors of type II DHQase was based on the structure of the known oxime inhibtor **1.36**.[1] The oxime functionality, which is thought to participate in stablising hydrogen bonding interactions with active site residues, is a major factor contributing to the strength of binding of **1.36** by type II DHQase. Potential inhibitors were therefore designed with other hydrophilic functionalities at C-3, while retaining the functionality and stereochemistry of the natural substrate at all other positions of the carbocyclic ring. This chapter describes the preparation of potential inhibitors with general structures **2.1**-**2.3**, where X is a hydrophilic functional group.

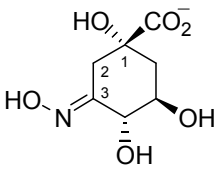

1.36

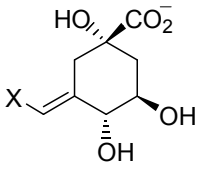

2.1

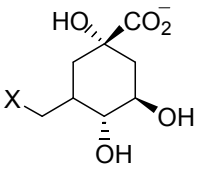

2.2

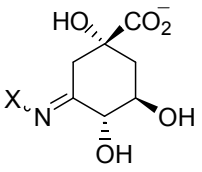

2.3

The activity of (2*R*)-2-fluorodehydroquinic acid **1.32** against type I dehydroquinase from *E. coli* suggested that other 2-fluorodehydroquinate derivatives could potentially display interesting biological activities against both types of DHQase. This chapter also describes an investigation into the synthesis of some (2*S*)-2-fluorodehydroquinate derivatives.

The synthesis of epoxide **2.4** is also reported in this chapter. It was thought that the epoxide of **2.4** would be susceptible to nucleophilic attack and ring-opening by the active site lysine of type I DHQase, resulting irreversible inhibition.

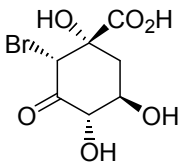

1.31

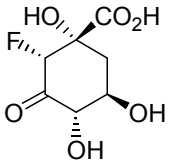

1.32

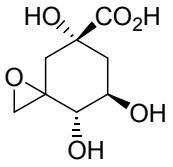

2.4

2.2 SELECTIVE OXIDATION OF THE C-3 HYDROXYL

The starting point for the synthesis of the proposed inhibitors was commercially available quinic acid **2.5**. This is a convenient starting material since it has the necessary substituents and stereochemistry at positions 1, 4 and 5. Selective oxidation of the C-3 hydroxyl was necessary, to furnish the corresponding ketone for subsequent derivatisation.

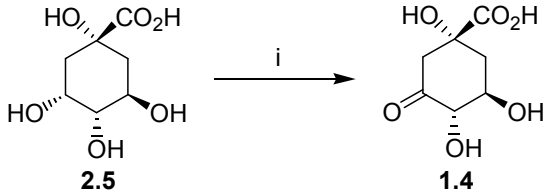

2.5 **1.4**

Scheme 2.1 Literature method for the direct oxidation of quinic acid **2.5**. *Reagents and conditions:* i. c.HNO_3(aq), 0ºC (45-50%).[2]

Methods for this selective oxidation reported in the literature included the direct oxidation of quinic acid **2.5** to dehydroquinic acid **1.4** by concentrated nitric acid (Scheme 2.1).[2] This method however, requires lengthy purification and is only low to moderate yielding. Dehydroquinic acid **1.4** is also synthetically inconvenient, requiring protection of the various functional groups prior to derivatisation.

An alternative route to oxidation of the C-3 hydroxyl *via* a more synthetically convenient protected dehydroquinate analogue was reported by Abell and co-workers (Scheme 2.2).[3] The quadruple protection of quinic acid **2.5** by *p*-toluenesulfonic acid catalysed reaction with benzaldehyde with azeotropic removal of water furnished the benzylidene acetal **2.6**. Catalytic hydrogenation to remove the benzylidene protecting group, followed by selective

protection of the C-4 hydroxyl group with *tert*-butyldimethylsilyl chloride (TBDMSCl) gave the selectively protected diol **2.7**. The secondary alcohol of this was then oxidised using pyridinium dichromate (PDC), to furnish the desired DHQ analogue **2.8**. This intermediate was then further derivatised to give reported inhibitors **1.31**, **1.32** and **1.36**.[1,3]

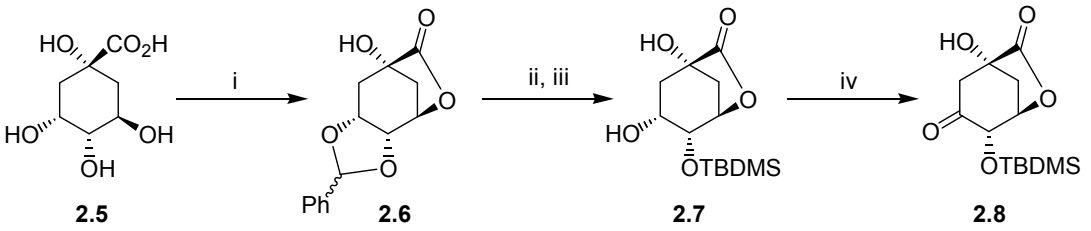

2.5 **2.6** **2.7** **2.8**

Scheme 2.2 Literature method for the preparation of protected dehydroquinate derivative **2.8**. *Reagents and conditions:* i. PhCHO, 4-TsOH, toluene, reflux (74%); ii. H_2, 10%Pd/C, AcOH, rt (94%); iii. TBDMSCl, DMAP, ET_3N, Bu_4NI, 90ºC (54%); iv. PDC, 4Å molecular sieves, CH_2Cl_2, rt (87%)[3]

A two step procedure for the selective protection of quinic acid using 2,2,3,3-tetramethoxybutane (TMB) **2.9** was reported by Montchamp *et al.* (Scheme 2.3).[4] This involved the preparation of TMB **2.9** by heating butane-2,3-dione and trimethyl orthoformate at reflux in the presence of sulphuric acid. Quinic acid methyl ester **2.10** was then reacted with **2.9** by heating at reflux with trimethyl orthoformate and camphorsulfonic acid (CSA) catalyst, in methanol, to furnish butane-2,3-bisacetal (BBA) protected quinic acid **2.11**. The $RuCl_3$ catalysed KIO_4 oxidation of the secondary hydroxyl of **2.11** gave protected dehydroquinate **2.12**, an important intermediate in the synthesis of tricarboxylate dehydroquinate synthase inhibitors.[5,6]

A more convenient one-pot procedure for the BBA protection of quinic acid **2.5** was subsequently employed by Armesto *et al.* in the synthesis of quinic and shikimic acid derivatives (Scheme 2.3).[7] This procedure involves heating quinic acid **2.5** at reflux with butane-2,3-dione, trimethyl orthoformate, and a catalytic amount of CSA in methanol for 1 h to furnish protected quinic acid **2.11**. The secondary hydroxyl at C-3 was then selectively oxidised using pyridinium chlorochromate (PCC) to yield ketone **2.12**.

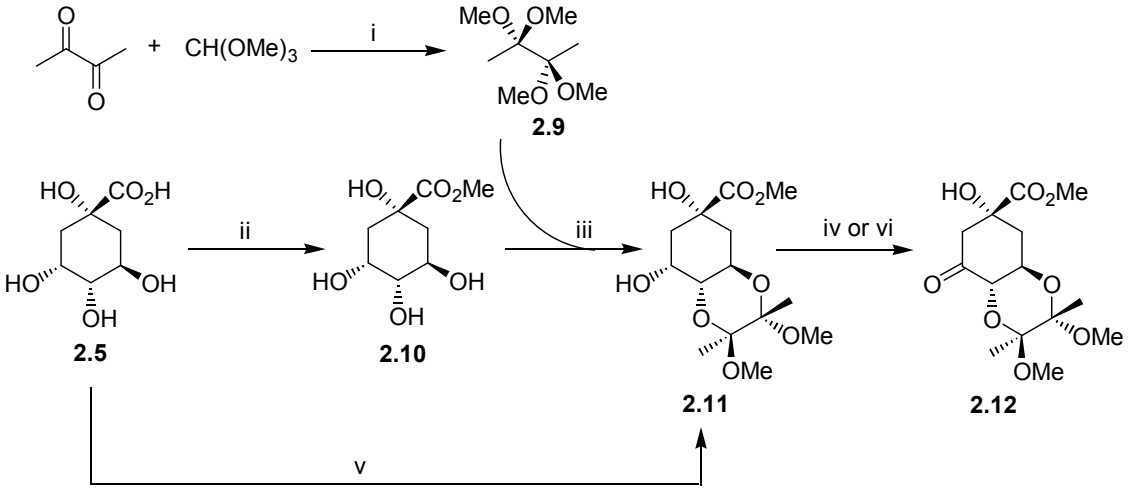

Scheme 2.3 Reported methods for the preparation of protected dehydroquinate **2.12**. *Reagents and conditions:* i. H_2SO_4, MeOH, reflux (53%); ii. Dowex 50 (H^+), MeOH, reflux; iii. $CH(OMe)_3$, (±)-CSA (87% over 2 steps);[4] iv. KIO_4, K_2CO_3, $RuCl_3$, H_2O, $CHCl_3$ (77%);[5] v. Butane-2,3-dione, CH(OMe)3, (±)-CSA, MeOH, reflux (90%);[7] vi. PCC, CH_2Cl_2 (82%).[7]

A modified version of the procedure of Armesto *et al*. was adopted by this group for the preparation of protected quinic acid **2.11** (Scheme 2.4).[8] However longer reaction times (16-20 h) were required and lower yields (70-80%) obtained than reported by Armesto *et al*.[7] Protected dehydroquinate **2.12** was prepared by PCC oxidation of **2.11** in CH_2Cl_2 over 4 Å molecular sieves for 18-48 h to produce the desired ketone in 70-80% yield. This key intermediate was utilised in the preparation of the majority of putative inhibitors described in this work.

The deprotected ketone **2.13** was also employed as an intermediate in cases where introduced functional groups where unstable under the acidic deprotection conditions (Scheme 2.4). Deprotection of **2.12** on treatment with 50% aqueous trifluoroacetic acid (TFA) at 60 ºC gave the desired product **2.13** in 42% yield, along with dehydroshikimate methyl ester **2.14** (13%), and other unidentified minor elimination products. However, when the reaction was carried out in 95% $TFA_{(aq)}$ over ice, the undesired side-products were virtually eliminated, and the desired product **2.13** obtained in 90% yield following flash chromatography. This second procedure often produced **2.13** in pure enough form, following evaporation of the solvent, that chromatographic purification was unnecessary. In such cases the yield was deemed to be quantitative although the sample generally contained some residual moisture which could not

be completely removed by drying under vacuum. Heating was avoided due to the sensitive nature of the compound.

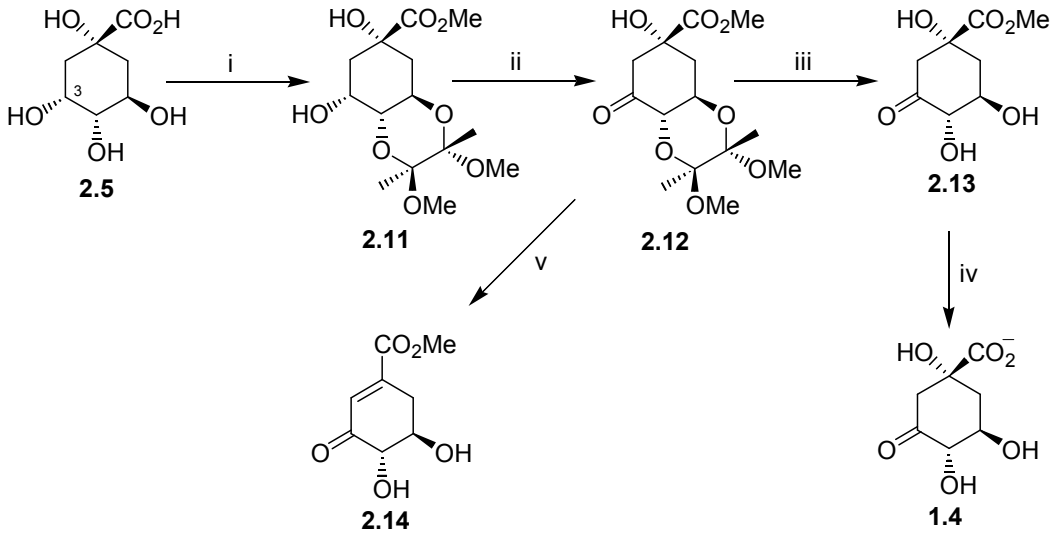

Scheme 2.4 Preparation of key intermediates **2.12** and **2.13** and enzymatic substrate DHQ **1.4**. *Reagents and conditions:* i. $(CH_3CO)_2$, $CH(OMe)_3$, (D)-CSA, MeOH, reflux (70-80%); ii. PCC, CH_2Cl_2, rt (70-80%); iii. 95% TFA/H_2O, 0 ºC (90-100%); iv. KOH, H_2O (100%); v. 50% TFA/H_2O, 60 ºC (**2.13** 42%, **2.14** 13%).

The enzymatic substrate DHQ **1.4**, required for the biological assays, was prepared from **2.13**. The ester of **2.13** was removed by basic hydrolysis in 1 equivalent of $KOH_{(aq)}$ over ice as described in the literature,[8] to furnish the substrate DHQ **1.4** quantitatively as the potassium salt. The potassium salt was employed directly in the biological assays without conversion to the carboxylic acid.

2.3 INHIBITORS WITH C ATTACHED AT C-3

2.3.1 Synthesis of the Inhibitors

It was anticipated that a Wittig reaction could be employed to functionalise ketone **2.12** at C-3 *en route* to inhibitors of general structures **2.1** and **2.2**. However, the strongly basic

conditions commonly employed in some Wittig reactions would be expected to be incompatible with the highly functionalised and sensitive nature of the substrate **2.12**. Consequently, the stabilised ylides (cyanomethylene)triphenylphosphorane (Scheme 2.5) and (carbethoxymethylene)triphenylphosphorane (Scheme 2.6) were used, eliminating the need for harsh basic conditions.

The proposed inhibitors **2.15**–**2.18** were prepared as described in Scheme 2.5. This initially involved the Wittig reaction of protected dehydroquinate **2.12** with (cyanomethylene)triphenylphosphorane (Scheme 2.5). This ylide was prepared from the commercially available (cyanomethyl)triphenylphosphonium chloride by addition of 50% $NaOH_{(aq)}$ to an aqueous solution of the salt. Protected deydroquinate **2.12** was then heated at reflux with the ylide to give protected allylic nitrile **2.19** as a single isomer, in 60% yield following recrystallisation. The configuration was assigned as (*E*)-, the expected thermodynamic product, however attempts to confirm this by NOESY NMR were unsuccessful with the only through-space interactions of the vinyl proton observed to be with the CH_3 groups of the protecting groups. Treatment of **2.19** with 95% $TFA_{(aq)}$ then gave the methyl ester **2.20** in 72% yield following recrystallisation. Hydrolysis of **2.20** in $KOH_{(aq)}$ furnished vinyl nitrile inhibitor **2.16** quantitatively as the potassium salt.

Protected nitrile **2.19** was also subjected to catalytic hydrogenation over palladium on charcoal, to give the diastereomeric nitriles **2.21** and **2.22** and the amine **2.23** in varying amounts depending on the conditions (Scheme 2.5). Reaction in CH_2Cl_2 with 40 mol% of 5% palladium on carbon gave a 1.2:3:1 ratio of **2.21**:**2.22**:**2.23**. Flash chromatography, followed by recrystallisation from pet. ether/EtOAc gave **2.21** and **2.22** in 5% and 19% yield respectively. Reaction in methanol however, with 10 mol% of 10% palladium on charcoal gave **2.22** and **2.23** in a ratio of 1:3 with only trace amounts of **2.21**. Flash chromatography gave **2.22** and **2.23** in 20% and 39% yields respectively. The configuration of the new asymmetric centre at C-3 was assigned for each of the products by ^1H NMR, as described in section 2.3.2.

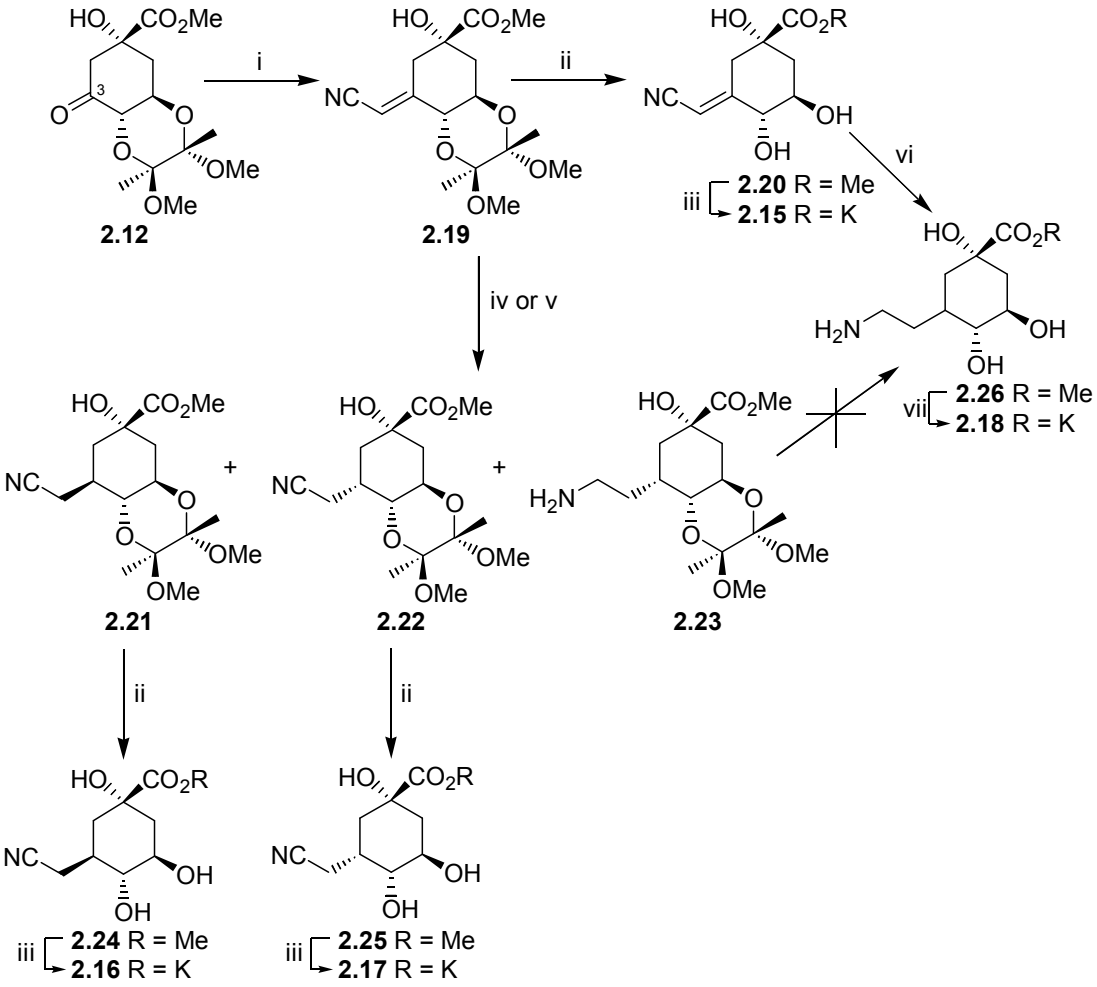

Scheme 2.5 Synthesis of nitrile inhibitors **2.15**-**2.17** and amine inhibitor **2.18**. *Reagents and conditions:* i. PPh_3CHCN, MeCN, reflux, (82%); ii. 95% $TFA_{(aq)}$, 0ºC, (**2.20** 72%, **2.24** 100%, **2.25** 100%); iii. KOH, H_2O, 0 ºC (**2.15** 100%, **2.16** 100%, **2.17** 100%); iv. H_2, 5% Pd/C, CH_2Cl_2 rt (**2.21** 5%, **2.22** 19%); v. H_2, 10% Pd/C, MeOH, rt (**2.22** 20%, **2.23** 38%); vi. H_2, 5% Pd/C, MeOH, rt; vii. KOH, H_2O, 0 ºC (71% over 2 steps).

Diastereomers **2.21** and **2.22** were separately subjected to TFA deprotection to furnish diols **2.24** and **2.25** respectively, the esters of which were hydrolysed with $KOH_{(aq)}$ to give **2.16** and **2.17** quantitatively as the potassium salts. A similar treatment of amine **2.23** with 95% $TFA_{(aq)}$ however, gave a mixture of compounds which proved unstable on attempted chromatographic purification. An alternative preparation of **2.26** was attempted by catalytic hydrogenation of olefin **2.20**. This gave what appeared to be the desired product amino ester **2.26**, with some loss of the ester. The poor resolution of the ^1H NMR spectrum of the mixture however, made it impossible to accurately assign and the mixture was not further characterised. The hydrolysis of the ester of **2.26** was completed in $KOH_{(aq)}$ to give the salt

2.18. The ^{1}H and ^{13}C NMR showed a single isomer but the ^{1}H NMR spectrum was again too poorly resolved to unambiguously assign the configuration at C-3. It seems likely however, that the configuration of the product would be the same as that obtained when the reaction was carried out in MeOH on the protected substrate **2.19** to furnish the 3*R*-epimers of the nitrile **2.22** and amine **2.23** as the major products.

The potential inhibitors **2.27**–**2.29** were prepared by Wittig reaction of protected dehydroquinate **2.12** with (carbethoxymethylene)triphenylphosphorane (Scheme 2.6). As with nitrile **2.19**, a single isomer was obtained in 89% yield and its NMR data were in agreement with the reported literature.[5] Diester **2.30** was deprotected in 95% $TFA_{(aq)}$ to give the *trans*-diol **2.31**, followed by basic hydrolysis of the ester to give the salt **2.27** quantitatively over 2 steps.

Diester **2.30** was also hydrogenated over palladium on charcoal to give diastereomers **2.32** and **2.33** in a ratio of 9:7. Chromatographic separation yielded the (3*R*)- and (3*S*)-epimers **2.32** and **2.33** respectively, both in 37% yield. The configuration at C-3 was assigned by ^{1}H NMR as discussed in Section 2.3.2.

Deprotection of **2.32** in 95% $TFA_{(aq)}$ gave the diester **2.34** which was treated with $KOH_{(aq)}$ to give the potential inhibitor **2.28** quantitatively as the potassium salt. Deprotection of **2.33** in 95% $TFA_{(aq)}$ furnished a product (obtained in 58% yield following chromatographic purification), the NMR of which indicated loss of the ethyl ester. This, coupled with an observed mass of 231 Da (MH^{+}), corresponding to a loss of 46 mass units (C_2H_5OH) relative to the expected product, suggested that lactonisation had occurred. Although there are three free hydroxyl groups which could potentially participate in the formation of a lactone, **2.35** is considered the most likely regioisomer on the basis of the ^{1}H NMR spectrum, as discussed in Section 2.3.2. Hydrolysis of the lactone **2.35** in aqueous KOH yielded dicarboxylate **2.29** quantitatively as the potassium salt.

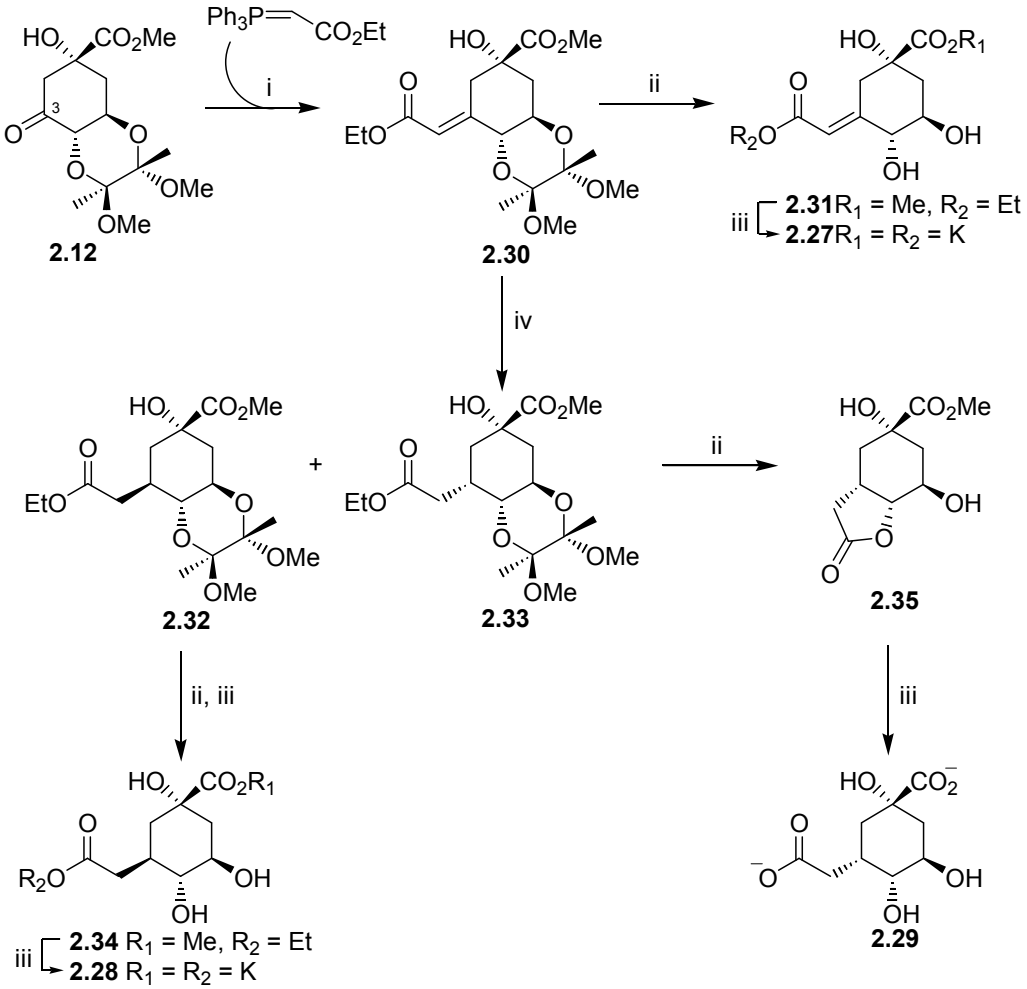

Scheme 2.6 Preparation of potential inhibitors **2.27**-**2.29**. *Reagents and conditions:* i. MeCN, reflux, (89%); ii. 95% TFA, 0ºC, (**2.31** 100%, **2.34** 100%, **2.35** 58%); iii. KOH, H_2O, 0 ºC (**2.27** 100%, **2.28** 100%, **2.29** 100%); iv. H_2, 10% Pd/C, EtOAc, rt (**2.32** 37%, **2.33** 37%).

2.3.2 Assignment of Configuration of Wittig Derivatives by ^{1}H NMR

The relative configuration at C-3 of the reduced Wittig derivatives **2.21**, **2.22**, **2.23**, **2.32** and **2.33** can be determined by ^{1}H NMR. The absolute configuration at C-3 can then be assigned on the basis of the known absolute configuration at C-4. The proton at C-3 (2.0-2.5 ppm) is coupled to five adjacent protons and its resonance is therefore very complex and generally too poorly resolved to be analysed. However, H-4 which is known to occupy the axial position, above the plane of the 6-membered ring, when in the preferred chair form (that in which the C-1 carboxyl and the C-4 and C-5 hydroxyls are all equatorial) has an appropriate resonance

for analysis. H-4 is coupled to only two protons, H-5 which also has an axial orientation, and H-3 whose orientation is to be determined. The H-4 signal therefore, is used to determine the relative configuration at C-3.

The vicinal coupling constants between H-4 and neighbouring H-3 and H-5 protons are indicative of the dihedral angle between the two protons as described by the Karplus relationship.[9] Both coupling constants for H-4 are large (9-11 Hz) and of similar magnitude when H-3 is in the axial position, resulting from the two *trans*-diaxial interactions with H-3 and H-5. However, the H-4 signal shows one large and one smaller (5-6 Hz) coupling constant when H-3 is in the equatorial position, resulting from the *trans*-diaxial interaction with H-5, and the *gauche*-interaction with the equatorial H-3 respectively.

2.3.2.1 Assignment of Configuration at C-3 for Nitriles 2.21 and 2.22

Figure 2.1 shows ^{1}H NMR spectra of the diastereomeric nitriles **2.21** and **2.22**. Figure 2.1A shows the spectrum of the (3*S*)-diastereomer **2.21**, in which the H-4 signal can be seen to be a double doublet at 3.50 ppm with two very similar coupling constants. One constant, of magnitude 9.8 Hz arises from the interaction with axial H-5. The second arises from the interaction with H-3 and has a magnitude of 10.7 Hz. This is large for a vicinal coupling constant and indicates that the dihedral angle between H-3 and H-4 is approximately 180º. This means that H-3 must be in the axial position, in a *trans*- relationship to H-4 as illustrated in Figure 2.1A.

Figure 2.1B shows the ^{1}H NMR spectrum of the (3*R*)-diastereomer **2.22**. In this case the H-4 signal can be seen to be a double doublet described by one large and one significantly smaller coupling constant. The diaxial interaction between H-4 and H-5 has a coupling constant of 10.5 Hz, similar to that for the (3*S*)-diastereomer. The coupling constant defining the interaction between H-4 and H-3 however, is a substantially smaller 5.6 Hz, consistent with a *gauche* relationship between H-3 and H-4. As H-4 is known to occupy the axial position, H-3 must therefore occupy the equatorial position at C-3 as illustrated in Figure 2.1B.

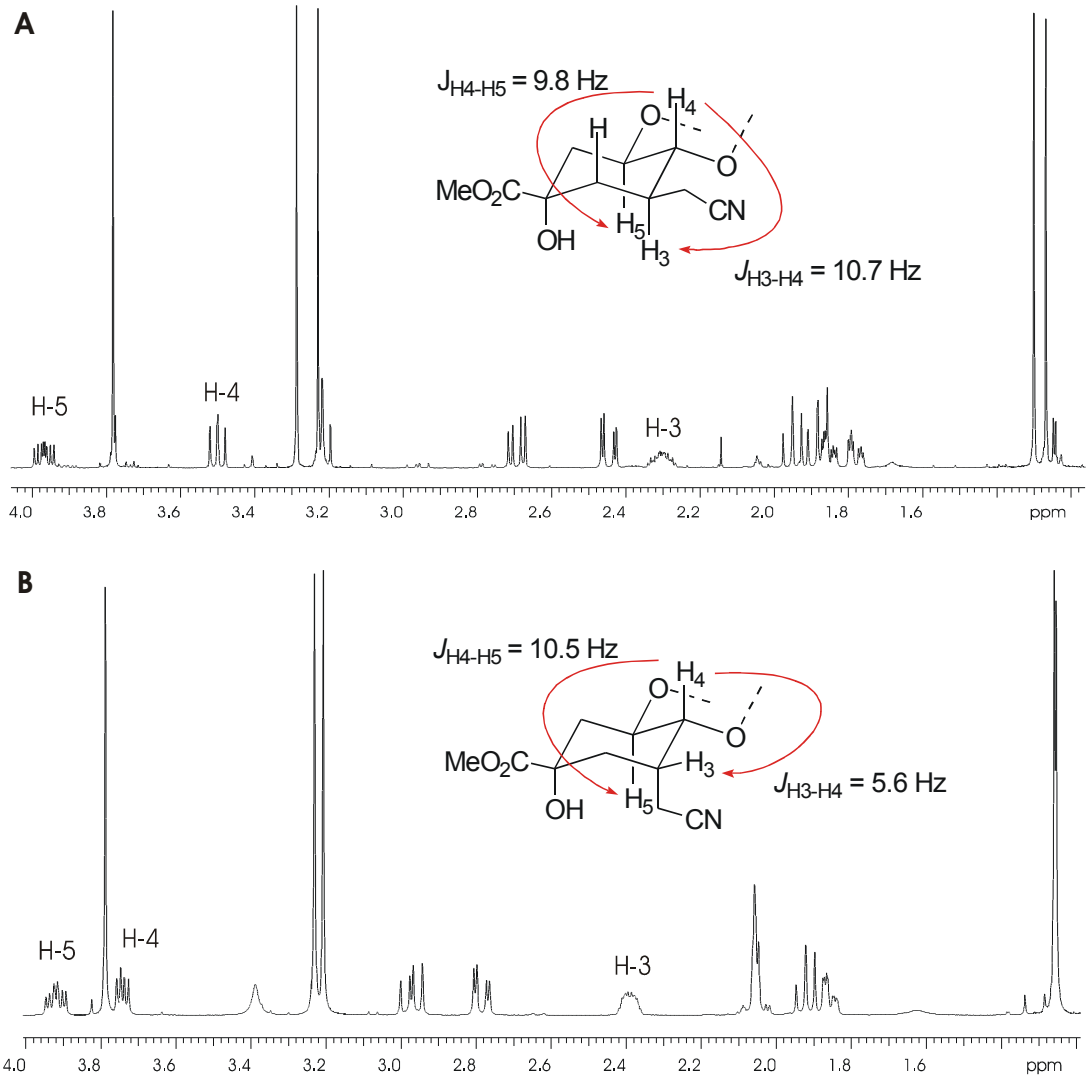

Figure 2.1 ^{1}H NMR spectra of diastereomeric nitriles **2.21** and **2.22**. A. ^{1}H NMR spectrum of **2.21**.[10] B. ^{1}H NMR spectrum of **2.22**.

2.3.2.2 Assignment of Configuration at C-3 for Amine 2.23

The H-3 resonance of amine **2.23** can not be used to assign the relative configuration as it overlaps with other signals in the spectrum. Therefore the configuration at C-3 must be determined by observing the influence of H-3 on the H-4 signal as described for **2.21** and **2.22**. The H-4 signal again exhibits two vicinal coupling interactions, one large (10.1 Hz) indicative of a *trans*-diaxial coupling to H-5 and one smaller (5.3 Hz) indicative of a *gauche* coupling to H-3. As H-4 is in an axial position, H-3 must therefore be in an equatorial position, in a *syn*- relationship to H-4 as illustrated in Figure 2.2.

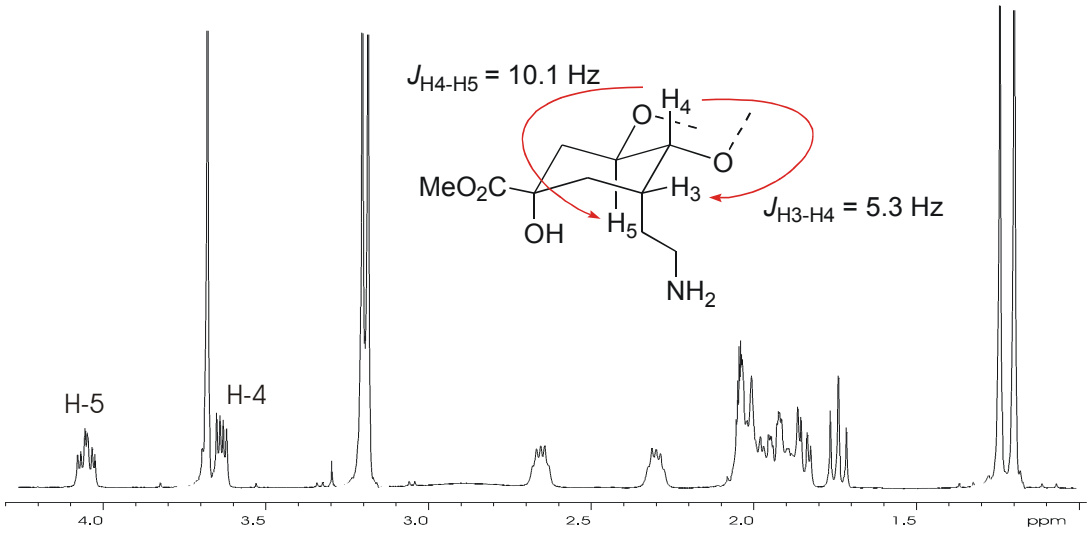

Figure 2.2 ^{1}H NMR spectrum of amine **2.23**.

2.3.2.3 Assignment of Configuration at C-3 for Diesters 2.32 and 2.33

The respective configurations of the diastereomeric esters **2.32** and **2.33** were assigned as for the nitriles **2.21** and **2.22**. Figure 2.3A shows the ^{1}H NMR spectrum of **2.32**, in which the H-4 resonance is a double doublet described by two relatively large coupling constants of 9.8 Hz and 10.7 Hz. This is consistent with a diaxial relationship between H-3 and H-4. H-3 must therefore be in the axial position as shown. The ^{1}H NMR of **2.33** (Figure 2.3B) shows a smaller coupling constant of 5.2 Hz between H-3 and H-4, relative to the larger constant of 10.5 Hz between H-4 and H-5 consistent with a *gauche* relationship between H-3 and H-4. As H-4 is axial, H-3 must therefore occupy an equatorial position as shown in Figure 2.3B.

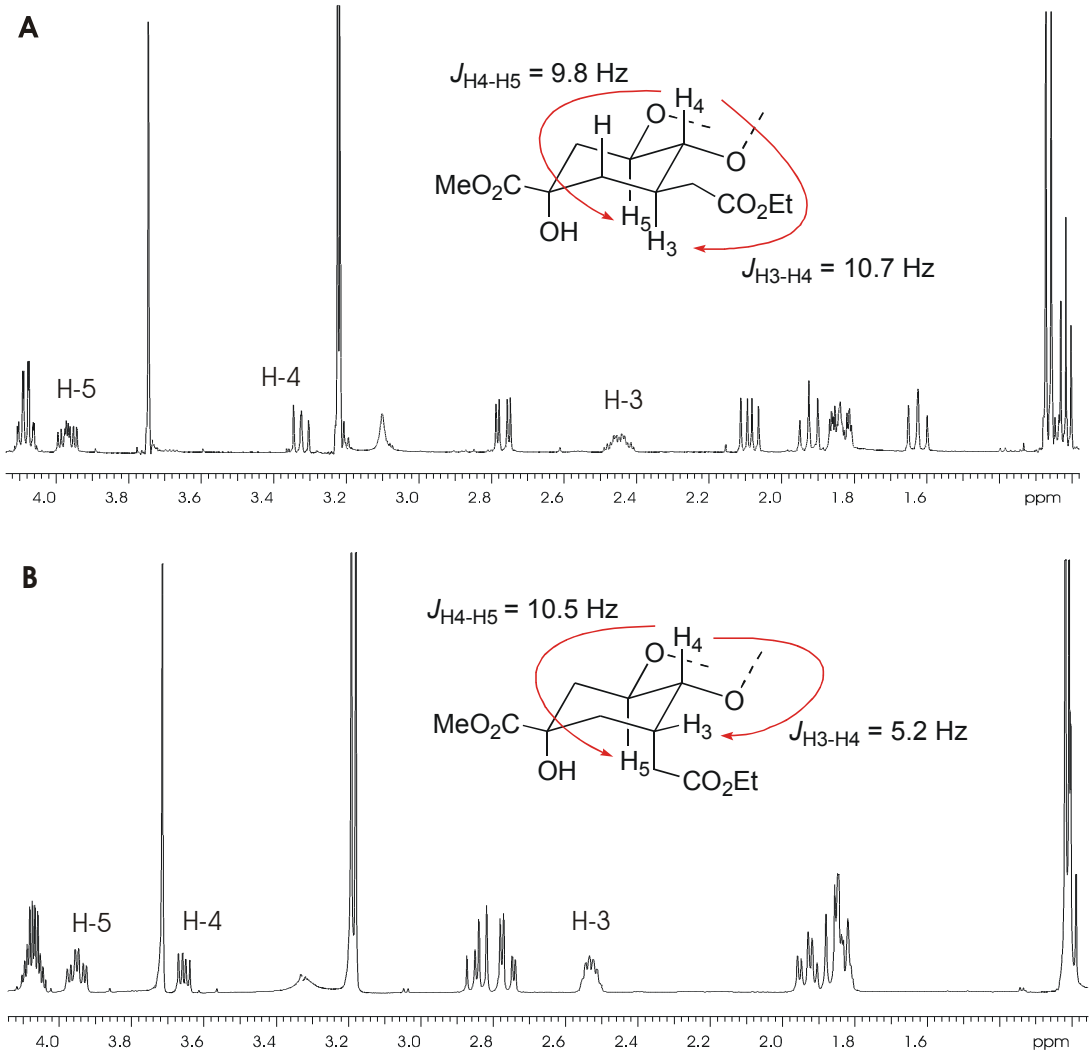

Figure 2.3 ^{1}H NMR spectra of diastereomeric esters **2.32** and **2.33**. A. ^{1}H NMR spectrum of **2.32**. B. ^{1}H NMR spectrum of **2.33**.

2.3.2.4 Structural Assignment of Lactone 2.35 by ^{1}H NMR

The ^{1}H and ^{13}C NMR spectra of the sample in question indicate the loss of the ethyl ester and a mass of 231 (MH^{+}), suggesting the formation of a lactone, rather than the free acid. The formation of a lactone could potentially take place with any of the three free hydroxyl groups at C-1, C-4 or C-5, giving rise to three possible regioisomeric products **2.36**, **2.35** and **2.37** respectively. An analysis of the proton NMR spectrum however, strongly supports the formation of the 3,4-lactone **2.35** (Figure 2.4).

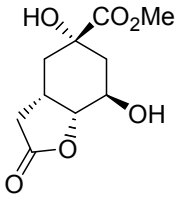

2.35

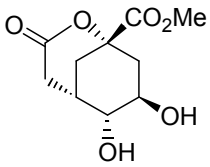

2.36

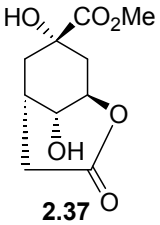

2.37

Again the diagnostic signal was that of H-4. The H-4 signal at 4.36 ppm displays a 0.8 ppm downfield shift relative to the to the corresponding signal (3.65 ppm) of the precursor **2.33** (Figure 2.3B), suggestive of acylation of the C-4 hydroxyl. The coupling constants for H-4 were also altered relative to **2.33**. The proton NMR spectrum of the precursor **2.33** shows one large constant (10.5 Hz) describing the diaxial interaction with H-5 and one smaller (5.2 Hz) constant describing the *gauche* coupling with H-3. The ^{1}H NMR spectrum of the lactone **2.35** however, shows the vicinal coupling of H-4 to H-3 and H-5 to be described by two intermediate, identical coupling constants of 7.8 Hz. This suggests a change in conformation from the usual chair form, with the dihedral angle between H-4 and H-5 becoming slightly less than 180º, and the dihedral angle between H-3 and H-4 becoming less than 60º, resulting in a decrease and an increase respectively, in the corresponding coupling constants. This is consistent with the formation of a bicyclic structure, resulting in a slight distortion of the original geometry.

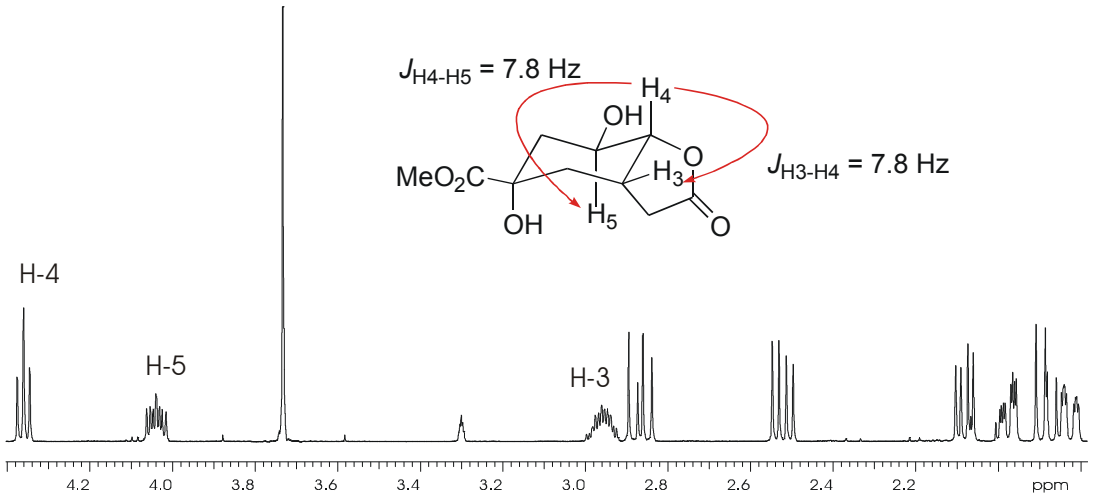

Figure 2.4 ^{1}H NMR spectrum of bicyclic lactone **2.35**.

Geometry optimisation of structure **2.35** using Spartan '04 quantum mechanics program suggests that the formation of lactone **2.35** would deform the usual geometry of the chair form

of the six-membered ring sufficiently to bring the H-3 and H-4 protons into an almost *syn* relationship and also skew the H-4 and H-5 protons slightly out of the normal diaxial relationship. The predicted structure of lactone **2.35** has a dihedral angle of 164º between H-4 and H-5, and a dihedral angle of 36º between H-3 and H-4 (Figure 2.5). This is consistent with the differences between the coupling constants exhibited by the H-4 signals of **2.33** and **2.35** as discussed above and supports the assigned structure as that of **2.35**.

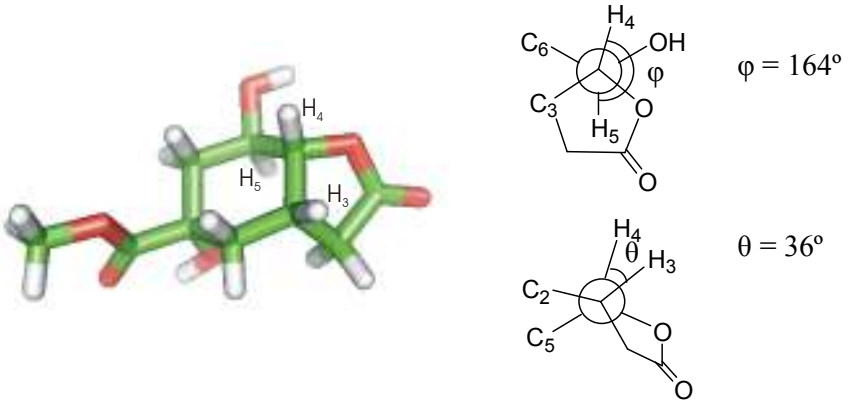

Figure 2.5 Calculated geometry of bicyclic lactone **2.35** with Newman projections illustrating the calculated dihedral angles between H-3, H-4 and H-5.

2.4 SYNTHESIS OF INHIBITORS WITH N ATTACHED AT C-3

The preparation of semicarbazone inhibitor **2.38** was initially attempted by reaction of protected ketone **2.12** with semicarbazide hydrochloride in the presence of NaOAc (Scheme 2.7). This produced two isomers of protected semicarbazone **2.39** in a 2:1 ratio. The stereochemistries of the isomers were not assigned, but it is likely that the major isomer was the thermodynamically more favourable (*E*)-isomer. The semicarbazone functionality however was not stable under the acidic conditions of the BBA protecting group removal, yielding dehydroquinate methyl ester **2.13** instead of the desired semicarbazone methyl ester **2.40**.

Methyl dehydroquinate **2.13** (prepared by deprotection of **2.12**) was subsequently employed as the intermediate ketone in the synthesis of semicarbazone inhibitor **2.38** (Scheme 2.7). Methyl dehydroquinate **2.13** was reacted with semicarbazide hydrochloride and sodium acetate (1:1.3) in water at 50-60 ºC to give a mixture of semicarbazone **2.40**, elimination products and highly coloured (yellow-brown) impurities. It was found that carrying out the reaction in a solution adjusted to pH 7 by addition of excess sodium acetate prevented the elimination of the hydroxyl groups and reduced the occurrence of the coloured impurities. This gave a mixture of isomers of **2.40** in a 10:1 ratio. The residual acetic acid and sodium acetate were removed from the product mixture by silica gel chromatography to furnish semicarbazone **2.40** as a 20:1 ratio of isomers in 82% yield. The ester of **2.40** was then hydrolysed in $KOH_{(aq)}$ to furnish salt **2.38** quantitatively.

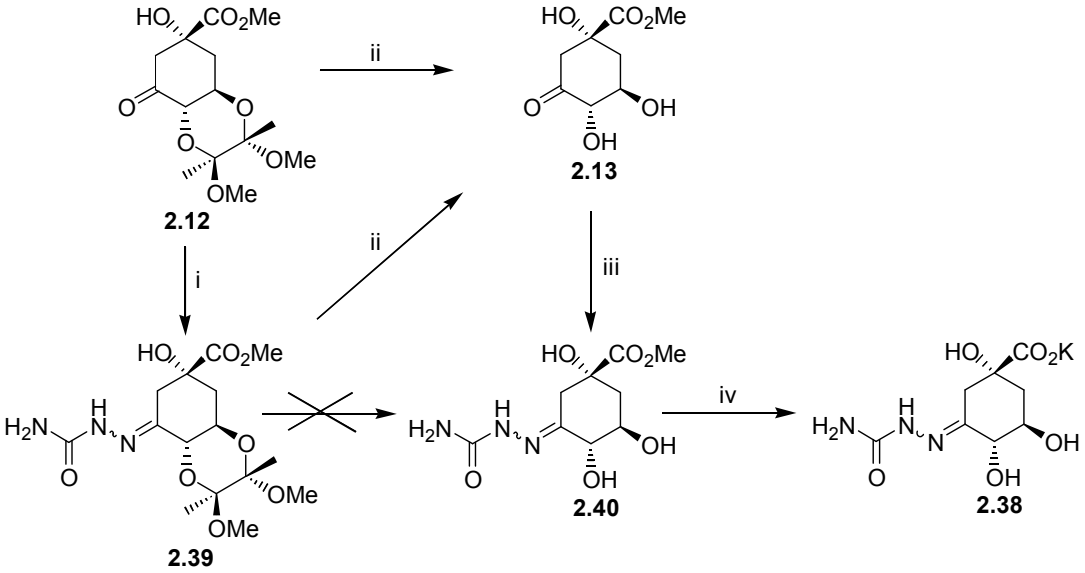

Scheme 2.7 Synthesis of semicarbazone inhibitor **2.38**. *Reagents and conditions:* i. $NH_2NHCONH_2{\cdot}HCl$, NaOAc, MeOH, H_2O, 50 ºC (53%); ii. 95% TFA/H_2O, 0 ºC (90%); iii. $NH_2NHCONH_2{\cdot}HCl$, NaOAc, MeOH, H_2O, 40 ºC (20:1 *E*:*Z*, 82%), iv. KOH, H_2O, 0 ºC (quant).

It is not known for certain whether the stereochemistry of the major isomer is *E* or *Z*. However, the known inhibitor **1.36** (see Scheme 2.8) was prepared as a single isomer by Abell and co-workers following a similar route.[1] The stereochemistry of **1.36** was assigned as *E* (the likely thermodynamic product) and confirmed by the crystal structure of *M. tuberculosis* DHQase with oxime **1.36** bound in the active site.[11] It seems likely that the hydrazone derivatives would follow a similar pattern, though apparently with less

stereoselectivity. On this basis the major isomer in each case was assumed to be the (*E*)-isomer.

Hydrazone methyl ester **2.41** was prepared from methyl dehydroquinate **2.13** and hydrazine hydrochloride (Scheme 2.8). The solution was adjusted to pH 7 by addition of excess NaOAc. The product **2.41** was obtained as 2:1 ratio of isomers containing a very intensely coloured brown impurity which was not detectable by NMR. It was observed that increasing the scale of the reaction from 50 mg to 1 g dramatically increased the apparent proportion of the coloured impurity. Repetitive flash chromatography on deactivated silica (1% Et_3N in the solvent used to pack the column to protect the acid-sensitive compound from the silica) only intensified the colour and left large amounts of Et_3N in the product which could not be removed *in vacuo*. Chromatography on non-deactivated silica was found to be preferable, however the recovery of the product from the column was low (10% overall yield), with the minor isomer not recovered.

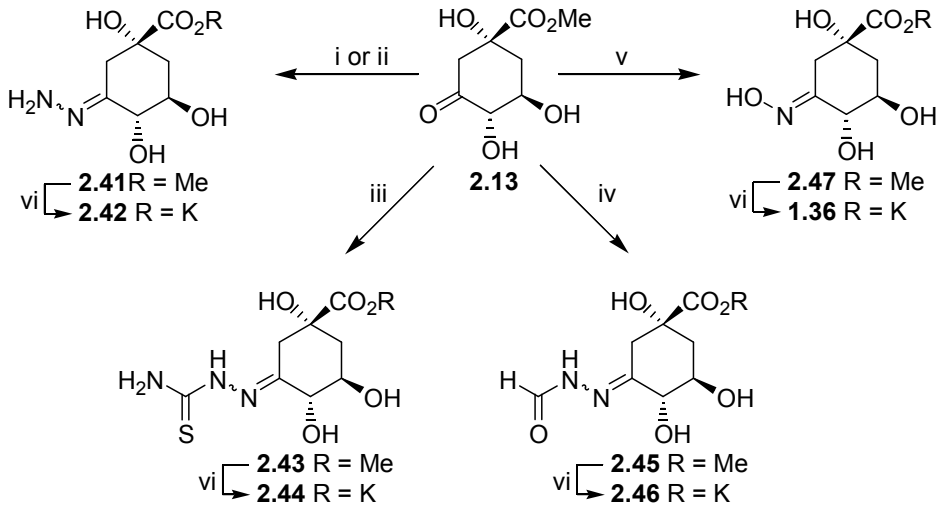

Scheme 2.8 Synthesis of hydrazone inhibitors **2.39**, **2.41**, **2.43** and **2.45**. *Reagents and conditions:* i. $NH_2NH_2{\cdot}2HCl$, NaOAc, H_2O, pH 7, rt (*E* only, 10%); ii. $NH_2NH_2{\cdot}H_2O$, H_2O, rt (3:1 *E*:*Z*, 44%); iii. $NH_2NHCSNH_2$, NaOAc/AcOH, H_2O, MeOH, 40 ºC. (9:1 *E*:*Z*, 51%); iv. NH_2NHCOH, H_2O, rt (3:2 *E*:*Z*, 24%); v. $NH_2OH{\cdot}HCl$, NaOAc. H_2O, pH 7, rt (55%); vi. KOH, H_2O, 0 ºC, (quant).

An alternative approach to the preparation of hydrazone **2.41** involved the reaction of methyl dehydroquinate **2.13** with one equivalent of hydrazine hydrate in water at ambient temperature. Though this method significantly reduced the amount of the coloured impurity, the reaction did not go to completion, and produced a mixture of the two isomers of **2.41**

(5:4), starting material and an unidentified side-product. The mixture was purified by column chromatography, without deactivating the silica, to furnish a 3:1 ratio of the isomers **2.41** in 44% yield. Increasing the amount of hydrazine hydrate in the reaction from 1 equivalent to 1.5 in an attempt to force the reaction to completion resulted in partial loss of the ester as indicated by ^{1}H NMR. The ester of **2.41** was hydrolysed in $KOH_{(aq)}$ to furnish **2.42** quantitatively.

Thiosemicarbazone methyl ester **2.43** was prepared by reaction of methyl dehydroquinate **2.13** with thiosemicarbazide (Scheme 2.8) in a mixture of 1.8 M acetate buffer (pH 7) and MeOH. A 9:1 ratio of isomers (with the major isomer assumed to be *E*) was obtained in 51% yield following chromatography on deactivated silica. The esters **2.43** were converted quantitatively to the potassium salts **2.44** by hydrolysis in aqueous KOH.

Formylhydrazone methyl ester **2.45** was prepared from methyl dehydroquinate **2.13** by reaction with formic hydrazide in H_2O at rt. Formic hydrazide was used as the free amine and as such it was not necessary to buffer the reaction mixture to prevent acid catalysed elimination of the hydroxyl groups. The crude sample contained the isomers **2.45** in a 4:3 ratio (*E*:*Z*) and 10% unidentified side-product (as determined by ^{1}H NMR). The undesired side-product was difficult to remove chromatographically. Therefore only the fraction shown by ^{1}H NMR to contain the least impurity (4%) was taken for deprotection and assay. This represented a 24% yield of **2.45**, in a 3:2 (*E*:*Z*) ratio of isomers. A further 39% was recovered from the column, containing 14% impurity and a 4:3 (*E*:*Z*) ratio of isomers. The esters **2.45** (3:2 *E*:*Z*) was converted quantitatively into the potassium salt by basic hydrolysis to yield inhibitor **2.46** as a 3:2 mixture of isomers.

Known dehydroquinase inhibitor, oxime **1.36** was also prepared as a standard with which to compare the assay results obtained for new inhibitors (Scheme 2.8). The oxime methyl ester **2.47** was prepared by reacting hydroxylamine hydrochloride with methyl dehydroquinate **2.13**, in the presence of NaOAc at pH 7. A single isomer (assigned as the (*E*)-isomer based on the literature)[1] was obtained, which was purified by silica gel chromatography to obtain oxime methyl ester **2.47** in 55% yield. The carboxyl group was deprotected by basic hydrolysis of the methyl ester to furnish oxime **1.36** quantitatively as the potassium salt, the ^{1}H NMR data of which agreed with the literature.[1,12]

2.5 INVESTIGATIONS INTO THE SYNTHESIS OF FLUORINATED DEHYDROQUINATE DERIVATIVES

2.5.1 Background

Dehydroquinate derivatives with fluorine incorporated at C-2, C-3 and C-6 have been prepared by various methods and these display a variety of biological activities.[3,13-18] (2*R*)-2-Fluorodehydroquinate **1.32** (Scheme 2.9) is a suicide inhibitor of type I DHQase and a substrate for type II DHQase.[17,18] The 3-fluoro-analogues **1.40** and **1.41** (Scheme 2.10) are competitive reversible inhibitors of type II DHQase and also poor competitive inhibitors of type I DHQase.[13,14] The 6-fluorodehydroquinate epimers **2.51a** and **2.51b** (Scheme 2.11) are substrates for both type I and II DHQase.[15]

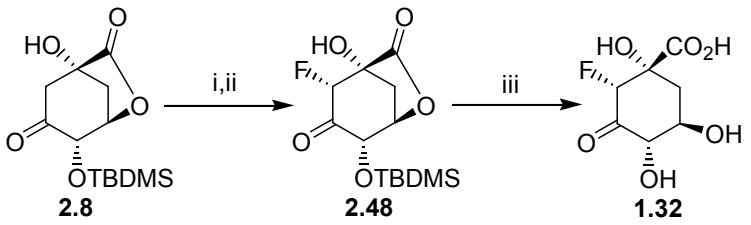

Scheme 2.9 Reported synthesis of (2*R*)-2-fluorodehydroquinate **1.32**.[3] *Reagents and conditions:* i. TMSOTf, Et3N, toluene, reflux; ii. Selectfluor®, DMF, rt (89%); iii. AcOH, H_2O, 50 ºC (90%).

The synthetic method used by Abell and coworkers to prepare type I DHQase inhibitor (2*R*)-2-fluorodehydroquinic acid **1.32** involved the initial selective protection and oxidation of quinic acid **2.5** to give protected dehydroquinic acid **2.8** (Scheme 2.2).[3,18] This was then converted into protected fluoroketone **2.48** by electrophilic fluorination of its corresponding silylenolether using Selectfluor® fluorinating reagent (Scheme 2.9). This was deprotected in aqueous acetic acid to give (2*R*)-2-fluorodehydroquinic acid **1.32**.

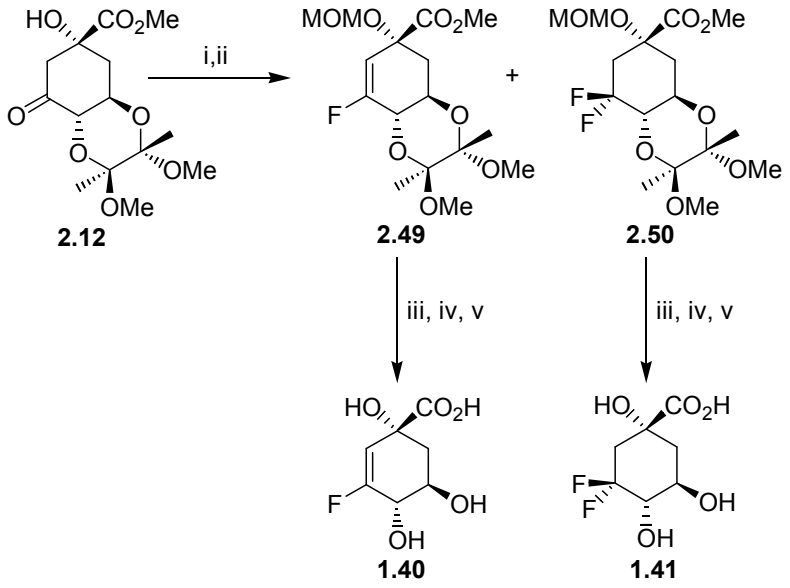

Scheme 2.10 Reported synthesis of fluorinated DHQase inhibitors **1.40** and **1.41**.[13,14] *Reagents and conditions:* i. $CH_2(OMe)_2$, P_2O_5, $CHCl_3$ (80%); ii. DAST, DME, 80 ºC (**2.49** 13%, **2.50** 45%); iii. TFA, H_2O, 60 ºC; iv. NaOH, H_2O; v. Amberlite IR-120(H) (**1.40** 63%, **1.41** 96% over 3 steps).

The 3-fluoro derivatives of dehydroquinic acid **1.40** and **1.41** were prepared by Abell and co-workers using BBA protected dehydroquinic acid **2.12** as an intermediate (Scheme 2.10).[13,14] The C-1 hydroxyl was protected as the methoxymethy (MOM) ether, and fluorine was introduced into the cyclohexanone ring upon treatment with diethylaminosulfur trifluoride (DAST) in 1,2-dimethoxyethane (DME), giving fluorinated products **2.49** and **2.50** in 13% and 45% yield respectively. Compounds **2.49** and **2.50** were separately deprotected over three steps to give the free acids **1.40** and **1.41** respectively.

An enzymatic approach was used by Abell *et al.* to prepare (6*R*)- and (6*S*)-fluorodehydroquinic acids (**2.51a** and **2.51b**), *en route* to the corresponding fluoroshikimic acids (**2.52a** and **2.52b**).[16] 6-Fluoroshikimate was prepared from 3-fluorophosphoenolpyruvate (**2.53a** and **2.53b**) and erythrose-4-phosphate **1.1** using the shikimate pathway enzymes DAHP synthase, dehydroquinate synthase, dehydroquinase and shikimate dehydrogenase. The fluorodehydroquinates **2.51a** and **2.51b** were employed in mechanistic studies on types I and II DHQase.[15]

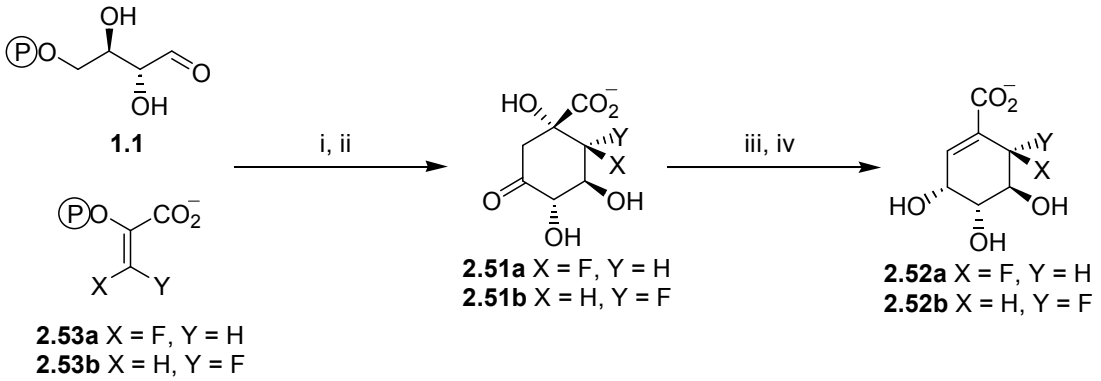

Scheme 2.11 Reported enzymatic synthesis of (6*R*)- and (6*S*)-fluorodehydroquinate **2.51a** and **2.51b**.[15,16] *Reagents and conditions:* i. DAHP synthase, Mn^{2+}; ii. DHQ synthase, Co^{2+}, NAD^{+}; iii. DHQase; iv. shikimate dehydrogenase, NADPH (**2.52a** 17%, **2.52b** 17%).

2.5.2 Synthesis of 2-Fluorodehydroquinate Derivatives

The participation of the C-2 protons of DHQ **1.4** in the mechanisms of both types of DHQase (Section 1.3), coupled with the known inhibitory activity of (2*R*)-2-fluorodehydroquinate **1.32** against type I DHQase (Section 1.4) suggested that other 2-fluorodehydroquinate derivatives might have interesting biological properties. The synthesis of 2-fluorodehydroquinate derivatives was therefore investigated. The method chosen was similar to that employed by Abell and coworkers in the synthesis of (2*R*)-2-fluorodehydroquinic acid **1.32**, however ketone **2.12** was employed in preference to **2.8** as the selectively protected intermediate (Scheme 2.12).

Protected dehydroquinate **2.12** was heated at reflux in toluene with trimethylsilyl trifluoromethanesulfonate (TMSOTf) and triethylamine, as described by Abell and coworkers.[3] This gave a mixture of the desired C-1 protected silylenolether **2.54** and the intermediate TMS protected ketone **2.55** in a ratio of 1.4:1 as determined by ^{1}H NMR. The TMS protection of the C-1 hydroxyl was not reported by Abell *et al.*[3] in their fluorination of the dehydroquinate 1,5-lactone **2.8** and was expected to have implications for the stereochemistry of the subsequent fluorination. The lack of completion of the reaction was attributed to the consumption of the silylating reagent by the tertiary hydroxyl.

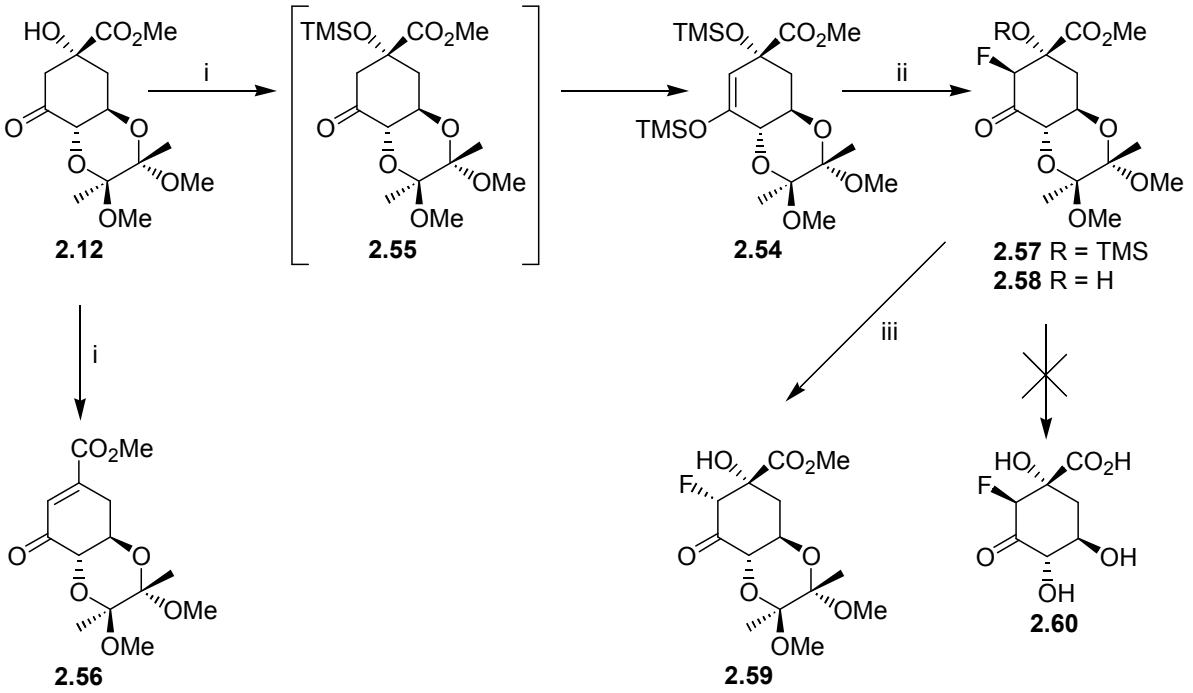

Scheme 2.12 Synthesis of 2-fluorodehydroquinate analogues **2.57** and **2.59**. *Reagents and conditions:* i. TMSOTf, Et_3N, toluene, reflux; ii. Selectfluor®, MeCN, 4 Å molecular sieves, rt (32% from **2.12**); iii. SiO_2, EtOAc/pet. ether/Et_3N (51% from **2.12**).

Attempts to increase the yield of silylenolether **2.54** by doubling the amount of TMSOTf in the reaction resulted in the formation of protected dehydroshikimate **2.56** as the major product. This was presumed to be due to the Lewis acidity of the TMSOTf, as dehydroquinate derivatives are known to undergo elimination of the C-1 hydroxyl under acidic conditions. The amount of Et_3N in the reaction mixture relative to the amount of TMSOTf was therefore increased. A combination of ketone starting material **2.12**, TMSOTf and Et_3N in a 1:6:10 ratio drove the reaction to completion and prevented the formation of the side-product **2.56**, giving silylenolether **2.54** as the sole product, which was used directly in the fluorination step without purification.

Silylenolether **2.54** was stirred with Selectfluor® in dry dimethylformamide (DMF) at rt to give a mixture of products containing TMS-protected ketone **2.55**, protected dehydroshikimate **2.56**, and α-fluoroketones **2.57** and **2.58** (4:2:2:1). An alternative solvent was chosen and the reaction carried out again over 4 Å molecular sieves in an attempt to maximise the formation of fluoroketone **2.57**.

The desired α-fluoroketone **2.57** was obtained as the major product on carrying out the reaction in acetonitrile, with ketone **2.55** also obtained as a minor product (6:1). The 2-fluoroketone **2.57** was obtained as a single diastereomer, and the configuration at C-2 assigned by ^{1}H NMR as discussed in section 2.5.3 (Figure 2.6). Unsurprisingly, given the expected steric hindrance due to the axial TMS-protected C-1 hydroxyl, the configuration at C-2 was found to be *S*, with the fluorine in the axial position. The Selectfluor® electrophilic fluorinating reagent (1-chloromethyl-4-fluoro-1,4-diazoniabicyclo[2.2.2]octane bis-(tetrafluoroborate)) is bulky, and it makes sense that it would be forced to approach from above the six-membered ring with the TMS group blocking approach from below.

Purification of (2*S*)-2-fluoroketone **2.57** proved problematic however, as its behaviour on attempted chromatographic separation was somewhat capricious. Flash chromatography on deactivated silica gave the (2*R*)-2-fluoroketone **2.59** as the main product, obtained in 51% yield (from **2.12**). Chromatography on alumina gave a mixture of both C-2 epimers as the free alcohols **2.58** and **2.59** in a ratio of 1:2 in 24% yield. Chromatography on silica (without deactivation) of a 1:1 mixture of **2.57** and **2.55** gave (2*S*)-2-fluoroketone **2.57** and ketone **2.55** in 32% and 31% yield respectively from **2.12**.

(2*S*)-2-Fluoroketone **2.57** was deprotected in 95% $TFA_{(aq)}$ to liberate the hydroxyl groups but attempts to deprotect the carboxyl group to give **2.60** were unsuccessful (Scheme 2.12). Basic hydrolysis in $KOH_{(aq)}$ destroyed the starting material. Acid hydrolysis in $AcOH/H_2O$ resulted in partial epimerisation at the fluorinated centre with no ester hydrolysis observed by ^{1}H NMR. The mixture of epimers (1:2.5 *R*:*S*) recovered from the attempted acid hydrolysis was subjected to nucleophilic dealkylation conditions using sodium cyanide, which destroyed the starting material.

(2*S*)-2-Fluorodehydroquinic acid **2.60**, whose synthesis has not been reported, was expected to exhibit interesting biological activity against types I and II DHQase. It was therefore desirable to solve the problem of the final deprotection of the carboxylate. As appropriate deprotection conditions could not be investigated further without preparing more (2*S*)-2-fluoroketone **2.57**, it was decided to incorporate an alternative carboxyl protecting group into the synthesis, which could be removed either under the conditions of the diol deprotection or under mild neutral conditions.

Two alternative esters were investigated, an allyl ester which can be cleaved by palladium(0) catalysed allyl transfer,[19,20] and an acid-labile *p*-methoxybenzyl ester (reported by Abell and co-workers to solve a related problem).[17] It was thought that this second ester could be removed simultaneously with the BBA protecting group in a single step, eliminating the need for a separate carboxyl deprotection step.

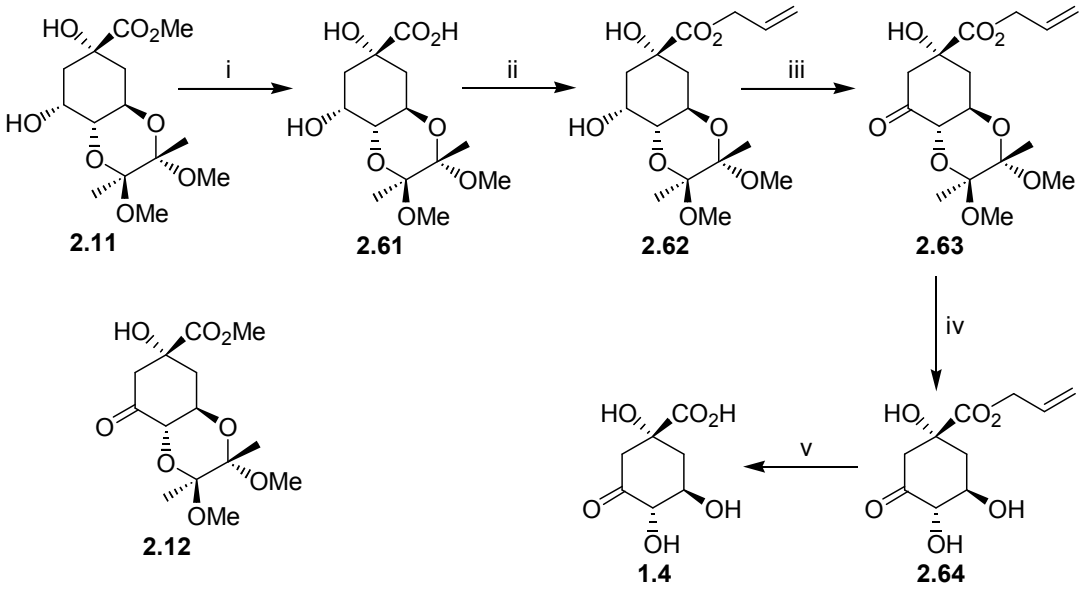

Scheme 2.13 Preparation of allyl ester protected intermediate **2.63**. *Reagents and conditions:* i. a) KOH, H_2O 0 ºC b) Amberlite IR-120(H) (95%); ii. AllBr, $KHCO_3$, DMF, rt (65%); iii. PCC, CH_2Cl_2, rt (71%); iv. 95% TFA, H_2O, 0 ºC (96%); v. $Pd(0)(PPh_3)_4$, dimedone, THF, rt (75%).

Allyl ester intermediate **2.63** was prepared as illustrated in Scheme 2.13. The key intermediate ketone **2.12** was not directly converted to the allyl ester **2.63** as it was known to decompose under the conditions of the basic ester hydrolysis.[21] Protected quinic acid **2.11** was therefore converted into the corresponding allyl ester by basic hydrolysis of the methyl ester followed by acidification over Amberlite IR-120(H) ion exchange resin to give the free acid intermediate **2.61**. This was followed by reaction with allyl bromide in the presence of $KHCO_3$ to furnish the allyl ester **2.62** in 65% yield following flash chromatography. This secondary alcohol was oxidised using PCC, to give protected dehydroquinic acid **2.63** in 71% yield following chromatography.

Deprotection conditions were investigated, using DHQ as a model system, prior to carrying out the fluorination reaction. The diol was successfully liberated employing 95% $TFA_{(aq)}$ to

furnish ester **2.64** in 96% yield. The allyl ester deprotection method of Kunz and Waldmann (employed in glycoprotein synthesis), using *tetrakis*-triphenylphosphine palladium (0) in THF with morpholine (10 equivalents) acting as the nucleophilic allyl acceptor, was initially attempted.[19] While this method was observed by ^{1}H NMR to remove the ester of **2.64**, the work up was problematic, due to the high water and low organic solubility of the product, and the residual morpholine could not be completely separated from the product. An alternative allyl acceptor was sought. It was desirable that the chosen nucleophile be taken up into the organic fraction during the work-up, without necessitating the use of any acids, bases or salts, as the solubility of the product was such that it would be extracted into the aqueous fraction.

Palladium catalysed deprotection methods for allyl protecting groups have been reviewed by Guibé.[20] Dimedone was used as an allyl scavenger in the deprotection of allyl carbamates by Kunz and coworkers.[22] It was thought that the excess dimedone might be more easily separated from the water soluble product by extraction than was the case for morpholine. The $Pd(PPh_3)_4$ catalysed removal of the ester from **2.64** did not go to completion with 10 equivalents of dimedone in acetonitrile. However, the use of THF as solvent and a 40 min reaction time resulted in complete conversion. Both catalyst and dimedone were removed by multiple extractions with chloroform and ethyl acetate to yield the free product dehydroquinic acid **1.4** in 75% crude yield.

The successful allyl ester methodology was subsequently applied to the preparation of (2*S*)-2-fluorodehydroquinate **2.60** (Scheme 2.14). Protected DHQ allyl ester **2.63** was converted into the silylenolether **2.65** and this was fluorinated using the conditions described for **2.57** (Scheme 2.12) to give a 3:1 mixture of the desired (2*S*)-2-fluoroketone **2.66** and the unfluorinated ketone **2.67**. Fluoroketone **2.66** was obtained in 37% yield following flash chromatography on silica. The fluorketone **2.66** was obtained as a single diastereomer, the stereochemistry of which was assigned by ^{1}H NMR (Section 2.5.3). The configuration at C-2 was found to be the same as that of **2.57**, with the fluorine in the axial position.

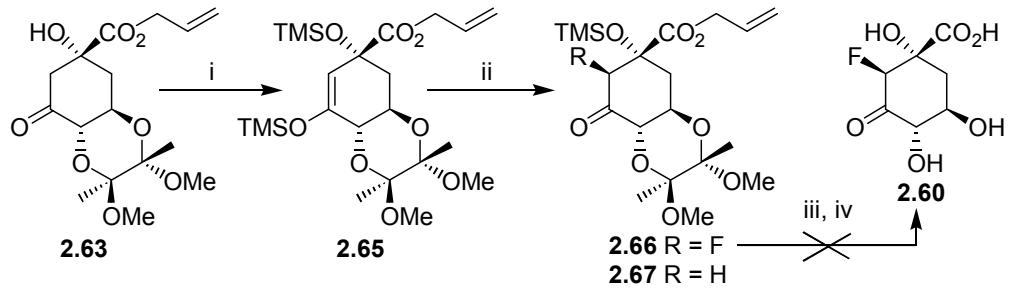

Scheme 2.14 Fluorination of protected dehydroquinate allyl ester **2.63**. *Reagents and conditions:* i. TMSOTf, Et_3N, toluene, reflux; ii. Selectfluor®, MeCN (37% over 2 steps); iii. 95% TFA, H_2O, 0 ºC; iv. Pd(0)(PPh3)4, dimedone, THF, rt.

Ketone **2.66** proved to be unstable under the TFA deprotection conditions, although some peaks which were consistent with the expected product were discernable in the ^{1}H NMR spectrum of the resulting mixture. The crude mixture was subjected to palladium catalysed removal of the allyl ester as described previously but peaks indicative of the desired product were not visible in the ^{1}H NMR spectrum.

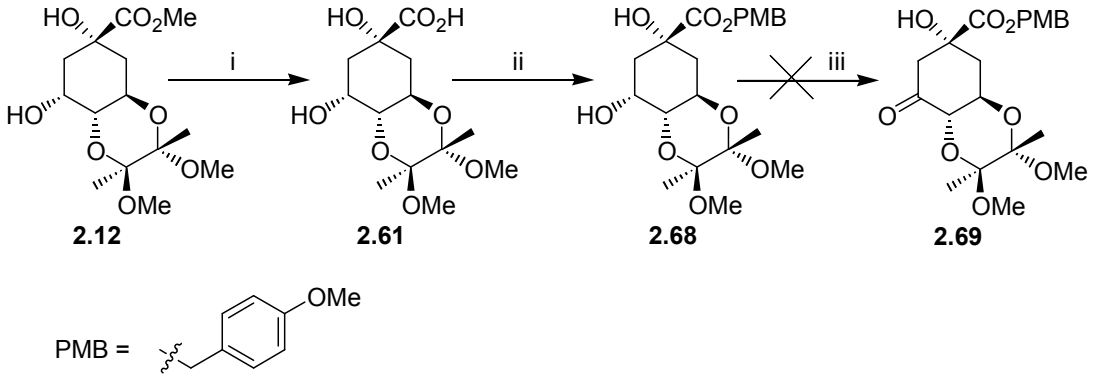

Scheme 2.15 Preparation of *p*-methoxybenzyl quinate derivative **2.68**. *Reagents and conditions:* i. a) KOH, H_2O, 0 ºC b) Amberlite IR-120(H); ii. *p*-methoxybenzyl chloride, $KHCO_3$, DMF, rt (41% over 2 steps); iii. PCC, CH_2Cl_2, rt

The *p*-methoxybenzyl (PMB) ester was also investigated as a carboxy protecting group. The PMB protected quinic acid **2.68** was prepared in the same way as the corresponding allyl ester **2.62** (Scheme 2.15). The methyl ester of **2.11** was hydrolysed in aqueous KOH and acidified over Amberlite IR-120(H) ion exchange resin. The free acid **2.61** was subsequently converted into the PMB protected derivative by reaction with *p*-methoxylbenzyl chloride in the presence of $KHCO_3$, to furnish **2.68** in 41% yield following column chromatography on silica. The

secondary alcohol **2.68** was then subjected to the conditions of the PCC oxidation, however the starting material proved to be unstable under the reaction conditions and neither starting material nor desired product **2.69** were recovered following filtration through silica.

It was subsequently elected not to continue further with the attempted synthesis of (2*S*)-2-fluorodehydroquinic acid **2.60** due to time constraints. The investigation of more appropriate protecting groups might be continued by others in the future. However, the (2*S*)-2-fluorodehydroquinate derivatives investigated thus far appear to be substantially less stable than the corresponding (2*R*)-2-fluorodehydroquinate derivatives and it may be that the desired product (2*S*)-2-fluorodehydroquinate **2.60** simply isn't stable enough for isolation and biological assay.

2.5.3 Assignment of the Configuration at C-2 of Fluorinated Dehydroquinate Derivatives by ^{1}H NMR

The relative configuration at C-2 of the α-fluoroketones **2.57**, **2.59** and **2.66** was determined by ^{1}H NMR. The absolute configurations of C-1, C-4 and C-5 are known (depicted in Figure 2.6 to Figure 2.8) and from this information the absolute configuration at C-2 can be inferred. The evidence of interactions of protons with the C-2 fluorine was considered, as well as the absence of interactions with the C-2 proton which was replaced by the fluorine. The specific details of the analysis of each spectrum, and comparisons to the spectra of each of the corresponding parent ketones **2.55**, **2.12** and **2.63** are discussed below.

2.5.3.1 Assignment of Configuration at C-2 for (2S)-2-Fluoroketone 2.57

The H-2eq proton of ketone **2.55** displays a long-range W-coupling of 2.5 Hz with H-6eq (Figure 2.6B). This interaction is also observed between H-6 and the remaining H-2 signal of the fluorinated analogue **2.57** (J = 1.5 Hz) suggesting that the remaining proton at C-2 retains its equatorial position in **2.57** (Figure 2.6A). The 1.2 Hz long-range coupling apparent between H-4 and H-2ax in the spectrum of ketone **2.55** is not observed in the H-4 signal of fluoroketone **2.57**, suggesting that there is no H-2ax proton present.

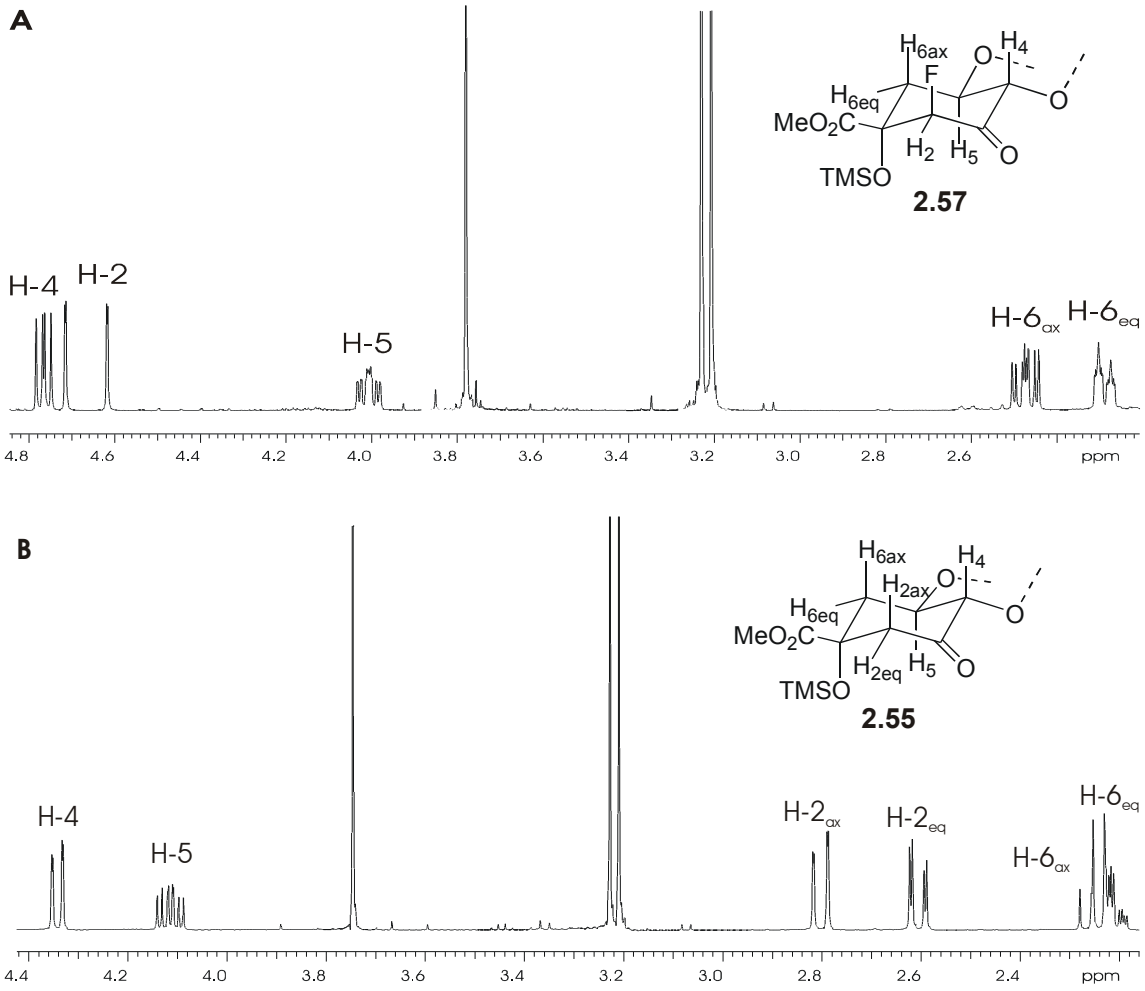

Figure 2.6 A. Partial ^{1}H NMR spectrum of **2.57**. B. Partial ^{1}H NMR spectrum of **2.55**.

The H-4 signal of **2.57** does display an additional 7.5 Hz coupling which is not observed in the corresponding resonance of the parent compound **2.55**, and is attributed to a long-range coupling to the C-2 fluorine atom. As H-4 is known to occupy an axial position, the occurrence of a long-range coupling to the fluorine atom suggests that the orientation of the fluorine is also axial. H-6ax also displays a coupling (4.7 Hz) which to the C-2 fluorine. Again, the long-range coupling to this axial proton suggests that the fluorine atom also occupies an axial position. However, H-6eq also displays a coupling to the fluorine atom, although it is weaker with a coupling constant of approximately 3 Hz. The ^{19}F NMR shows a multiplet, with a large geminal coupling to H-2 (48.9 Hz) and several other interactions with smaller coupling constants. However, the resolution is such that only the geminal coupling constant could be determined.

2.5.3.2 Assignment of Configuration at C-2 for (2R)-2-Fluoroketone 2.59

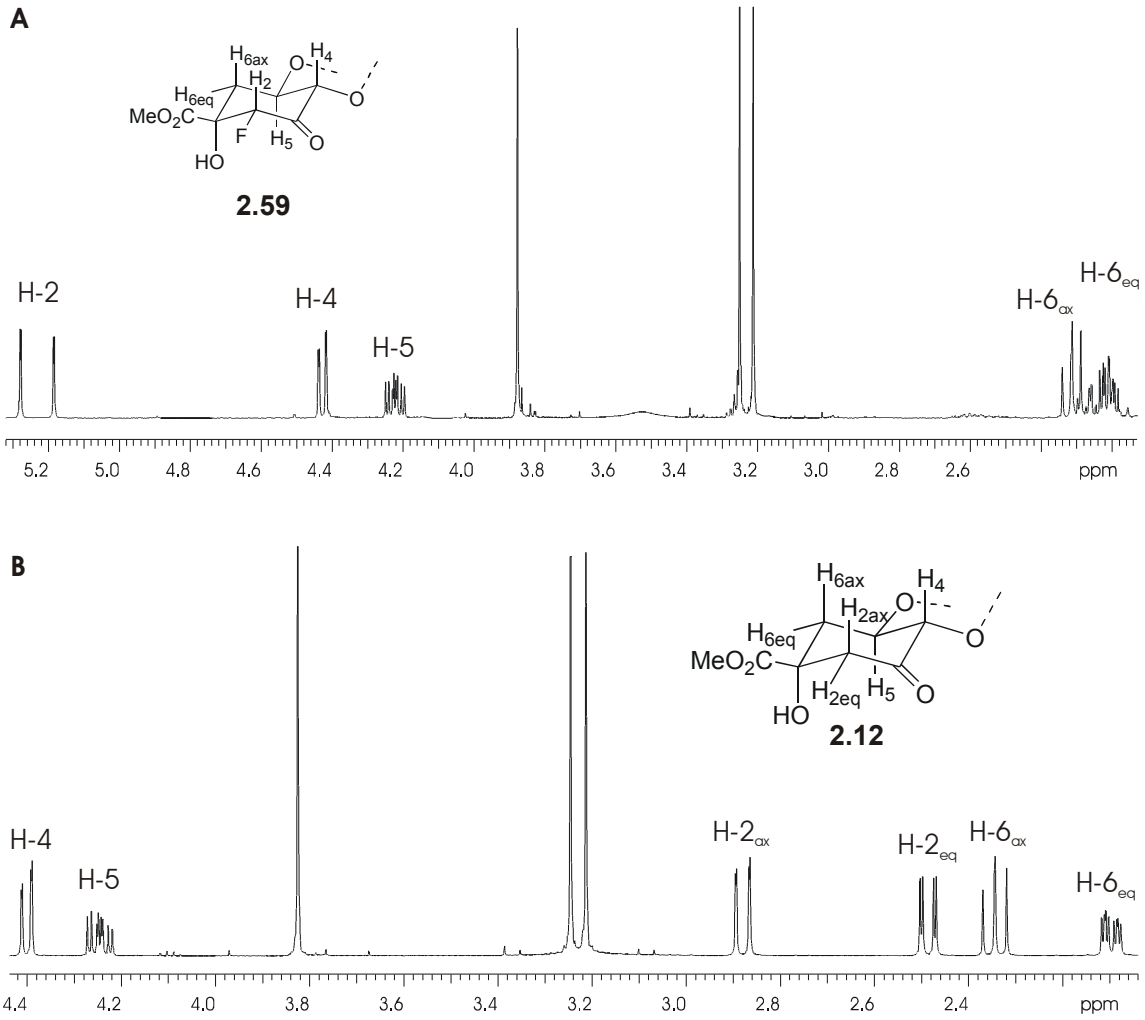

Figure 2.7 A. Partial ^{1}H NMR spectrum of **2.59**. B. Partial ^{1}H NMR spectrum of **2.12**.

The 1.5 Hz long-range di-axial coupling between H-4 and H-2ax, seen in the spectrum of **2.12** (Figure 2.7B), is also evident between H-4 and the remaining H-2 proton signal of **2.59** (Figure 2.7A), suggesting that the H-2 proton is axial in **2.59**. In contrast to the spectrum of **2.57** (Figure 2.6A), the H-4 signal of **2.59** (Figure 2.7A) does not display an additional di-axial coupling to the fluorine atom, but is identical to the H-4 signal of the parent ketone **2.12** (Figure 2.7B), suggesting that the fluorine does not occupy the axial position in **2.59**. The H-6eq resonance on the other hand, displays a 4.8 Hz coupling to the fluorine atom. This replaces the 2.9 Hz long-range W-coupling with H-2eq observed in the spectrum of **2.12**, indicating that the fluorine occupies the equatorial position in **2.59**. The equatorial fluorine of

ketone **2.48** (Scheme 2.9), whose configuration at C-2 was assigned in a similar manner, was also reported by Manthey *et al*. to be coupled to H-6eq, with J = 8 Hz.[3]

2.5.3.3 Assignment of Configuration at C-2 for (2S)-2-Fluoroketone 2.66

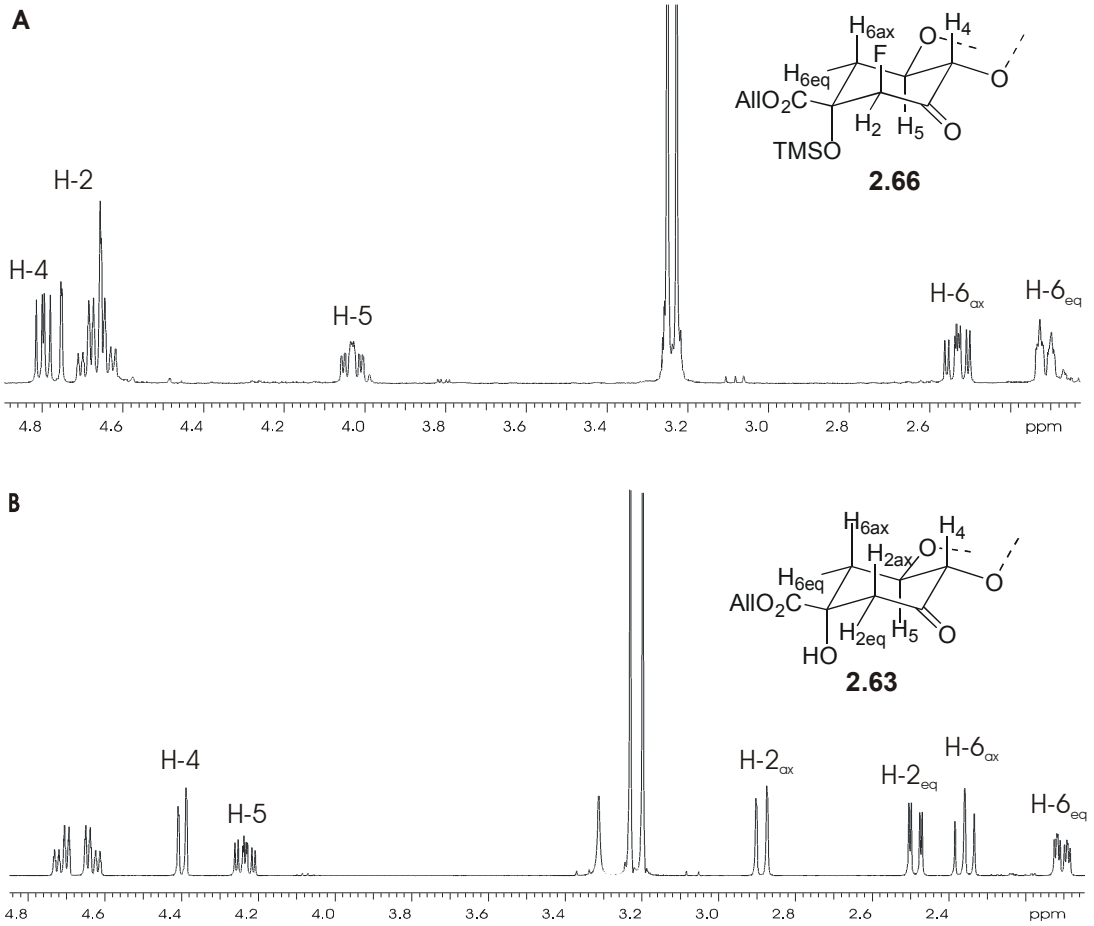

Figure 2.8 A. Partial ^{1}H NMR spectrum of **2.66**. B. Partial ^{1}H NMR spectrum of **2.63**.

The ^{1}H NMR spectrum of fluorinated allyl ester **2.66** (Figure 2.8A) is very similar to that of the methyl ester **2.57** (Figure 2.6A). The long-range W-coupling interaction between H-6eq and H-2eq, observed in the spectra of the parent ketone **2.63** (Figure 2.8B) and **2.57**, is also apparent for α-fluoroketone **2.66** (Figure 2.8A). However, the 1.1 Hz long-range coupling to H-2ax visible in the H-4 resonance of the parent ketone **2.63** is not evident in the corresponding resonance of fluoroketone **2.66**. The H-4 signal of **2.66** does, however, display a 7.4 Hz coupling to the fluorine atom. Like H-4, H-6ax also appears to be coupled (4.7 Hz)

to the C-2 fluorine. These factors indicate that, as in the case of fluoroketone **2.57**, the fluorine occupies the axial position in **2.66**.

2.6 SYNTHESIS OF AN EPOXIDE-BASED INHIBITOR

Proposed epoxide inhibitor **2.4** was thought to be a possible candidate for an inhibitor of both types I and II DHQase. The epoxide provides both an electronegative atom at C-3 for inhibition of type II DHQase, and a site for irreversible alkylation by the active site lysine of type I DHQases. The synthesis of **2.4** is described in Scheme 2.16 and Scheme 2.18.

Olefin **2.70** was prepared as an intermediate in the synthesis of both the desired epoxide **2.4** and allylic bromide **2.71**, a potentially useful intermediate in the synthesis of a range of C-2 – C-3 unsaturated analogues (Scheme 2.16). In order to avoid the harsh basic conditions required for carbonyl methylenation *via* the Wittig reaction, Takai's method was employed, as described by Frost for the methylenation of protected dehydroquinic acid **2.12**.[6,23] The C-1 tertiary hydroxyl was reacted with trimethylsilyl (TMS) chloride to give the TMS protected ketone **2.55** in 96% yield. This was then treated with diiodomethane, titanium (IV) chloride, and activated zinc to give protected olefin **2.70**. This reaction was found to be somewhat fickle. It did not go to completion unless the THF used as solvent was not only anhydrous, but oxygen free (judged by formation of a deep purple, rather than blue, complex with sodium/benzophenone).

The successful reaction also produced mixtures of the three products **2.70**, **2.72** and **2.73**. Typically the fully protected olefin **2.70** was obtained in 64% yield, along with the partially protected product **2.72** in 10% yield, following flash chromatography. On one occasion, the partially protected product **2.72** and the free triol **2.73** were obtained in 50% and 25% yields respectively, following column chromatography. This partial deprotection was most likely due to the acidic nature of the workup and seemed to be exacerbated by increasing the scale of the reaction, perhaps due to the greater amount of heat liberated when the zinc metal dissolved in the cold 1 N $HCl_{(aq)}$. Although this was carried out over an ice bath, the

precaution may not have been sufficient, or the reaction mixture may have been added too quickly.

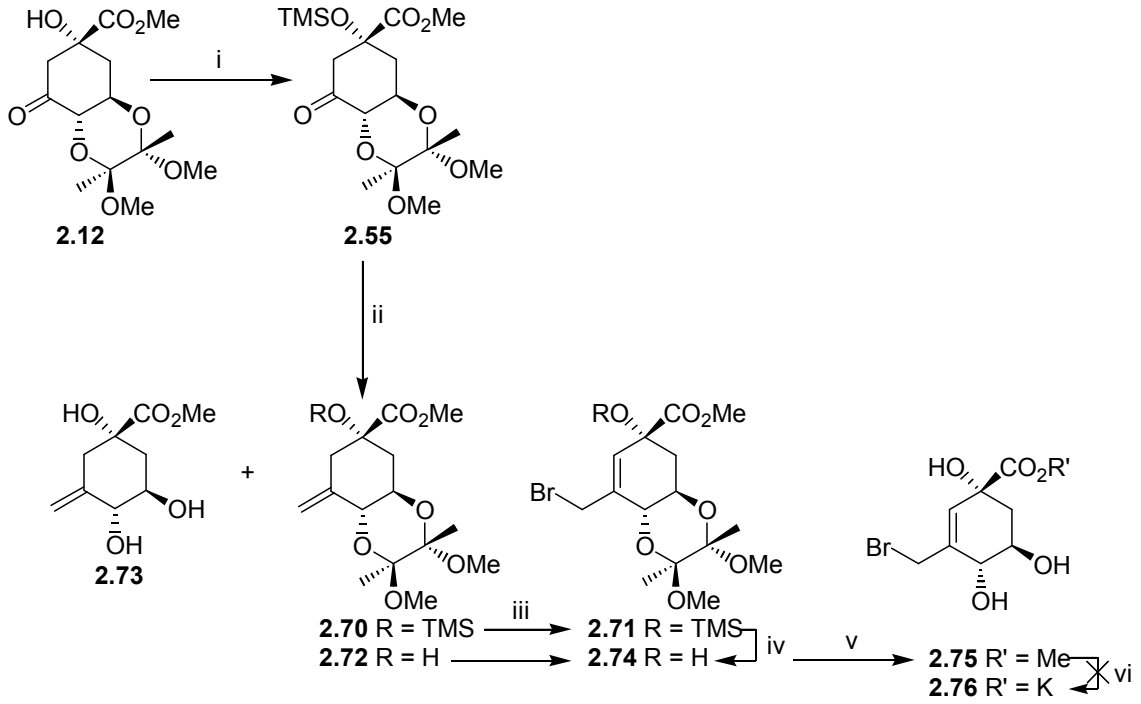

Scheme 2.16 Synthesis and derivatisation of olefin intermediates **2.70**-**2.72** and allylic bromide intermediates **2.73**-**2.75**. *Reagents and conditions:* i. TMSCl, HMDS, pyridine, rt (96%); ii. Zn, CH_2I_2, $TiCl_4$, THF, 0 ºC – rt (**2.70** 64%, **2.72** 50%, **2.73** 25%); iii. a) PhSeBr, Na_2CO_3, CH_2Cl_2, -78 ºC, b) *m*-CPBA, pyridine, CH_2Cl_2, -78 ºC – rt (**2.74** 42%); iv. SiO_2 (40%, 2 steps); v. 95% TFA, H_2O, 0 ºC (100%); vi. $KOH_{(aq)}$, 0 ºC.

The allylic bromide intermediate **2.71** was prepared from olefin **2.70** according to the method of Kolt[24] as employed by Frost.[6] The regiospecific anti- Markovnikov addition of phenylselenyl bromide to olefin **2.70** was carried out at -78 ºC for 23 h. The adduct thus obtained was converted into the allylic bromide **2.71** *in situ* by oxidative elimination with *m*-chloroperbenzoic acid (*m*-CPBA) in the presence of pyridine. Purification of the crude product by flash chromatography on silica resulted in the loss of the TMS group to give **2.74** in 40% yield. This reaction was also successfully carried out on the free alcohol **2.72** to yield the corresponding allylic bromide **2.74** in 42% yield following flash chromatography.

Time constraints meant that it was not practical to pursue the derivatisation of allylic bromide **2.74** in the preparation other C-2–C-3 unsaturated DHQ analogues. The deprotection of **2.74** was attempted however, as it was thought that the free allylic bromide **2.76** was worth

investigating. The similarity to anhydroquinic acid **1.37**, a potent inhibitor of type II DHQase from *S. coelicolor*, and the expected susceptibility of the allylic bromide to nucleophilic attack by the active site lysine of type I DHQase suggested that **2.75** could potentially be an inhibitor of both types of DHQase. Deprotection of **2.74** in 95% $TFA_{(aq)}$ furnished **2.75** quantitatively, however, this proved to be unstable under the conditions of the basic ester hydrolysis.

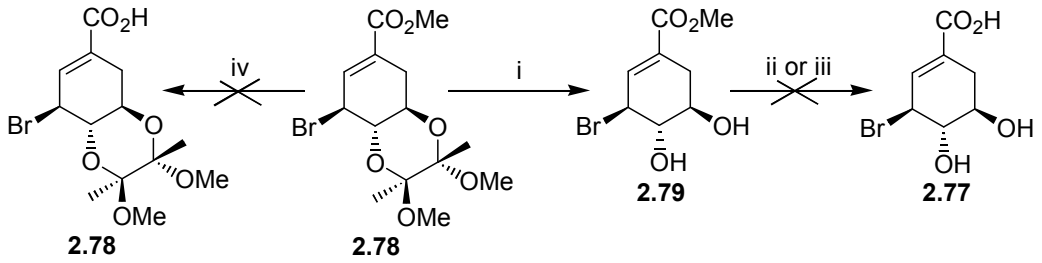

Scheme 2.17 Attempted deprotection of allylic bromide derivative **2.78**. *Reagents and conditions:* i. 95% $TFA_{(aq)}$, 0 ºC (91%); ii. $KOH_{(aq)}$, 0 ºC; iii. $HCl_{(aq)}$, reflux; iv. TMSCl, NaI, MeCN, reflux.

It was thought that **2.77** might also be susceptible to nucleophilic attack by type I DHQase. Deprotection of allylic bromide **2.78**[25] in 95% $TFA_{(aq)}$ was therefore carried out to furnish the free diol **2.79** in 91% yield following chromatography (Scheme 2.17). Like allylic bromide **2.75** however, **2.79** was unstable to basic hydrolysis. Acidic conditions and TMSCl/NaI were equally unsuccessful for **2.79** and **2.78** respectively. The investigation of deprotection conditions for allylic bromides **2.75** and **2.79** was not pursued.

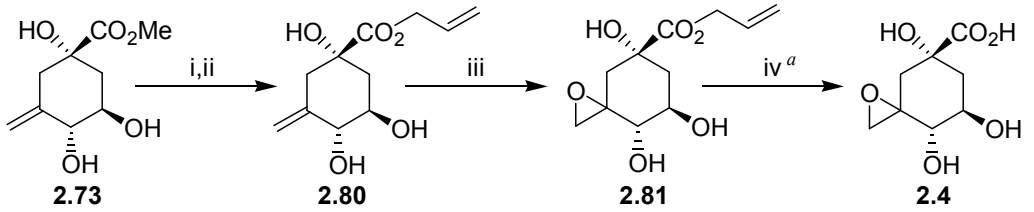

Scheme 2.18 Synthesis of epoxide inhibitor **2.4**. *Reagents and conditions:* i. a) KOH, H_2O, 0 ºC b) Amberlite IR-120(H); ii. AllBr, $KHCO_3$, DMF, rt (45% over 2 steps); iii. *m*-CPBA, CH_2Cl_2, rt (major isomer 60%, minor isomer 13%); iv. $Pd(0)(PPh_3)_4$, dimedone, THF, rt (72%).

[a] This reaction was carried out on the major isomer only.

The epoxide of proposed inhibitor **2.4** was expected to be unstable under the acidic and basic conditions of the usual diol and ester deprotection steps. The epoxide was therefore prepared

from the free triol **2.73**, and an allyl ester employed in preference to a methyl ester as the carboxy protecting group (Scheme 2.18).

The triol **2.73,** obtained as a side product in the methylenation step (Scheme 2.16), was converted to the allyl ester **2.80** in two steps (Scheme 2.18). The methyl ester was hydrolysed in aqueous KOH, followed by acidification over amberlite IR-120(H) ion exchange resin. The resulting acid was then reacted with allyl bromide in the presence of $KHCO_3$ to furnish the olefin allyl ester **2.80** in 45% yield following column chromatography. The olefin **2.80** was then reacted with just over one equivalent of *m*-CPBA to give the epoxide **2.81** as two isomers in a ratio of 1:4 as determined by ^{1}H NMR. Flash chromatography separated the major and minor isomers, giving 60% and 13% yields respectively. The yields were determined by ^{1}H NMR as both isomers contained some residual reagent (15% in the case of the minor isomer and 11% in the case of the major isomer). The major isomer was used in the subsequent step, and the impurity removed during the work-up. The carboxyl deprotection conditions developed for the deprotection of the DHQ allyl ester **2.64** (Scheme 2.13) were applied to the major isomer of **2.81** and the allyl ester removed by $Pd(0)(PPh_3)_4$ catalysed allyl transfer to dimedone to yield the free acid **2.4** in 72% yield.

2.7 CONCLUSION

A series of potential inhibitors with general structures **2.1**, **2.2** and **2.3** were prepared, where X is a hydrophilic functionality.

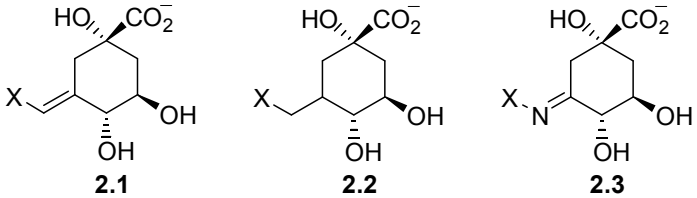

2.1 **2.2** **2.3**

Potential inhibitors of general structure **2.1** were prepared by Wittig reaction of the protected ketone **2.12** with the corresponding stabilised ylide. Single isomers, presumed to be the *E*-

isomers, were obtained in each case. The hydroxyl and carboxyl groups were then deprotected to give compounds **2.15** and **2.27**.

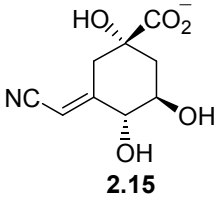

2.15

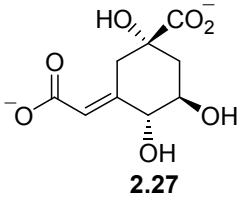

2.27

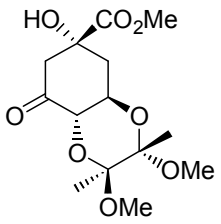

2.12

Compounds of general structure **2.2** were also prepared Wittig reaction of ketone **2.12**. This was followed by catalytic hydrogenation of the double bond to give mixtures of the 3*R*- and 3*S*- epimers. Separation of the products by chromatography, followed by deprotection gave potential inhibitors **2.16**, **2.17**, **2.18**, **2.28** and **2.29**.

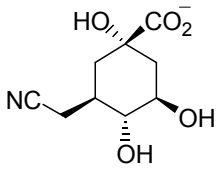

2.16

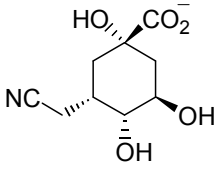

2.17

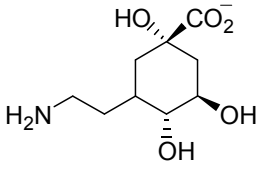

2.18

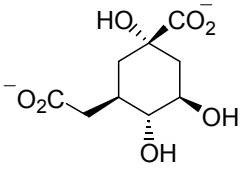

2.28

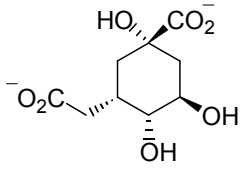

2.29

Compounds of general structure **2.3**, were prepared from ketone intermediate **2.13,** as the hydrazone functionality was unstable under the acidic conditions of the diol deprotection. Ketone **2.13** was reacted with the corresponding hydrazide to give mixtures of *E*- and *Z*-isomers, with the major isomer presumed to be *E*. Subsequent deprotection of the C-1 carboxyl gave potential inhibitors **2.38**, **2.42**, **2.44** and **2.46** as mixtures of isomers.

The epoxide-based derivative **2.4** was prepared by carbonyl methylenation of ketone **2.12,** and deprotection of the *trans*-diol. The methyl ester was then exchanged for an allyl ester as the carboxy protecting group. Epoxidation of the double bond, followed by palladium(0) catalysed allyl transfer gave potential inhibitor **2.4** as the free acid.

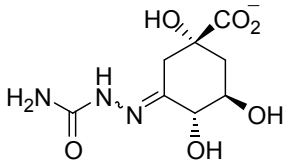
2.38

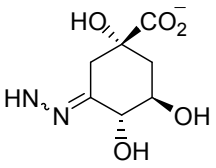
2.42

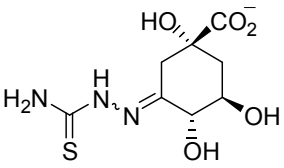
2.44

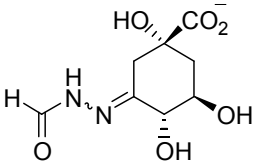
2.46

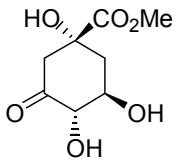
2.13

The synthesis of potential inhibitors **2.59**, **2.76** and **2.77** was investigated but was unsuccessful due to the instability of the compounds to the deprotection conditions. The possibility of employing alternative deprotection conditions and/or carboxy protecting groups warrants further investigation.

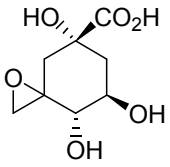
2.4

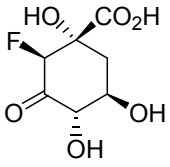
2.59

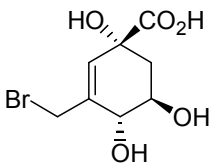
2.76

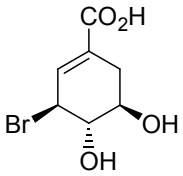
2.77

The potential inhibitors whose preparation is described in this chapter were tested for biological activity against type II DHQases from *M. tuberculosis* and *S. coelicolor* and in the case of epoxide **2.4**, against type I DHQase from *S. typhi*. The results of these studies are discussed in the following chapters.

2.8 REFERENCES FOR CHAPTER 2

(1) Frederickson, M.; Parker, E. J.; Hawkins, A. R.; Coggins, J. R.; Abell, C. *J. Org. Chem.* **1999**, *64*, 2612.

(2) Grewe, R.; Haendler, H. *Biochemical Preparations* **1966**, 21-26.

(3) Manthey, M. K.; Gonzales-Bello, C.; Abell, C. *J. Chem. Soc., Perkin Trans. 1* **1997**, 625.

(4) Montchamp, J.-L.; Tian, F.; Hart, M. E.; Frost, J. W. *J. Org. Chem.* **1996**, *61*, 3897.

(5) Tian, F.; Montchamp, J.-L.; Frost, J. W. *J. Org. Chem.* **1996**, *61*, 7373.

(6) Montchamp, J.-L.; Frost, J. W. *J. Am. Chem. Soc.* **1997**, *119*, 7645-7653.

(7) Armesto, N.; Ferrero, M.; Fernandez, S.; Gotor, V. *Tetrahedron Lett.* **2000**, *41*, 8759.

(8) Le Sann, C.; Abell, C.; Abell, A. D. *Synthetic Communications* **2003**, *33*, 527-533.

(9) Karplus, M. *J. Am. Chem. Soc.* **1963**, *85*, 2870-2871.

(10) This sample contains 8% 2.22. This spectrum was chosen for the purposes of this discussion as it is better resolved than that of pure 2.21.

(11) Roszak, A. W.; Frederickson, M.; Abell, C.; Coggins, J. R.; Lapthorn, A. J. In *RCSB Protein Databank* 2003.

(12) Le Sann, C.; Abell, C.; Abell, A. D. *J. Chem. Soc., Perkin Trans. 1* **2002**, 2065-2068.

(13) Frederickson, M.; Coggins, J. R.; Abell, C. *Chem. Commun.* **2002**, 1886-1887.

(14) Frederickson, M.; Roszak, A. W.; Coggins, J. R.; Lapthorn, A. J.; Abell, C. *Org. Biomol. Chem.* **2004**, *2*, 1592-1596.

(15) Parker, E. J.; Gonzales-Bello, C.; Coggins, J. R.; Abell, C. *Bioorganic and Medicinal Chemistry Letters* **2000**, *10*, 231.

(16) Duggan, P. J.; Parker, E. J.; Coggins, J. R.; Abell, C. *Bioorg. Med. Chem. Lett.* **1995**, *5*, 2347-2352.

(17) González-Bello, C.; Manthey, M. K.; Harris, J.; Hawkins, A. R.; Coggins, J. R.; Abell, C. *J. Org. Chem* **1998**, *63*, 1591-1597.

(18) González-Bello, C.; Harris, J. M.; Manthey, M. K.; Coggins, J. R.; Abell, C. *Bioorg. Med. Chem. Lett.* **2000**, *10*, 407.

(19) Kunz, H.; Waldmann, H. *Angew. Chem. Int. Ed. Engl.* **1984**, *23*, 71-72.

(20) Guibé, F. *Tetrahedron* **1998**, *54*, 2967-3042.

(21) Le Sann, C.; Abell, A. D. *Aust. J. Chem.* **2004**, *57*, 355-358.

(22) Kunz, H.; Unverzagt, C. *Angew. Chem. Int. Ed. Engl.* **1984**, *23*, 436-437.

(23) Hibino, J.-i.; Okazoe, T.; Takai, K.; Nozaki, H. *Tetrahedron Lett.* **1985**, *26*, 5579-5580.

(24) Ho, P.-K.; Kolt, R. J. *Can. J. Chem.* **1982**, *60*, 663-666.

(25) Compound 2.78 was prepared by R. Payne

3 Biological Studies: Spectrophotometric Assay

3.1 INTRODUCTION

3.1.1 Steady-State Enzyme Kinetics

A simple mechanism for the enzymatic conversion of substrate to product is depicted in Scheme 3.1, where S is the substrate, E the enzyme, ES the enzyme-substrate complex and P the enzymatic product. The rate constants for the binding and dissociation of the substrate from the enzyme are represented by k_1 and k_{-1} respectively, while k_2 represents the rate constant for the conversion of the ES complex to product.

$$E + S \underset{k_{-1}}{\overset{k_1}{\rightleftharpoons}} ES \xrightarrow{k_2} E + P$$

Scheme 3.1 Generalised mechanism for an enzymatic reaction.

The steady-state approach to enzyme kinetics relies on the assumption that the concentration of the ES complex remains constant within a finite period and thus the rate of the enzymatic reaction ($d[P]/dt = k_2[ES]$) also remains constant (i.e. the reaction progress curve remains linear within a defined period of time). It is also assumed that the product formation step is irreversible, or that the concentration of product is sufficiently small that the contribution of the competing back-reaction is negligible. These assumptions are valid during the initial stage of the reaction.

$$v = \frac{V_{max}[S]}{K_M + [S]} \qquad (3.1)$$

From these assumptions is derived the fundamental equation of enzyme kinetics: the Michaelis-Menten equation (Equation 3.1).[1-4] In the equation as written, v is the initial rate of reaction, V_{max} is the limiting rate, and K_M is the Michealis constant. For the simplified mechanism depicted in Scheme 3.1 K_M is defined as $(k_{-1} + k_2)/k_1$ and V_{max} as $k_2[E]_t$ (where $[E]_t$ is the total enzyme concentration). However, the equation is also applicable to more general circumstances than Scheme 3.1 in which V_{max} is defined as $k_{cat}[E]_t$ where k_{cat} is the rate constant for the conversion of the enzyme-substrate complex ES to product and does not necessarily represent a single step. In the general case, K_M is not necessarily equal to $(k_{-1} + k_2)k_1$. It can be shown that K_M is equal to the substrate concentration at which the rate is half the limiting rate V_{max}, and this is taken as a working definition of K_M.[1] The curve defined by the Michaelis-Menten equation is depicted in Figure 3.1.

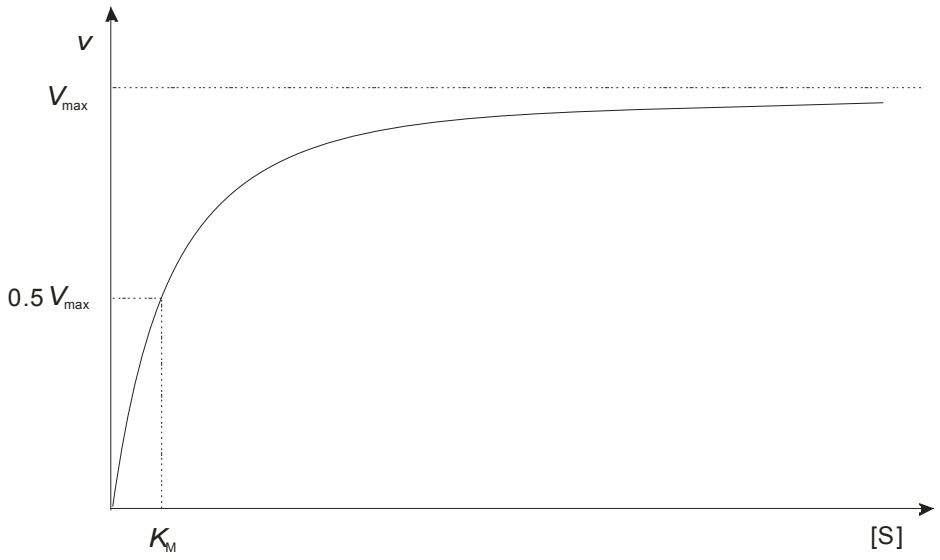

Figure 3.1 Generalised Michaelis–Menten curve.

3.1.2 Competitive Reversible Inhibition

Competitive inhibition occurs when an inhibitor competes with the substrate for binding at the active site of the enzyme. The inhibitor cannot be converted to product and thus remains bound in the active site, preventing the binding and catalysis of substrate by the enzyme. A mechanism for competitive inhibition (specific inhibition) may be represented in general terms by Scheme 3.2, where I is the competitive inhibitor and EI the enzyme-inhibitor

complex. In the case of reversible competitive inhibition, the inhibitor binds reversibly and equilibrium is established, as indicated in Scheme 3.2.

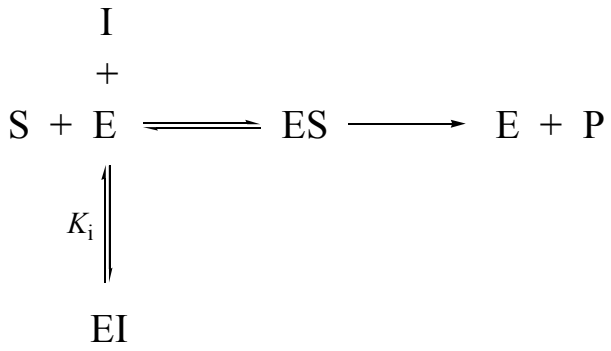

Scheme 3.2 Generalised mechanism for competitive reversible inhibition.

The equilibrium constant for dissociation of the enzyme-inhibitor complex is known as the inhibition constant, K_i. However, irreversible competitive inhibition can also occur, in which the inhibitor becomes covalently attached to the enzyme active site. The effect of competitive inhibition on the rate of product formation v, is defined by equation 3.2. This equation is of the same form as the Michaelis-Menten equation and can be written as shown in equation 3.3.[1]

$$v = \frac{V_{max}[S]}{K_M(1 + [I]/K_i) + [S]} \qquad (3.2)$$

$$v = \frac{V^{app}[S]}{K_M^{app} + [S]} \qquad (3.3)$$

The inhibition constant K_i is a convenient means of quantifying inhibitor potency. The smaller K_i, the more potent the inhibitor and the more strongly it is bound by the enzyme. K_i can be determined experimentally by Dixon plot.[1,2] The inverse rate ($1/v$) is plotted against inhibitor concentration for a series of substrate concentrations. From equation 3.2 it can be shown that the intersection of the different series occurs at the point ($-K_i$, $1/V_{max}$) (Figure 3.2).[1]

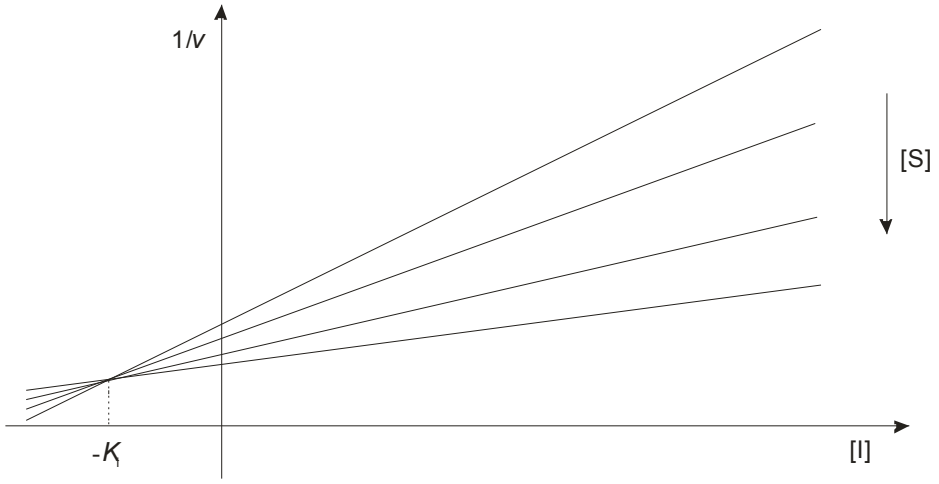

Figure 3.2 Generalised Dixon plot.

3.2 GENERAL METHOD

In order to determine inhibition constants (K_i) for the potential inhibitors **2.4**, **2.15**-**2.18**, **2.27**-**2.29**, **2.38**, **2.42**, **2.44** and **2.46**, whose synthesis was discussed in the previous chapter, a means of monitoring the progress of the DHQase catalysed conversion of dehydroquinate (DHQ) **1.4** to dehydroshikimate (DHS) **1.5** (Scheme 3.3) was required. The method of choice was UV/visible spectroscopy as the enone-carboxylate chromophore of the enzymatic product DHS **1.5** gives rise to a strong absorbance at 234 nm. The initial rate of the enzymatic reaction can be determined by monitoring the increase in absorbance at 234 nm due to the formation of DHS **1.5** for the initial stage of the reaction, during which the reaction progress curve is approximately linear. A straight line is fitted to the absorbance vs. time data and the slope of the line, dA/dt is determined. From this the initial rate of product formation d[DHS]/dt is calculated using Beer's Law (Eq. 3.4), where A is the measured absorbance, ε is the molar absorptivity in $Lmol^{-1}cm^{-1}$ of DHS, c is the concentration of DHS in $molL^{-1}$ and l is the path length in cm.

$$A = \varepsilon c l \qquad (3.4)$$

Initial rate data is obtained for a series of samples, consisting of 3 or 4 substrate concentrations and 4-8 inhibitor concentrations. A Dixon plot is prepared by plotting the inverse of a series of initial rates, determined as described above, against the corresponding inhibitor concentrations. A straight line is fitted to the $1/v$ vs. [I] data for each substrate concentration to give a Dixon plot as illustrated in Figure 3.2. The inhibition constant K_i is determined from the intersection point.

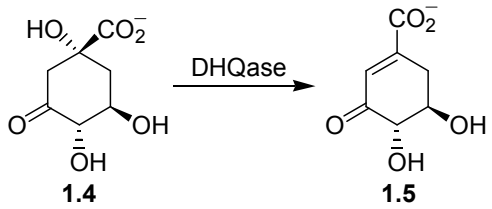

1.4 **1.5**

Scheme 3.3 Enzymatic conversion of DHQ **1.4** to DHS **1.5**.

3.3 ENZYMATIC STUDIES ON *S. COELICOLOR* TYPE II DHQASE

3.3.1 Michaelis-Menten Curve

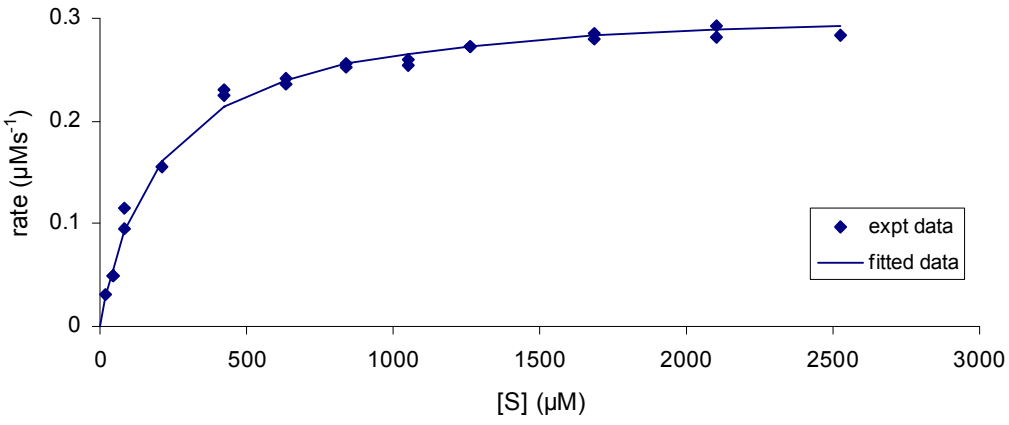

Figure 3.3 Michaelis-Menten curve for *S. coelicolor* DHQase at 25ºC and pH 7.

Kinetic parameters for the *S. coelicolor* DHQase catalysed conversion of DHQ **1.4** to DHS **1.5** at an enzyme concentration of 25.5 $ngmL^{-1}$ at 25ºC and pH 7 were determined by obtaining initial rate data for a series of substrate concentrations. Non-linear least squares fitting of the data to the Michaelis-Menten equation (Equation 3.1) gave the curve shown in Figure 3.3. A Michaelis constant K_M of 200 ± 20 μM and a limiting rate V_{max} of 0.32 μMs^{-1} were obtained. This value of K_M is slightly lower than the value of 250 μM reported by Abell *et al*. for the same conditions.[5]

3.3.2 Assay Results for *S. coelicolor* DHQase

Preliminary investigations with potential inhibitors **2.15**-**2.17**, **2.38** and **2.44** at low inhibitor concentrations ([I] < 100 μM) yielded no useful result. The range of data on which the extrapolation was based was insufficient, and when the linear substrate series were extrapolated, the error introduced was too great for the series to intersect at a common point. This suggested that the inhibitors were likely to have a K_i well in excess of 100 μM, and that substantially higher inhibitor concentrations would be required for the assay.

The oxime inhibitor **1.36**, upon which the design of the new potential inhibitors was based, was known to be less active against *S. coelicolor* DHQase than *M. tuberculosis* DHQase by more than one order of magnitude. If the new inhibitors were expected to exhibit activity on the order of that of oxime **1.36**, inhibitor concentrations in excess of 500 μM would be required for the assay, in order to obtain sufficient data for the extrapolation back to $-K_i$.

The assay against *S. coelicolor* DHQase was initially attempted at higher inhibitor concentrations with the new inhibitors **2.15** and **2.44**. However, the absorbance at 234 nm due to the inhibitors was extremely high at the concentrations employed and caused too much interference to obtain meaningful rate data. Acquisition of UV/vis spectra for the inhibitors revealed that all of the sp^2 hybridised inhibitors **2.15**, **2.27**, **2.38**, **2.42**, **2.44** and **2.46** absorbed at 234 nm. Inhibitors with sp^3 character at C-3 (**2.16**-**2.18**, **2.28** and **2.29**) did not absorb at 234 nm.

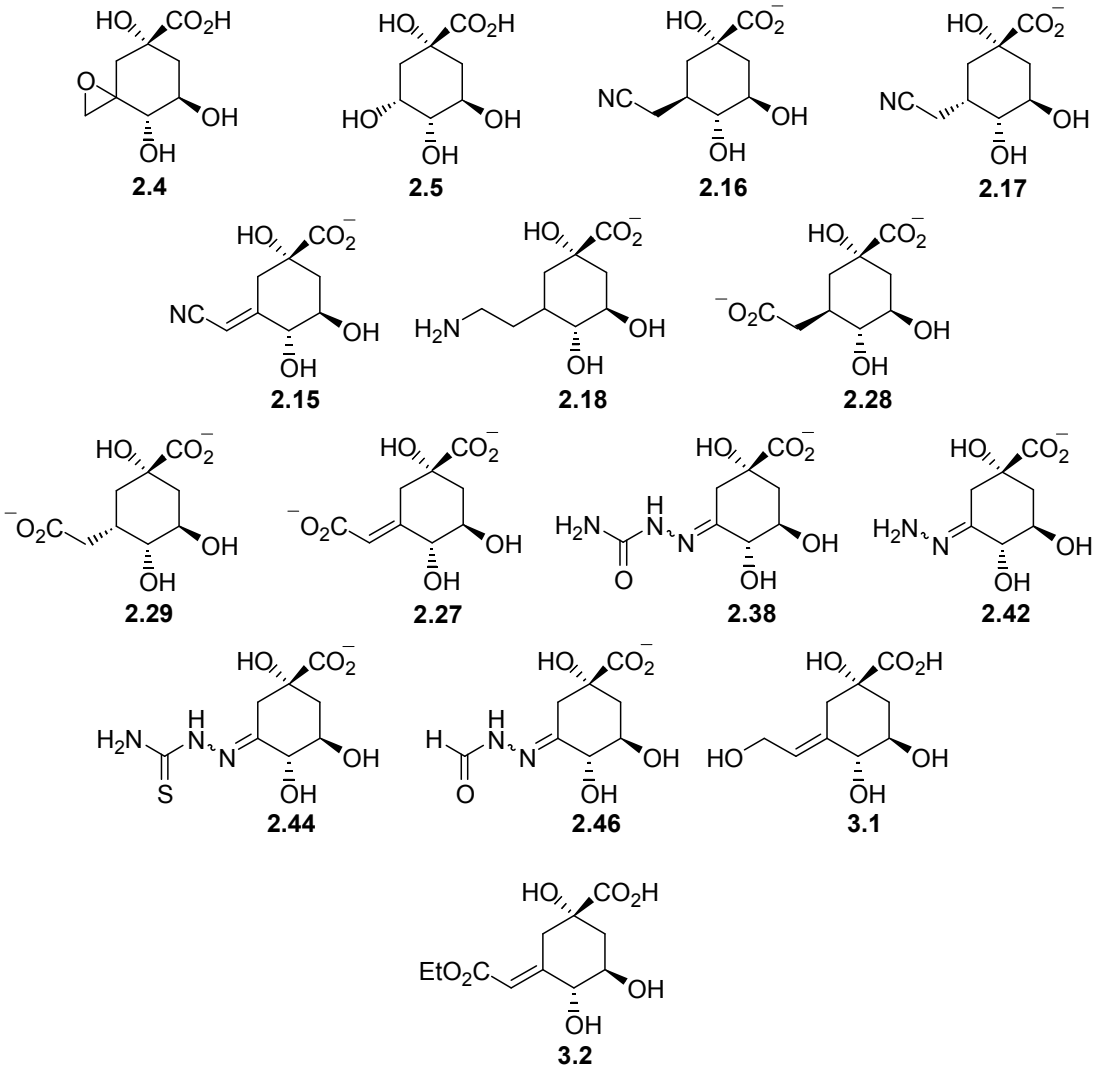

It was apparent that the strongly absorbing inhibitors could not be assayed against *S. coelicolor* DHQase by this method. By analogy with oxime **1.36**, it was anticipated that the new potential inhibitors would be substantially more active against *M. tuberculosis* DHQase than *S. coelicolor* DHQase. Future assays with *M. tuberculosis* DHQase could therefore be expected to require lower inhibitor concentrations than was the case for *S. coelicolor* DHQase, and so could be conducted by this method.

Known oxime inhibitor **1.36**, which absorbed only weakly at 234 nm, was assayed against *S. coelicolor* DHQase in order to test the method. A Dixon plot was prepared and a K_i of 530 ± 80 μM determined (Figure 3.4). This was in agreement with the result of 500 ± 200 μM reported by Abell and coworkers for this inhibitor with *S. coelicolor* DHQase.[6]

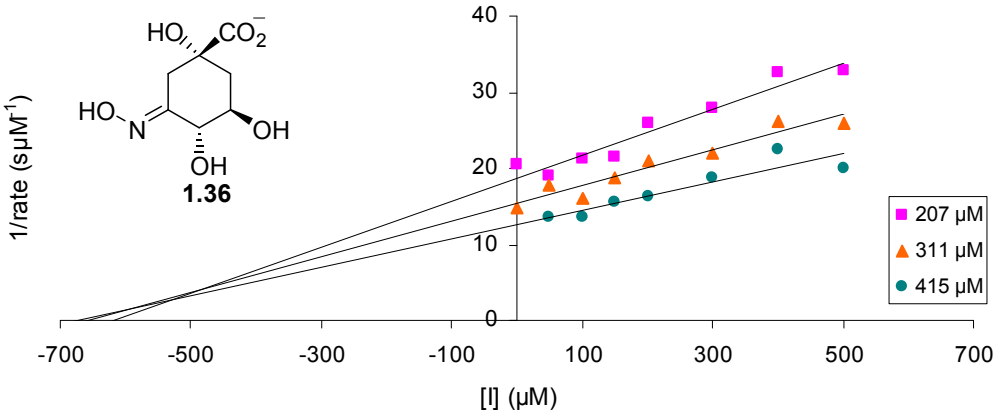

Figure 3.4 Dixon plot for known inhibitor oxime **1.36** against *S. coelicolor* DHQase.

Saturated inhibitors **2.16-2.18**, **2.28** and **2.29**, which did not absorb at 234 nm, were assayed against *S. coelicolor* DHQase. Inhibitor **2.17** was assayed against *S. coelicolor* DHQase in the form of a 2:1 mixture with the C-3 epimer **2.16**. It was thought that the commercially available quinic acid **2.5** might inhibit DHQase and so it was also assayed against *S. coelicolor* DHQase. Absorbance vs. time data obtained at 234 nm was analysed as described previously to obtain Dixon plots for each of the inhibitors (Figure 3.5 to Figure 3.10). The inhibition constants thus obtained are reported in Table 3.1.

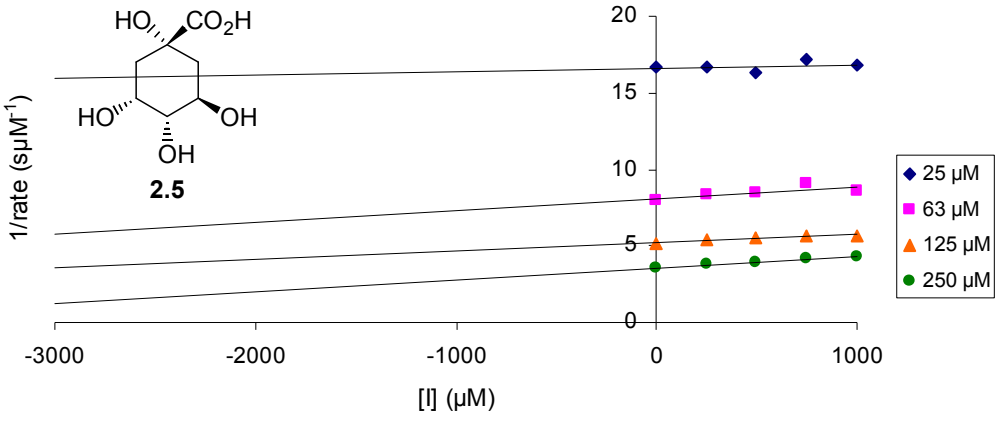

Figure 3.5 Dixon plot for Quinic acid **2.5** against *S. coelicolor* DHQase.

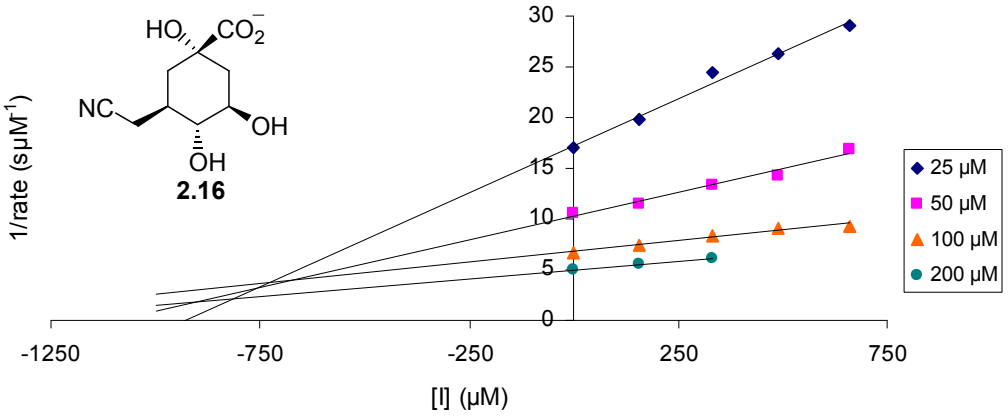

Figure 3.6 Dixon plot for inhibitor **2.16** against *S. coelicolor* DHQase.

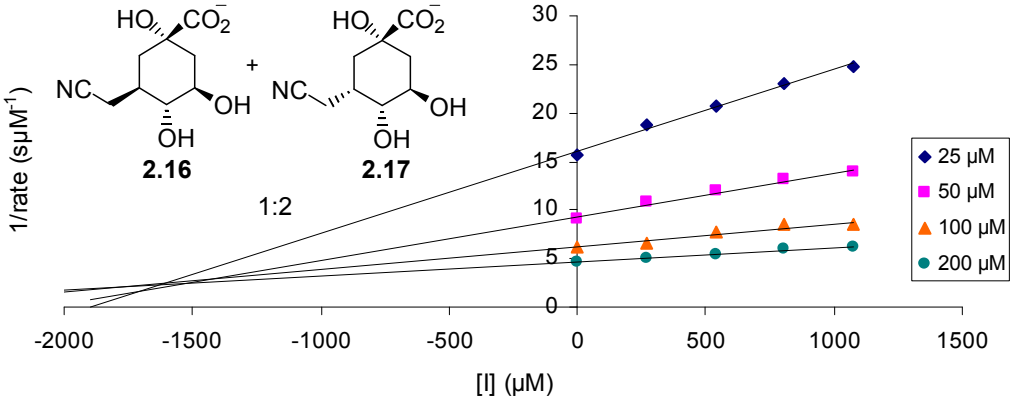

Figure 3.7 Dixon plot for a 1:2 mixture of diastereomers **2.16** and **2.17** against *S. coelicolor* DHQase with the x-axis showing the combined concentration of both diastereomers.

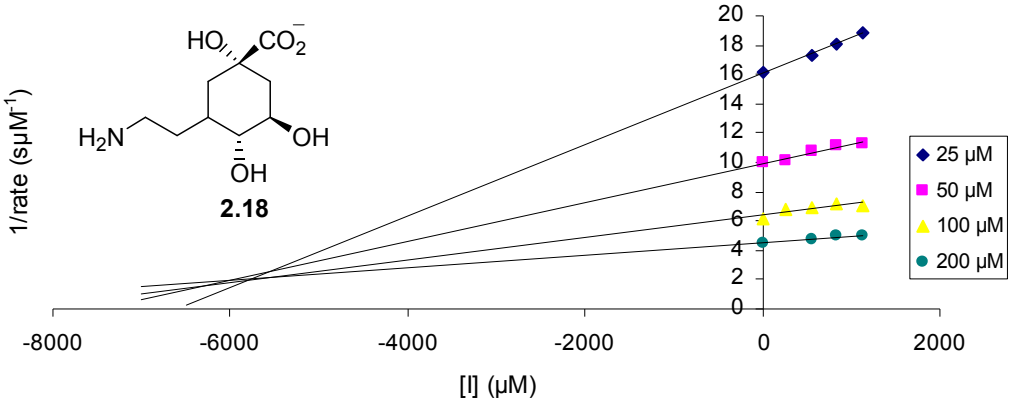

Figure 3.8 Dixon plot for inhibitor **2.18** against *S. coelicolor* DHQase.

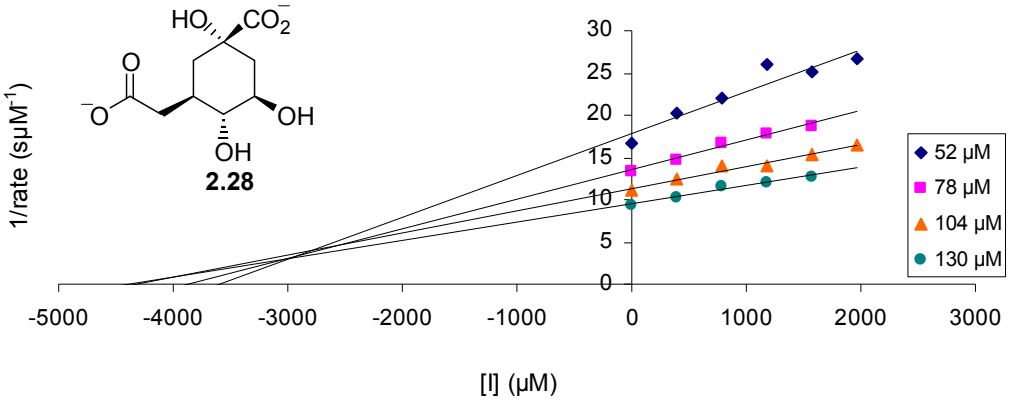

Figure 3.9 Dixon plot for inhibitor **2.28** against *S. coelicolor* DHQase.

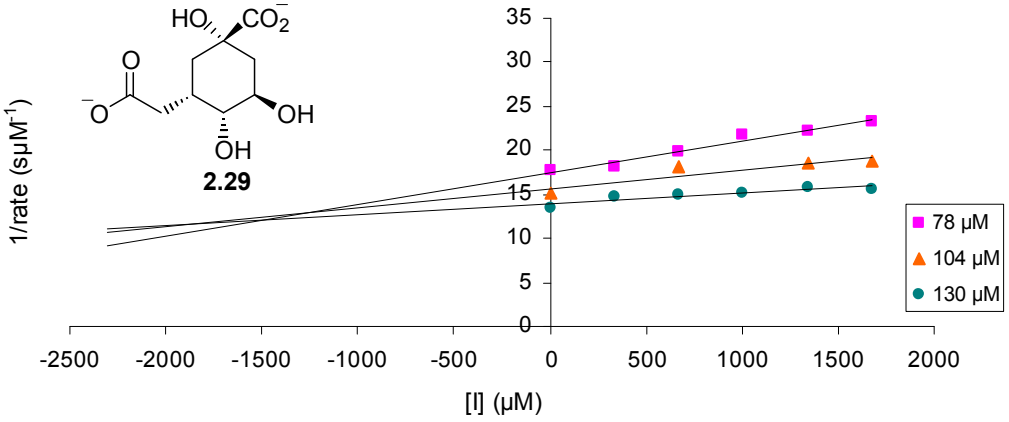

Figure 3.10 Dixon plot for inhibitor **2.29** against *S. coelicolor* DHQase.

Table 3.1 Inhibition constants (K_i) for inhibitors **2.16-2.18**, **2.28** and **2.29** against *S. coelicolor* DHQase.

Inhibitor	**K_i (μM)** *S. coelicolor* DHQase
K_M	200 ± 20
2.16	800 ± 100
2.17[a]	1600 ± 200
2.18	6000 ± 500
2.28	3000 ± 1000
2.29	1500 ± 500

[a] K_i for a 2:1 mixture of **2.17** and **2.16**.

3.3.3 Discussion of *S. coelicolor* DHQase Assay Results

The inhibition constants obtained from the assays of inhibitors **2.16**-**2.18**, **2.28** and **2.29** against *S. coelicolor* DHQase are shown in Table 3.1. The inhibition constants reported for some known inhibitors are given in Table 3.2.

Table 3.2 Inhibition constants for reported inhibitors of *S. coelicolor* DHQase.

Inhibitor	K_i **(μM)** *S. coelicolor* DHQase
1.36[a]	500 ± 200
1.37[a]	30 ± 10
1.38[a]	2500 ± 500
1.39[a]	600 ± 200
1.43[b]	420 ± 50
1.44[b]	>20000
1.45[b]	180 ± 20
1.46[b]	3000 ± 500
1.47[b]	1200 ± 450
1.48[b]	530 ± 50
1.49[b]	>20000
1.50[b]	3500 ± 400
1.53[c]	33 ± 5.4
1.54[c]	84 ± 13
1.55[c]	220 ± 50

[a] Ref. 6. [b] Ref. 5. [c] Ref. 8.

Inhibitor **2.17** was assayed against *S. coelicolor* as a 2:1 mixture of **2.17** and **2.16**. The K_i was determined by plotting the inverse rate against the total combined concentration of the two isomers (Figure 3.7). This method of determining K_i gives an averaged approximation of the activity of the mixture. It is clear that **2.17** is a substantially less potent inhibitor of *S. coelicolor* DHQase than its C-3 epimer **2.16**, as the activity of the 2:1 mixture of **2.17** and **2.16**, with a K_i of 1600 ± 200 μM is a factor of 2 less potent than **2.16** alone, which has a K_i of 800 ± 100 μM. Amine **2.18**, whose absolute configuration at C-3 is not known, but is suspected to be the same as that of **2.17** (i.e. with the C-3 substituent in the axial position), was substantially less active than the nitriles **2.16** and **2.17**, with an inhibition constant of 6000 ± 500 μM. The fact that **2.16**, for which the C-3 side-chain is equatorial, is more active than **2.17** (and **2.18**), for which the side chain is axial, suggests that the equatorial

configuration is preferred by the enzyme. This is consistent with results reported by Abell *et al*. for epimeric inhibitors **1.47** (K_i = 1200 ± 450) and **1.49** (K_i > 20000) and **1.48** (K_i = 530 ± 50) and **1.50** (K_i = 3500 ± 400).[5]

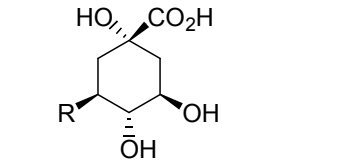

1.47 R = $OCH_2CH{=}CH_2$
1.48 R = $OCH_2CH(OH)CH_2OH$

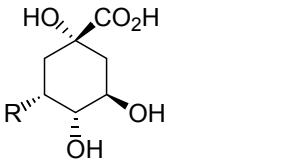

1.49 R = $OCH_2CH{=}CH_2$
1.50 R = $OCH_2CH(OH)CH_2OH$

In the case of carboxylate inhibitors **2.28** and **2.29** however, the enzyme appeared to show a preference for the axial side-chain. Inhibitor **2.29**, for which the C-3 substituent is in the axial position, has a K_i of 1500 ± 500. This is twice as potent as its C-3 epimer **2.28**, which has a K_i of 3000 ± 1000. This is inconclusive however, as the inhibition constants could be said to be in agreement within the stated errors.

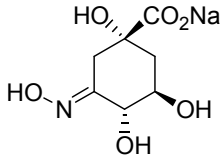

1.36

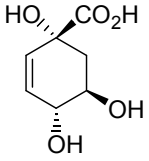

1.37

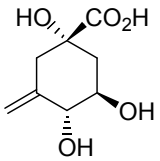

1.38

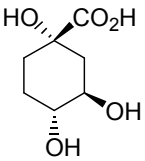

1.39

All of the new inhibitors assayed thus far against *S. coelicolor* DHQase are less potent than the known inhibitors **1.36** (K_i = 500 ± 200) and **1.37** (K_i = 30 ± 10).[6] The inhibition constant for nitrile **2.16** however, is close to that of **1.36** and the values could be said to be in agreement within the stated errors. A comparison of the inhibition constants of known inhibitors **1.36** and **1.38** (K_i = 2500 ± 500) indicates that exchanging the oxime for carbon at the 3-position leads to a loss of potency against *S. coelicolor* DHQase. As such it is perhaps not so surprising that these new inhibitors, all of which have carbon at C-3, were in general less potent than **1.36**.

With the exception of **2.18** and **2.28,** the new inhibitors were more potent than *exo*-methylene **1.38**. This suggests that extending the C-3 side-chain could be a favourable modification, possibly enabling the inhibitor to occupy additional binding sites such as the glycerol binding pocket reported by Abell *et al*.[7] However, when compared to the new inhibitors, the complete

lack of a C-3 side-chain seems to be preferred, as shown by the lower K_i of the unsubstituted analogue **1.39** (K_i of 600 ± 200). A number of *S. coelicolor* DHQase inhibitors **1.43**-**1.46** have been reported by Abell *et al*. which bear a side-chain at C-3. In some cases the carbon chain was found to increase the potency relative to the unsubstituted analogue **1.39** and in some cases to decrease the potency, depending on the specific nature of the side-chain. The lack of potency of the new inhibitors described in this thesis relative to the unsubstituted analogue **1.39** suggests that these particular side chains do not form favourable interactions with the active site.

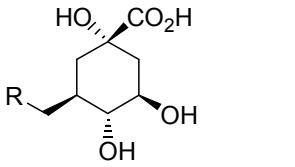

1.43 R = $CH{=}CH_2$
1.44 R = $CH(OH)CH_3$
1.45 R = CH_2CH_2OH
1.46 R = $CH(OH)CH_2OH$

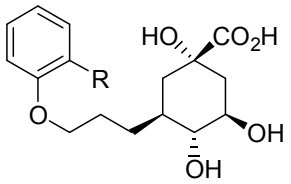

1.53 R = H
1.54 R = NO_2
1.55 R = CO_2H

Compounds **1.43** (K_i = 420 ± 50) and **1.45** (K_i = 180 ± 20) were reported by Abell *et al*. to be more potent than the corresponding unsubstituted derivative **1.39**.[5] Compounds **1.44** (K_i > 20000) and **1.46** (K_i = 3000 ± 500) which have a secondary hydroxyl group on the side-chain, two carbons removed from the six-membered ring, are substantially less potent than their corresponding non-hydroxylated equivalents **1.43** (K_i = 420 ± 50) and **1.45** (180 ± 120). They are also less potent than the unsubstituted analogue **1.39**. The side-chain carboxylate oxygen atoms of the inhibitors **2.28** and **2.29** are in a corresponding position to the secondary hydroxyl groups of **1.44** and **1.46.** The carboxylate inhibitor **2.28** (K_i = 3000 ± 1000), in which the C-3 side-chain is in the equatorial position (as in **1.43**-**1.46**) shows a substantial loss of potency relative to the corresponding nitrile analogue **2.16** (K_i = 800 ± 100). This is consistent with the lack of potency of **1.44** and **1.46** relative to **1.43** and **1.45** respectively and suggests that having an oxygen containing group at this particular position on the equatorial side chain may result in an unfavourable interaction with the enzyme active site. The inhibitors **2.17** and **2.29**, in which the C-3 side-chain is in the axial position, have very similar activities, suggesting that there is no additional unfavourable interaction of the carboxyl group when the side chain has this orientation. An unfavourable interaction of the carboxylate of the equatorial side-chain might account for the apparent preference of *S. coelicolor* DHQase

for the carboxylate inhibitor **2.29**, bearing the axial side-chain, over **2.28**, in contrast to the preference for the equatorial side-chain observed for nitrile inhibitors **2.26** and **2.17** and reported inhibitors **1.47**-**1.50**.[5] A similar trend was observed by Abell *et al*. in the substitution of the phenyl ring of inhibitors **1.53**-**1.55** in which increasing hydrophilicity of the *ortho*-substituent was found to decrease the strength of binding to *S. coelicolor* DHQase.[8]

Although quinic acid **2.5** was seen to inhibit *S. coelicolor* DHQase (as shown by the increase in inverse rate with inhibitor concentration in Figure 3.5), the data series were more or less parallel i.e. the inhibition appeared to be independent of substrate concentration. This suggests that the inhibition is not of a competitive nature.

3.4 Enzymatic Studies on *M. tuberculosis* Type II DHQase

Oxime inhibitor **1.36** has been shown to be more potent against type II DHQase from *M. tuberculosis* than that from *S. coelicolor* by a factor of 25.[6] The design of the putative inhibitors prepared in this work was based on the hypothesis that inhibitors with hydrophilic groups at C-3 would mimic the structure and activity of oxime **1.36**. It was perhaps unsurprising therefore, that the new inhibitors showed relatively poor activity against type II DHQase from *S. coelicolor*. It was anticipated however, by analogy with oxime **1.36**, that the same inhibitors would demonstrate significantly increased potency against type II DHQase from *M. tuberculosis*, relative to the *S. coelicolor* enzyme. More potent inhibitors would require lower inhibitor concentrations in the spectrophotometric assay, as the data would not need to be extrapolated back so far to reach $-K_i$. All of the putative inhibitors whose preparation was described in Chapter 2, as well as compounds **3.1** and **3.2** (prepared by K. Smith)[9] where thus assayed against type II DHQase from *M. tuberculosis*. In the cases where the inhibitors absorbed at 234 nm, the maximum inhibitor concentration that could be used was limited by the absorbance due to the inhibitor.

3.4.1 Michaelis-Menten Curve

Rate vs. substrate concentration data was obtained for *M. tuberculosis* DHQase at an enzyme concentration of 0.5 μgmL^{-1} at 25ºC and pH 7 and the Michaelis-Menten curve plotted (Figure 3.11). Non-linear least squares fitting of the data to equation 3.1 gave a Michaelis constant K_M of 15 ± 1 μM and a limiting rate V_{max} of 0.028 ± 0.002 μMs^{-1}. This value of K_M is slightly higher, though very close to the value of 13 μM reported by Abell *et al*. for the same conditions.[10]

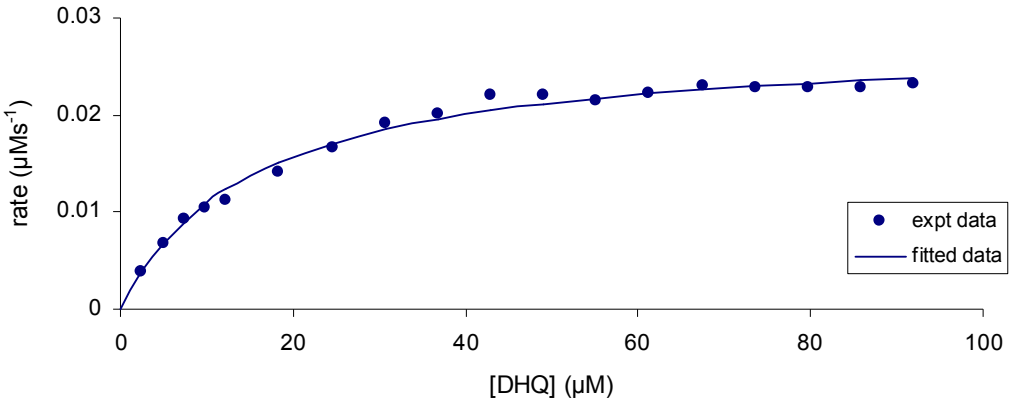

Figure 3.11 Michaelis-Menten curve for *M. tuberculosis* DHQase.

3.4.2 Assay Results for *M. tuberculosis* DHQase

3.4.2.1 Inhibitors with C Attached at C-3

Inhibitors **2.4**, **2.15**, **2.16**, **2.17**, **2.18**, **2.27**, **2.28**, **2.29**, **3.1** and **3.2** were assayed against type II DHQase from *M. tuberculosis* by the method described in Section 3.2. The Dixon plots are shown in Figure 3.12 to Figure 3.21 and the K_i values thus obtained are listed in Table 3.3.

In order to conserve the sample of epoxide inhibitor **2.4** for further experiments, only the minimum data required to estimate a value of K_i was obtained. Thus the accuracy of the K_i value obtained was not verified by multiple data sets and so is only an approximate value.

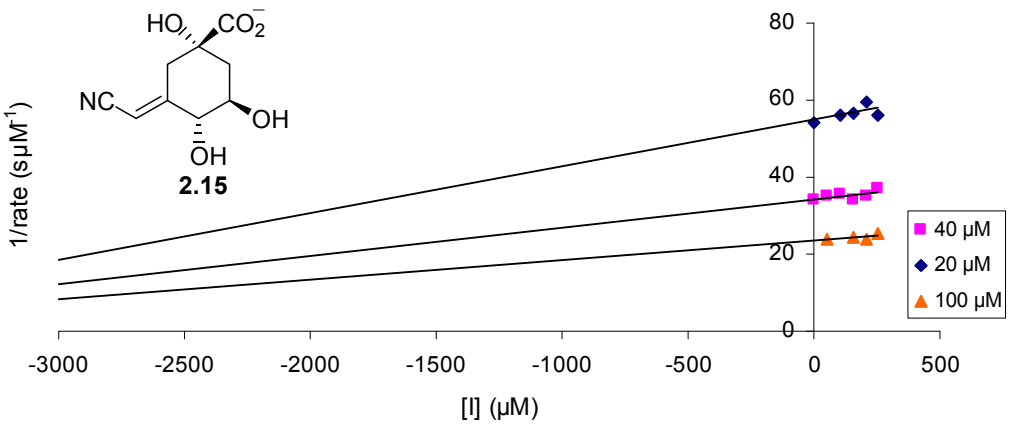

Figure 3.12 Dixon plot for inhibitor **2.15** against *M. tuberculosis* DHQase**.**

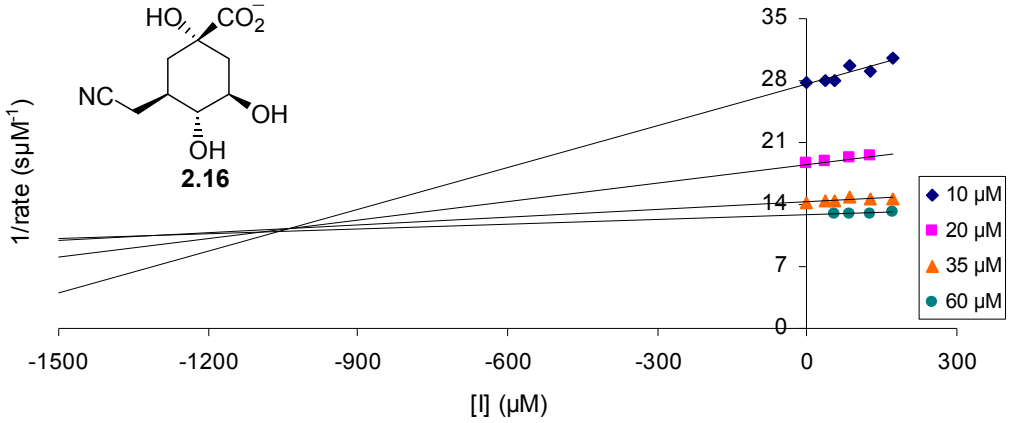

Figure 3.13 Dixon plot for inhibitor **2.16** against *M. tuberculosis* DHQase.

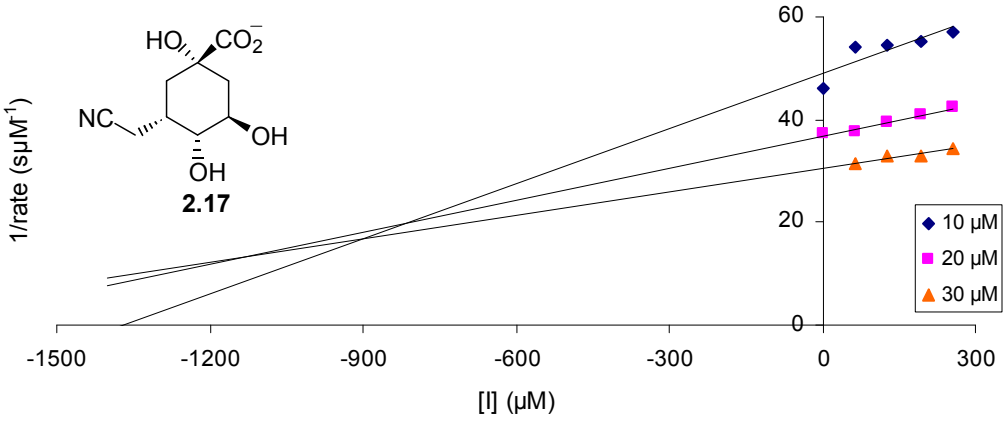

Figure 3.14 Dixon plot for inhibitor **2.17** against *M. tuberculosis* DHQase.

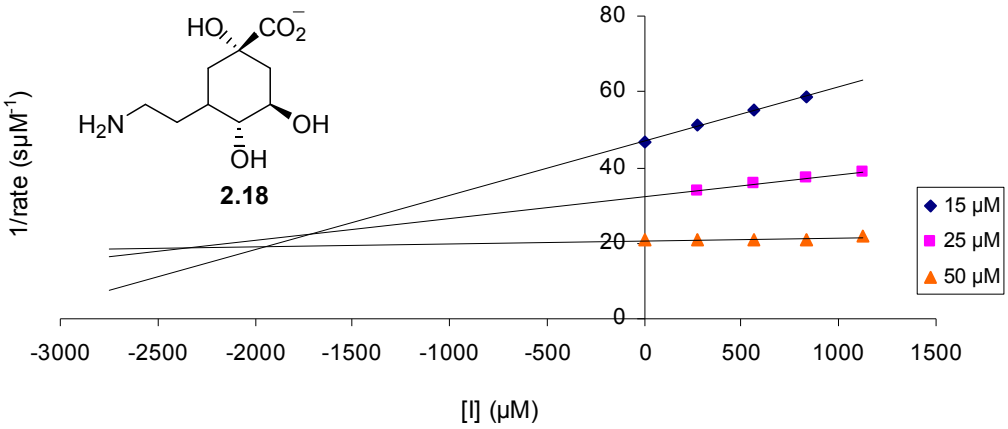

Figure 3.15 Dixon plot for inhibitor **2.18** against *M. tuberculosis* DHQase.

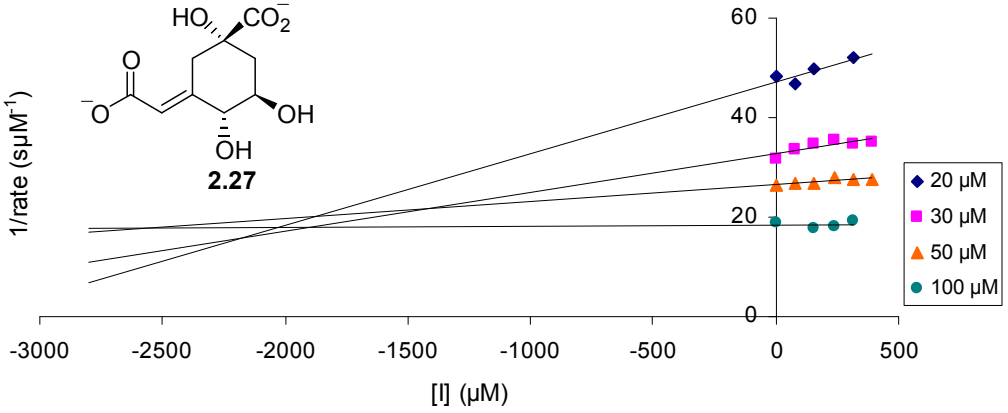

Figure 3.16 Dixon plot for inhibitor **2.27** against *M. tuberculosis* DHQase.

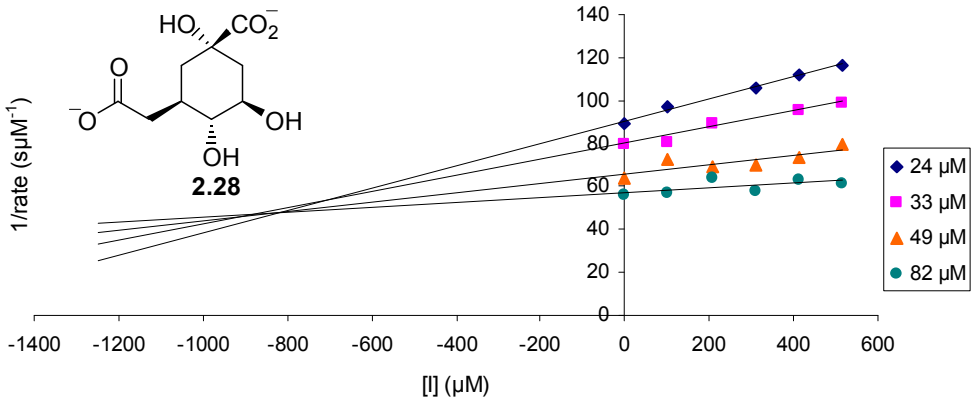

Figure 3.17 Dixon plot for inhibitor **2.28** against *M. tuberculosis* DHQase.

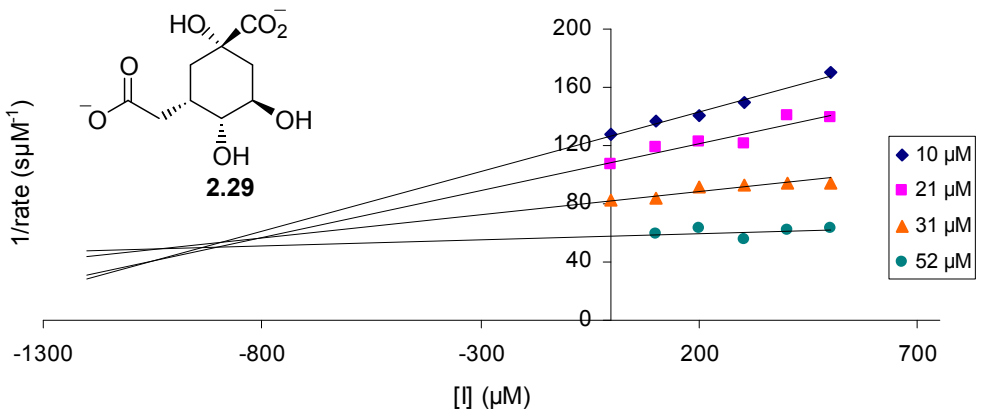

Figure 3.18 Dixon plot for inhibitor **2.29** against *M. tuberculosis* DHQase.

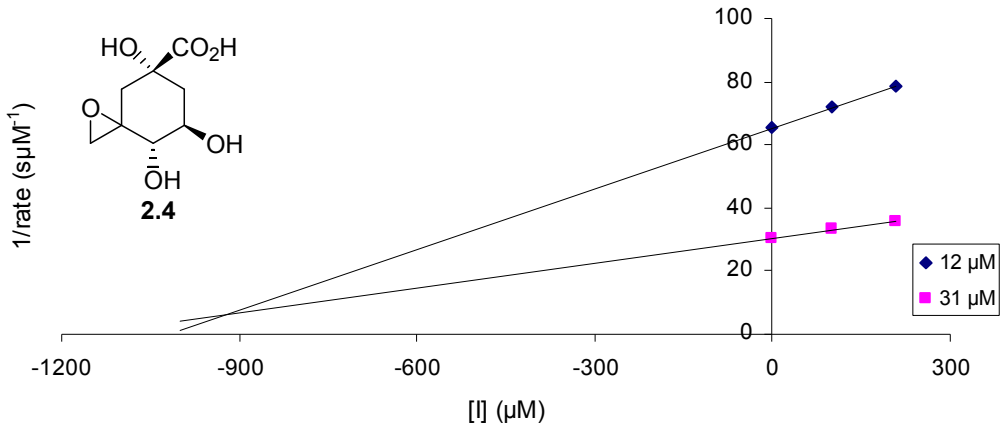

Figure 3.19 Dixon plot (minimal data) for inhibitor **2.4** against *M. tuberculosis* DHQase.

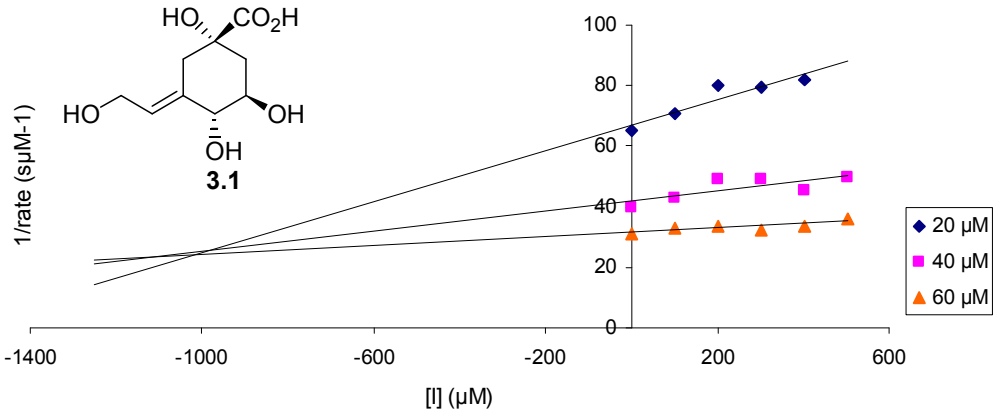

Figure 3.20 Dixon plot for inhibitor **3.1** against *M. tuberculosis* DHQase.

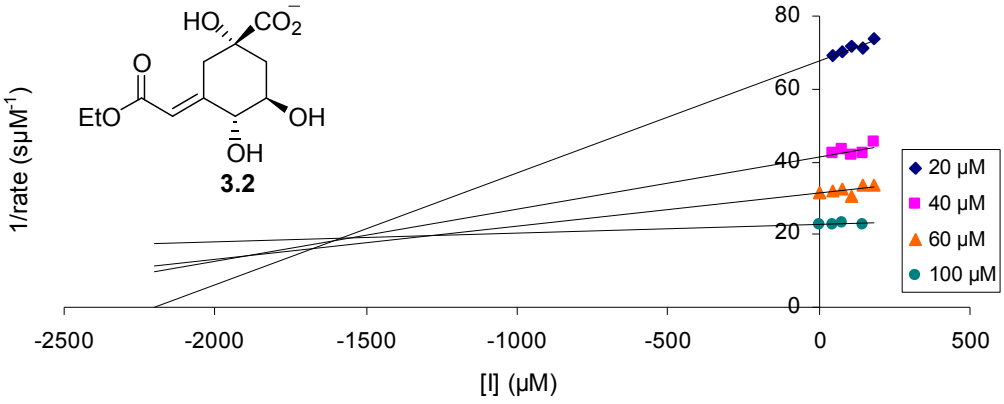

Figure 3.21 Dixon plot for inhibitor **3.2** against *M. tuberculosis* DHQase.

Inhibitors **2.15**, **2.16**, **2.17**, **2.27**, **2.28**, **2.29**, **2.4**, **3.1** and **3.2** were found to be less potent against *M. tuberculosis* DHQase than was anticipated (Table 3.3). The range of inhibitor concentrations used was therefore not really sufficient in some cases to reliably extrapolate the data back to such low values of $-K_i$, especially in the cases of inhibitors **2.15**, **2.16**, **2.27** and **3.2**. No K_i was obtained for inhibitor **2.15** as it seemed pointless to continue the extrapolation beyond -3000 μM given the range of inhibitor concentrations was less than 300 μM.

The saturated nitrile and carboxylate inhibitors **2.16**, **2.17**, **2.28** and **2.29** appear to be preferred to the corresponding olefinic analogues **2.15** and **2.27** which are less potent by a factor of two.

There is no apparent preference for axial or equatorial configuration at C-3 as the inhibition constants for both pairs of epimers **2.16** and **2.17** and **2.28** and **2.29** are in agreement within the experimental error.

There may be a slight preference for the saturated carboxylate inhibitors **2.28** and **2.29** over the nitrile equivalents **2.16** and **2.17** but this is uncertain as the respective inhibition constants can also be said to be in agreement within the stated errors. It was expected that ester **3.2** would be a poorer inhibitor than the corresponding free carboxylate **2.27**, due to reduced hydrophilicity. This is not evident in the results for K_i however, as **3.2** is as active, or slightly

more so, than **3.1**. This would suggest that the carboxylate does not participate in any significant binding interactions with the active site of *M. tuberculosis* DHQase.

Table 3.3 Inhibition constants K_i for inhibitors with C attached at C-3.

Inhibitor	K_i **(μM)** *M. tuberculosis* DHQase
K_M	15 ± 1
1.36[a]	20 ± 2
2.4	~ 900
2.15	>3000
2.16	1150 ± 150
2.17	1000 ± 200
2.18	2000 ± 400
2.27	2000 ± 600
2.28	850 ± 150
2.29	900 ± 150
3.1	1100 ± 100
3.2	1600 ± 400

[a] Ref. 6.

3.4.2.2 Inhibitors with N Attached at C-3 (and Quinic Acid)

Hydrazone inhibitors **2.38**, **2.42, 2.44** and **2.46** were assayed against *M. tuberculosis* DHQase by the method described previously and the Dixon plots are shown in Figure 3.22 to Figure 3.25. The inhibition constants obtained are listed in Table 3.4. Quinic, thought to be a potential inhibitor, was also assayed against *M. tuberculosis* DHQase and the corresponding Dixon plot is shown in Figure 3.26.

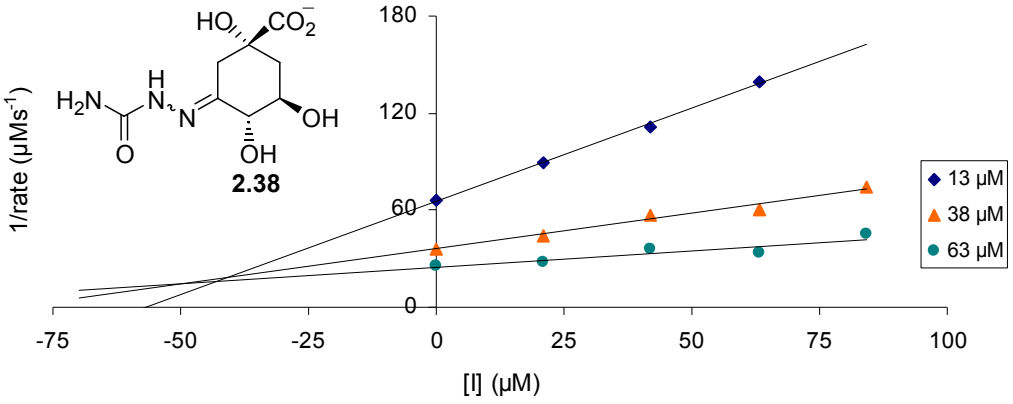

Figure 3.22 Dixon plot for inhibitor **2.38** (20:1 *E*:*Z*) against *M. tuberculosis* DHQase.

The sample of inhibitor **2.46** contained both *E* and *Z* isomers in a ratio of 3:2. The inhibition constant was therefore determined by plotting the inverse rate against the total concentration and so is an average result for the mixture rather than for either of the individual isomers. It is to be expected therefore that the K_i obtained is higher than the actual K_i of the more active component of the mixture. Inhibitor samples **2.38** and **2.44** were also assayed as mixtures of *E* and *Z* isomers (20:1 and 9:1 respectively). In these cases the minor isomer amounted to no more than 10% of the total inhibitor concentration and the reported inhibition constants are therefore based on the concentration of the major isomer alone. The sample of inhibitor **2.42** contained only the major isomer.

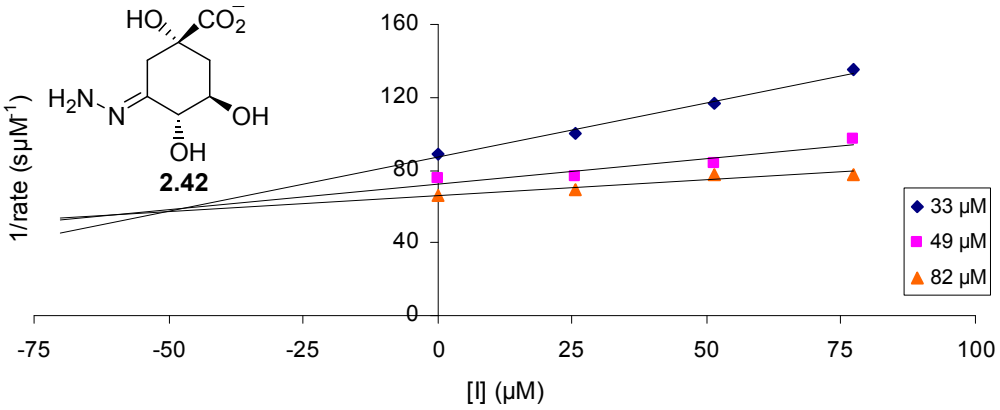

Figure 3.23 Dixon plot for inhibitor **2.42** against *M. tuberculosis* DHQase.

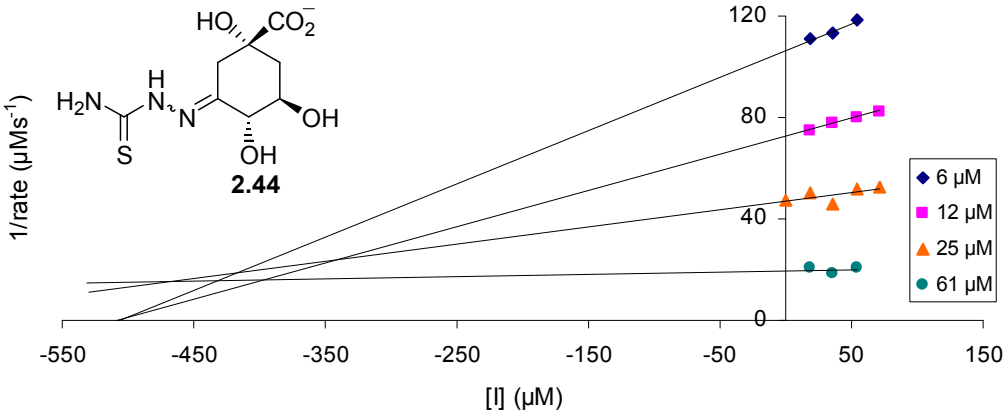

Figure 3.24 Dixon plot for inhibitor **2.44** (9:1 *E*:*Z*) against *M. tuberculosis* DHQase.

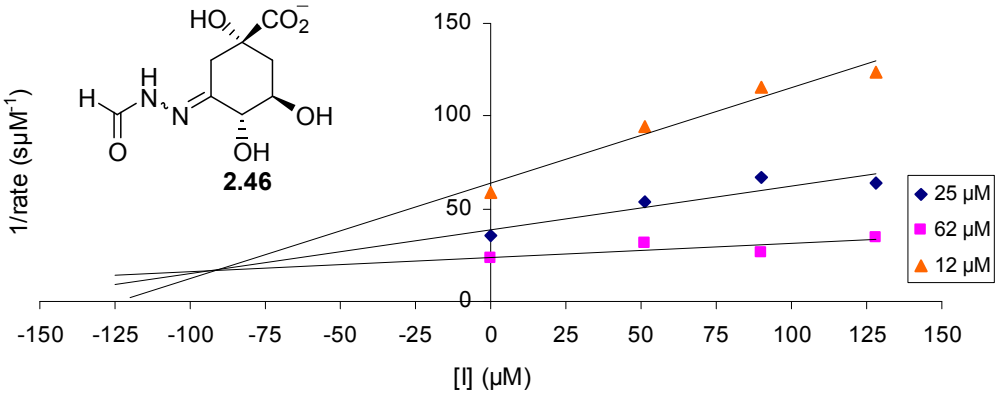

Figure 3.25 Dixon plot for inhibitor **2.46** (3:2 *E*:*Z*) against *M. tuberculosis* DHQase, with the x-axis showing the combined concentration of both isomers.

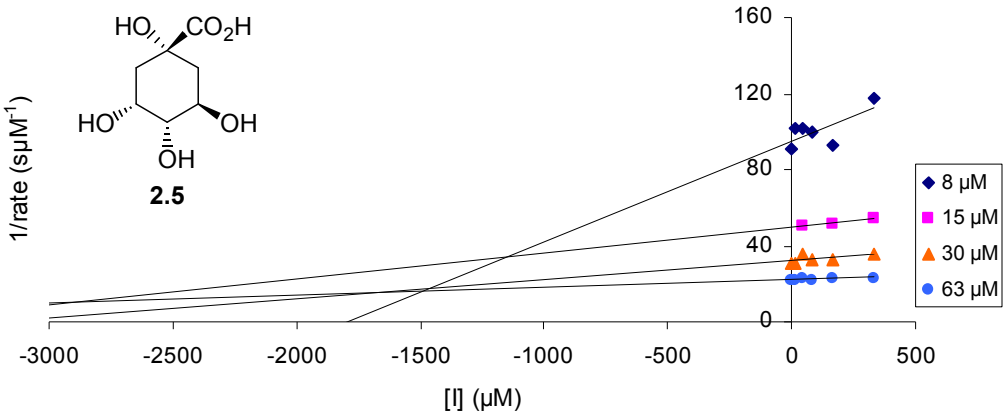

Figure 3.26 Dixon plot for Quinic acid **2.5** against *M. tuberculosis* DHQase.

The inhibitors with nitrogen at C-3, particularly **2.38** and **2.42**, are almost as active against *M. tuberculosis* DHQase as known inhibitor oxime **1.36**. A comparison of the inhibition constants obtained for inhibitors **2.38**, **2.42** and **2.46**, as shown in Table 3.4, suggests no apparent trend in activity with increasing size of the substituent at C-3 and the inhibitors with the shortest and longest side-chains (**2.42** and **2.38** respectively) have approximately equal inhibition constants.

Semicarbazone inhibitor **2.38** is more potent than the corresponding sulphur analogue **2.44** by a factor of 10, indicating that hydrogen bonding to the carbonyl oxygen must be a contributing factor in the potency of these inhibitors.

Table 3.4 Inhibition constants K_i for inhibitors with N attached at C-3 and quinic acid.

Inhibitor	**K_i (μM)** *M. tuberculosis* DHQase
K_M	15 ± 1
1.36[a]	20 ± 2
2.38[b]	45 ± 5
2.42	50 ± 5
2.44[b]	425 ± 75
2.46[c]	90 ± 10
2.5	2000 ± 800

[a] Ref. 6. [b] Based on the concentration of the major isomer only. [c] Based on the combined concentration of a 3:2 mixture of isomers.

3.4.3 Discussion of *M. tuberculosis* DHQase Assay Results

The most striking observation that can be made about the results of the *M. tuberculosis* DHQase assays is that although all of the inhibitors assayed have a hydrophilic group attached at the 3-position, those which have a non-hydrogen bonding carbon atom directly adjacent to the ring are substantially less active than those with a nitrogen atom at the same position. The K_i values in Table 3.3 indicate that all of the inhibitors with C attached at C-3 (**2.15**-**2.18**, **2.27**-**2.29**, **3.1** and **3.2**) are relatively poor inhibitors of type II DHQase from *M. tuberculosis*

compared to oxime **1.36**.[6] In contrast, the nitrogen containing inhibitors (**2.38**, **2.42**, **2.44** and **2.46**) were roughly one order of magnitude more potent, with activities similar to that of oxime **1.36**.

The general lack of potency of the carbon based inhibitors relative to the nitrogen based inhibitors would appear to be consistent with the findings of Frederickson *et al*.[6] and Evans *et al*.[11] which suggest that the C-3 carbonyl is particularly important in substrate recognition for *M. tuberculosis* DHQase, relative to *S. coelicolor* DHQase, possibly interacting with the active site residue Arg-19.[11]

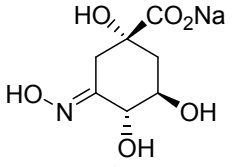

1.36

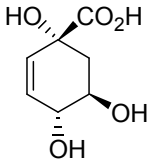

1.37

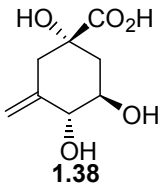

1.38

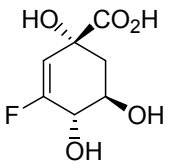

1.40

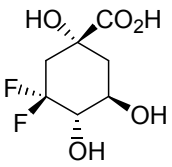

1.41

The importance of the C-3 carbonyl in substrate recognition by *M. tuberculosis* DHQase may be such that the enzyme cannot easily accommodate substitutions at this position. It may be necessary to have an electronegative element such as nitrogen, oxygen or fluorine directly attached to the ring at the 3-position in order to maximise the strength of binding by the enzyme. Known potent inhibitors of *M. tuberculosis* DHQase **1.36** (K_i = 20 ± 2 μM) and **1.40** (K_i = 10 ±2 μM) as well as the substrate DHQ **1.4** all meet this criterion, having nitrogen, fluorine and oxygen atoms respectively at this position (Table 3.5).[6,12] Inhibitor **1.37**, a good inhibitor of *S. coelicolor* DHQase but with no electronegative atom at C-3 is a much less potent inhibitor of *M. tuberculosis* DHQase, with a K_i of 200 ± 2 μM.[6]

An apparent contradiction to this hypothesis can be seen in the inhibition constants for epoxide inhibitor **2.4** and quinic acid **2.5**, which have K_i values of approximately 900 and 2000 ± 800 respectively. Although the epoxide inhibitor **2.4** has an oxygen atom directly attached to the ring at the 3-position, it is no more potent than the majority of the other inhibitors with C at C-3. This might be a consequence of the stereochemistry of the epoxide being such that the oxygen atom is not well positioned for binding to the relevant active site residue(s) and that the carbon of the epoxide ring is instead positioned in the preferential

binding position. It could therefore provide potentially useful information to assay the C-3 epimer of epoxide **2.4**.

Quinic acid **2.5** however, which has no carbon atom at C-3, only the axial hydroxyl group, also proved to be a poor inhibitor of *M. tuberculosis* DHQase. The results of the assays of compounds **2.4** and **2.5** with *M. tuberculosis* DHQase suggest that the presence of an electronegative element adjacent to the ring at C-3 is alone insufficient to insure a strong interaction with this enzyme. This is also observed with the 3-fluoro analogue **1.41** (K_i = 700 ± 100 μM), which has fluorine at C-3, but is not a very good inhibitor of *M. tuberculosis* DHQase.

Table 3.5 Inhibition constants for reported inhibitors of *M. tuberculosis* DHQase.

Inhibitor	**K_i (μM)** *M. tuberculosis* DHQase
1.36[a]	20 ± 2
1.37[a]	200 ± 20
1.38[a]	700 ± 200
1.40[b]	10 ± 2
1.41[b]	700 ± 100

[a] Ref. 6. [b] Ref. 12,13.

There are two possible factors which could be influencing the activity of the inhibitors against *M. tuberculosis* DHQase, in addition to having an electronegative atom at C-3. The first is stereochemistry. The C-3 hydroxyl of quinic acid **2.5** is known to be in the axial position (though the configuration of **2.4** at C-3 is unknown). It was suggested in the discussion of the *S. coelicolor* DHQase assay results (Section 3.3.3) that the equatorial position was the preferred position for substituents at C-3. This may also be the case here, even though configuration at C-3 was not observed to significantly affect the activities of the nitrile epimers **2.16** and **2.17** or the carboxylate epimers **2.28** and **2.29**. With an electronegative atom in place of C at the 3-position, the potential for interaction with the active site residues responsible for carbonyl recognition may make the influence of configuration at C-3 more substantial. It might therefore be informative to assay the C-3 epimer of **2.5**. However, the difluoro inhibitor **1.41** has fluorine atoms occupying *both* the equatorial *and* axial positions at

C-3 and yet is a fairly poor inhibitor of *M. tuberculosis* DHQase. This would suggest that configuration at C-3 is not a major factor in determining affinity for *M. tuberculosis* DHQase and that the poor activity of **2.4** and **2.5**, relative to the N containing inhibitors, may be a result of some other factor.

The second factor potentially affecting the activity of the inhibitors against *M. tuberculosis* DHQase, in addition to the presence of the electronegative atom at C-3, is the presence of a double bond to C-3. Known potent inhibitors of *M. tuberculosis* DHQase **1.36** and **1.40** along with the enolate intermediate **1.19** and the substrate **1.4**, have an sp^2 carbon at the 3-position. Although sp^2 character at C-3 alone does not make a good inhibitor of *M. tuberculosis* DHQase (as shown by the modest activity of inhibitors **1.37** and **1.38**), in combination with an element such as N, O or F attached to C-3, it could potentially make the difference between a good and a poor inhibitor. This makes sense when one considers that the natural substrate DHQ **1.4** has a carbonyl group at C-3, i.e. it has both an electronegative atom and a double bond to C-3. Perhaps a double bond is necessary, either to the attached atom, as in the substrate, or between C-2 and C-3, as in the enolate intermediate, in order to correctly position the electronegative atom for optimal binding. Such a contribution can be observed in the differing potencies of 3-fluoro analogues **1.40** and **1.41**. Inhibitor **1.40** has an sp^2 centre at C-3 and is the most potent *M. tuberculosis* DHQase inhibitor reported to date. Inhibitor **1.41** however, has an sp^3 centre at C-3 and is a comparatively weak inhibitor.[12,13]

In summary, the results of the assays against *M. tuberculosis* DHQase, along with comparisons to reported results, suggest that the most crucial factor in determining whether a dehydroquinate analogue, retaining the functionality and stereochemistry of the natural substrate at all positions except C-3, will be a good inhibitor of *M. tuberculosis* DHQase, is the *combination* of an electronegative element directly attached to the carbocyclic ring at C-3 and sp^2 character at C-3. That the presence of the electronegative element alone is insufficient, is indicated by the poor activity of **2.4**, **2.5** and **1.41**, relative to **2.38**, **2.42** and **1.40**. That sp^2 character at C-3 is insufficient on its own is indicated by the poor activity of **2.15**, **2.27**, **3.1** and **3.2** relative to **2.38**, **2.42**, and **2.46**.

3.4.4 Anomalous Interaction of Inhibitors 2.38 and 2.46 with Type II DHQases.

On carrying out the assay of hydrazone derivatives **2.38** and **2.46** (Scheme 3.4) an increase in absorbance in the absence of substrate was observed which increased with increasing inhibitor concentration.

The observed increase in absorbance of solutions of inhibitors **2.38** and **2.46** in the presence of both *M. tuberculosis* and *S. coelicolor* DHQases led to the investigation of the reaction of inhibitor **2.46** with DHQase by ^{1}H NMR. Inhibitor **2.46** was chosen as a representative example as the reaction progress could be followed by monitoring the intensity of the aldehyde proton signals of the isomers. It seemed likely that the product of the reaction of inhibitor **2.46** with type II DHQases might be either the C-1–C-2 unsaturated inhibitor-product analogue **3.3**, or the natural enzymatic product DHS **1.5**, with the hydrazone functionality being lost (Scheme 3.4).

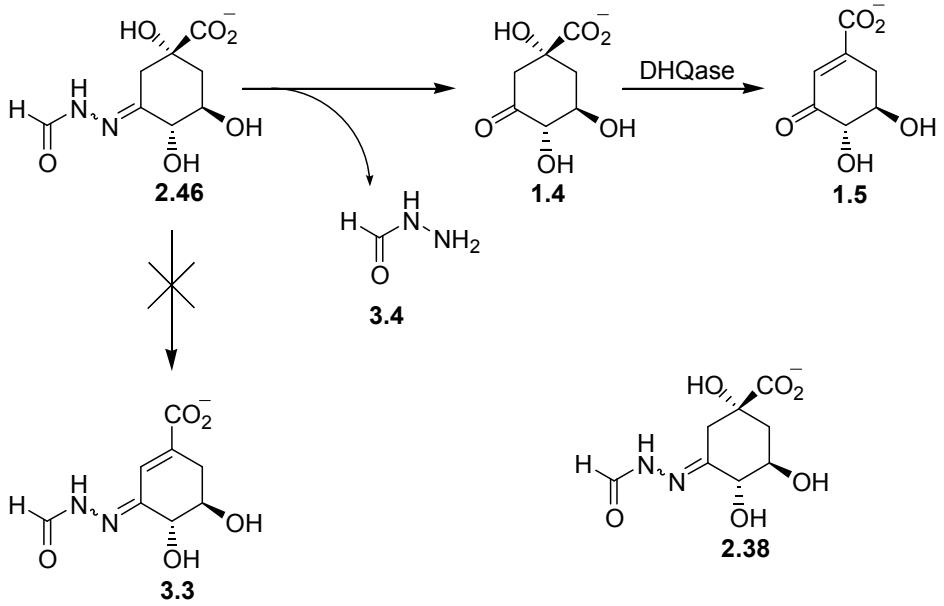

Scheme 3.4 Hydrolysis of formylhydrazone isomers **2.46** in the presence of DHQase.

The mixture of inhibitor isomers **2.46** (3:2 *E*:*Z*) was incubated with *S. coelicolor* DHQase at room temperature in a 5 mm NMR tube with a D_2O filled insert and the progress of the reaction recorded periodically by ^{1}H NMR (Figure 3.27). If the product was in fact **3.3**, then

two sets of product signals for the two isomers would be expected in the ^{1}H NMR spectrum. If the product was the natural product DHS **1.5** however, then only one set of new signals would be observed. (Scheme 3.4).

Observation of the proton signals at 8.0 and 8.6 ppm of the isomers **2.46**, showed the signals of both isomers decreasing, but only one corresponding signal appearing at 7.8 ppm (Figure 3.27). It is unlikely that two isomers of **2.46** would be converted into only one product isomer. The most likely explanation therefore, was that the isomers were being converted into the natural product DHS **1.5** and liberating the formyl hydrazone functionality as formic hydrazide **3.4** (Scheme 3.4). To confirm this, ^{1}H NMR spectra of formic hydrazide and DHS were obtained under the same conditions. These showed identical signals to those observed in the spectrum of the product of the enzymatic reaction of the isomers **2.46**.

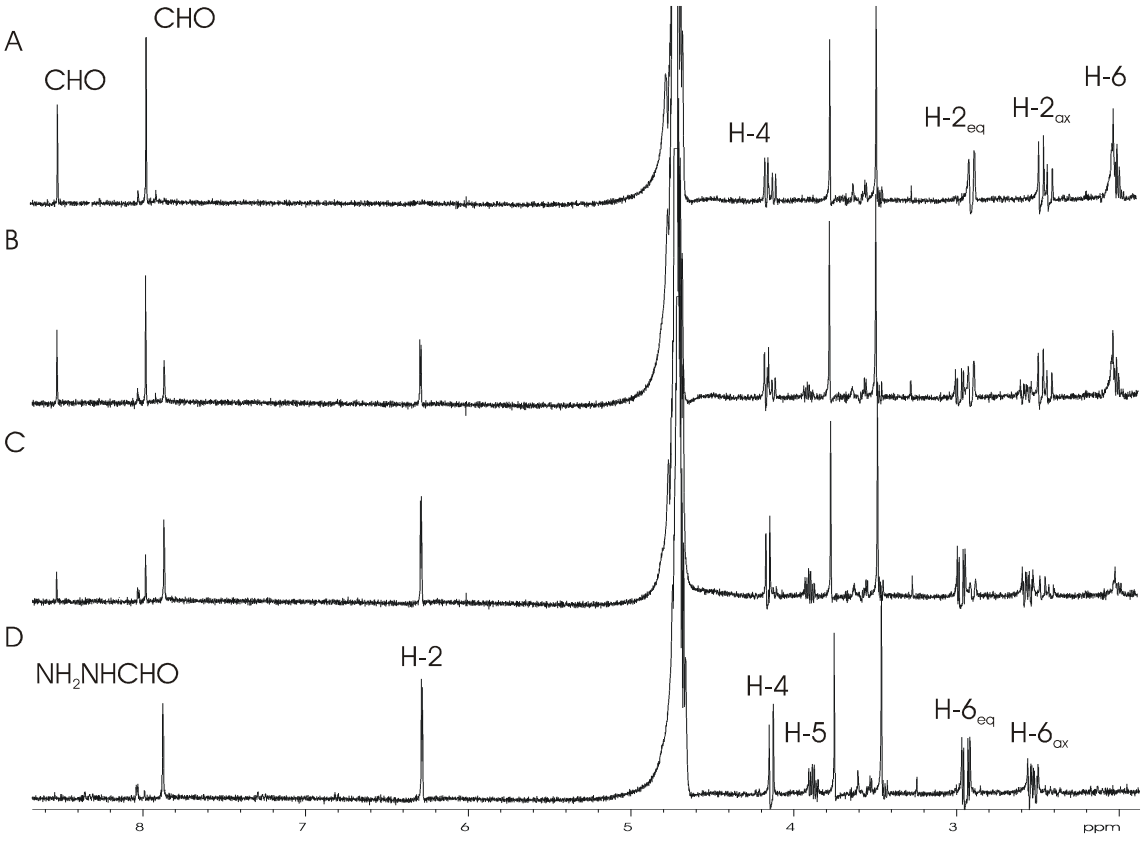

Figure 3.27 ^{1}H NMR spectra showing the enzymatic conversion of formylhydrazone isomers **2.46** into DHS and formic hydrazide at A. 0 h; B. 42 h; C. 138 h and D. 306 h.

The progress of the enzymatic reaction as monitored by ^{1}H NMR can be seen in Figure 3.27, showing A) the initial spectrum of the enzymatic reaction of **2.46**, with only the two isomers of inhibitor **2.46**, B) the NMR spectrum of the reaction at 42 h, C) the spectrum at 138 h and D) the final spectrum at 306 h, showing only the products DHS **1.5** and formic hydrazide **3.4**. The spectra were acquired with simultaneous suppression of the buffer and water signals. The residual water signal (4.7 ppm) and buffer satellite peaks (3.45 and 3.75 ppm) can still be seen. The spectra clearly show the decrease in concentration of the signals due to the isomers of **2.46** (particularly those at 8.0 and 8.6 ppm). The corresponding increase in a single proton signal at 7.8 ppm belonging to formic hydrazide **3.4**, along with signals belonging to DHS **1.5** (especially the olefinic H-2 signal at 6.3 ppm) can also be seen.

The next question was whether the enzyme itself was catalysing the removal of the hydrazone functionality, or if the hydrazone was being non-enzymatically hydrolysed under the assay conditions, liberating free DHQ **1.4**, which was then converted to DHS **1.5** by the enzyme. Inhibitor **2.46** was incubated under the assay conditions, but in the absence of enzyme, in an NMR tube and spectra acquired periodically over several days. The spectra did indeed show a decrease in the signals of the isomers **2.46** and an increase in that corresponding to formic hydrazide as well as those corresponding to the natural substrate DHQ **1.4**.

In order to determine whether the hydrolysis of the hydrazone functionality in the presence of type II DHQase was occurring enzymatically or non-enzymatically, the rates of reaction in the presence and absence of the enzyme were compared. The enzymatic reaction showed a 57% conversion of the isomers **2.46** to formic hydrazide **3.4** after 5.1 days, whereas the non-enzymatic reaction showed a 51% conversion after 4.9 days. These rates were deemed to be equivalent within a reasonable experimental error. The fact that the enzymatic rate was the same as the non-enzymatic rate indicates that the rate-determining step in each case is the non-enzymatic removal of the hydrazone functionality.

Such a rate of hydrolysis of the hydrazone functionality under the assay conditions was considered to be too low to cause a significant decrease in inhibitor concentration over the few minutes required to prepare the assay samples and acquire the data. This instability of the inhibitors would be expected to be a deterrent to their development as potential therapeutics as it seems likely that such compounds would be unstable under physiological conditions.

They do, however, provide useful information about structure-activity relationships and insights into the active site structure of type II DHQase.

The rate of hydrolysis of the hydrazone functionality is also too low to account for the increase in absorbance observed over a short period (<30 min) by UV/vis spectroscopy in the presence of type II DHQases. No reaction other than the disappearance of the inhibitor signals and appearance of the formic hydrazide and DHS signals was observed in the ^{1}H NMR of the assay solution. At higher inhibitor concentrations however, the ^{1}H NMR shows the presence of a small amount of contaminating substrate in the inhibitor solution, which is barely detectable by NMR, but is sufficient for the formation of the product to be observed by the more sensitive UV/vis spectroscopy.

3.4.5 Whole-Cell Testing Against *M. tuberculosis*

Compounds **1.36**, **2.27**, **2.31**, **2.34**, **2.35**, **2.38**, **2.43**, **2.44** and **2.47** were screened for activity against *M. tuberculosis* strain H_{37}Rv by the Tuberculosis Antimicrobial Acquisition & Coordinating Facility (TAACF) Southern Research Institute in Birmingham Alabama. It was anticipated that the free carboxylate salts might exhibit little ability to permeate the plasma membrane. The corresponding esters were therefore screened instead of or in addition to the salts in the hope that these would traverse the cell membrane more easily. Although it was not expected that the esters themselves would be very active against *M. tuberculosis* DHQase, as the C-1 carboxylate is thought to contribute to substrate recognition,[11,14] it was thought that the esters might be hydrolysed *in vivo*, freeing the carboxylate for binding.

Compounds were tested at a concentration of 6.25 μgmL^{-1}. None of the compounds were found to be active at this concentration, demonstrating no inhibition of the growth of the *M. tuberculosis* strain. This is not very surprising in the case of the inhibitors with carbon at C-3, or even thiosemicarbazone inhibitors **2.43** and **2.44** which were shown to be poor inhibitors of *M. tuberculosis* DHQase. Compounds **1.36** and **2.38** however, are good inhibitors of *M. tuberculosis* DHQase and so it is a little disappointinng that the oximes **1.36** and **2.47** and the semicarbazone **2.38** showed no activity against *M. tuberculosis*. It is possible that the lack of activity of the salts is due to an inability to traverse the cell membrane. In the case of the ester

2.47, the compound may still be too hydrophilic to permeate the membrane, or it might be that the ester could not be hydrolysed by the organism.

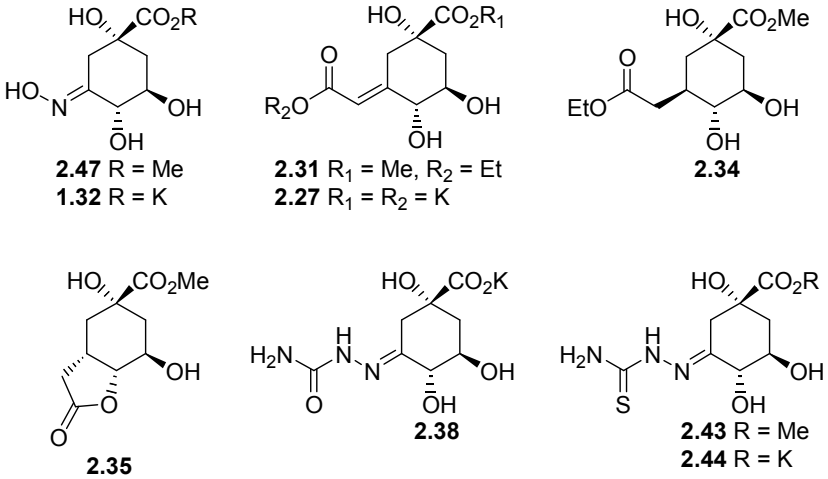

A possible strategy for overcoming both membrane permeability and ester hydrolysis issues might be to adopt a prodrug approach which utilises an ester that is known to be susceptible to enzymatic hydrolysis and which would also make the inhibitors more lipophilic, enabling them to more easily traverse the plasma membrane. The standard spectrophotometric assay for DHQase could easily be adapted, by incorporation of a suitable esterase, to test whether the carboxyl group could be unmasked to regenerate the free inhibitor and restore its activity.

3.5 ENZYMATIC STUDIES ON *S. TYPHI* TYPE I DHQASE

3.5.1 Michaelis-Menten Curve

Data for a Michaelis-Menten curve was obtained for *S. typhi* DHQase at 25ºC and pH 7 (Figure 3.28). Non-linear least-squares fitting of the data to the Michealis-Menten equation (equation 3.1) gave K_M = 17 ± 1 and V_{max} = 0.045 ± 0.005 μMs^{-1} at a total enzyme concentration of 46 ngmL^{-1}. The Michaelis constant obtained is in agreement with that reported by Abell and co-workers who obtained K_M = 16 under the same conditions.[5]

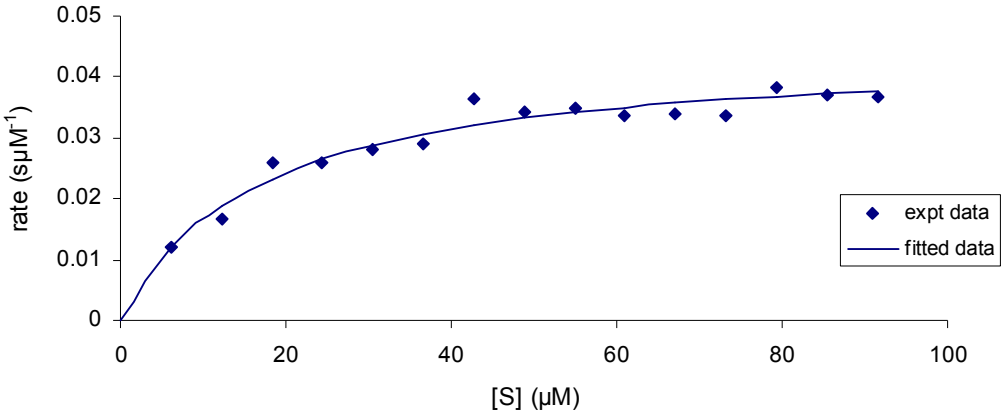

Figure 3.28 Michaelis-Menten curve for Type I DHQase from *S. typhi*.

3.5.2 Assay Results and Discussion

The only inhibitor synthesised with the type I DHQase in mind was the epoxide inhibitor **2.4**. It was thought that the active site lysine residue of the type I enzyme might ring-open the epoxide, causing the inhibitor to become covalently bound to the enzyme, irreversibly inhibiting the enzyme.

Precedent has shown that inhibitors of type II DHQase are type selective and thus poor inhibitors of type I DHQase.[5,6,12] It was therefore deemed unnecessary to waste the prepared type II DHQase inhibitors on an assay against type I DHQase. Epoxide inhibitor **2.4** was therefore the only inhibitor assayed against type I DHQase from *S. typhi*.

3.5.2.1 Reversible Competitive Inhibition Study

Epoxide inhibitor **2.4** was first assayed for competitive inhibition against *S. typhi* DHQase. Minimal data was collected in order to conserve the inhibitor for future experiments. A Dixon plot was prepared and is shown in Figure 3.29.

This Dixon plot gives a value of K_i for this inhibitor of 1.1 mM. This K_i is an approximation and is unconfirmed, as multiple data sets leading to a common intersection point on the Dixon

plot were not obtained. This result for K_i indicates that epoxide **2.4** is a relatively weak inhibitor of *S. typhi* DHQase.

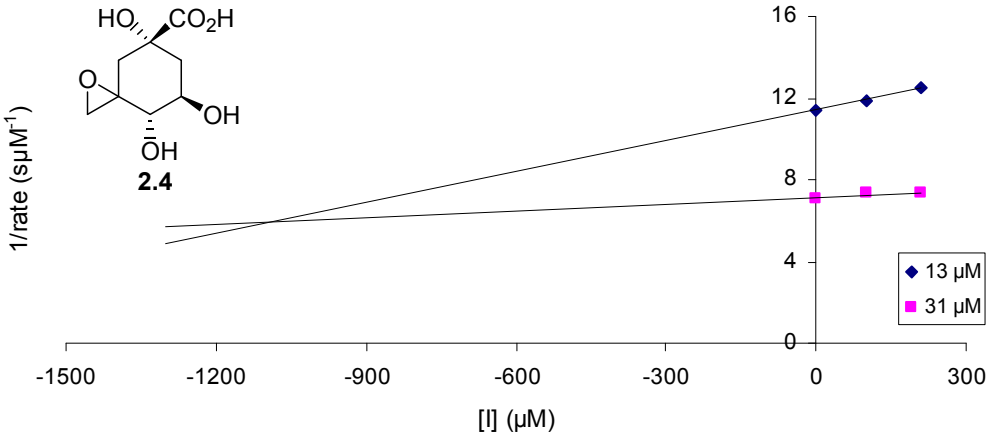

Figure 3.29 Dixon plot (minimal data) for inhibitor **2.4** against *S. typhi* DHQase.

Table 3.6 shows reported inhibition constants for some inhibitors of type I DHQases from *S. typhi* and *E. coli*. By comparison, epoxide inhibitor **1.24** was a more potent inhibitor of *E. coli* DHQase with a reported K_i of 400 μM.[15] Known inhibitor fluoroketone **1.32** was much more potent an inhibitor of type I DHQase from *E. coli*, with a reported K_i of 80 μM.[16] The activities of these inhibitors have not been reported for *S. typhi* DHQase however and so no direct comparison to the activity of epoxide **2.4** can be made. Epoxide **2.4** is marginally more potent than **1.37** and **1.40**, the most potent competitive inhibitors reported for *S. typhi* DHQase, however these inhibitors are type selective and thus more active against type II DHQase.[6] Epoxide **2.4** however, is no more active type II DHQase from *M. tuberculosis* than type I DHQase from *S. typhi*.

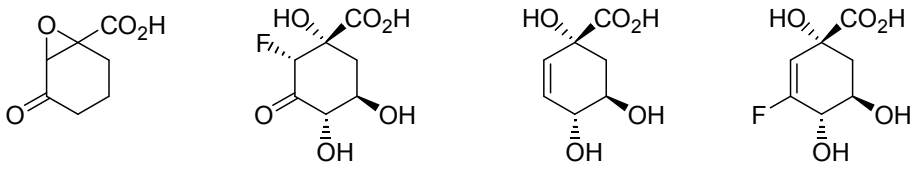

Table 3.6 Reported inhibition constants for known type I DHQase inhibitors.

Inhibitor	K_i (μM)	
	S. typhi DHQase	*E. coli* DHQase
2.4	1100	
1.24[a]		400
1.32[b]		80
1.37[c]	3000 ± 1000	
1.40[d]	1500 ± 500	

[a] Ref. 15. [b] Ref. 16. [c] Ref. 6. [d] Ref. 12,13.

3.5.2.2 Time-Dependent Inhibition Study

Epoxide inhibitor **2.4** was incubated with type I DHQase from *S. typhi* at ambient temperatutre. A control sample was also incubated, identical except for the absence of inhibitor. Aliquots of the enzyme incubation were taken at intervals, added to a solution containing substrate and buffer, and absorbance vs. time data collected for the enzymatic reaction.

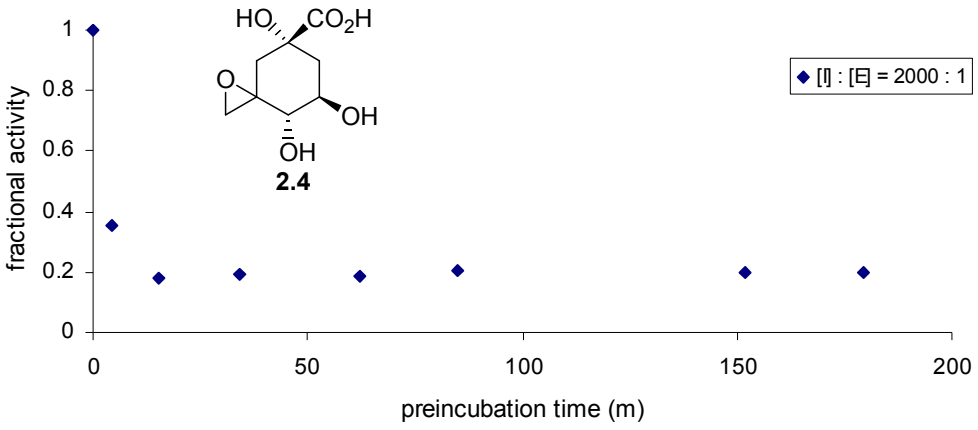

Figure 3.30 Plot of fractional activity vs. pre-incubation time for inhibitor **2.4** (400 μM) against showing time-dependent inhibition of *S. typhi* DHQase.

On addition of the enzyme-inhibitor solution to the buffered substrate solution an initial induction period was observed before picking up to the steady-state rate. The fractional rate v_i/v_0, where v_i is the steady state rate of the sample containing inhibitor **2.4** and v_0 is the initial (steady-state) rate of the control sample, was plotted against time. The activity of the enzyme was seen to drop off quite quickly confirming that epoxide **2.4** is a time dependent inhibitor of type I DHQase from *S. typhi* (Figure 3.30). The full activity (i.e. that of the control sample) was not recovered after dilution into the substrate solution, indicating that epoxide **2.4** is, as anticipated, an irreversible inhibitor of type I DHQase from *S. typhi*.

A second experiment was carried out in which an incubation of *S. typhi* DHQase and inhibitor **2.4** was prepared for LCMS, to determine whether the inhibitor was in fact becoming covalently bound to the enzyme. A solution containing inhibitor and enzyme (200 : 1) at pH 7 was incubated for 93 hours. An aliquot was taken and diluted into a solution containing substrate and the absorbance was recorded over a period of 3 hours. The data showed an extended induction period, followed by a linear period (the steady-state) after which the rate tailed off as the substrate was consumed (Figure 3.31). The steady-state rate was compared to the control enzyme incubation (lacking inhibitor) and showed a 90% loss of activity over the 93 hours (Figure 3.32).

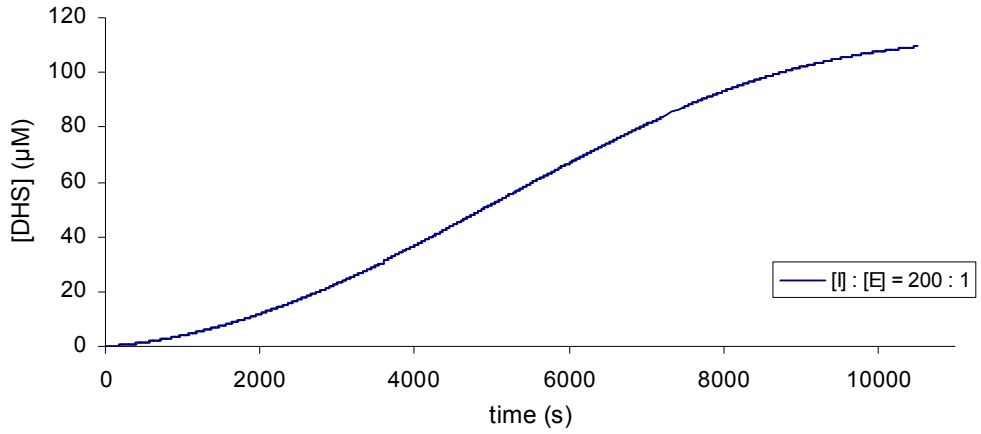

Figure 3.31 Reaction progress curve for *S. typhi* DHQase after incubation for 93 hours in the presence of inhibitor **2.4**.

The enzyme incubation containing 200:1 inhibitor **2.4** : *S. typhi* DHQase was subjected to LCMS. The resulting spectrum showed a pair of peaks, one at 27462 Da representing the

subunit mass of the free enzyme and the second at 27665 Da representing the enzyme subunit with a gain in mass of 203 Da. This is in agreement (within an acceptable margin of error) with the mass gain that would be expected (204 Da) if inhibitor **2.4** had become covalently attached to the enzyme, by ring opening of the epoxide.

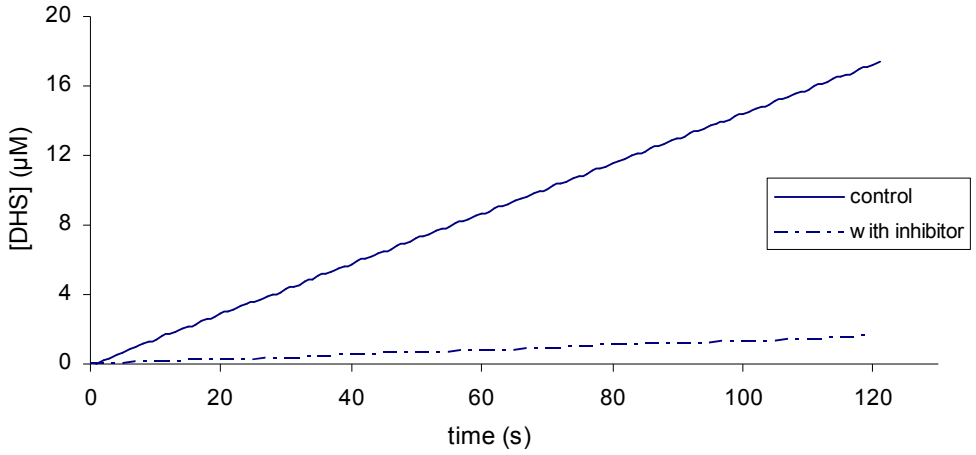

Figure 3.32 Illustration of time dependent inhibition of *S. typhi* DHQase by inhibitor **2.4** by comparison of steady-state rates of control incubation ([I] = 0 μM) and experimental incubation ([I] = 9 mM) after 93 h.

The proposed mechanism of the time-dependent inhibition is one in which the epoxide is opened by the active site lysine residue of type I DHQases. This is the lysine residue responsible for nucleophilic attack at the carbonyl carbon (C-3) and Schiff base formation during normal substrate turnover and so it seems reasonable to expect that the lysine would also attack the epoxide at C-3 to form enzyme bound adduct **3.5** (Scheme 3.5).

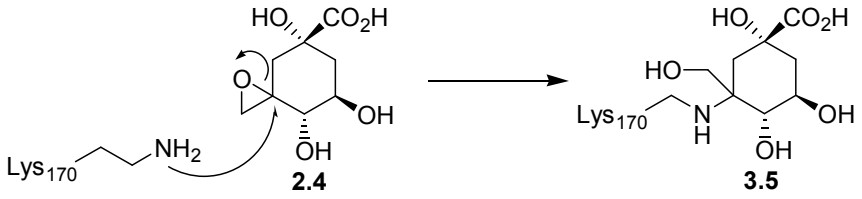

Scheme 3.5 Proposed mechanism of *S. typhi* DHQase time-dependent inhibition by epoxide **2.4**.

However, it is equally possible that the active site lysine attacks instead at the carbon *exo* to the carbocyclic ring, opening the epoxide to form adduct **3.6** (Scheme 3.6). This is the chemically preferred pathway but the steric requirements of the enzyme may influence the site of attack. As both possible products have identical mass, it is not possible to determine from

the LCMS result which is being formed. This question could be answered however, if crystal structures of the enzyme-inhibitor adduct could be obtained. The preferred mode of attack might also be predicted by computer modelling studies.

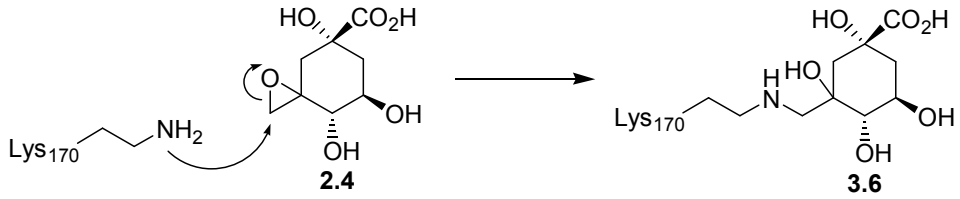

Scheme 3.6 Alternative mechanism of time-dependent inhibition of *S. typhi* DHQase by epoxide **2.4**.

3.6 CONCLUSION

A spectrophotometric assay was used to evaluate the biological activity of the inhibitors whose preparation was described in Chapter 2.

All of the inhibitors were assayed against type II DHQase from *M. tuberculosis*. Inhibitors with a carbon atom attached at the 3-position were found to be universally weak inhibitors of *M. tuberculosis* DHQase. Inhibitors with a nitrogen atom double bonded to C-3, on the other hand, were found to be more active than the carbon containing inhibitors by a factor ten or more. These inhibitors displayed activity similar that of known inhibitor oxime **1.36**. The importance of the combination of an electronegative atom directly attached to the carbocyclic ring at the 3-position, and sp^2 character at C-3, offers a clear direction for the design and synthesis of future generations of *M. tuberculosis* DHQase inhibitors.

Epoxide inhibitor **2.4** was found to be a weak competitive inhibitor of type I DHQase from *S. typhi* which displayed rapid time-dependent irreversible inhibition of the enzyme. LCMS confirmed that the inhibitor was becoming covalently attached to the enzyme, most likely by ring-opening of the epoxide by the active site lysine residue. An x-ray crystal structure of the inactivated enzyme-inhibitor adduct could confirm this.

Inhibitors with sp^3 character and C at C-3 were assayed against *S. coelicolor* DHQase. These were found to be poor to moderate inhibitors of this enzyme. The enzyme appeared to favour an equatorial side-chain at C-3 over an axial one, however, increasing the hydrophilicity of the equatorial side-chain appeared to result in a decrease in activity.

Inhibitors with sp^2 character at C-3 were not assayed against type II DHQase from *S. coelicolor* DHQase by this method due to their high absorbance at 234 nm. In order to evaluate the biological activity of these inhibitors against *S. coelicolor* DHQase an alternative assay methodology was investigated. This is discussed in the following chapter.

3.7 REFERENCES FOR CHAPTER 3

(1) Cornish-Bowden, A. *Fundamentals of enzyme kinetics*; Portland Press Ltd.: London, 1995.

(2) Copeland, R. A. *Enzymes: A practical introduction to structure, mechanism, and data analysis*; Wiley-VCH, Inc.: New York, 1996.

(3) Briggs, G. E.; Haldane, J. B. S. *Biochem. J.* **1925**, *19*, 338-339.

(4) Michaelis, L.; Menten, M. L. *Biochem. Z.* **1913**, *49*, 333-369.

(5) Toscano, M. D.; Frederickson, M.; Evans, D. P.; Coggins, J. R.; Abell, C.; González-Bello, C. *Org. Biomol. Chem.* **2003**, *1*, 2075-2083.

(6) Frederickson, M.; Parker, E. J.; Hawkins, A. R.; Coggins, J. R.; Abell, C. *J. Org. Chem.* **1999**, *64*, 2612.

(7) Roszak, A. W. R., D. A.; Krell, T.; Hunter, I. S.; Frederickson, M.; Abell, C.; Coggins, J. R.; Lapthorn, A. J. *Structure* **2002**, *10*, 493-503.

(8) Toscano, M. D.; Stewart, K. A.; Coggins, J. R.; Lapthorn, A. J.; Abell, C. *Org. Biomol. Chem.* **2005**, *3*, 3102-3104.

(9) Smith, K. A., University of Canterbury, 2002.

(10) González-Bello, C.; Manthey, M. K.; Harris, J.; Hawkins, A. R.; Coggins, J. R.; Abell, C. *J. Org. Chem* **1998**, *63*, 1591-1597.

(11) Evans, L. D. B.; Roszak, A. W.; Noble, L. J.; Robinson, D. A.; Chalk, P. A.; Matthews, J. L.; Coggins, J. R.; Price, N. C.; Lapthorn, A. J. *FEBS Lett.* **2002**, *530*, 24-30.

(12) Frederickson, M.; Roszak, A. W.; Coggins, J. R.; Lapthorn, A. J.; Abell, C. *Org. Biomol. Chem.* **2004**, *2*, 1592-1596.

(13) Frederickson, M.; Coggins, J. R.; Abell, C. *Chem. Commun.* **2002**, 1886-1887.

(14) Vaz, A. D. N.; Butler, J. R.; Nugent, M. J. *J. Am. Chem. Soc.* **1975**, *97*, 5914-5915.

(15) Bugg, T. D. H.; Abell, C.; Coggins, J. R. *Tetrahedron Lett.* **1988**, *29*, 6783.

(16) González-Bello, C.; Harris, J. M.; Manthey, M. K.; Coggins, J. R.; Abell, C. *Bioorg. Med. Chem. Lett.* **2000**, *10*, 407.

4 Biological Studies: ^{1}H NMR Assay

4.1 INTRODUCTION

The highly UV active nature the inhibitors with sp^2 character at C-3 prohibited using the spectrophotometric assay (described in Chapter 3) to obtain inhibition constants for their activity against *S. coelicolor* DHQase. The spectrophotometric assay for DHQase consists of measuring the initial rate of the enzymatic conversion of dehydroquinate (DHQ) **1.4** to dehydroshikimate (DHS) **1.5** by monitoring the increase in absorbance at 234 nm due to the enone-carboxylate chromophore of the product DHS **1.5** (Scheme 4.1). At the inhibitor concentrations required for the *S. coelicolor* DHQase assay, the absorbance due to the inhibitors was too great to obtain meaningful rate data spectrophotometrically. In the initial stages of this work, *S. coelicolor* DHQase was the only type II enzyme available against which to assay the putative inhibitors. An alternative means of measuring the rate of the enzymatic reaction was required. This meant finding an alternative method for detecting either the appearance of the product, or the disappearance of the substrate.

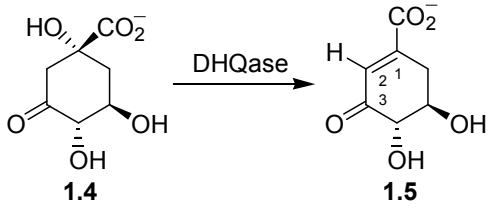

1.4 **1.5**

Scheme 4.1 Conversion of substrate DHQ **1.4** to product DHS **1.5** by DHQase.

Two possibilities were considered for an alternative detection method. The first was ^{1}H NMR. The change in concentration of substrate or product could be measured by monitoring the decrease or increase respectively in an appropriate signal in the ^{1}H NMR spectrum of the assay sample. The second possibility was HPLC. The concentration changes could be determined by stopping the enzymatic reaction after a certain interval and the various

components separated by HPLC and the amounts determined. The discontinuous HPLC assay method seemed time consuming and inconvenient. The continuous NMR method seemed preferable as the data could be acquired during the course of the reaction and no subsequent separation of the reaction components would be necessary.

^{1}H NMR would be expected to possess certain advantages over UV/vis spectroscopy as a detection method for the *S. coelicolor* assay. It would allow the independent resolution of signals from the different components of the sample, enabling product, substrate and inhibitor to be distinguished in the spectrum. This would avoid the problem of interference by the inhibitor encountered when attempting to monitor the formation of the product during the spectrophotometric assay.

4.2 Determination of DHS Concentration by ^{1}H NMR

4.2.1 Choice of the Signal to be Monitored

In order to measure the rate of the enzymatic reaction by ^{1}H NMR, an appropriate signal from either the substrate **1.4** or the product **1.5** needed to be chosen, by which to monitor the concentration changes. Such a signal must not overlap or be subject to interference from any of the other signals arising from the components of the assay solution. Ideally it would be an intense peak as this would maximise the signal to noise ratio.

The preferable choice would be to monitor the decrease in a substrate signal, however, all signals in the substrate spectrum were coupled to at least one other proton and usually more, making the signals broader and less intense. All of the substrate signals also occur in the busy region of the spectrum between 2 and 5 ppm, in close proximity to other signals arising from the substrate itself, the product or from the intense signals due to the buffer and solvent. The doublet (J = 2.9 Hz) at 6.3 ppm in the product spectrum was chosen instead as it is a narrow signal relative to all others in the substrate and product spectra (there are no singlets in either spectrum), but more importantly, is well removed from any other signals in the assay

spectrum. This signal arises from the olefinic proton at the 2-position of the product DHS **1.5**. Figure 4.1 shows the ^{1}H NMR spectrum of the product DHS **1.5**.

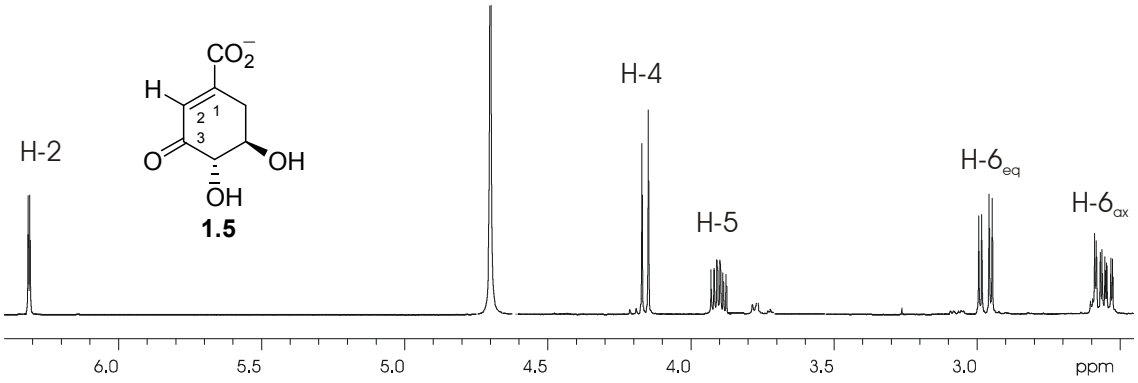

Figure 4.1 ^{1}H NMR spectrum of DHS **1.5** in D_2O (the solvent peak has been partially deleted for convenience).

4.2.2 Choice of a Reference Substance

The relative concentrations of the components of the assay mixture could be determined by measuring peaks integrals. However, for the purposes of the assay, the absolute concentration of the product at a given time needed to be measured. This required the introduction of a known amount of a reference substance into the sample. The absolute concentration of the product DHS **1.5** could then be calculated from the relative areas of the product and reference signals.

4.2.2.1 Internal vs. External Reference

Two possible means existed for introducing a reference substance into the assay sample. An internal reference could be employed, in which case the reference substance is added directly to the assay solution. Alternatively an external reference could be chosen whereby a known amount of the reference substance is added to the D_2O in the NMR tube insert and so is detected by the NMR spectrometer but does not come into contact with the assay solution.

An external reference has the advantage of being isolated from the assay sample, negating any potential interaction of the reference with the components of the sample, particularly the

enzyme. The known *amount* of reference would then be used to determine the *amount* of product present from the integrals of the respective NMR signals. This would require the transferral of the assay sample into the NMR tube to be quantitative, or else introduce a significant source of error to the experiment by altering the relative amounts of product and reference.

On the other hand, in the case of an internal reference, the reference would be in the solution with the other components of the assay and so the *concentration* of DHS would be determined from the *concentration* of the reference. If the transferral of the assay sample to the NMR tube were not quantitative, the concentrations of the product and reference in the solution would not be affected.

In practice, all of the components of the assay sample are combined in a vial, the reaction is initiated by the addition of enzyme, and the sample transferred to the NMR tube. It is quite common for droplets of the aqueous solution to adhere to the pipette used to transfer the solution, to the walls of the NMR tube and to the sides of the NMR tube insert. Minor spillages also occasionally occur. It was thought that an internal reference was a more practical choice than an external one, as it eliminated these factors as a source of error.

4.2.2.2 Nature of the Reference

Choosing a reference substance imposed certain constraints. The substance had to have an appropriate signal to monitor in its ^{1}H NMR spectrum. The requirements for the reference signal were the same as those for the product signal. A signal well removed from all others in the assay spectrum was required and a narrow, intense signal was preferred. It was desirable that the reference spectrum contained only the signal to be monitored and no others to avoid complicating the spectrum further. It was also preferred that the signal to be monitored be an intense, uncoupled signal such as that for a methyl or *tert*-butyl group as this would reduce the concentration of reference required to get a good signal and minimise any interactions with the components of the assay.

The decision to use an internal rather than external reference imposed the additional requirement that the reference compound must not inhibit the enzyme. Therefore any

potential reference compound must first be assayed to determine whether or not it demonstrated any inhibitory activity against DHQase and thus whether it could be adopted as the standard reference for the ^{1}H NMR assay.

4.2.2.2.1 ^{t}BuOH as a Reference

Tertiary butanol was the first substance trialled as a reference. It gave a very intense, singlet signal at 1.2 ppm, well removed from substrate and product signals. It also showed no competitive inhibition of *S. coelicolor* DHQase by the standard spectrophotometric assay described in Chapter 3.

Figure 4.2 shows a ^{1}H NMR spectrum of an assay sample with ^{t}BuOH used as the reference. The details of the spectrum about the very intense suppressed water signal and unsuppressed buffer signal are difficult to see clearly due to the distortion of the baseline arising from the baseline correction. The baseline correction is used to bring the DHS **1.5** and ^{t}BuOH signals into line with each other so that the respective integral regions may be directly compared. The apparent distortion increases as the concentration of DHS **1.5** is reduced due to the greater vertical expansion of the spectrum required to clearly view the DHS **1.5** peak.

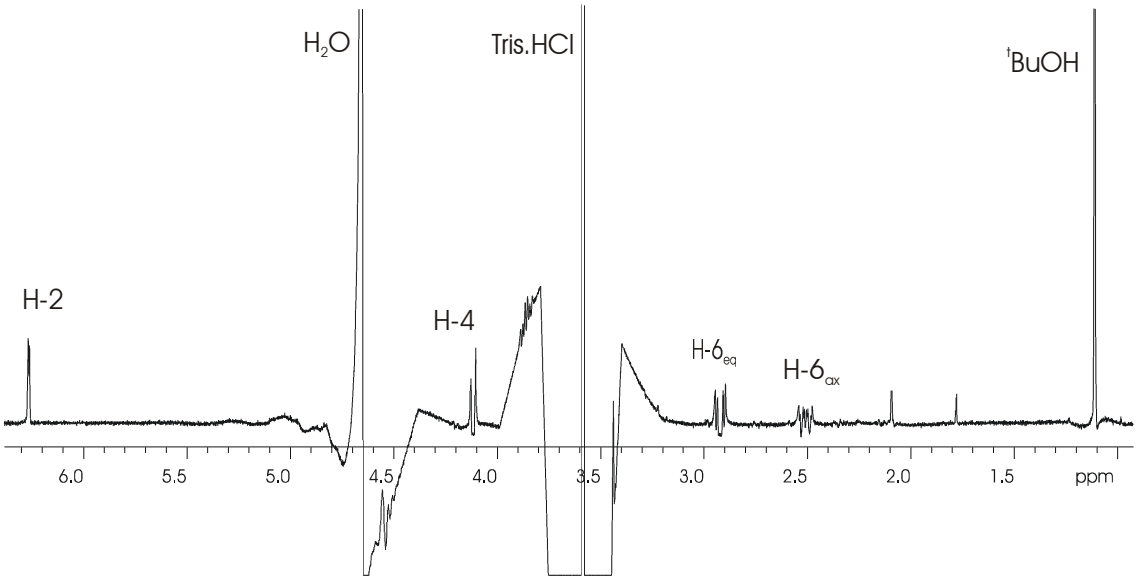

Figure 4.2 ^{1}H NMR spectrum showing enzymatic product DHS **1.5** H-2 and ^{t}BuOH reference signals.

Although ^{t}BuOH proved to be an adequate reference the large separation of the reference signal from the product signal made processing of the spectrum inconvenient and time consuming. Because the regions about the peaks cannot be viewed in great detail, it makes optimising the phasing and integral regions of both peaks by eye difficult.

It was thought that using an alternative reference substance with a signal that was closer in chemical shift to that of the DHS H-2 proton at 6.3 ppm would circumvent the extreme distortion of the central region of the spectrum resulting from the baseline correction. It would also allow significant expansion during processing of the region of the spectrum about the two peaks to be monitored, allowing the regions around the signals of interest to be viewed in more detail. This in turn would allow optimisation of the resulting data by increasing the precision with which the spectra could be phased and the integral regions selected.

4.2.2.2.2 An Aromatic Compound as Reference

It was thought that an aromatic proton would give a signal in the desired region of the spectrum, near the product H-2 signal but not too near the distortion arising from the water signal (Figure 4.2). The signal would ideally be a singlet and would not overlap any other signals arising from the same compound. Polyhydroxylated aromatics hydroquinone **4.1** ($\delta_H(D_2O)$ = 6.7 ppm), and phloroglucinol **4.2** ($\delta_H(D_2O)$ = 5.9 ppm) seemed likely candidates as they would be expected to be sufficiently soluble in the aqueous assay solution. Both showed a single singlet in their ^{1}H NMR spectra, which was close to that of H-2 of DHS **1.5**, but not so close as to overlap.

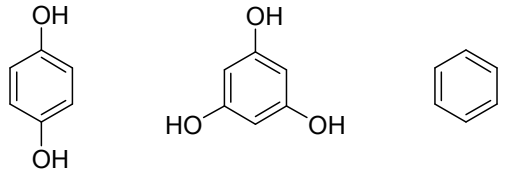

4.1 **4.2** **4.3**

Hydroquinone **4.1** however, was found to inhibit *S. coelicolor* DHQase, i.e. the initial rate of the enzymatic reaction was observed (spectrophotometrically) to decrease with increasing concentration of **4.1** (Figure 4.3) and it was thought that this was also likely to be the case for

phloroglucinol **4.2**. Benzene **4.3** ($\delta_H(D_2O)$ = 7.3 ppm) however, might be less likely to inhibit the enzyme as it lacked the potential for hydrogen bonding interactions of hydroxyl groups with the enzyme active site. Benzene was therefore tested for inhibition of *S. coelicolor* DHQase, however a decrease in initial rate with increasing benzene concentration was still observed (Figure 4.3). It is apparent that monocyclic aromatic compounds of this type would not make appropriate reference substances for a ^{1}H NMR assay for *S. coelicolor* DHQase. However, their potential as inhibitors of DHQase warrants further investigation.

4.2.2.2.3 A Small Molecule as Reference

It was thought that a small molecule would be less likely to inhibit *S. coelicolor* DHQase and so small molecules with a signal above 5 ppm in their proton NMR spectrum were considered. Chloroform ($\delta_H(D_2O)$ = 7.3 ppm), dichloromethane (DCM) ($\delta_H(D_2O)$ = 5.4 ppm) and *N*,*N*-dimethylformamide (DMF) ($\delta_H(D_2O)$ = 7.8 ppm for the COH proton) were considered the most likely candidates. The chlorocarbons were considered preferable to DMF as each contained only a single proton signal in their respective NMR spectra, and chloroform was preferable to DCM as its proton signal was further removed from possible interference by the very intense water signal at 4.7 ppm.

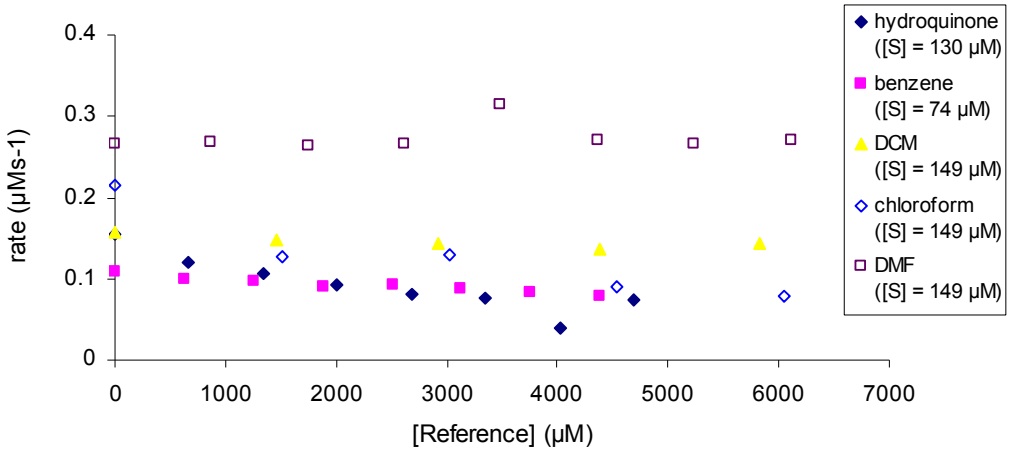

Figure 4.3 Comparison of the effect of the possible alternative references on the initial rate of the enzymatic reaction.

The small molecules were consequently investigated for inhibition of *S. coelicolor* DHQase (Figure 4.3). In the cases of chloroform and dichloromethane, a definite decrease in the rate

of the enzymatic reaction was observed with increasing concentration of the small molecule. DMF however, displayed no such trend. When tested for time dependent inhibition of *S. coelicolor* DHQase, DMF, at a concentration of 2 mM, caused no apparent decrease in enzyme activity over a period of 4 h. This met the necessary requirements for a reference substance, as the enzyme would only be in contact with approximately 500 μM solutions of the reference, for reaction times of less than 15 minutes.

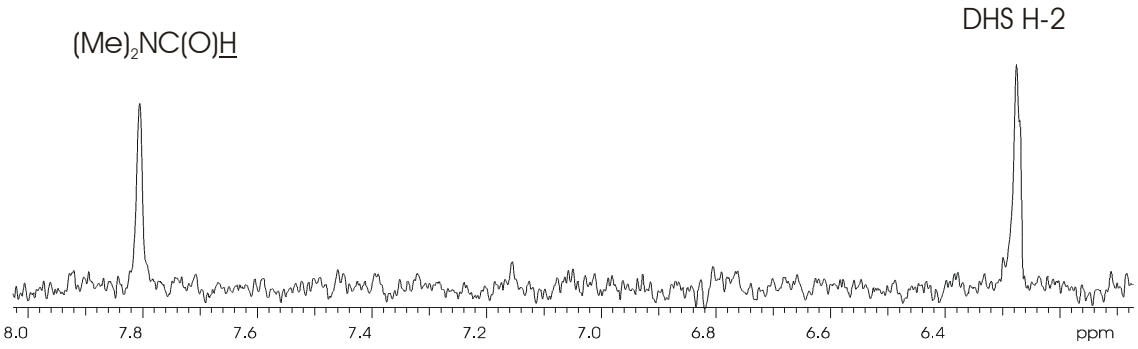

Figure 4.4 Partial ^{1}H NMR spectrum of an assay sample showing DHS **1.5** H-2 and DMF signals (lb = 2).

DMF was consequently selected as the most appropriate of the potential reference compounds investigated. Although the DMF spectrum contains more than one proton resonance, the methyl peaks are well removed from the signals to be monitored during the assay. With DMF as the reference, only the region of the spectrum between 6 and 8 ppm need be considered when processing the data (Figure 4.4). All other signals arising from the substrate, product, buffer and solvent, which occur up field of this region, can be ignored. Figure 4.4 shows the region of the spectrum from which the data is extracted for a typical assay using DMF as the reference. The improvement in clarity, when compared to the spectrum using ^{t}BuOH as the reference (Figure 4.2) is obvious. As anticipated, the use of a reference compound with a signal closer in chemical shift to that of the DHS **1.5** proton, made processing the spectral data easier, more efficient and, most importantly, more precise.

4.2.2.3 Spin-Lattice Relaxation Times

An accurate concentration of product relative to reference can not be directly obtained from the respective peak integrals. This is because the spin-lattice relaxation times (T1) for the protons in question are different. While the DHS H-2 has a T1 of 6.0 s (averaged over both

peaks of the doublet), the DMF signal has a T1 of 8.4 s. To allow for full relaxation of the protons between acquisitions (in order to obtain quantitative data from the integrals), a relaxation delay (d1) of approximately 5T1 is required. This amounts to a necessary relaxation delay (d1) of 42 s. This was completely inappropriate as data acquisition would take much too long. An alternative value of d1 needed to be chosen.

The longer the time interval between pulses, the greater the extent of relaxation of the proton, and the greater the intensity of the resulting signal. The effect of the value of d1 on the intensity of the signals to be monitored and the quality of the data obtained was investigated. Increasing the value of d1 in 1 s increments from 0 up to 5 seconds showed a corresponding significant increase in the intensity of the product signal. Beyond this point however, the improvement in the signal with each 1 s increase in d1 was less dramatic. Values for d1 of 5 s and 10 s were considered as a compromise between maximum signal intensity and minimum acquisition time. While d1 = 10 gave slightly better data, with better signal to noise in the NMR spectrum and less scatter in the rate data, it also took much longer to acquire the data, meaning that fewer data points could be obtained for the [DHS] vs. time curve during the initial phase of the reaction.

4.2.2.3.1 Calibration Curves

A relaxation delay (d1) significantly below the time required for full relaxation of both DHS and reference peaks results in a ratio of signal areas which is *not* equal to the ratio of the concentrations. This necessitates the construction of a calibration curve, in order to obtain a constant of proportionality, allowing the ratio of the concentrations of DHS and DMF to be calculated from the ratio of signal areas.

$$[\mathrm{DHS}]_{\mathrm{calc}} = \frac{\text{DHS integral}}{\text{Reference integral}} \times [\text{Reference}] \qquad (4.1)$$

To obtain a calibration curve for the reference, spectra were acquired for samples of known product and DMF concentrations and the integrals measured for the reference and product signals. A calculated value for the concentration of the product DHS **1.5** ($[\mathrm{DHS}]_{\mathrm{calc}}$) was obtained by measuring the integrals and calculated according to Equation 4.1. Calibration

curves were prepared with $[DHS]_{calc}$ on the abscissa and the actual known product concentration $[DHS]_{actual}$ on the ordinate axis.

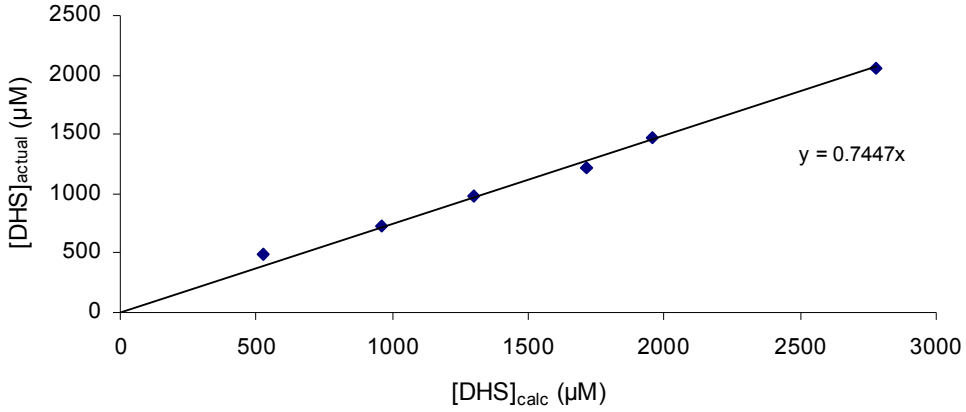

Figure 4.5 Calibration curve for DMF as reference (d1 = 5).

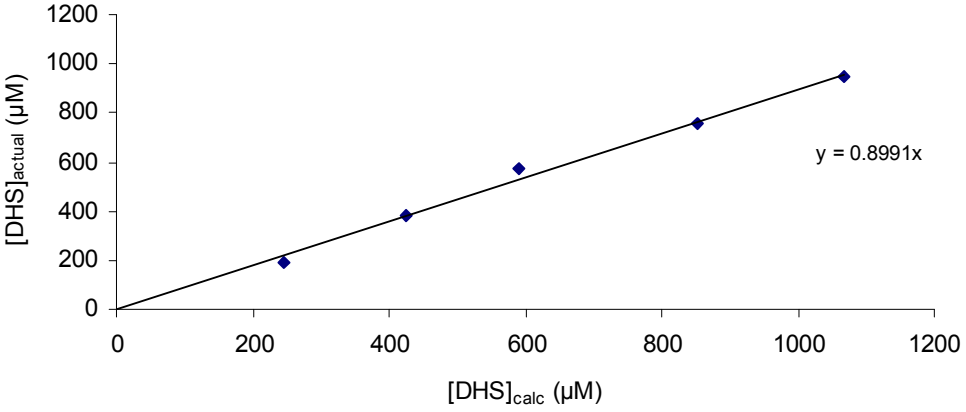

Figure 4.6 Calibration curve for DMF as reference (d1 =10).

Calibration curves were obtained for DMF as a reference with d1 = 5 s (Figure 4.5) and 10 s (Figure 4.6). Both of the calibration curves have a slope that is less than 1, indicating that the actual DHS concentration ($[DHS]_{actual}$) is less than the DHS concentration calculated from the spectrum ($[DHS]_{calc}$) using equation 4.1. This overestimation of calculated DHS concentration is due to the shorter spin-lattice relaxation time of the DHS proton relative to the reference proton, giving a more intense DHS signal relative to the reference signal at equal concentrations. The actual concentration of DHS in the assay samples can therefore be

calculated from the ^{1}H NMR spectra according to equation 4.2 where the calibration constant **C** is equal to the slope of the calibration curve.

$$[DHS]_{actual} = \frac{\text{DHS integral}}{\text{Reference integral}} \text{ x } \mathbf{C}[\text{Reference}] \qquad (4.2)$$

The DMF calibration curves illustrate that using a value of d1 equal to 10 s gives a better approximation of the DHS concentration than does a value of d1 equal to 5 s (Figure 4.5 and Figure 4.6). In spite of this, d1 = 10 s was deemed to increase the acquisition time to too great a degree, and a value of d1 = 5 s was adopted.

4.3 Optimisation of the Experiment

With the establishment of a serviceable method for determining the concentration of DHS **1.5** in the assay solution by ^{1}H NMR, it became necessary to optimise the experiment in order to obtain the most reliable rate data possible by this method. Various factors were taken into consideration in optimising the experiment, including the choice of reference as discussed in section 4.2.2, the reaction conditions of the assay, the way the ^{1}H NMR experiment was set up and the way the data was processed.

4.3.1 Optimisation of the Assay Conditions

In optimising the reaction conditions of the assay, the best substrate and enzyme concentrations had to be chosen. In order to construct a Dixon plot (Section 3.1.2) to determine K_i for the inhibitor, 3 or 4 different substrate concentrations are required. The substrate and enzyme concentrations chosen would determine the rate of the reaction to be monitored. The tailoring of the assay conditions to give an appropriate rate was a crucial factor in establishing a working assay. The time available for collection of initial rate data and the concentration of the product present in the solution would be determined by the rate

of the reaction, these factors therefore had to be taken into account when selecting the substrate and enzyme concentrations for the assay.

4.3.1.1 Detection Limit for Product Concentration

The use of ^{1}H NMR as a detection method imposes a limiting concentration of DHS **1.5**, below which the signal to noise ratio is extremely poor, or the signal cannot be observed at all. It was found that 50 μM was the practical minimum DHS concentration which could be readily observed by ^{1}H NMR. The substrate and enzyme concentrations therefore, must be sufficient to give rise to a DHS concentration of at least 50 μM within 2-3 minutes of initiating the reaction (the time required to set up the NMR experiment) in order to give a measurable signal for the duration of the data collection. The greater the rate of the reaction, the earlier the limiting concentration of DHS would be reached. However, the greater the rate of substrate turnover, the briefer the interval over which the progress curve remains linear. The change in absorbance at 234 nm due to formation of DHS was monitored for different concentrations of DHQ **1.4** and *S. coelicolor* DHQase in order to determine which combinations would produce 50 μM concentrations of DHS within 2 minutes of initiation of the reaction.

4.3.1.2 Linearity of Initial Rate

Substrate and enzyme concentrations had to be chosen such that there was sufficient substrate for the reaction progress curve to remain linear (to a reasonable approximation) over the time required to acquire the data. The minimum time required to set up the NMR experiment and collect the data was 12 minutes (2 minutes to set up the experiment and 10 minutes to collect the data). The reaction progress for different combinations of enzyme and substrate concentrations was followed spectrophotometrically in order to find a combination which gave a reaction progress curve which remained linear for at least 12 minutes but also produced a product concentration of 50 μM within the first 2 minutes (as discussed in the preceding section). The lower the concentration of enzyme relative to substrate, the longer the period over which the progress curve remained linear. However if the rate of reaction

was too low, sufficient quantities of DHS **1.5** would not be produced within the necessary time frame of the experiment.

4.3.1.3 Dependence of Rate on Substrate Concentration

Another issue to take into consideration was the degree of dependence of the rate of the reaction on the substrate concentration. Obviously, attaining high concentrations of product in the initial stages of the reaction and maintaining a linear progress curve for an extended time interval would be favoured by a high substrate concentration relative to the enzyme concentration. However, at very high substrate concentrations the rate becomes virtually independent of substrate concentration, as described by the Michaelis-Menten equation (equation 3.1) and illustrated in Figure 3.3. To construct a Dixon plot, a series of substrate concentrations is required, each giving rise to a different initial rate. Thus the chosen substrate concentrations must be low enough that there is a measurable difference between the resulting initial rates.

4.3.1.4 Test Run

Substrate concentrations in the region of 500-1250 μM and an enzyme concentration of 0.04 μgmL^{-1} were initially chosen to satisfy the above criteria. The ^{1}H NMR assay method was tested by determining the initial rates of reaction for duplicate samples from the chosen series of substrate concentrations in the absence of inhibitor. It was found that although the rates of reaction at such high substrate concentrations could easily be distinguished spectrophotometrically, the differences between the rates were too small and the ^{1}H NMR method not sufficiently sensitive to measure such small differences. The result being that the measured initial rates for the different substrate concentrations were found to be approximately equal, within the range of error, by ^{1}H NMR. Figure 4.7 shows the rate data obtained by ^{1}H NMR at substrate concentrations of 500, 750, 1000 and 1250 μM along with corresponding data obtained by UV/vis spectroscopy. Choosing a series of lower substrate concentrations to obtain a larger difference between rates gave product concentrations which were too low to obtain useful data.

There seemed to be no practical solution offering a series of substantially different rates all at high substrate concentrations. It was decided instead to obtain rate data for one high substrate concentration only, which would then be used to construct a dose-response plot, from which could be determined the IC_{50} for an inhibitor.

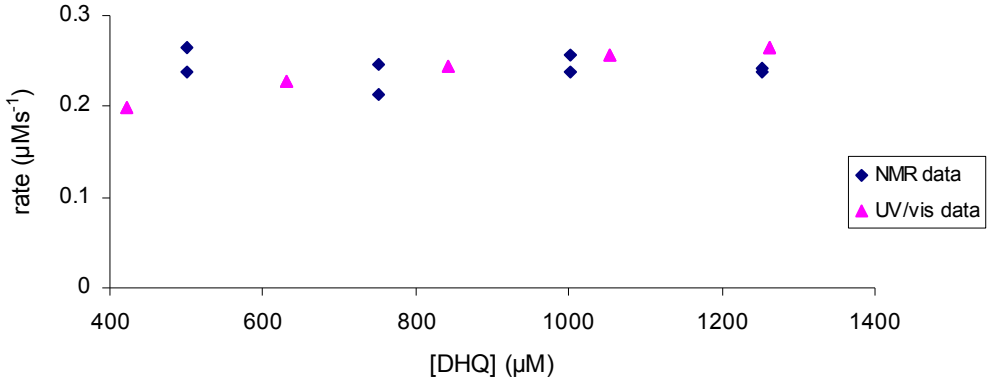

Figure 4.7 Comparison of rate data by ^{1}H NMR with data obtained by UV/vis spectroscopy.

4.3.2 Optimisation the NMR Experiment

Several parameters were investigated in an attempt to optimise the NMR data obtained. In general, two main sets of parameters were considered. The parameters used when setting up the NMR experiment, and the parameters used when processing the spectra in order to extract the best quality data from the spectra obtained.

4.3.2.1 Experimental Parameters

The two main factors which need to be considered when selecting the parameters for setting up the ^{1}H NMR experiment are signal-to-noise ratio and time-scale. There is always a compromise between choosing parameters that give the best signal-to-noise ratio, and keeping the time-scale of the experiment within the period for which the progress curve is known to remain linear.

4.3.2.1.1 Signal-to-Noise Ratio

A poor signal to noise ratio is one of the greatest contributing factors to error in the experimental data. Irregularities in the baseline that overlap with the signals to be measured cause significant variations in the integrals and hence the concentrations calculated. As the assay is conducted at very low concentrations relative to a normal NMR spectrum obtained for the purposes of product characterisation, the signals to be measured are weak and the baseline noise substantial. A number of parameters can be adjusted in order to improve the signal to noise ratio.

4.3.2.1.1.1 Number of Transients

The number of transients acquired has a great affect on the quality of the spectra obtained. The greater the number of transients acquired, the better the signal to noise ratio. In order to optimise the data obtained, a large number of transients ought to be collected. However, the more transients acquired, the more time required to collect the spectra. With a non-zero delay between acquisitions of transients, the time required to collect each spectrum becomes substantial.

It was found that increasing the number of transients per spectrum from 8 to 16 resulted in an observable improvement in the smoothness of the baseline and consistency of the concentration vs. time data obtained. However, without decreasing d1 below the allotted 5 s, a minimum of 20 minutes was required to collect 10 data points. This was too long, as the progress curve only remained linear for a little longer than 12 minutes. Increasing the number of transients acquired by 1 or 2 made no appreciable difference to the data. As a compromise between quality of spectra and time required to collect the data, 8 transients were collected for each spectrum. A value of d1 equal to 5 s allowed a series of 10 spectra to be collected over a period of 10 minutes.

4.3.2.1.1.2 Relaxation Delay (d1)

As discussed previously in section 4.2.2.3, the value of d1 chosen has an effect on the intensity of the resulting signal. Increasing the relaxation delay increases the intensity of the signal by increasing the proportion of protons allowed to relax back to the ground state before subsequent re-excitation. As relaxation is described by a decay curve (the half-life being

equal to the spin-lattice relaxation time T1), incremental increases in d1 correspond to consecutively smaller corresponding increases in the extent of relaxation and thus intensity of the signal. Beyond a certain point, increasing d1 by 1 s makes minimal difference to the signal intensity. In the interests of completing the data collection within an acceptable time interval, in this case, the 12 minutes for which the reaction progress curve was known to be approximately linear, a value of d1 equal to 5 s was chosen. Some experiments were also carried out with d1 = 10 s, however, in order to reduce the time required to acquire the data, fewer data points were able to be obtained. Although d1 = 10 seemed to give marginally more consistent data (i.e. the concentration vs. time data showed less scatter), it was deemed to be in the interests of experimental accuracy to obtain as many data points as possible in order to minimise the contribution of outlying points. Therefore the majority of experiments were carried out with d1 = 5 s.

4.3.2.1.1.3 Signal Suppression

The assay experiments were carried out with water as the solvent and it was therefore necessary to suppress the water signal in order to observe the required resonances. However, the signal due to the Tris.HCl buffer at a concentration of 50 mM was very large relative to the micromolar concentrations of DHS and reference, and overwhelmed much of the central region of the spectrum. It was thought that a simultaneous suppression of both water and buffer signals might decrease the experimental error associated with the method, resulting in more consistent concentration vs. time data.

Figure 4.8 shows the ^{1}H NMR spectrum of a sample acquired with simultaneous suppression of water and buffer signals (spectrum A) and without suppression of the buffer signal i.e. with suppression of the water signal alone (spectrum B). Note the absence of the very intense buffer peak at 3.6 ppm from spectrum A and the presence of the buffer satellite peaks, which were not apparent in spectrum B due to the distortion of the baseline resulting from the baseline correction. No significant improvement was observed in the integrity of the rate data however, and so the double suppression approach was abandoned as the result did not justify the additional time required to set up the experiment. The assay was therefore carried out with suppression of the water signal only.

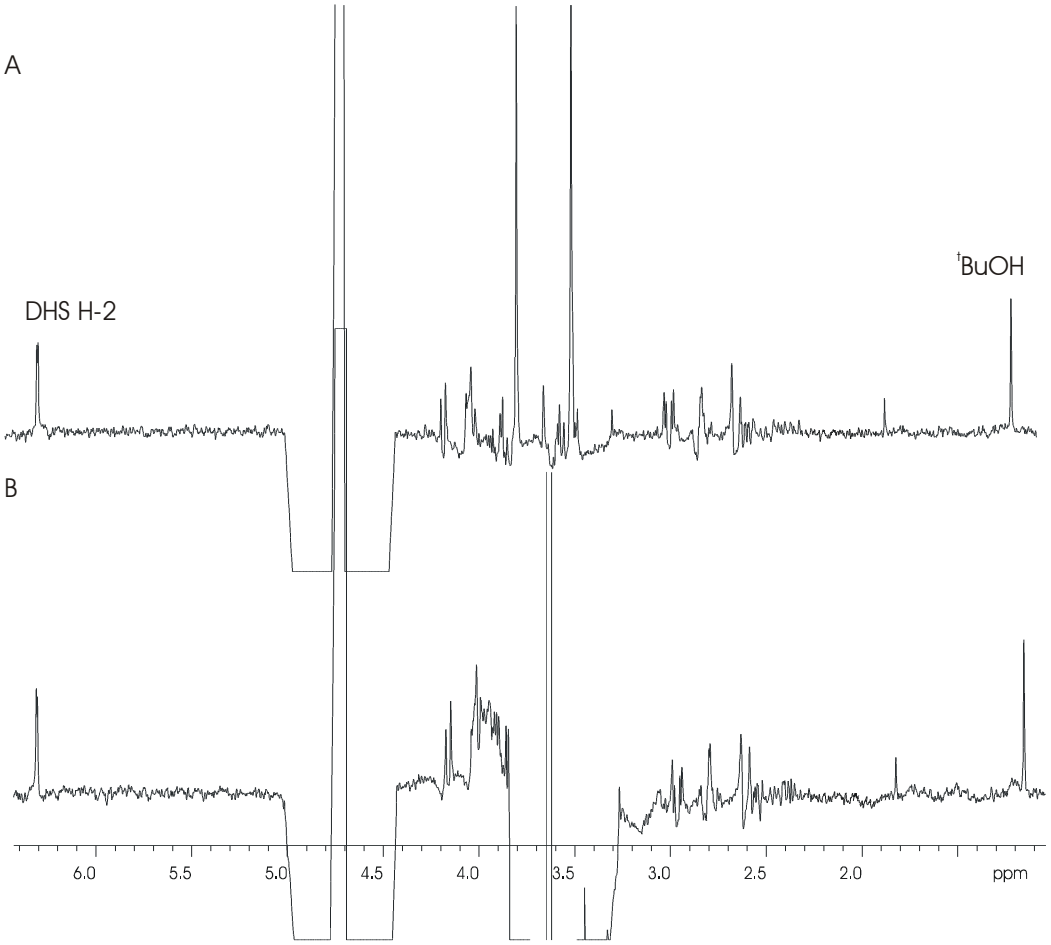

Figure 4.8 ^{1}H NMR spectra of an assay sample A. with suppression of the buffer signal and B. without suppression of the buffer signal.

4.3.2.1.1.4 Decoupling of the Doublet Product Signal

Another approach employed in an attempt to increase the signal to noise ratio by increasing the intensity of the DHS **1.5** signal was to decouple the signal by irradiating H-6_{ax} ($\delta_H(D_2O)$ = 2.6 ppm), the proton to which it is coupled (J = 2.9 Hz). However, the increase in intensity of the signal when collapsed to a singlet was minor relative to the initial signal intensity. It was concluded that this minimal gain in signal intensity did not justify the additional time and inconvenience required to set up the experiment with decoupling of the DHS **1.5** proton.

4.3.2.1.2 Time-Scale

The ^{1}H NMR assay depends on measuring the *initial* rate of reaction, that is, the linear part of the reaction progress curve. The time required to collect the data therefore needs to be as short as is practically possible. Every action taken to improve the quality of the data obtained increases the time required to collect the data. In addition to the number of transients collected and the relaxation delay (d1) discussed above, factors that affect the time required to collect the data include the number of spectra acquired (i.e. the number of data points on the final concentration vs. time curve) and the time between acquisition of each spectrum.

4.3.2.1.2.1 Number of Spectra Collected

Each spectrum collected for an assay sample gives one point on the [DHS] vs. time curve. There is a substantial amount of scatter amongst these points and so, ideally, a large number of points would be collected to minimise the contribution of outliers. However, the more points obtained, the more spectra that must be acquired and the longer the time required to collect the data. The maximum number of spectra that could be acquired in one experiment was 12. It was decided that 10 points would be taken for each curve, thus 10 spectra. With a relaxation delay d1 of 5 s, 10 spectra could be collected in 12 minutes, including the 2 minutes required to set up the experiment subsequent to initiation of the reaction.

4.3.2.1.2.2 Pre-acquisition Delay

The pre-acquisition delay is the time interval between the completion of acquisition of one spectrum and the start of acquisition of another. In order to minimise the time taken to complete the experiment, a small delay was needed. It was also felt that it would be best to choose a pre-acquisition delay at least equal to the relaxation delay d1 and so a pre-acquisition delay of 5 seconds was chosen. Collecting 8 transients per spectrum, with a 5 s relaxation delay between transients, and a 5 s pre-acquisition delay between spectra, for a total of 10 spectra, required a total data acquisition time of 10 minutes.

4.3.2.2 Data Processing Parameters

Once the spectra have been acquired they must be processed in order to extract the concentration data. There are several parameters that can be optimised in order to obtain the best possible data. The two factors that can be influenced subsequent to acquiring the spectra are peak shape and integrals.

4.3.2.2.1 Peak Shape

The shapes of the peaks to be measured have a large impact on the quality of the concentration data. If the shape of the peak varies significantly from one spectrum to another in a series, a significant error is introduced and the concentration vs. time data can manifest a great deal of scatter. Thus the optimal peak shape must be obtained before selecting the integral regions.

4.3.2.2.1.1 Fourier Number (fn)

This parameter determines the number of points included in the Fourier transform of the free-induction decay (FID). Increasing the Fourier number can be used to increase the resolution of the resulting spectrum by zero-filling. The better the resolution, the closer the signals appear to their true shape, and the more accurately the relative peak areas reflect the relative concentrations.

4.3.2.2.1.2 Phasing

If the signals to be measured are not phased properly and consistently, the area under the peak is not a good measure of the substance concentration. The DHS **1.5** and reference signals must be phased manually and the optimum phasing for each signal judged by eye. The manual phasing carried out on one spectrum of the series also phases every other spectrum in that series to the same degree. However, there is still a certain amount of unavoidable inconsistency in the shapes of the peaks from one spectrum to the next, arising mainly from irregularities in the baseline, and contributing significantly to the scatter observed in the concentration vs. time data.

4.3.2.2.1.3 Line broadening (lb)

Another way of smoothing out the shapes of the peaks is to use line broadening. Although the broadening of the signal makes it appear less intense, it also decreases significantly the baseline noise which can interfere with the measured signals. Varying degrees of line broadening (lb) were trialled, from the standard 0 up to 3. A value of lb = 2 was found to give the greatest improvement in the data. Figure 4.9 shows the appearance of a typical assay spectrum after processing with A) lb = 0 and B) lb = 2. It is plain to see that the line broadening makes the spectrum clearer so that the integral regions may be selected incorporating the minimum contribution from nearby baseline features.

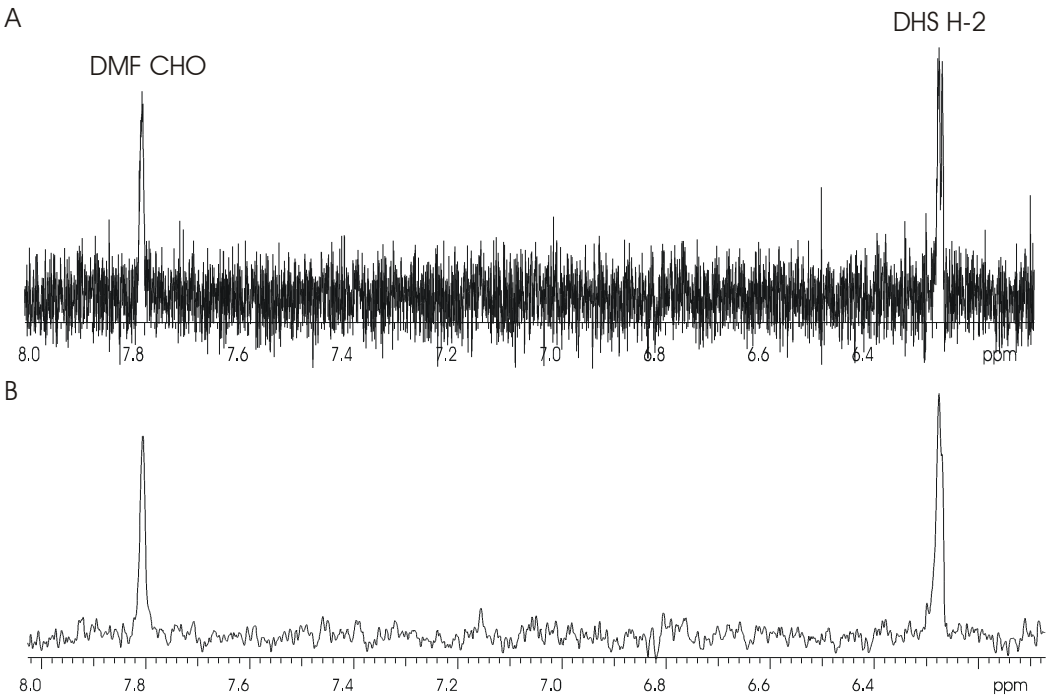

Figure 4.9 Partial ^{1}H NMR spectrum of an assay sample showing the effect of line broadening (lb) on the appearance of the spectrum. A. lb = 0; B. lb = 2.

4.3.2.2.2 Integrals

The shape and position of the integral regions has a significant effect on the resulting data. Thus great care must be taken in determining exactly which areas of the spectrum will be taken into account in the calculation of relative peak area.

4.3.2.2.2.1 Selection of Integral Regions

When selecting the integral regions, the spectrum is expanded as much as possible about the two peaks to be measured. Ideally, the integral region must include the entire signal to be measured, without including any nearby irregularities in the baseline. This can sometimes be problematic as the signals often overlap with significant baseline irregularities and judgement must be exercised in determining the best positioning of the integral region to best reflect the true peak area.

4.3.2.2.2.2 Baseline Correction

Once the integral regions have been selected, the baseline correction straightens and evens out the baseline around the selected integral regions, bringing the two signals into line with one another. This is necessary because both the phasing of the signals and the large vertical expansion of the spectrum required to view the signals of the dilute DHS **1.5** and reference components can severely distort the baseline.

4.3.2.2.2.3 Level Tilt

The level tilt can be used to ensure that any parts of the integral that extend beyond the edge of the signal and over the baseline are as near as possible to horizontal. Any non-horizontal peripheral parts of integrals will add to (or subtract from) the measured relative peak area.

4.4 GENERAL METHOD

Based on the above considerations, a general method was developed for the ^{1}H NMR assay. The assay samples consisted of 550 μL of solution, containing substrate, inhibitor, DMF, Tris.HCl buffer (50 mM), and water and were prepared in 2 mL vials. The reaction was initiated by addition *S. coelicolor* DHQase solution in 50 mM buffer. The sample was then transferred to a 5 mm NMR tube with a D_2O-filled insert and inserted into the spectrometer, at a temperature of 25 ºC.

After locking and shimming the sample one transient was acquired in order to set up the solvent peak suppression. The experiment was then set up to collect 10 spectra, with a 5 s pre-acquisition delay before the start of acquisition of each spectrum. Each spectrum consisted of 8 transients, with a relaxation delay (d1) of 5 s between each transient. The set-up took approximately 2 minutes and acquisition of each spectrum took 55 s plus an extra 5 s delay before acquisition of the succeeding spectrum, leading to a total of 10 minutes for complete data acquisition.

The spectra obtained were processed with fourier number (fn) = 128k and line-broadening (lb) = 2. The spectrum was expanded vertically and horizontally so the DHS and DMF peaks could be seen clearly. The two signals at 6.3 and 7.8 ppm were then phased manually. The integral regions were selected, then the baseline corrected. The level-tilt was adjusted if necessary. The integral regions were displayed and their values recorded. The baseline correction and recording of the integrals was repeated for each spectrum in the series.

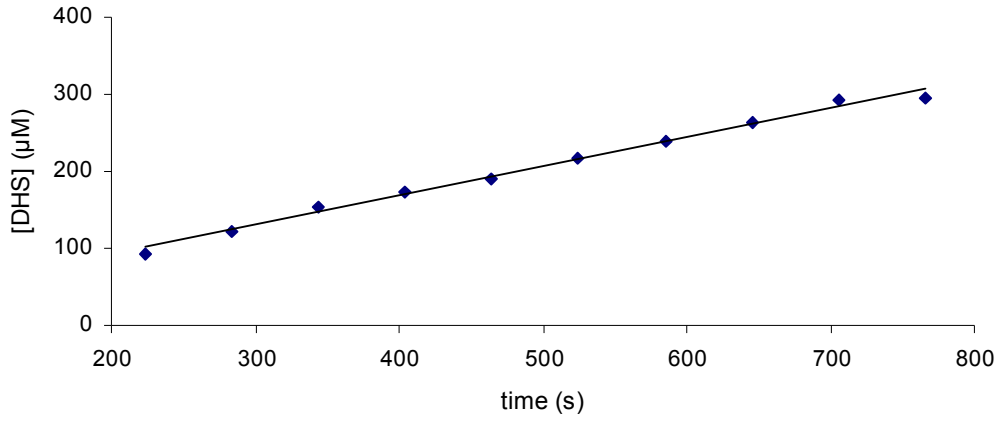

Figure 4.10 An example of a partial product concentration vs. time curve for the conversion of DHQ **1.4** to DHS **1.5** by DHQase obtained by ^{1}H NMR.

The product concentrations were calculated for each spectrum using equation 4.2 and plotted against the time of completion of acquisition of each spectrum. The rate was determined by fitting a straight line to the data and taking the slope. An example of a [DHS] vs. time curve obtained by ^{1}H NMR for the initial stage of the enzymatic reaction is shown in Figure 4.10.

4.5 ASSAY RESULTS AND DISCUSSION

4.5.1 Dose-Response Curves for Inhibitors

The activity of the inhibitors with sp^2 character at C-3, **2.15**, **2.27**, **2.38**, **2.44**, **2.46** and **3.1**, against *S. coelicolor* DHQase was assessed by ^{1}H NMR assay. Dose-response curves were obtained in preference to Dixon plots, as the NMR method lacked the sensitivity of the spectrophotometric method and so was unable to distinguish such small differences in rates. The IC_{50} for the inhibitor could then be determined from the dose-response plot by non-linear least-squares fitting of the data to Equation 4.3.[1] The inhibition constant K_i can be calculated from the IC_{50} using the Cheng and Prusoff relationship for competitive inhibition (Equation 4.4).[1,2]

$$\frac{v_i}{v_0} = \frac{1}{1 + \frac{[I]}{IC_{50}}} \qquad (4.3)$$

$$K_i = \frac{IC_{50}}{1 + \frac{[S]}{K_M}} \qquad (4.4)$$

4.5.1.1 Dose-Response Curve for Dicarboxylate Inhibitor 2.27

Inhibitor **2.27** was assayed against *S. coelicolor* DHQase using the ^{1}H NMR method. A dose-response curve was compiled and is shown in Figure 4.11, where v_i is the rate in the presence of inhibitor, v_0 is the rate in the absence of inhibitor and v_i/v_0 is the fractional rate. As can be seen in the figure, the curve is incomplete, in that it does not extend as far as $v_i/v_0 = 0$. This is because it was not possible to obtain data for sufficiently high inhibitor concentrations to observe the full curve because the signals due to the inhibitor overwhelm those due to DHS **1.5** and the reference DMF at such high concentrations. The other obvious contributing factor to the incomplete state of the curve is the lack of potency of the inhibitor **2.27**. The fact that the fractional rate v_i/v_0 does not reach zero within an inhibitor

concentration of 30 mM indicates that **2.27** is not a very good inhibitor of *S. coelicolor* DHQase. Also, the substrate concentration at which the experiment was carried out was high (800 μM) in order to generate a sufficient product concentration during the initial stage of the reaction. Given the dependence of the IC_{50} on substrate concentration, using a lower concentration of substrate would give a lower IC_{50} and thus a more complete dose-response plot could be obtained using the same inhibitor concentrations. Least squares fitting of the data to equation 4.3 gives a value of IC_{50} = 61 ± 9 mM. Using equation **3.2** and K_M = 200 μM to calculate K_i for [S] = 800 μM gives an inhibition constant of 12 ± 2 mM. This result confirms that **2.27** is a very poor inhibitor of *S. coelicolor* DHQase.

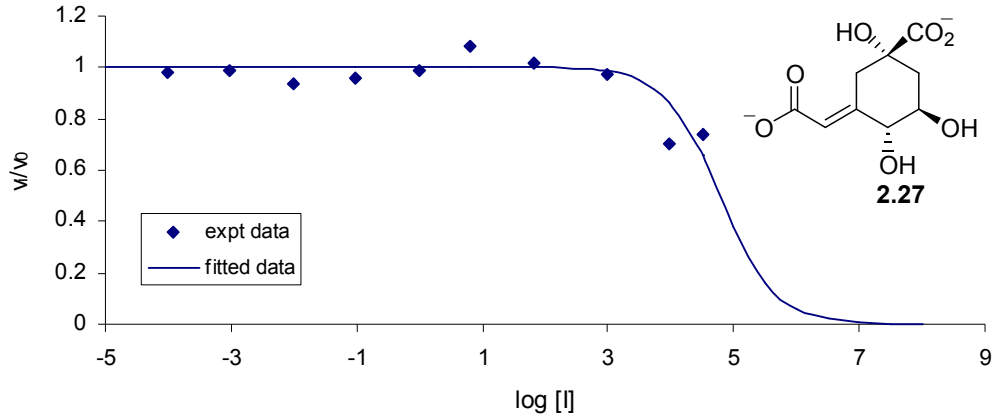

Figure 4.11 Dose-response plot for inhibitor **2.27**. Reference = DMF, d1 = 10.

4.5.1.2 Dose-Response Curve for Oxime Inhibitor 1.36

It was necessary to validate the method by using it to determine an inhibition constant for a known inhibitor and also to attempt to obtain a more complete dose-response plot using a more potent inhibitor. Therefore the known inhibitor **1.36** was assayed against type II DHQase from *S. coelicolor* at a substrate concentration of 800 μM. As in the case of inhibitor **2.27**, the dose-response curve does not extend to a fractional rate of zero, although the curve for oxime **1.36** is more complete than that for **2.27**. Least squares fitting of the data gave an IC_{50} of 2600 ± 800 μM. A K_i of 520 ± 150 μM was obtained using Equation 3.2. This is in agreement with the both the K_i of 530 ± 80 μM obtained using the spectrophotometric assay and the reported value of 500 ± 200 μM.[3] This attainment of a K_i

for a known inhibitor, in agreement the values previously obtained using a spectrophotometric assay, proves that this is a valid method for assaying inhibitors of *S. coelicolor* DHQase.

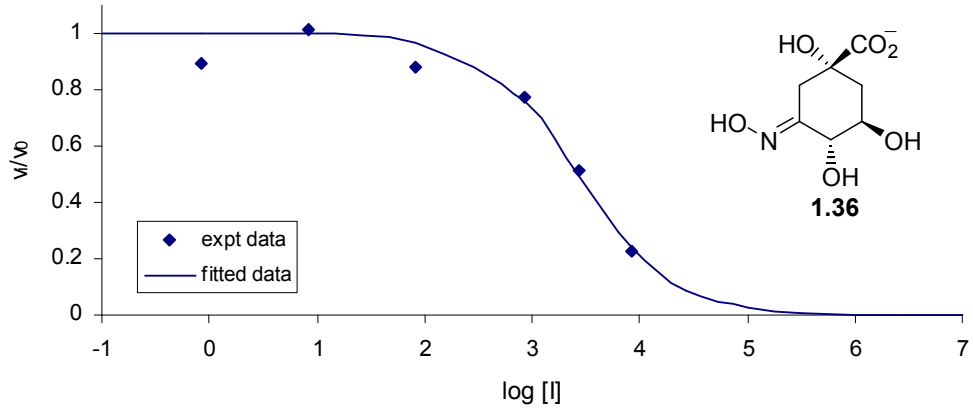

Figure 4.12 Dose-response plot for known oxime inhibitor **1.36** against *S. coelicolor* DHQase.

4.5.1.3 Single-Point Inhibition Studies

The incomplete nature of the dose-response curves obtained indicated that full curves would only be obtained for more potent inhibitors. It was therefore decided not to obtain dose-response plots for other inhibitors unless prior experiments indicated that the inhibitors would be sufficiently potent to obtain reasonably complete curves. For inhibitors **2.15**, **2.38**, **2.44**, **2.46** and **3.1** therefore, the degree of inhibition was determined at fixed inhibitor and substrate concentrations. The initial rates of reaction were measured both in the presence and absence of inhibitor, at the same substrate concentration and the activity remaining determined as a percentage of the initial activity in the absence of inhibitor. The inhibition at the given inhibitor concentration was then defined as being equal to 100% minus the activity remaining. The experiments were carried out at a substrate concentration of 800 μM. The inhibitor concentrations employed were subject to availability of material and are shown, along with the inhibition results, in Table 4.1. The inhibitor concentrations listed are for the major isomer only in the cases of **2.38** and **2.44**, and the combined concentration of both isomers for **2.46**. The % inhibition by **2.27** that would be expected at an inhibitor

concentration of 5000 μM was calculated from the data obtained for the dose-response curve and is included in the table for the sake of comparison.

Table 4.1 Inhibition results for inhibitors **2.15**, **2.38**, **2.44**, **2.46** and **3.1** against *S. coelicolor* DHQase as determined by ^{1}H NMR spectroscopy.

Inhibitor	[DHQ] (μM)	[I] (μM)	Enzyme Activity Remaining (%)	Inhibition (%)
2.15	800	5000	62 ± 17	38 ± 17
2.27[a]	800	5000	92	8
2.38[b]	800	5000	89 ± 16	11 ± 16
2.44[c]	800	4500	11 ± 6	89 ± 6
2.46[d]	800	1100	89 ± 7	11 ± 7
3.1	800	5000	10 ± 5	90 ± 5

[a] Calculated from data obtained for the dose-response plot. [b] 20:1 (*E*:*Z*). [c] 9:1 (*E*:*Z*). [d] 3:2 (*E*:*Z*).

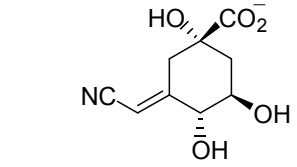

2.15

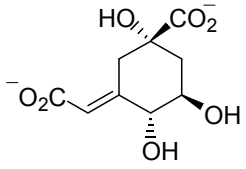

2.27

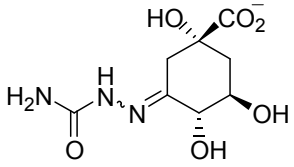

2.38

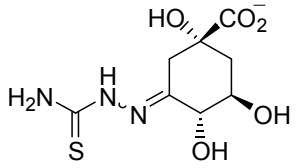

2.44

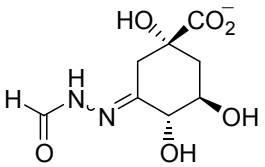

2.46

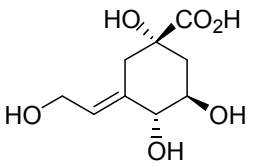

3.1

Two of the inhibitors whose activity was evaluated in this way were found to display substantial activity against *S. coelicolor* DHQase. Allylic alcohol inhibitor **3.1** and thiosemicarbazone inhibitor **2.44** showed 90% and 89% inhibition respectively of *S. coelicolor* DHQase. Dose-response plots for these inhibitors against *S. coelicolor* DHQase were therefore obtained by ^{1}H NMR spectroscopy. The remaining inhibitors **2.15**, **2.38** and **2.46** were deemed to be insufficiently active to justify obtaining dose-response plots.

4.5.1.4 Dose-Response Curve for Thiosemicarbazone Inhibitor 2.44

Thiosemicarbazone inhibitor **2.44** was assayed as a 9:1 mixture of *E* and *Z* isomers and the calculated IC_{50} is based on the concentration of the major isomer. The dose-response plot obtained for inhibitor **2.44** is shown in Figure 4.13. The x-axis shows the $\log_{10}$ of the concentration (in μM) of the major isomer. The experimental data is shown as points and the curve obtained by least squares fitting of the data to equation 4.3 is shown as a solid line. An IC_{50} of 1100 ± 200 μM was obtained, which corresponds to an inhibition constant (at 800 μM substrate concentration) of 220 ± 40 μM, according to the Cheng and Prusoff relationship (equation **3.2**).

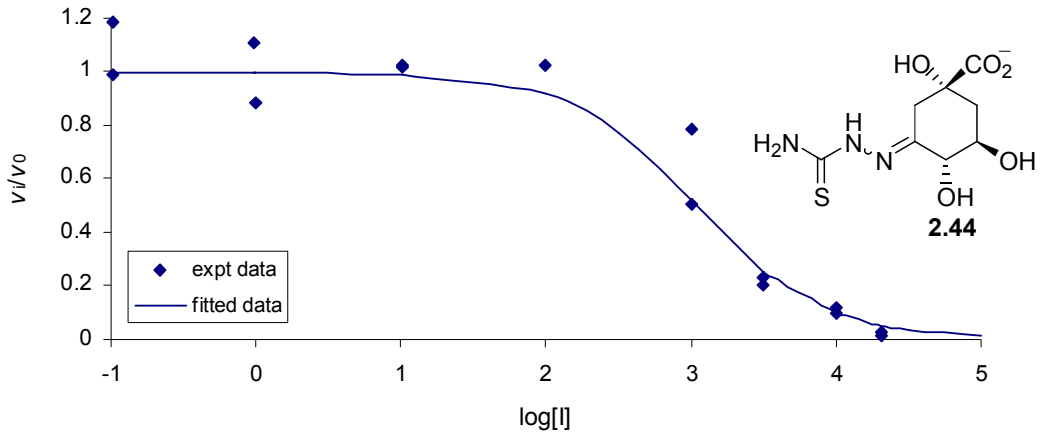

Figure 4.13 Dose-response curve for thiosemicarbazone inhibitor **2.44**, in a 9:1 ratio of isomers (*E*:*Z*), with the x-axis displaying the log of the concentration (μM) of the major isomer.

4.5.1.5 Dose-Response Curve for Alcohol 3.1

The dose-response plot obtained for inhibitor **3.1** is shown in Figure 4.14. The plot shows two curves obtained by least-squares fitting of the data to Equation 4.3. The upper curve shows the fit including the outlying point at log[I] = 3.75, and the lower curve shows the fit calculated without including this point. The upper fit gives an IC_{50} of 500 μM and the lower fit an IC_{50} of 280 μM. The Cheng and Prusoff relationship (Equation **3.2**) gives

corresponding inhibition constants K_i of 98 μM and 56 μM respectively. Averaging the two results gives a K_i of 77 ± 21 μM.

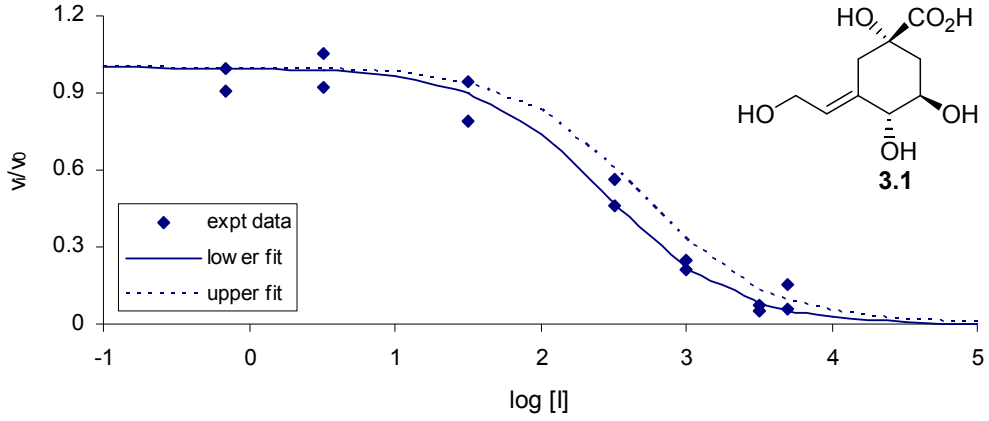

Figure 4.14 Dose-response plot for inhibitor **3.1** against *S. coelicolor* DHQase.

4.5.2 Discussion of ^{1}H NMR Assay Results

The three inhibitors with C at C-3 and with sp^2 character at C-3 (**2.15**, **2.27** and **3.1**), showed dramatically different activities against *S. coelicolor* DHQase. Nitrile **2.15** was found to be a fairly poor inhibitor of *S. coelicolor* DHQase. This was unsurprising given the moderate activity observed for the reduced analogues **2.16** and **2.17** by spectrophotometric assay (Chapter 3). The dicarboxylate inhibitor **2.27** was an even poorer inhibitor of *S. coelicolor* DHQase. This is consistent with the lower activity of the saturated, equatorial carboxylate inhibitor **2.28** relative to the corresponding nitrile **2.16**. What is slightly surprising is the substantially greater activity displayed by allylic alcohol **3.1** against *S. coelicolor* DHQase relative to the other sp^2 inhibitors **2.15** and **2.27**.

The x-ray crystal structure of *S. coelicolor* DHQase with the inhibitor 2,3-anhydroquinic acid **1.37** bound in the active site indicates that this enzyme is able to bind a glycerol molecule in the active site, as well as the inhibitor.[4] This is the basis of the design of the series of inhibitors **1.43**-**1.50** prepared by Abell and co-workers (Chapter 1).[5] Inhibitor **3.1** is more active against *S. coelicolor* DHQase than the most potent of these inhibitors, compound **1.45**. It is however less potent than the parent inhibitor **1.37**. It is possible that the side-chain

hydroxyl of **3.1** is able to enhance binding by binding in the glycerol binding pocket. However, if this is the case, the carboxylate side-chain of **2.27**, expected to be of similar length to that of **3.1**, ought also to extend into the glycerol binding pocket, leading to enhanced binding. This is clearly not the case, supporting the assumption that the carboxylate group participates in a particularly disadvantageous interaction when the side chain is equatorial (see discussion of spectrophotometric assay results for *S. coelicolor* DHQase in Section 3.3.3) or joined to the carbocyclic ring *via* a double bond.

Table 4.2 Some inhibition constants for *S. coelicolor* DHQase.

Inhibitor	**K_i (μM)** *S. coelicolor* DHQase
1.37[a]	30 ± 10
1.45[b]	180 ± 20
2.16	800 ± 100
2.27	12000 ± 2000
2.28	3000 ± 1000
2.44	220 ± 40
3.1	77 ± 21

[a] Ref. 3. [b] Ref. 5. [c] 2:1 **2.17**:**2.16**.

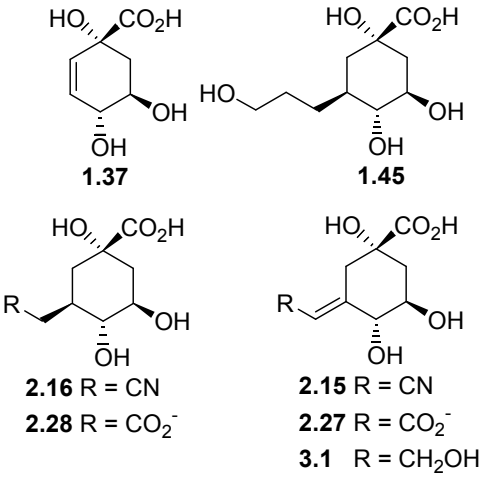

The inhibitors with N at C-3 (**2.38**, **2.44** and **2.46**) also showed interesting activity against *S. coelicolor* DHQase. In general, they appear to be no more active than the carbon based inhibitors, in contrast to the results obtained for the *M. tuberculosis* enzyme. This is consistent with the moderate activity of reported oxime inhibitor **1.36** against *S. coelicolor* DHQase. In complete contrast to the results obtained for type II DHQase from *M. tuberculosis* (Section 3.4.2.2), the thiosemicarbazone inhibitor **2.44** was substantially more active against *S. coelicolor* DHQase than the semicarbazone **2.38** or the formylhydrazone **2.46** (Table 4.1). This is consistent however, with the observation that more hydrophilic side-chains at C-3 appear to be disfavoured by *S. coelicolor* DHQase, as indicated by the poorer activity of the carboxylate inhibitors **2.27** and **2.28** relative to the corresponding nitriles **2.15** and **2.16** and alcohol **3.1**.

4.6 CONCLUSION

^{1}H NMR spectroscopy was investigated as an alternative detection method for conducting biological studies with *S. coelicolor* type II DHQase. A new method using ^{1}H NMR spectroscopy as the means of determining reaction rate was developed to obtain biological data in cases where the traditional spectrophotometric assay was inappropriate. The ^{1}H NMR method was used successfully to obtain inhibition constants for three new inhibitors and one previously reported inhibitor, and was shown to give a result in good agreement with that reported in the literature. The method is more practical for determining the % inhibition at a fixed inhibitor concentration, than for determining inhibition constants, except in cases where the inhibitors are reasonably active (K_i < 500 μM).

Although the method proved useful in enabling the acquisition of kinetic data that could not have been obtained using the spectrophotometric assay it is by no means an ideal assay for DHQase. The particular attributes of the DHQase reaction which make it not well suited to this method are the absence of a good substrate signal, so that the formation of product must be monitored instead, and that the signal to be monitored is not a very intense one. The sensitivity of the detection method is poor relative to UV/visible spectroscopy requiring high substrate concentrations and high reaction rates in order to generate sufficient product concentrations. Such high substrate concentrations lessen the observable effect of inhibitors on the rate of reaction so that unless the inhibitor is particularly potent, only partial data can be obtained for the dose-response curves required to determine the inhibition constants. The necessity for a high rate of reaction also means that the method would not be very appropriate for evaluating the activity of inhibitors against enzymes with a low k_{cat} such as *M. tuberculosis* DHQase.

An alternative methodology which would perhaps be more appropriate to the DHQase system is a coupled assay. A coupled assay for DHQase would incorporate the subsequent enzyme on the shikimate pathway, shikimate dehydrogenase, which utilises the UV active co-factor NADPH. NADPH has a λ_{max} of 340 nm,[6] which does not overlap with the signals from the product dehydroshikimate or any of the inhibitors. If sufficient shikimate dehydrogenase and NADPH were added, such that the DHQase reaction became the rate limiting step, the rate of

the DHQase reaction could be determined by monitoring the decrease in absorbance due to NADPH.

The ^{1}H NMR assay method would be more appropriate for a biological system in which the decrease in substrate concentration could be monitored in place of the increase in product concentration. This would mean that lower substrate concentrations could be used without the necessity of allowing the product concentration to build up to detectable levels. Systems possessing a very intense signal in the ^{1}H NMR spectrum of the substrate, such as a methyl group, which could more easily be monitored by NMR spectroscopy with improved signal to noise ratio, allowing lower substrate concentrations to be employed would be particularly amenable to this method.

4.7 REFERENCES FOR CHAPTER 4

(1) Copeland, R. A. *Enzymes: A practical introduction to structure, mechanism, and data analysis*; Wiley-VCH, Inc.: New York, 1996.

(2) Cheng, Y.-C.; Prusoff, W. H. *Biochem. Pharmacol.* **1973**, *22*, 3099.

(3) Frederickson, M.; Parker, E. J.; Hawkins, A. R.; Coggins, J. R.; Abell, C. *J. Org. Chem.* **1999**, *64*, 2612.

(4) Roszak, A. W. R., D. A.; Krell, T.; Hunter, I. S.; Frederickson, M.; Abell, C.; Coggins, J. R.; Lapthorn, A. J. *Structure* **2002**, *10*, 493-503.

(5) Toscano, M. D.; Frederickson, M.; Evans, D. P.; Coggins, J. R.; Abell, C.; González-Bello, C. *Org. Biomol. Chem.* **2003**, *1*, 2075-2083.

(6) Nandi, D. L.; Westley, J. *International Journal of Biochemistry & Cell Biology* **1998**, *30*, 973-977.

5 Summary and Future Work

5.1 SUMMARY

A series of potential DHQase inhibitors were prepared, based on the structure of known inhibitor oxime **1.36**. Two main classes of inhibitors were prepared. Those of general structure **2.3** with N attached at C-3 (**2.38**, **2.42**, **2.44** and **2.46**) and those of general structures **2.1** and **2.2** with C attached at C-3 *via* a single or double bond respectively (**2.15**-**2.18** and **2.27**-**2.29**). Epoxide based inhibitor **2.4** was also prepared.

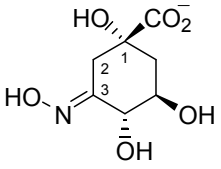
1.36

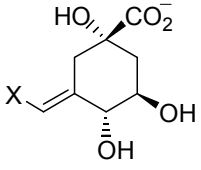
2.1

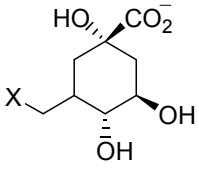
2.2

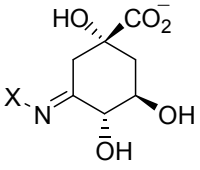
2.3

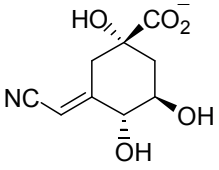
2.15

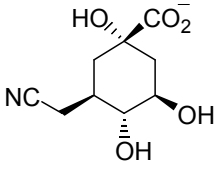
2.16

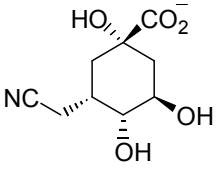
2.17

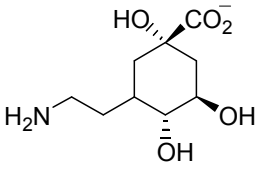
2.18

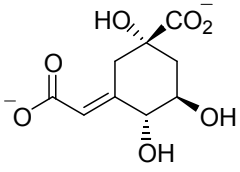
2.27

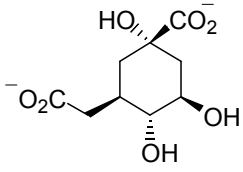
2.28

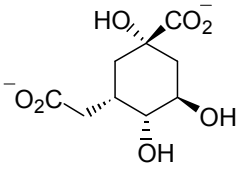
2.29

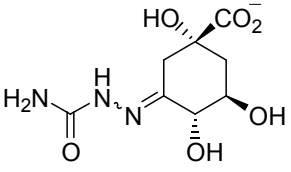
2.38

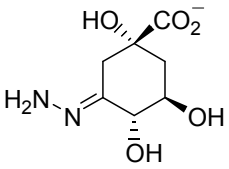
2.42

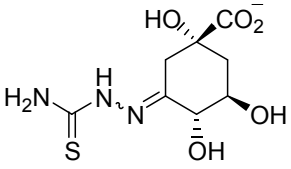
2.44

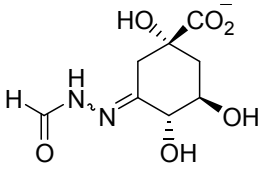
2.46

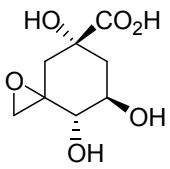
2.4

The preparation of potential inhibitors **2.59**, **2.76** and **2.77** was also investigated, and was ultimately unsuccessful due to problems with the protecting group chemistry.

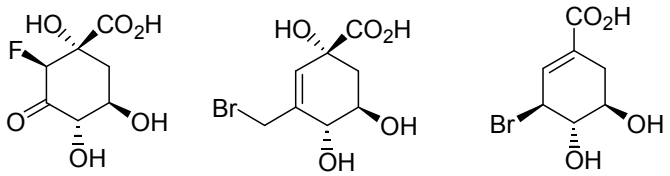

The potential inhibitors were assayed against *M. tuberculosis* and *S. coelicolor* DHQase spectrophotometrically, by monitoring the increase in absorbance at 234 nm due to the enone-carboxylate chromophore of the product dehydroshikimate. This assay proved to be unsuitable for assaying UV active inhibitors against *S. coelicolor* DHQase as the high inhibitor concentrations required gave rise to too great a degree of background absorbance. An alternative ^{1}H NMR based assay methodology was therefore developed. This involved monitoring the appearance of the C-2 proton resonance of dehydroshikimate at 6.3 ppm. The concentration of DHS was determined by integrating the H-2 signal relative to the CHO signal of a known concentration of the reference DMF.

Table 5.1 Assay results for inhibitors against *M. tuberculosis* and *S. coelicolor* type II DHQases

Inhibitor	**K_i (μM)**		**% inhibition**
	M. tuberculosis DHQase	*S. coelicolor* DHQase	*S. coelicolor* DHQase
K_M	15 ± 1	200 ± 20	
2.4	~ 925	[e]	
2.15	>3000		38 ± 17
2.16	1150 ± 150	800 ± 100	
2.17	1000 ± 200	1600 ± 200[a]	
2.18	2000 ± 400	6000 ± 500	
2.27	2000 ± 600	12000 ± 2000	
2.28	850 ± 150	3000 ± 1000	
2.29	900 ± 150	1500 ± 500	
2.38[b]	45 ± 5		11 ± 16
2.42	50 ± 5		[e]
2.44[c]	425 ± 75	220 ± 40	89 ± 6
2.46[d]	90 ± 10		11 ± 7
3.1	1100 ± 100	77 ± 21	90 ± 5
3.2	1600 ± 400		[e]

[a] 2:1 **2.17**:**2.16**. [b] 20:1 *E*:*Z*. [c] 9:1 *E*:*Z*. [d] 3:2 *E*:*Z*. [e] Not determined due to lack of material.

Inhibitors with N attached at C-3 (**2.38**, **2.42**, **2.44** and **2.46**) were found to be more potent against *M. tuberculosis* DHQase than those with C at the corresponding position by roughly one order of magnitude, displaying activities ranging from 45-90 μM, with the exception of **2.44** which had a K_i of 425 μM (Table 5.1). The most potent of these inhibitors, **2.38**, displayed a K_i of 45 μM, similar to that of oxime **1.36** which had a reported K_i of 20 μM.[1] Inhibitors with C at C-3 on the other hand, displayed inhibition constants ranging from 850 μM to >3000 μM.

Inhibition constants for inhibitors with sp^3 character and C at C-3 (**2.26**-**2.18**, **2.28** and **2.29**) against *S. coelicolor* DHQase, determined by spectrophotometric assay, ranged from 800 to 6000 μM, a similar range to that observed for the *M. tuberculosis* enzyme. Inhibitors with sp^2 character and C at C-3 (**2.15**, **2.27** and **3.1**) were evaluated by ^{1}H NMR assay. Inhibitors **2.15** and **2.27** were found to be poor inhibitors of *S. coelicolor* DHQase. Allylic alcohol inhibitor **3.1** proved to be the exception, with a K_i of 77 ± 21 μM. The activity of inhibitors with N at C-3 against *S. coelicolor* DHQase was also evaluated by ^{1}H NMR assay. Inhibitors **2.38** and **2.46** showed only 11% inhibition at concentrations of 5 mM and 1.1 mM respectively. The sulphur analogue of **2.44** on the other hand, displayed 89% inhibition at 5 mM, with a K_i of 220 ± 40 μM, in direct contrast to the trend observed for the N containing inhibitors against *M. tuberculosis* DHQase.

Inhibitor **2.4** was found to be a weak competitive inhibitor of Type I DHQase from *S. typhi* ($K_i \approx 1100$ μM), and also displayed irreversible inhibition of the enzyme.

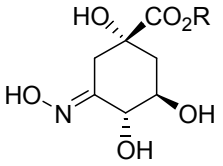

2.47 R = Me
1.36 R = K

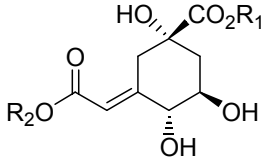

2.31 R_1 = Me, R_2 = Et
2.27 R_1 = R_2 = K

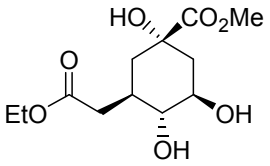

2.34

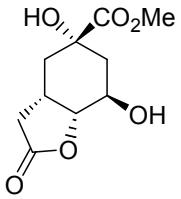

2.35

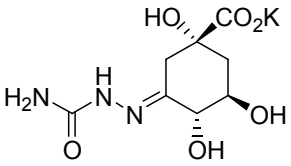

2.38

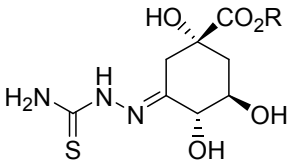

2.43 R = Me
2.44 R = K

A selection of the inhibitors, **2.27**, **2.38** and **2.44**, along with the esters **2.31**, **2.34** **2.35** and **2.43** and the oximes **1.36** and **2.47**, were submitted for biological evaluation against *M. tuberculosis* strain $H_{37}Rv$. None of the compounds, including the two oximes, were found to be active against the bacterium at a concentration of 6.25 μgmL^{-1}.

5.2 FUTURE WORK

Possible future directions for this work include pursuing the work that was begun with the synthesis of allylic bromide **2.74**. Alternative deprotection conditions and/or carboxy protecting groups ought to be explored for this compound as the deprotected form **2.76** could be a potential inhibitor of both type I and type II DHQase (*S. coelicolor* type II DHQase more than *M. tuberculosis*). The preparation of analogues of potent *S. coelicolor* DHQase inhibitor **1.37**[1] by nucleophilic displacement of bromide from **2.74** might also be explored. Azide **5.1** for example, could be prepared from **2.74**, and from that, the allylic amine **5.2**. This could be deprotected to give potential inhibitor **5.3**. Various nucleophiles (such as sugar derivatives), might also be employed in the derivitisation of **2.74**, to produce compounds of general structure **5.4**, which could be deprotected to give **5.5**, with the nucleophile potentially binding in the glycerol binding site of *S. coelicolor* described by Roszak *et al*.[2]

It is thought that lactam **5.6a** (Scheme 5.2) would, through its resonance contributors, be particularly able to fulfil the structural requirements for binding by *M. tuberculosis* DHQase as discussed in Section 3.4.3. That is, it displays both sp^2 character and an electronegative atom at C-3. It is also a good mimic for the structural features of the type II DHQase enolate intermediate **1.21** and would therefore be expected to be a good inhibitor of Type II DHQases in general, not just that from *M. tuberculosis*.

In contrast to the dehydroquinate analogues described in this work, the lactam **5.6a**, which contains an N atom at the 2-position of the carbocyclic ring, could not be prepared from the usual starting material, quinic acid **2.5**. It might however, be prepared *via* ring-closing metathesis, followed by epoxidation of the double bond and ring-opening to form the *trans*-

diol, as illustrated in Scheme 5.2. The C-1 hydroxyl would pose a problem however, as the α-hydroxyamino acid **5.7a** is not expected to be stable. Alternative α-allylamino acids **5.7b** and **5.7c** might be more practical options, eventually leading to lactams **5.6b** and **5.6c**. The replacement of the C-1 hydroxyl however, might be expected to reduce the binding affinity, particularly for *S. coelicolor* DHQase, for which binding of the C-1 hydroxyl and carboxyl is important for substrate recognition. It might be less of a problem for *M. tuberculosis* DHQase, for which C-3 carbonyl recognition is thought to be more important. The affect of replacing the C-1 hydroxyl might be explored by preparing the substrate analogues **5.8b** and **5.8c** and some of their C-3 derivatives.

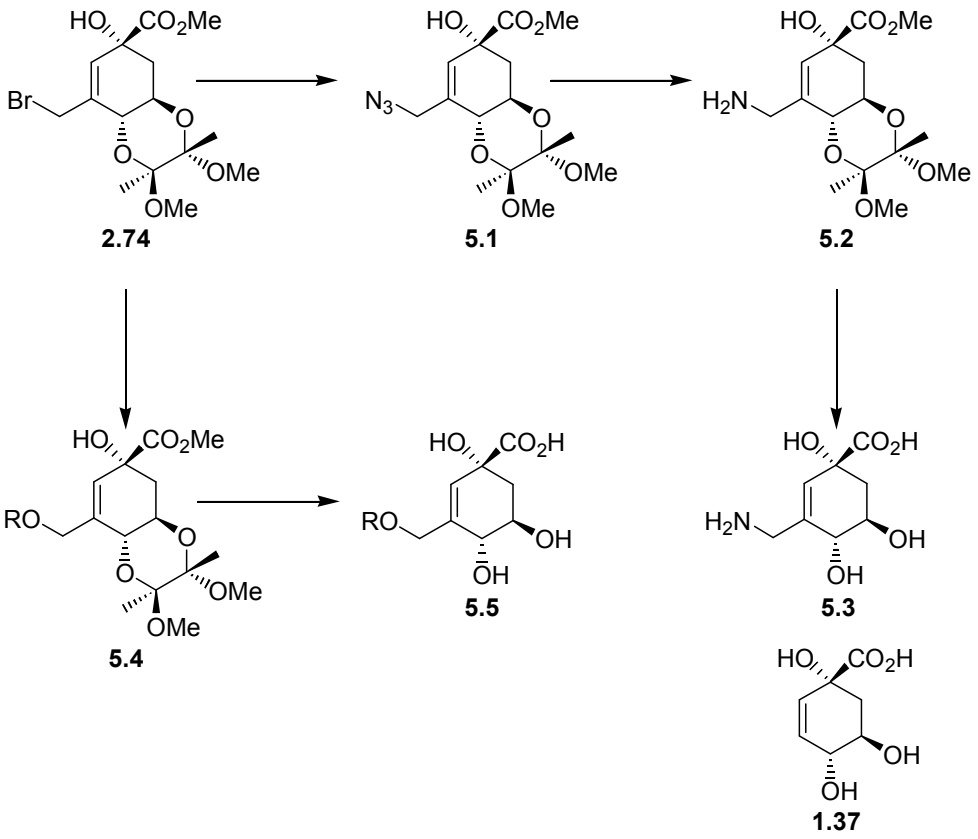

Scheme 5.1 Proposed synthesis of derivatives of allylic bromide **2.74**.

It would also be useful to investigate improving the drug-like properties of dehydroquinate derivatives. The choice of protecting group for the C-1 carboxyl in particular ought to be investigated. The carboxyl group could be masked with a lipophilic ester, which could facilitate the uptake of the inhibitor into a cell, and be subsequently hydrolysed *in vivo* to produce the inhibitor in its active form.

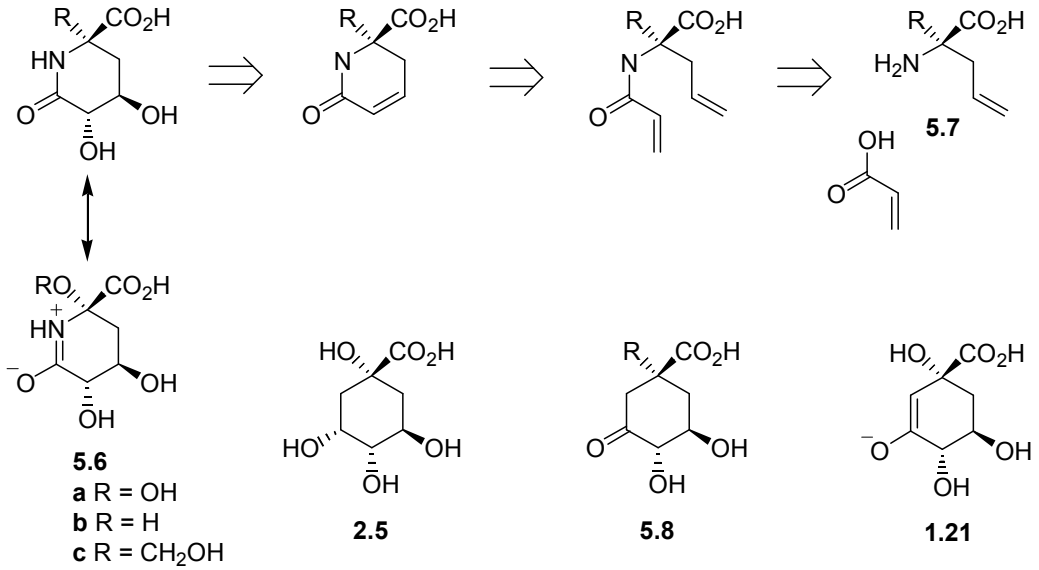

Scheme 5.2 Retrosynthetic analysis of lactam **5.6**.

5.3 REFERENCES FOR CHAPTER 5

(1) Frederickson, M.; Parker, E. J.; Hawkins, A. R.; Coggins, J. R.; Abell, C. *J. Org. Chem.* **1999**, *64*, 2612.

(2) Roszak, A. W. R., D. A.; Krell, T.; Hunter, I. S.; Frederickson, M.; Abell, C.; Coggins, J. R.; Lapthorn, A. J. *Structure* **2002**, *10*, 493-503.

6 Experimental Details

6.1 GENERAL

Melting points were obtained on an Electrothermal apparatus and are uncorrected.

^{1}H NMR spectra were recorded on a Varian Unity 300 or Varian Inova 500 spectrometer operating at 500 MHz. ^{13}C NMR spectra were recorded on a Varian Unity 300 spectrometer operating at 75 Mz with a relaxation delay (d1) of 1 s. ^{19}F NMR spectra were recorded on a Varian Unity 300 NMR spectrometer. Spectra were obtained at 23 ºC unless otherwise stated. Chemical shifts are reported in parts per million (ppm).

Electron impact (EI) mass spectra were recorded on a Kratos MS80 RFA mass spectrometer operating at a 4000 V accelerating potential and 70 eV ionization energy. The source temperature was 200-250 ºC. Electrospray (ES) mass spectra were detected on a micromass LCT TOF mass spectrometer, with a probe voltage of 3200 V and temperature of 150 ºC and a source temperature of 80 ºC. Direct ionization used 10 µL of an 8 or 10 μgmL^{-1} solution, with 50% MeCN/H_2O as the carrier solvent at a flow rate of 20 $\mu Lmin^{-1}$. Ionisation was assisted by the addition of 0.5% formic acid.

UV/vis spectra were recorded on a GBC 920 UV VIS spectrophotometer with a slit width of 0.2 nm and an integration time of 1 s in 3 mL 1 cm path-length quartz cuvettes.

Optical rotations were recorded on a Perkin Elmer 341 polarimeter with a 10 cm path length. Optical rotations are given in units of 10^{-1}deg cm^2 g^{-1}. Concentrations are quoted in g/100 mL.

Starting material and reagents were obtained commercially and used without further purification unless otherwise stated. Solvents for organic synthesis and chromatography were

dried and distilled prior to use. THF was dried by distillation from Na/benzophenone. Pet. ether, EtOAc, CH_2Cl_2, MeCN, toluene, Et_3N and pyridine were dried by distillation from CaH_2. Methanol was dried by distillation from Mg/I_2. DMF was dried over 4 Å activated molecular sieves, replacing the sieves two times over 48 h. Pet. ether refers to the fraction boiling between 50 and 70 ºC.

Flash chromatography was carried out using 230-400 mesh Merck Silica Gel 60 under positive pressure. Deactivated silica refers to silica that has been neutralised by the addition of Et_3N (1%) to the solvent used to pack the column. The column was then rinsed with eluent prior to loading the material to be separated. Analytical thin-layer chromatography was carried out on Merck Keiselgel $KG60F_{254}$ silica plates and visualised using $KMnO_4$.

Assay solutions were prepared using water from a Milli-Q MilliPore ($\geq$ 18 MΩ cm^{-1}) water purification system in which distilled water was sequentially passed through a Super-C carbon cartridge, Ion-ex anion and cation exchange cartridges, an Organex-Q cartridge and finally a Millipak 0.22 μm pore size filter.

Evaporation of solvents from reaction products was carried out using a rotary evaporator, connected to a diaphragm pump. Drying of samples was carried out under high-vacuum, using a rotary oil pump. Lyophilisation was carried out using either a Chriss Alpha I-5 freeze dryer or a rotary oil high vacuum pump with a cold-finger.

For the purpose of naming compounds, the mono- and bi-cyclic ring systems were named and numbered as follows:

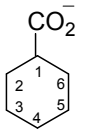

cyclohexane-1-carboxylate

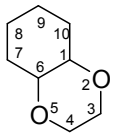

2,5-dioxabicyclo[4.4.0]decane

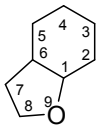

9-oxabicyclo[4.3.0]nonane

6.2 SYNTHETIC DETAILS

Methyl (1*R*,3*S*,4*S*,6*R*,7*R*,9*S*)-7,9-dihydroxy-3,4-dimethoxy-3,4-dimethyl-2,5-dioxabicyclo[4.4.0]decane-9-carboxylate 2.11

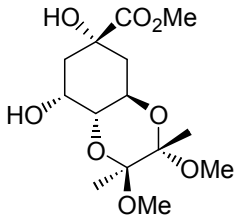

Quinic acid **2.5** (6.28 g, 32.7 mmol), 2,3-butanedione (5.5 mL, 63 mmol), trimethyl orthoformate (17.0 mL, 155 mmol) and D-camphorsulphonic acid (332 mg, 1.03 mmol) were heated at reflux under an inert atmosphere for 20 h. The reaction mixture was allowed to cool to rt, quenched with solid $NaHCO_3$ and the solvent evaporated. The residue was re-dissolved in EtOAc and heated at reflux over activated charcoal for 2.5 h. The reaction mixture was cooled to rt, then filtered through silica, eluting with 10% MeOH/EtOAc. The solvent was evaporated *in vacuo* to give a yellow oil which crystallised on standing (12.38 g). The product was purified by repetitive recrystallisations from EtOAc to give **2.11** as a white solid (7.63g, 73% yield).

^{1}H NMR ($CDCl_3$): δ 4.31 (1H, ddd, J = 4.4, 10.3, 12.2 Hz), 4.20 (1H, ddd, J = 2.9, 2.9, 2.9 Hz), 3.79 (3H, s), 3.60 (1H, dd, J = 2.9, 10.3 Hz), 3.26 (3H, s), 3.26 (3H, s), 2.19 (1H, ddd, J = 2.9, 2.9, 14.7 Hz), 2.11 (1H, ddd, J = 2.9, 4.4, 12.7 Hz), 2.04 (1H, dd, J = 2.9, 14.7 Hz), 1.92 (1H, dd, J = 12.2, 12.7 Hz), 1.34 (3H, s), 1.30 (3H, s).

^{13}C NMR ($CDCl_3$): δ 174.3, 100.3, 99.7, 75.8, 72.7, 69.1, 62.4, 52.9, 47.9, 47.9, 38.6, 37.3, 17.8, 17.6.

mp: 136-139 ºC (lit.: 138-140 ºC)[1]

Anal.: Calculated for $C_{14}H_{24}O_8$: C 52.49; H 7.55. Found C 52.51; H 7.49.

Optical rotation: $[\alpha]_D^{20}$ +139.7 (*c*. 1.05, CH_2Cl_2); lit.: +121.9 (*c*. 1.08, CH_2Cl_2).[2]

TOF MS ES+: 453.0531; $C_{14}H_{24}O_8Cs$ $[MCs]^+$ requires 453.0526.

Methyl (1*R*,3*S*,4*S*,6*S*,9*R*)-9-hydroxy-3,4-dimethoxy-3,4-dimethyl-7-oxo-2,5-dioxabicyclo[4.4.0]decane-9-carboxylate 2.12

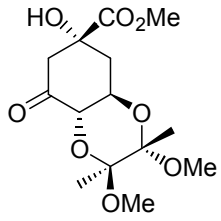

A suspension of protected quinic acid **2.11** (7.58 g, 23.7 mol) and pyridinium chlorochromate (26.03 g, 120.8 mmol) in CH_2Cl_2 were stirred over 4 Å molecular sieves at rt until reaction was complete by TLC (20 h). The reaction mixture was filtered through silica, washing with 15% MeOH/EtOAc (300 mL) and the solvent evaporated. The residue was heated at reflux in EtOAc over activated charcoal for 3.5 h then cooled and filtered through silica as above. The solvent was evaporated leaving a white solid which was recrystallised from EtOAc to give **2.12** as white crystals (5.89 g, 78%).

^{1}H NMR ($CDCl_3$): δ 4.40 (1H, d, *J* = 10.3 Hz), 4.25 (1H, ddd, *J* = 4.4, 10.3, 12.0Hz), 3.83 (3H, s), 3.25 (3H, s), 3.21 (3H, s), 2.88 (1H, d, *J* = 14.2 Hz), 2.49 (1H, dd, *J* = 2.9, 14.2 Hz), 2.35 (1H, dd, *J* = 12.0, 13.0 Hz), 2.10 (1H, ddd, *J* = 2.9, 4.4, 13.0 Hz), 1.38 (3H, s), 1.28 (3H, s).

^{13}C NMR ($CDCl_3$): δ 199.5, 174.1 100.5, 99.6, 77.2, 74.0, 67.0, 53.6, 49.0, 48.3, 48.0, 37.8, 17.6, 17.5.

mp: 211-214 ºC (lit.: 212-214 ºC)[1]

Anal.: Calculated for $C_{14}H_{22}O_8$: C 52.83; H 6.97. Found: C 52.95; H 6.96.

Optical rotation: $[\alpha]_D^{20}$ +114.2 (*c*. 1.04, $CHCl_3$); lit.: +105.1 (*c*. 1.05, $CHCl_3$).[2]

Methyl (1*R*,4*S*,5*R*)-1,4,5-trihydroxy-3-oxocyclohexane-1-carboxylate (Methyl 3-dehydroquinate) 2.13

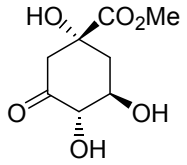

Protected dehydroquinate **2.12** (542 mg, 1.70 mmol) was stirred in 95% $TFA_{(aq)}$ (5 mL) over ice for 1 h and the solvent evaporated. The residue was subjected to flash chromatography on deactivated silica to give methyl dehydroquinate **2.13** as a colourless oil (312 mg, 90%).

^{1}H NMR (D_2O): δ 4.18 (1H, dd, *J* = 1.0, 9.3 Hz), 3.79 (1H, ddd, *J* = 5.9, 9.3, 9.3 Hz), 3.65 (3H, s), 3.03 (1H, dd, *J* = 1.0, 14.2 Hz), 2.46 (1H, dd, *J* = 2.4, 14.2 Hz), 2.18-2.21 (2H, m).

^{13}C NMR (D_2O): δ 207.8, 174.7, 80.6, 74.1, 71.1, 53.4, 47.4, 39.4.

Anal.: Calculated for $C_8H_{12}O_6 \cdot 0.25\ H_2O$: C 46.04; H 6.04. Found: C 46.06; H 5.98.

Optical rotation: $[\alpha]_D^{20}$ -35.07 (*c*. 1.50, CH_3OH); lit.: -34.8 (*c*. 1.50, CH_3OH).[2]

Methyl (4*S*,5*R*)-4,5-dihydroxy-3-oxocyclohex-1-ene-1-carboxylate (Methyl 3-dehydroshikimate) 2.14

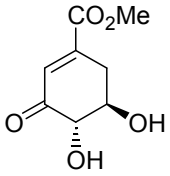

Protected dehydroquinate **2.12** (2.54 g, 7.97 mmol) was stirred in 50% $TFA_{(aq)}$ for 45 min at 60 ºC. The solvent was removed to give a colourless oil (1.52 g). A portion of the crude product (571 mg) was subjected to flash chromatography on silica gel, eluting with 1-3% MeOH/EtOAc to furnish methyl dehydroquinate **2.13** (350 mg, 58%) as a colourless oil and methyl dehydroshikimate **2.14** (74 mg 13%) as a white solid whose NMR data were consistent with the literature.[3]

^{1}H NMR (CD_3OD): δ 6.70 (1H, d, J = 3.4 Hz), 4.06 (1H, d, J = 10.7 Hz), 3.86 (1H, ddd, J = 5.4, 9.8, 10.7 Hz), 3.83 (3H, s), 3.08 (1H, dd, J = 5.4, 18.6 Hz), 2.54 (1H, ddd, J = 3.4, 9.8, 18.6 Hz).

^{13}C NMR (CD_3OD): δ 201.2, 167.7, 147.7, 132.5, 80.4, 72.6, 53.6, 34.5.

mp: 127-130 ºC.

Potassium 3-dehydroquinate (Potassium (1*R*,4*S*,5*R*)-1,4,5-trihydroxy-3-oxocyclohexane-1-carboxylate) 1.4

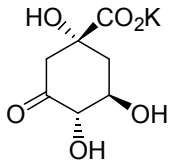

$KOH_{(aq)}$ (0.48 M, 0.80 mL, 0.38 mmol) and H_2O (0.5 mL) were added, over ice, to methyl dehydroquinate **2.13** (76 mg, 0.37 mmol). The solution was stirred over ice for 5 min then freeze-dried. The dehydroquinate potassium salt **1.4** was obtained as a hygroscopic pale yellow glass (84 mg, quant) whose ^{1}H NMR data were in agreement with the literature.[2]

^{1}H NMR (D_2O): δ 4.24 (1H, d, J = 9.8 Hz), 3.82 (1H, ddd, J = 5.4, 9.8, 11.2 Hz), 3.01 (1H, d, J = 14.2 Hz), 2.40 (1H, dd, J = 2.9, 14.2 Hz), 2.20 (1H, dd, J = 11.2, 13.7 Hz), 2.13 (1H, ddd, J = 2.9, 5.4, 13.7 Hz).

Methyl (1*R*,3*S*,4*S*,6*R*,7*E*,9*S*)-7-(cyanomethylene)-9-hydroxy-3,4-dimethoxy-3,4-dimethyl-2,5-oxabicyclo[4.4.0]decane-9-carboxylate 2.19

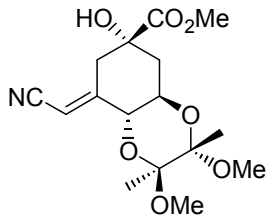

A solution of protected dehydroquinate **2.19** (4.07 g, 12.8 mmol) and (cyanomethylene)triphenylphosphorane (7.01 g, 23.3 mmol) in MeCN (100 mL) was heated at reflux over 4 Å molecular sieves until the reaction was judged complete by TLC (1.25 h). The reaction mixture was filtered, evaporated and subjected to flash chromatography on deactivated silica, eluting with 20% pet. ether/EtOAc. A pale yellow oil was obtained which crystallized on cooling (3.58 g, 82%). Recrystallisation from 50% pet. ether/EtOAc furnished **2.19** as a white crystalline solid (2.64 g, 60%).

^{1}H NMR ($CDCl_3$): δ 5.70 (1H, dd, *J* = 2.0, 2.0 Hz), 4.22 (1H, dd, *J* = 2.0, 9.6 Hz), 3.96 (1H, ddd, *J* = 4.9, 9.6, 12.2 Hz), 3.84 (3H, s), 3.24 (3H, s), 3.23 (3H, s), 2.99 (1H, dd, *J* = 2.4, 14.2 Hz), 2.65 (1H, dd, *J* = 2.0, 14.6 Hz), 2.12 (1H, dd, *J* = 12.2, 12.7 Hz), 1.98 (1H, ddd, *J* = 2.4, 4.9, 12.7 Hz), 1.36 (3H, s), 1.30 (3H, s).

^{13}C NMR ($CDCl_3$): δ 174.5, 156.7, 116.4, 100.4, 99.7, 94.9, 73.3, 72.6, 67.8, 53.5, 48.1, 48.0, 40.8, 37.6, 17.6, 17.6.

mp: 142.5-144 ºC

Anal.: Calculated for $C_{16}H_{23}NO_7$: C 56.29; H 6.79; N 4.10. Found C 56.54; H 6.85; N 4.17.

Optical rotation: $[\alpha]_D^{20}$ +59.8 (*c*. 1.06, CH_2Cl_2).

TOF MS ES+: 364.1374; $C_{16}H_{23}NO_7Na$ $[MNa]^+$ requires 364.1372.

Preparation of the reagent (cyanomethylene)triphenylphosphorane

50% $NaOH_{(aq)}$ (5 mL) was added drop-wise with stirring to solution of (Cyanomethyl)triphenylphosphonium chloride (10.03 g, 29.69 mmol) in H_2O (200 mL) and stirred for a further 10 min. The precipitate was filtered, washed with H_2O and dried under vacuum to give a white solid (7.95 g, 89%). The product was used without further purification.

Methyl (1*S*,3*E*,4*R*,5*R*)-3-(cyanomethylene)-1,4,5-trihydroxycyclohexane-1-carboxylate 2.20

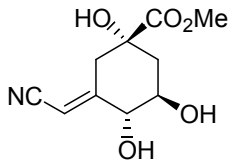

Protected derivative **2.19** (142 mg, 0.42 mmol) was stirred in 95% $TFA_{(aq)}$ over ice for 2 h. The solvent was removed *in vacuo*. The residue was re-dissolved in MeOH and evaporated again to give a colourless oil which crystallised on standing. Recrystallisation from EtOAc furnished **2.20** as a white solid (69 mg, 72%).

^{1}H NMR (D2O, 300 MHz): δ 5.69 (1H, dd, *J* = 2.0, 2.0 Hz), 4.09 (1H, dd, *J* = 2.0, 9.1 Hz), 3.71 (3H, s), 3.62 (1H, ddd, *J* = 5.2, 9.1, 11.2 Hz), 2.96 (1H, dd, *J* = 2.9, 14.9 Hz), 2.76 (1H, dd, *J* = 2.0, 14.9 Hz), 2.13 (1H, ddd, *J* = 2.9, 5.2, 13.7 Hz), 1.98 (1H, dd, *J* = 11.2, 13.7 Hz).

^{13}C NMR (D_2O): δ 175.2, 162.8, 117.5, 95.1, 76.1, 74.7, 70.9, 53.4, 39.7, 39.6.

Anal.: Calculated for $C_{10}H_{13}NO_5$: C 52.86; H 5.77; N 6.17. Found: C 52.99; H 5.67; N 6.16.

Optical rotation: $[\alpha]_D^{20}$ -68.2 (*c*. 1.06, MeOH).

+*EI MS*: 227.0794; $C_{10}H_{13}NO_5$ M^+ requires 227.0794.

Potassium (1*S*,3*E*,4*R*,5*R*)-3-(cyanomethylene)-1,4,5-trihydroxycyclohexane-1-carboxylate 2.15

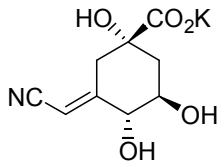

To a solution of **2.20** (14 mg, 0.06 mmol) in H_2O over ice was added 0.30 M $KOH_{(aq)}$ (200 µL, 0.06 mmol) and the solution stirred for 10 min. The solvent was evaporated and the residue dried under vacuum to give the potassium salt **2.15** as a colourless glass (15 mg, quant)

^1H NMR (D_2O): δ 5.59 (1H, dd, *J* = 1.5, 1.7 Hz), 4.04 (1H, dd, *J* = 1.7, 9.3 Hz), 3.54 (1H, ddd, *J* = 5.4, 9.3, 11.2 Hz), 2.78 (1H, dd, *J* = 2.7, 14.2 Hz), 2.63 (1H, d, *J* = 1.5, 14.2 Hz), 1.94 (1H, ddd, *J* = 2.7, 5.4, 13.5 Hz), 1.90 (1H, dd, *J* = 11.2, 13.5 Hz).

^{13}C NMR (D_2O): δ 180.2, 164.6, 117.9, 93.9, 76.4, 76.0, 71.9, 40.7, 40.6.

TOF MS ES+: 196.0609; $C_9H_{10}NO_4$ $[MH_2 - K - H_2O]^+$ requires 196.0610.

Methyl (1*R*,3*S*,4*S*,6*R*,7*S*,9*S*)-7-(cyanomethyl)-9-hydroxy-3,4-dimethoxy-3,4-dimethyl-2,5-dioxabicyclo[4.4.0]decane-9 carboxylate 2.21 and **Methyl (1*R*,3*S*,4*S*,6*R*,7*R*,9*S*)-7-(cyanomethyl)-9-hydroxy-3,4-dimethoxy-3,4-dimethyl-2,5-dioxabicyclo[4.4.0]decane-9 carboxylate 2.22**

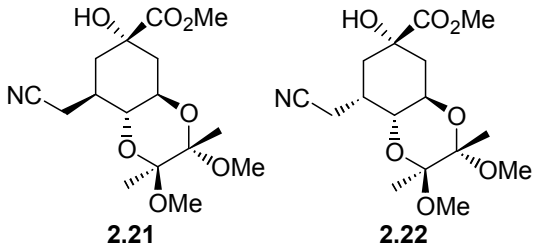

2.21 **2.22**

Olefin **2.19** (512 mg, 1.50 mmol) was stirred at rt over 5% Pd/C (1.20 g) in CH_2Cl_2 (5 mL) under 1 atm $H_{2(g)}$ for 44 h. The suspension was filtered through celite and rinsed with CH_2Cl_2. Evaporation of the solvent gave a yellow foam (478 mg) containing **2.21**, **2.22** and **2.23** in a ratio of 1.2:3:1. The foam was subjected to flash chromatography on silica, eluting with 20% pet. ether/EtOAc, giving partial separation of the isomers. Fractions containing mixtures of isomers were combined and evaporated and the chromoatographic separation repeated. Fractions containing mostly one diastereomer (less than 20% of the alternate isomer) were combined and evaporated. Recrystallisation of the sample enriched in the major (3*R*-) epimer from 25% EtOAc/pet. ether gave **2.22** as a white solid (98 mg, 19%). Recrystallisation of the sample enriched in the minor (3*S*-) epimer from 33% EtOAc/pet. ether gave **2.21** as a white solid (23 mg, 5%).

(7S)-Epimer 2.21

^{1}H NMR ($CDCl_3$): δ 3.94 (1H, ddd, *J* = 4.9, 9.8, 12.2 Hz), 3.78 (3H, s), 3.50 (1H, dd, *J* = 9.8, 10.9 Hz), 3.29 (3H, s), 3.23 (3H, s), 3.22 (1H, br s), 2.69 (1H, dd, *J* = 6.1, 16.6 Hz), 2.45 (1H, dd, *J* = 3.9, 16.6 Hz), 2.30 (1H, ddddd, *J* = 3.9, 3.9, 6.1, 10.9, 12.7 Hz), 1.95 (1H, dd, *J* = 12.2, 12.7 Hz), 1.88 (1H, dd, *J* = 12.7, 13.2 Hz), 1.85 (1H, ddd, *J* = 2.4, 4.9, 12.7 Hz), 1.78 (1H, ddd, *J* = 2.4, 3.9, 13.2 Hz), 1.30 (3H, s), 1.27 (3H, s).

^{13}C NMR ($CDCl_3$): δ 175.7, 117.7, 99.9, 99.6, 73.4, 72.3, 66.6, 53.3, 48.2, 48.0, 38.6, 37.9, 32.0, 18.4, 17.7, 17.5.

(7R)-Epimer 2.22

^{1}H NMR ($CDCl_3$): δ 3.94 (1H, ddd, *J* = 4.9, 10.3, 11.5 Hz), 3.81 (3H, s), 3.76 (1H, dd, *J* = 5.4, 10.3 Hz), 3.25 (3H, s), 3.23 (3H, s), 2.99 (1H, dd, *J* = 12.2, 16.6 Hz), 2.80 (1H, dd, *J* = 3.9, 16.6 Hz), 2.41 (1H, m), 2.08 (2H, m), 1.94 (1H, dd, *J* = 11.5, 12.7 Hz), 1.88 (1H, ddd, *J* = 2.0, 4.9, 12.7 Hz), 1.28 (3H, s), 1.27 (3H, s).

^{13}C NMR ($CDCl_3$): δ 175.7, 120.2, 99.9, 99.5, 74.9, 70.7, 62.4, 53.4, 47.9, 38.5, 35.0, 34.4, 17.7, 17.6, 16.8.

mp: 95-97 ºC

Anal.: Calculated for $C_{16}H_{25}NO_7$: C 55.96; H 7.34; N 4.08. Found C 56.13; H 7.54; N 4.00.

Optical rotation: $[\alpha]_D^{20}$ +117.19 (*c*. 1.02, CH_2Cl_2).

TOF MS ES+: 476.0684; $C_{16}H_{25}NO_7Cs$ $[MCs]^+$ requires 476.0685.

Methyl (1*R*,3*S*,4*S*,6*R*,7*R*,9*S*)-7-(2-aminoethyl)-9-hydroxy-3,4-dimethoxy-3,4-dimethyl-2,5-dioxabicyclo[4.4.0]decane-9 carboxylate 2.23

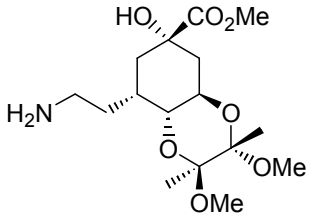

Nitrile **2.19** (1.53 g, 4.49 mmol) was added to a suspension of 10% Pd/C (325 mg) in MeOH under $H_{2(g)}$ (1 atm). The system was evacuated then stirred under $H_{2(g)}$ at rt. TLC showed starting material remaining after 48 h so a further 100 mg of catalyst was added. The starting material was no longer evident after 68 h and the reaction was filtered through celite, washing with MeOH. The solvent was evaporated to give a pale yellow foam (1.58 g) containing **2.22** and **2.23** in a ratio of 1:3 (plus trace **2.21**). Flash chromatography on deactivated silica, eluting with a gradient of 20% pet. ether/EtOAc to 20% MeOH/EtOAc gave nitrile **2.22** as a colourless oil (309 mg, 20%), amine **2.23** as a yellow oil (601 mg, 39%) and a 2:1 mixture of the epimers **2.21** and **2.22** (43 mg, 3%). A portion of the amine **2.23** (320 mg) was columned again, eluting with 15% MeOH/CH_2Cl_2 to give **2.23** (153 mg, 10%) as a white glass.

^{1}H NMR ($(CD_3)_2CO$): δ 4.18 (1H, ddd, J = 4.5, 10.2, 11.9 Hz), 3.81 (3H, s), 3.73 (1H, dd, J = 5.3, 10.2 Hz), 3.33 (3H, s), 3.32 (3H, s), 2.79 (1H, m), 2.43 (1H, m), 2.01-2.15 (5H, m), 1.97 (1H, dd, J = 5.4, 14.6 Hz), 1.87 (1H, dd, J = 11.9, 12.2 Hz), 1.37 (3H, s), 1.33 (3H, s).

^{13}C NMR ($(CD_3)_2CO$): δ 176.4, 100.2, 99.9, 75.9, 73.6, 64.0, 53.0, 52.5, 47.8, 39.0, 36.3, 35.5, 24.2, 18.2, 18.2.

Methyl (1*S*,3*S*,4*R*,5*R*)-3-(cyanomethyl)-1,4,5-trihydroxycyclohexane-1-carboxylate 2.24

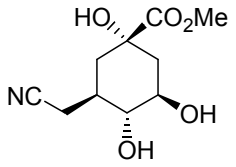

Nitrile **2.21** (21 mg, 0.06 mmol) was stirred in 95% $TFA_{(aq)}$ (0.5 mL) over ice for 35 min. The solvent was evaporated and the residue re-dissolved in MeOH and evaporated again. The residue was dried under vacuum for 18 h to give the free diol **2.24** as a colourless oil (16 mg, quant).

^1H NMR (D_2O): δ 3.60-3.65 (1H, m), 3.62 (3H, s), 3.12 (1H, dd, *J* = 9.0, 10.5 Hz), 2.59 (1H, dd, *J* = 4.5, 17.1 Hz), 2.53 (1H, dd, *J* = 6.5, 17.1 Hz), 1.96-2.02 (2H, m), 1.81 (1H, ddd, *J* = 3.4, 3.9, 14.1 Hz), 1.69-1.75 (2H, m).

^{13}C NMR (D_2O): δ 176.3, 119.8, 76.3, 74.0, 53.1, 39.5, 37.1, 34.4, 19.2.

Methyl (1*S*,3*R*,4*R*,5*R*)-3-(cyanomethyl)-1,4,5-trihydroxycyclohexane-1-carboxylate 2.25

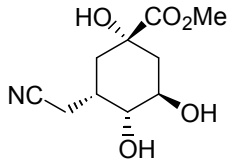

Nitrile **2.22** (84 mg, 0.25 mmol) was stirred in 95% $TFA_{(aq)}$ (0.5 mL) over ice for 2.5 h. The solvent was evaporated and the residue re-dissolved in MeOH and evaporated again. The residue was dried under vacuum for 3 h to give the free diol **2.25** as a colourless oil (59 mg, quant).

^1H NMR (D_2O): δ 3.86 (1H, m), 3.67 (1H, m), 3.64 (3H, s), 2.60 (1H, dd, *J* = 7.8, 17.1 Hz), 2.55 (1H, dd, *J* = 7.8, 17.1 Hz), 2.39 (1H, m), 2.03-2.10 (2H, m), 1.89 (1H, dd, *J* = 3.9, 13.7 Hz), 1.62 (1H, dd, *J* = 8.3, 13.7 Hz).

^{13}C NMR (D_2O): (from a 2:1 mixture of **2.25** and **2.24**) δ 175.8, 121.0, 73.6, 70.6, 67.8, 52.8, 37.6, 33.7, 33.1, 18.3.

Potassium (1*S*,3*S*,4*R*,5*R*)-3-(cyanomethyl)-1,4,5-trihydroxycyclohexane-1-carboxylate 2.16

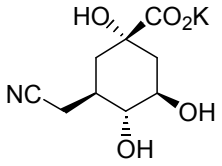

To a solution of ester **2.24** (16 mg, 0.07 mmol) in H_2O (100 μL) was added $KOH_{(aq)}$ (0.30 M, 260 μL, 0.08 mmol) and the reaction was stirred over ice for 15 min. The solvent was evaporated and the residue dried under vacuum to give the potassium salt **2.16** as a colourless glass (17 mg, quant).

^{1}H NMR (D_2O): *δ* 3.65 (1H, ddd, *J* = 4.9, 9.3, 11.7 Hz), 3.18 (1H, dd, *J* = 9.3, 10.7 Hz), 2.64 (1H, dd, *J* = 4.9, 17.1 Hz), 2.59 (1H, dd, *J* = 6.5, 17.1 Hz), 2.00 (1H, m), 1.91 (1H, dd, *J* = 4.9 13.2 Hz), 1.71-1.77 (3H, m).

^{13}C NMR (D_2O): δ 182.3, 120.8, 77.5, 75.9, 71.5, 41.4, 38.8, 35.8, 20.1.

TOF MS ES$^-$: 214.0933; $C_9H_{12}NO_5$ $[M-K]^-$ requires 214.0716.

Potassium (1*S*,3*R*,4*R*,5*R*)-3-(cyanomethyl)-1,4,5-trihydroxycyclohexane-1-carboxylate 2.17

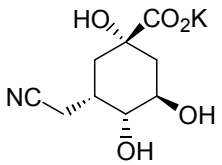

To a solution of ester **2.25** (7 mg, 0.03 mmol) in H_2O (100 μL) was added $KOH_{(aq)}$ (0.30 M, 103 μL, 0.03 mmol) and the reaction was stirred over ice for 5 min. The solvent was evaporated and the residue dried under vacuum to give the potassium salt **2.17** as a colourless glass (7 mg, quant).

^{1}H NMR (D_2O): δ 3.79 (1H, m), 3.69 (1H, dd, J = 3.9, 5.9 Hz), 2.59 (2H, d, J = 7.8 Hz), 2.36 (1H, m), 1.80-1.88 (3H, m), 1.67 (1H, dd, J = 8.3, 13.7 Hz).

^{13}C NMR (D_2O): (from a 2:1 mixture of **2.17** and **2.16**) δ 182.6, 121.87, 76.2, 72.6, 68.7, 38.2, 36.1, 34.1, 19.0.

TOF MS ES$^-$: 214.0943; $C_9H_{12}NO_5$ $[M-K]^-$ requires 214.0716.

Potassium (1*S*,4*R*,5*R*)-3-(2-aminoethyl)-1,4,5-trihydroxycyclohexane-1-carboxylate 2.18

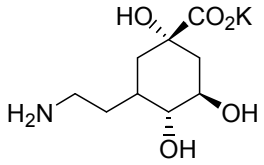

A solution of nitrile **2.20** (71 mg, 0.31 mmol) in MeOH was stirred over 5% Pd/C (220 mg) under 1 atm $H_{2(g)}$ at rt for 67 h. The suspension was filtered through celite and the residue washed with MeOH. The combined filtrates were evaporated to give a colourless oil (50 mg).

A portion of the oil (7 mg) was dissolved in H_2O (400 μL) and 1.0 M $KOH_{(aq)}$ (32 μL, 0.03 mmol) added over ice. The solution was stirred over ice for 10 min and the solvent removed by lyophilisation. ^{1}H NMR showed a small amount of the ester remaining and so a further 0.01 mmol of 1.0 M $KOH_{(aq)}$ was added under the same conditions. The solvent was again removed by lyophilisation to give the potassium salt **2.18** as a yellow glass which was not purified further (9 mg, 71% over 2 steps).

^{1}H NMR (D_2O): δ 3.78 (1H, m), 3.57 (1H, m), 2.82-2.92 (2H, m), 1.84-1.91 (3H, m), 1.60-1.74 (3H, m), 1.52 (1H, dd, *J* = 10.3, 13.2 Hz).

^{13}C NMR (D_2O): δ 182.4, 75.5, 72.0, 68.7, 46.0, 36.8, 35.7, 33.0, 27.1.

TOF MS ES+: 220.1178; $C_9H_{18}NO_5$ $[MH_2\text{-}K]^+$ requires 220.1186.

Methyl (1*R*,3*S*,4*S*,6*R*,7*E*,9*S*)-7-(carbethoxymethylene)-9-hydroxy-3,4-dimethoxy-3,4-dimethyl-2,5-dioxabicyclo[4.4.0]decane-9-carboxylate 2.30

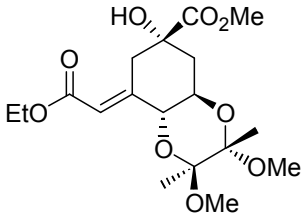

Protected dehydroquinic acid **2.12** (1.03 g, 3.24 mmol) was heated at reflux with (carbethoxymethylene)triphenylphosphorane (1.90 g, 5.46 mmol) in dry MeCN (25 mL) over 4 Å molecular sieves until the reaction was judged complete by TLC (1.75 h). The reaction mixture was cooled, filtered and the filtrate evaporated to give a yellow oil. The oil was subjected to flash chromatography on silica, eluting with 25% pet. ether/EtOAc. Fractions containing the product were combined and the solvent evaporated to give the diester **2.30** as an off-white foam (1.12 g, 89%), whose NMR data was consistent with the literature.[4]

^{1}H NMR ($CDCl_3$): δ 6.22 (1H, dd, *J* = 1.5, 2.0 Hz), 4.13 (3H, m), 4.01 (1H, dd, *J* = 2.7, 14.5 Hz), 3.93 (1H, ddd, *J* = 4.9, 9.8, 12.0 Hz), 3.77 (3H, s), 3.21 (3H, s), 3.19 (3H, s), 2.31 (1H, dd, *J* = 1.5, 14.5 Hz), 2.09 (1H, dd, *J* = 12.0, 13.0 Hz), 1.97 (1H, ddd, *J* = 2.7, 4.9, 13.0 Hz), 1.33 (3H, s), 1.27 (3H, s), 1.25 (3H, t, *J* = 7.3 Hz).

^{13}C NMR ($CDCl_3$): δ 174.8, 166.8, 150.6, 115.2, 100.1, 99.4, 74.9, 72.9, 68.5, 60.0, 53.0, 48.0, 47.9, 37.4, 36.9, 17.7, 14.2.

Anal.: Calculated for $C_{18}H_{28}O_9$: C 55.66; H 7.27. Found C 56.06; H 7.21.

Methyl (1*S*,3*E*,4*R*,5*R*)-3-(carbethoxymethylene)-1,4,5-trihydroxycyclohexane-1-carboxylate 2.31

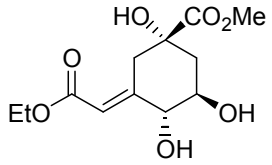

Diester **2.30** (75 mg, 0.19 mmol) was stirred in 95% $TFA_{(aq)}$ over ice for 1 h. The solvent was evaporated and the residue re-dissolved in MeOH and evaporated again. The residue was dried under vacuum for 18 h to give **2.31** as a colourless oil (60 mg, quant).

^{1}H NMR (D_2O): δ 6.09 (1H, dd, *J* = 2.0, 2.0 Hz), 4.08 (2H, q, *J* = 7.3 Hz), 4.00 (1H, dd, *J* = 2.0, 9.3 Hz), 3.76 (1H, dd, *J* = 2.9, 14.5 Hz), 3.70 (3H, s), 3.59 (1H, ddd, *J* = 4.9, 9.3, 11.2 Hz), 2.43 (1H, d, *J* = 14.5 Hz), 2.10 (1H, ddd, *J* = 2.9, 4.9, 13.7 Hz), 1.96 (1H, dd, *J* = 11.2, 13.7 Hz), 1.17 (3H, t, *J* = 7.3 Hz).

^{13}C NMR (D_2O): δ 175.8, 168.5, 155.1, 115.4, 76.3, 74.2, 71.2, 61.4, 53.2, 39.8, 35.6, 13.3.

Dipotassium (1*S*,3*E*,4*R*,5*R*)-3-(carboxylatomethylene)-1,4,5-trihydroxycyclohexane-1-carboxylate 2.27

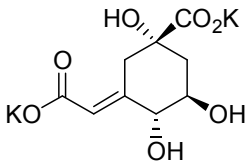

To a solution of diester **2.31** (34 mg, 0.12 mmol) in H_2O (100 µL) was added 0.30 M $KOH_{(aq)}$ (846 µL, 0.25 mmol) and the reaction was stirred over ice for 5 min. The solvent was removed by lyophilisation to give dicarboxylate **2.27** as a yellow glass (40 mg, quant).

^1H NMR (D_2O): δ 5.98 (1H, s), 3.91 (1H, d, *J* = 9.8 Hz), 3.56 (1H, ddd, *J* = 5.4, 9.8, 10.7 Hz), 3.14 (1H, dd, *J* = 2.4, 14.5 Hz), 2.31 (1H, d, *J* = 14.5 Hz), 1.94 (1H, ddd, *J* = 2.4, 5.4, 13.7 Hz), 1.89 (1H, dd, *J* = 10.7, 13.7 Hz).

^{13}C NMR (D_2O): δ 181.5, 176.5 144.3, 120.9, 76.4, 76.0, 72.0, 40.7, 37.4.

TOF MS ES-: 231.0512. $C_9H_{11}O_7$ $(MH-2K)^-$ requires 231.0505.

Methyl (1*R*,3*S*,4S,6*R*,7*R*,9*S*)-7-(carbethoxymethyl)-9-hydroxy-3,4-dimethoxy-3,4-dimethyl-2,5-dioxabicyclo[4.4.0]decane-9-carboxylate 2.32 and **Methyl (1*R*,3*S*,4*S*,6*R*,7*S*,9*S*)-7-(carbethoxymethyl)-9-hydroxy-3,4-dimethoxy-3,4-dimethyl-2,5-dioxabicyclo[4.4.0]decane-9-carboxylate 2.33**

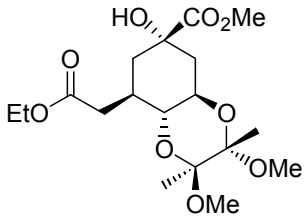

2.32

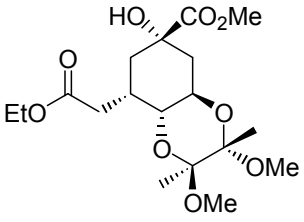

2.33

A solution of olefin **2.30** (179 mg, 0.46 mmol) in EtOAc (3 mL) was stirred over 10% Pd/C (274 mg) under 1 atm $H_{2(g)}$ for 26 h. The suspension was filtered through celite, washing with EtOAc and the filtrate evaporated to give a colourless oil (175 mg) containing both (*R*)- and (*S*)- epimers in a 1.25:1 ratio by ^1H NMR. The oil was subjected to flash chromatogtaphy on silica, eluting with 20% EtOAc/pet. ether. Fractions containing each epimer were combined and evaporated to give 67 mg of the (*R*)-epimer **2.32** (37%) and 67 mg of the (*S*)-epimer **2.33** (37%), both as colourless oils.

(7R)-Epimer 2.32

^{1}H NMR ($CDCl_3$): δ 4.08 (1H, dq, *J* = 1.5, 7.3 Hz), 3.97 (1H, ddd, *J* = 4.4, 9.8, 12.2 Hz), 3.75 (3H, s), 3.32 (1H, dd, *J* = 9.8, 10.7 Hz), 3.23 (3H, s), 3.22 (3H, s), 3.10 (1H, br s), 2.77 (1H, dd, *J* = 4.4, 15.1 Hz), 2.44 (1H, m), 2.09 (1H, dd, *J* = 8.8, 15.1 Hz), 1.93 (1H, dd, *J* = 12.2, 12.2 Hz), 1.80-1.87 (2H, m), 1.62 (1H, dd, *J* = 13.2, 13.2 Hz), 1.27 (3H, s), 1.26 (3H, s), 1.22 (3H, t, *J* = 7.3 Hz).

^{13}C NMR ($CDCl_3$): δ 176.0, 172.2, 99.7, 99.4, 73.7, 73.6, 66.8, 60.3, 53.0, 47.9, 39.3, 37.8, 35.6, 32.3, 17.7, 17.7, 14.2.

TOF MS ES+: 391.1982. $C_{18}H_{31}O_9$ $(MH)^+$ requires 391.1968.

(7S)-Epimer 2.33

^{1}H NMR ($CDCl_3$): δ 4.07 (2H, m), 3.95 (1H, ddd, *J* = 4.8, 10.5, 11.1 Hz), 3.72 (3H, s), 3.65 (1H, dd, *J* = 5.2, 10.5 Hz), 3.33 (1H, br s), 3.19 (3H, s), 3.18 (3H, s), 2.84 (1H, dd, *J* = 11.1, 16.3 Hz), 2.76 (1H, dd, *J* = 4.4, 16.3 Hz), 2.53 (1H, m), 1.94 (1H, dd, *J* = 5.2, 15.1 Hz), 1.81-1.90 (3H, m), 1.22 (3H, s), 1.21 (3H, s), 1.20 (3H, t, *J*= 7.5 Hz).

^{13}C NMR ($CDCl_3$): δ 176.3, 174.0, 99.7, 99.3, 75.2, 71.5, 63.0, 60.2, 53.1, 47.8, 47.8, 38.5, 35.6, 33.3, 32.3, 17.8, 17.6, 14.2.

TOF MS ES+: 391.1986. $C_{18}H_{31}O_9$ $(MH)^+$ requires 391.1968.

Methyl (1*S*,3*R*,4*R*,5*R*)-3-(carbethoxymethyl)-1,4,5-trihydroxycyclohexane-1-carboxylate 2.34

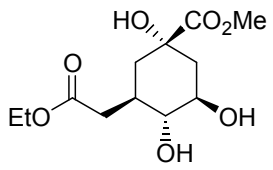

Diester **2.32** (28 mg, 0.07 mmol) was stirred in 95% $TFA_{(aq)}$ (0.5 mL) over ice for 40 min. The solvent was evaporated and the residue re-dissolved in MeOH and the solvent evaporated again. The residue was dried under vacuum for 20 h to give **2.34** as a yellow oil (21 mg, quant).

^{1}H NMR (D_2O): δ 4.07 (2H, dq, *J* = 2.0, 7.3), 3.67 (4H, m), 3.13 (1H, dd, *J* = 9.8, 9.8 Hz), 2.62 (1H, dd, *J* = 5.0, 15.0 Hz), 2.22 (1H, dd, *J* = 8.0, 15.0 Hz), 2.14 (1H, m), 2.02 (1H, ddd, *J* = 2.9, 4.4, 13.7 Hz), 1.73-1.78 (2H, m), 1.65 (1H, dd, *J* = 12.7, 13.7 Hz), 1.16 (3H, t, *J*= 7.3 Hz).

^{13}C NMR (D_2O): δ 176.6, 175.5, 77.3, 74.2, 70.1, 61.7, 53.0, 39.6, 37.6, 36.96, 35.0, 13.3.

Dipotassium (1*S*,3*R*,4*R*,5*R*)-3-(carboxylatomethyl)-1,4,5-trihydroxycyclohexane-1-carboxylate 2.28

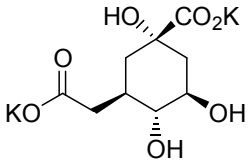

To an ice-cooled solution of diester **2.34** (13 mg, 0.05 mmol) in H_2O (160 µL) was added 0.30 M $KOH_{(aq)}$ (340 µL, 0.10 mmol) and the reaction was stirred over ice for 10 min. The solvent was removed by lyophilisation to give **2.28** as a pale brown glass (16 mg, quant).

^{1}H NMR (D_2O): δ 3.63 (1H, ddd, *J* = 4.9, 9.3, 11.7 Hz), 3.04 (1H, dd, *J* = 9.3, 10.3 Hz), 2.60 (1H, dd, *J* = 4.4, 14.2 Hz), 1.97 (1H, m), 1.83-1.88 (2H, m), 1.72 (1H, dd, *J* = 11.7, 13.2 Hz), 1.59 (1H, ddd, *J* = 3.9, 3.9, 14.2 Hz), 1.51 (1H, dd, *J* = 12.2, 14.2 Hz).

^{13}C NMR (D_2O): δ 182.2, 78.2, 75.5, 71.2, 40.8, 40.7, 38.8, 36.2.

TOF MS ES-: 233.0666; $C_9H_{13}O_7$ $[MH-2K]^-$ requires 233.0661.

Methyl (1*R*,2*R*,4*S*,6*S*)-2,4-dihydroxy-8-oxo-9-oxabicyclo[4.3.0]nonane-4-carboxylate 2.35

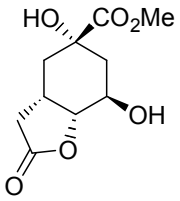

Diester **2.33** (46 mg, 0.12 mmol) was stirred in 95% $TFA_{(aq)}$ (0.5 mL) over ice for 30 min and the solvent removed by lyophilisation to give a brown oil (36 mg). The oil was subjected to flash chromatography on silica, eluting with 20% pet. ether/EtOAc, to give the lactone **2.35** as a colourless oil (16 mg, 58%).

^{1}H NMR (CD_3OD): δ 4.36 (1H, dd, *J* = 7.3, 7.8 Hz), 4.04 (1H, ddd, *J* = 4.4, 7.8, 11.2 Hz), 3.73 (3H, s), 2.96 (1H, m), 2.87 (1H, dd, *J* = 10.7, 17.1 Hz), 2.52 (1H, dd, *J* = 8.3, 17.1 Hz), 2.08 (1H, dd, *J* = 6.4, 14.7 Hz), 1.98 (1H, ddd, *J* = 2.4, 4.4, 13.7 Hz), 1.88 (1H, dd, *J* = 11.2, 13.7 Hz), 1.83 (1H, ddd, *J*= 2.4, 3.4, 14.7 Hz).

^{13}C NMR (D_2O): δ 180.8, 176.3, 84.7, 74.7, 66.7, 53.0, 37.8, 33.9, 33.3, 31.9.

TOF MS ES+: 231.1276. $C_{10}H_{15}O_6$ $[MH]^+$ requires 231.0869.

Dipotassium (1*S*,3*S*,4*R*,5*R*)-3-(carboxylatomethyl)-1,4,5-trihydroxycyclohexane-1-carboxylate 2.29

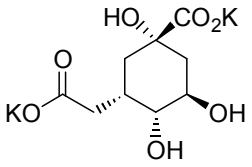

To a solution of lactone **2.35** (11 mg, 0.05 mmol) in H_2O (160 µL) over ice was added 0.30 M $KOH_{(aq)}$ (340 µL, 0.10 mmol) and the reaction was stirred over ice for 10 min. The solvent

was removed by lyophilisation to give dicarboxylate inhibitor **2.29** as a pale yellow glass (16 mg, quant).

^{1}H NMR (D_2O): δ 3.76 (1H, m), 3.57 (1H, m), 2.26 (2H, m), 2.16 (1H, dd, *J* = 10.7, 15.6 Hz), 1.85 (2H, m), 1.68 (1H, dd, *J* = 3.4, 13.7 Hz), 1.51 (1H, dd, *J* = 9.3, 13.7 Hz).

^{13}C NMR (D_2O): δ 182.5, 182.2, 75.5, 72.6, 68.8, 39.4, 36.5, 36.0, 33.0.

TOF MS ES+: 233.0702; $C_9H_{13}O_7$ [MH-2K]$^-$ requires 233.0661.

Methyl (1*R*,3*S*,4*S*,6*R*,7*E*/*Z*,9*S*)-7-[(aminocarbonyl)hydrazono]-9-hydroxy-3,4-dimethoxy-3,4-dimethyl-2,5-dioxabicyclo[4.4.0]decane-9-carboxylate 2.39

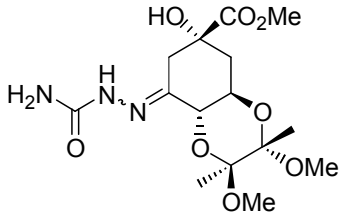

Protected dehydroquinate **2.12** (51 mg, 0.16 mmol) was added to a solution of semicarbazide hydrochloride (97 mg, 0.87 mmol) and sodium acetate trihydrate (152 mg, 1.11 mmol) in H_2O (1 mL). MeOH (1 mL) was added and the solution heated at 50 ºC for 1.5 h. The reaction mixture was cooled to rt and extracted with CH_2Cl_2 (3×). The combined organic extracts were dried ($MgSO_4$), filtered and the solvent evaporated to give two isomers (2:1 ratio) of the protected semicarbazone **2.39** as a pale yellow glass (32 mg, 53%).

^{1}H NMR ($CDCl_3$, 300 MHz): δ (major isomer from 2:1 mixture) 9.79 (1H, s), 5.46 (2H, br s), 4.22 (1H, d, *J* = 9.3 Hz), 3.98 (1H, m), 3.70 (3H, s), 3.22 (3H, s), 3.15 (3H, s), 2.24 (1H, d, *J* = 14.7 Hz), 1.98-2.10 (3H, m), 1.30 (3H, s), 1.23 (3H, s) (minor isomer from 2:1 mixture) 10.21 (1H, s), 4.52 (1H, d, *J* = 10.3 Hz), 4.13-4.24 (1H, m), 3.73 (3H, s), 3.26 (3H, s), 3.17 (3H, s), 2.58 (1H, d, *J* = 14.2 Hz), 2.38 (1H, d, *J* = 14.2 Hz), 1.98-2.10 (2H, m), 1.37 (3H, s), 1.20 (3H, s).

^{13}C NMR ($CDCl_3$): δ (both isomers in 2:1 mixture) 174.7, 174.4, 159.9, 157.4, 145.8, 139.6, 100.5, 100.0, 99.3, 77.0, 74.2, 73.7, 72.8, 68.4, 66.3, 53.1, 52.8, 48.6, 48.1, 47.9, 47.8, 43.7, 37.6, 37.0, 35.3, 17.7, 17.6, 17.5.

Methyl (1*S*,3*E*/*Z*,4*R*,5*R*)-3-[(aminocarbonyl)hydrazono]-1,4,5-trihydroxycyclohexane-1-carboxylate 2.40

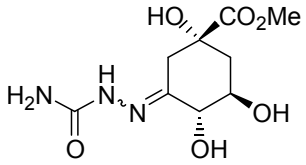

To a solution of methyl dehydroquinate **2.13** (104 mg, 0.51 mmol) in MeOH (0.5 mL) and H_2O (1 mL) was added semicarbazide hydrochloride (60 mg, 0.54 mmol). Sodium acetate trihydrate was added (212 mg, 1.56 mmol) until the solution reached pH 7, as judged by universal indicator paper. The solution was heated to 40 ºC and stirred for 4 h. The solvent was evaporated. The resulting yellow oil showed a 10:1 ratio of isomers by ^1H NMR. The residue was purified by flash chromatography on deactivated silica, eluting with 30% MeOH/EtOAc to give the isomers **2.40** (20:1 ratio, major isomer presumed to be *E*) as a pale yellow glass (111 mg, 82%).

^1H NMR (D_2O, 300 MHz): δ (major isomer from 20:1 mixture) 4.08 (1H, d, J = 9.3 Hz), 3.68-3.76 (1H, m), 3.70 (3H, s), 2.98 (1H, dd, J = 2.7, 14.8 Hz), 2.48 (1H, d, J = 14.8 Hz), 2.14 (1H, ddd, J = 2.7, 4.9, 13.7 Hz), 2.02 (1H, dd, J = 11.2, 13.7 Hz).

^{13}C NMR (D_2O): δ (major isomer from 20:1 mixture) 175.1, 160.0, 149.2, 75.8, 74.2, 71.3, 53.4, 39.4, 33.8.

Anal. Calculated for $C_9H_{15}N_3O_6 \cdot 2H_2O$: C 36.36; H 6.44; N 14.14. Found C 36.86; H 5.42; N 13.80.

Optical rotation: $[\alpha]_D^{20}$ -18.24 (*c*. 1.03, CH_3OH).

TOF MS ES+: 262.1032; $C_9H_{16}N_3O_6$ $[MH]^+$ requires 262.1039.

Potassium (1*S*,3*E*/*Z*,4*R*,5*R*)-3-[(aminocarbonyl)hydrazono]-1,4,5-trihydroxycyclohexane-1-carboxylate 2.38

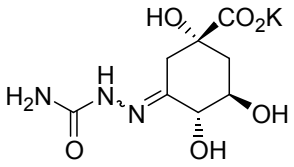

To a solution of ester **2.40** (20:1 mixture of *E*/*Z* isomers) (27 mg, 0.10 mmol) in H_2O (0.5 mL) over ice was added 0.30 M $KOH_{(aq)}$ (320 μL, 0.10 mmol) and the reaction was stirred over ice for 5 min. The solvent was evaporated and the residue dried under vacuum to give the isomers **2.38** (20:1) as a yellow glass (34 mg, quant).

^{1}H NMR (D2O, 300 MHz): δ (major isomer from 20:1 mixture) 3.95 (1H, d, *J* = 9.6 Hz), 3.59 (1H, ddd, *J* = 6.3, 9.6, 10.3 Hz), 3.02 (1H, dd, *J* = 2.0, 14.7 Hz), 2.20 (1H, d, *J* = 14.7 Hz), 1.88-1.92 (2H, m).

^{13}C NMR (D_2O): δ (major isomer from 20:1 mixture) 180.9, 165.0, 150.3, 76.5, 75.7, 72.7, 40.3, 34.8.

Optical rotation: $[\alpha]_D^{20}$ -18.05 (c. 1.03, CH_3OH).

TOF MS ES+: 286.0427; $C_8H_{13}N_3O_6K$ $[MH]^+$ requires 286.0441.

Methyl (1*S*,3*E*/*Z*,4*R*,5*R*)-3-hydrazono-1,4,5-trihydroxycyclohexane-1-carboxylate 2.41

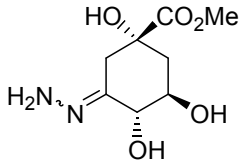

To a solution of hydrazine hydrochloride (55 mg, 0.53 mmol) in H_2O (2 mL) was added NaOAc·3H_2O until the solution reached pH 7 (720 mg, 5.29 mmol). Methyl dehydroquinate **2.13** (107 mg, 0.52 mmol) was added and the solution stirred at rt for 22 h. The solvent was removed by lyophilisation to give a dark brown solid containing *E* and *Z* isomers of the product in a 2:1 ratio (with the major isomer presumed to be *E*). The solid was subjected to flash chromatography on deactivated silica eluting with 20% MeOH/EtOAc to give a red oil (71 mg). The oil was again subjected to flash chromatography, this time without deactivating the silica, again eluting with 20% MeOH/EtOAc to give only the major (*E*) isomer of **2.41** as a beige solid (12 mg, 10%).

Alternative Method

To a solution of methyl dehydroquinate **2.13** (36 mg, 0.18 mmol) in H_2O (0.5 mL) over ice was added hydrazine hydrate (8.65 µL, 0.18 mmol). The solution was stirred at rt f or 47 h, 30 ºC for 5 h and rt for 18 h. The reaction did not appear to be progressing any further by TLC and so the solution was freeze-dried to give a yellow glass (36 mg) containing two isomers of the product, starting material and an unidentified side-product in a 5:4:2:1 ratio respectively. The yellow glass was subjected to flash chromatography on silica, eluting with 20% MeOH/EtOAc, to give a 3:1 ratio of the isomers **2.41** as a pale yellow solid (17 mg, 44%).

^{1}H NMR (D_2O): δ (major isomer only) 4.16 (1H, d, *J* = 9.3 Hz), 3.85 (1H, ddd, *J* = 4.9, 9.3, 11.5 Hz), 3.69 (3H, s), 2.99 (1H, dd, *J* = 2.9, 14.9 Hz), 2.34 (1H, d, *J* = 14.9 Hz), 2.17 (1H, ddd, *J* = 2.9, 4.9, 13.7 Hz), 2.03 (1H, dd, *J* = 11.5, 13.7 Hz).

^{13}C NMR (D_2O): δ (major isomer only) 175.1, 160.2, 75.9, 74.4, 71.0, 53.3, 39.0, 34.6.

TOF MS ES+: 219.1665; $C_8H_{15}N_2O_5$ $[MH]^+$ requires 219.0981.

Potassium (1*S*,3*E*,4*R*,5*R*)-3-hydrazono-1,4,5-trihydroxycyclohexane-1-carboxylate 2.42

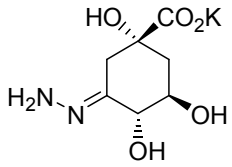

To a solution of the major (*E*) isomer of **2.41** (4 mg, 0.02 mmol) in H_2O (200 μL) over ice was added 0.30 M $KOH_{(aq)}$ (70 μL, 0.02 mmol). The solution was stirred over ice for 10 min and the solvent removed by lyophilisation to give the *E*-isomer **2.42** as a brown glass (6 mg, quant).

^{1}H NMR (D_2O, 300 MHz): δ 4.17 (1H, d, J = 9.3 Hz), 3.86 (1H, ddd, J = 5.4, 9.3, 11.2 Hz), 2.94 (1H, dd, J = 2.4, 14.9 Hz), 2.33 (1H, d, J = 14.9 Hz), 2.08 (1H, ddd, J = 2.4, 5.4, 13.7 Hz), 1.99 (1H, dd, J = 11.2, 13.7 Hz).

^{13}C NMR (D_2O): δ 180.5, 162.2, 76.3, 75.8, 71.9, 40.2, 35.6.

TOF MS ES-: 203.0663; $C_7H_{11}N_2O_5$ $[M-K]^-$ requires 203.0668.

Methyl (1*S*,3*E*/*Z*,4*R*,5*R*)-3-[(aminocarbonothioyl)hydrazono]-1,4,5-trihydroxycyclohexane-1-carboxylate 2.43

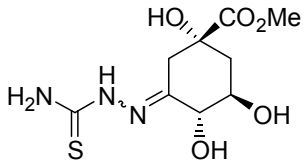

Methyl dehydroquinate **2.13** (1.02 g, 4.99 mmol) and thiosemicarbazide (510 mg, 5.59 mmol) were heated at 40 ºC in a mixture of MeOH (3 mL) and acetate buffer (pH 7, 1.8 M, 2 mL) for 7 h then the solvent evaporated. The residue (a brown oil) was subjected to flash chromatography on deactivated silica, eluting with 5% MeOH/EtOAc to give the isomers **2.43** in a 9:1 ratio (major isomer presumed to be *E*) as a beige solid (704 mg, 51%).

^{1}H NMR (D_2O, 300 MHz): δ (major isomer from a 9:1 mixture) 4.11 (1H, d, J = 8.8 Hz), 3.71 (1H, ddd, J = 4.7, 8.8, 11.0 Hz), 3.68 (3H, s), 3.05 (1H, dd, J = 2.4, 14.9 Hz), 2.52 (1H, d, J = 14.9 Hz), 2.13 (1H, ddd, J = 2.4, 4.7, 13.7 Hz), 2.00 (1H, dd, J = 11.0, 13.7 Hz).

^{13}C NMR (D_2O): δ (major isomer from a 9:1 mixture) 177.6, 174.9, 152.6, 75.9, 74.2, 71.4, 53.4, 39.2, 34.4.

Anal. Calculated for $C_9H_{15}N_3O_5S \cdot H_2O$: C 36.60; H 5.80; N 14.23; S 10.86. Found C 36.64; H 5.82; N 15.13; S 11.42.

Optical rotation: $[\alpha]_D^{20}$ -31.46 (*c*. 1.03, CH_3OH).

TOF MS ES+: 278.0818; $C_9H_{16}N_3O_5S$ $[MH]^+$ requires 278.0811.

Potassium (1*S*,3*E*/*Z*,4*R*,5*R*)-3-[(aminocarbonothioyl)hydrazono]-1,4,5-trihydroxycyclohexane-1-carboxylate 2.44

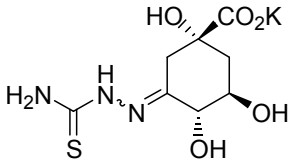

To a solution of thiosemicarbazone **2.43** (114 mg, 0.41 mmol) (9:1 *E*:*Z*) in H_2O (1 mL) over ice was added 0.30 M $KOH_{(aq)}$ (1.38 mL, 0.41 mmol). The solution was stirred 5 min over ice then freeze-dried. ^{1}H NMR showed a small amount of the ester remaining so a second aliquot of $KOH_{(aq)}$ (0.17 mL, 0.05 mmol) was added with 1 mL H_2O. After stirring over ice for another 5 min the reaction was freeze-dried to give **2.44** (9:1 *E*:*Z*) as a brown glass (123 mg, quant).

^{1}H NMR (D_2O, 300 MHz): δ (major isomer from 9:1 mixture) 4.08 (1H, d, J = 9.3 Hz), 3.64 (1H, ddd, J = 5.4, 9.3, 11.2 Hz), 2.94 (1H, dd, J = 2.4, 14.7 Hz), 2.37 (1H, d, J = 14.7 Hz), 1.97 (1H, ddd, J = 2.4, 5.4, 13.7 Hz), 1.92 (1H, dd, J = 11.2, 13.7 Hz).

^{13}C NMR (D_2O): δ (major isomer from 9:1 mixture) 180.0, 177.3, 154.4, 76.3, 75.5, 72.5, 40.2, 35.6.

Anal. Calculated for $C_8H_{12}N_3O_5KS{\cdot}2.5H_2O$: C 27.74; H 4.95; N 12.13; S 9.26. Found C 27.69; H 4.50; N 12.62; S 9.60.

Optical rotation: $[\alpha]_D^{20}$ -24.51 (*c*. 1.02, H_2O).

TOF MS ES+: 264.0655; $C_8H_{14}N_3O_5S$ $[MH_2\text{-}K]^+$ requires 264.0654.

Methyl (1*S*,3*E*/*Z*,4*R*,5*R*)-3-(formylhydrazono)-1,4,5-trihydroxycyclohexane-1-carboxylate 2.45

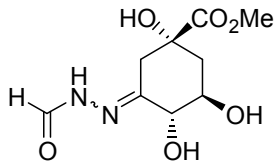

Methyl dehydroquinate **2.13** (78 mg, 0.38 mmol) and formic hydrazide (21 mg, 0.35 mmol) were stirred in H_2O (1.5 mL) at rt for 55 h. The solution was freeze dried to give a yellow glass containing the product, an unidentified side-product and methyl dehydroquinate (8:1:0.75). The product was present as a pair of isomers (3:4). The mixture was subjected to flash chromatography on silica, eluting with 15% MeOH/EtOAc. Fractions containing the product **2.45** were evaporated separately and analysed by ^1H NMR. The fraction containing the least side product (25:1 product:side-product) was set aside for deprotection and assay (22 mg, 24%). This fraction contained a 3:2 ratio of isomers, with the major isomer presumed to be the *E*-isomer. The remaining fractions were combined to give a 6:1 mixture of product and side-product (39 mg, 4:3 *E*:*Z*, 39%).

^1H NMR (CD_3OD): δ (major isomer from 3:2 mixture) 8.07 (1H, s), 4.05 (1H, d, *J* = 8.8 Hz), 3.79 (1H, ddd, *J* = 4.9, 8.8, 10.7 Hz), 3.76 (3H, s), 3.04 (1H, dd, *J* = 2.4, 14.7 Hz), 2.54 (1H,

d, *J* = 14.7 Hz), 2.15 (1H, m), 2.01 (1H, m) (minor isomer from 3:2 mixture) 8.68 (1H, s), 4.01 (1H, d, *J* = 8.6 Hz), 3.79 (1H, ddd, *J* = 4.9, 8.6, 10.7 Hz), 3.76 (3H, s), 3.04 (1H, dd, *J* = 2.4, 14.7 Hz), 2.50 (1H, d, *J* = 14.7 Hz), 2.15 (1H, m), 2.01 (1H, m).

^{13}C NMR (D_2O): δ (both isomers from 3:2 mixture) 175.0, 174.9, 168.0, 160.6, 158.5, 153.5, 75.8, 75.6, 74.3, 74.2, 71.3, 71.1, 53.4, 48.9, 39.1, 39.0, 34.5, 34.2.

TOF MS ES+: 247.0963. $C_9H_{15}N_2O_6$ $(MH)^+$ requires 247.0930.

Potassium (1*S*,3*E*/*Z*,4*R*,5*R*)-3-(formylhydrazono)-1,4,5-trihydroxycyclohexane-1-carboxylate 2.46

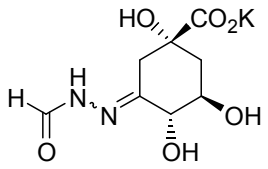

To ester **2.45** (23 mg, 0.09 mmol) in H_2O (200 μL) was added 0.30 M $KOH_{(aq)}$ (350 μL, 0.10 mmol) and the reaction stirred over ice for 5 min. The solvent was removed by lyophilisation to give a brown glass **2.46** as a 2:3 mixture of isomers (24 mg, quant)

^{1}H NMR (D_2O): δ (major isomer from a 3:2 mixture) 7.96 (1H, s), 4.15 (1H, d, *J* = 9.3 Hz), 3.71 (1H, m), 2.90 (1H, dd, *J* = 2.4, 14.9 Hz), 2.43 (1H, d, *J* = 14.9 Hz), 1.93-2.03 (2H, m), (minor isomer from a 3:2 mixture) 8.57 (1H, s), 4.08 (1H, d, *J* = 9.3 Hz), 3.69 (1H, m), 2.95 (1H, dd, *J* = 2.4, 14.9 Hz), 2.36 (1H, d, *J* = 14.9 Hz), 1.93-2.03 (2H, m).

^{13}C NMR (D_2O): δ (both isomers from a 3:2 mixture) 180.1, 179.9, 169.1, 160.8, 159.7, 155.3, 76.5, 76.1, 75.5, 72.6, 72.3, 40.2, 35.8, 35.5.

TOF MS ES-: 231.0652. $C_8H_{11}N_2O_6$ $(M-K)^-$ requires 231.0617.

Methyl (1*S*,3*E*,4*R*,5*R*)-3-(hydroxyimino)-1,4,5-trihydroxycyclohexane-1-carboxylate 2.47

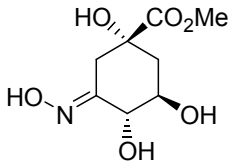

To a solution of hydroxylamine hydrochloride (21 mg, 0.30 mmol) in H_2O (1 mL) was added NaOAc·$3H_2O$ until the solution reached pH 7 (212 mg, 1.56 mmol). Methyl dehydroquinate **2.13** (41 mg, 0.20 mmol) was added and the reaction stirred at rt for 18 h. The solvent was removed by lyophilisation and the residue subjected to flash chromatography on silica, eluting with EtOAc. Fractions containing the product were evaporated, then re-dissolved in H_2O and freeze-dried to remove traces of EtOAc and CH_3COOH. A single isomer of the product **2.47** was obtained as colourless glass (23.8 mg, 55%), whose ^{1}H NMR data were in agreement with the literature.[5]

^{1}H NMR (D_2O): δ 4.06 (1H, d, J = 9.3 Hz), 3.74 (1H, ddd, J = 4.4, 9.3, 11.2 Hz), 3.68 (3H, s), 3.31 (1H, dd, J = 2.9, 14.9 Hz), 2.33 (1H, d, J = 14.9 Hz), 2.11 (1H, ddd, J = 2.9, 4.4, 13.7 Hz), 1.97 (1H, dd, J = 11.2, 13.7 Hz).

Potassium (1*S*,3*E*,4*R*,5*R*)-3-(hydroxyimino)-1,4,5-trihydroxycyclohexane-1-carboxylate 1.32

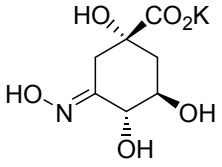

To a solution of oxime methyl ester **2.47** (11.8 mg, 0.06 mmol) in H_2O (300 µL) over ice was added 0.30 M $KOH_{(aq)}$ (200 µL, 0.06 mmol). The reaction was stirred over ice for 10 min then freeze-dried to give the potassium salt of **1.32** as a pale yellow glass (15 mg, quant), whose ^{1}H NMR data were in agreement with the literature.[5]

^{1}H NMR (D_2O): δ 4.03 (1H, d, *J* = 9.3 Hz), 3.69 (1H, ddd, *J* = 4.9, 9.3, 10.7 Hz), 3.18 (1H, dd, *J* = 2.4, 14.7 Hz), 2.18 (1H, d, *J* = 14.7 Hz), 1.97 (1H, ddd, *J* = 2.4, 4.9, 13.2 Hz), 1.90 (1H, dd, *J* = 10.7, 13.2 Hz).

Methyl (1*R*,3*S*,4S,6*S*,9*R*)-9-hydroxy-3,4-dimethoxy-3,4-dimethyl-7,9-bis(trimethylsiloxy)-2,5-dioxabicyclo[4.4.0]dec-7-ene-9-carboxylate 2.55

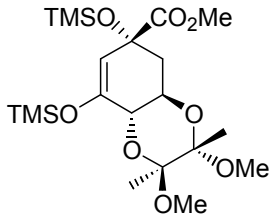

To a solution of protected dehydroquinate **2.12** (101 mg, 0.32 mmol) in dry toluene (4 mL) under Ar was added dry Et_3N (0.45 mL, 3.2 mmol), then trimethylsilyl trifluoromethanesufonate (0.35 mL, 1.9 mmol) and the reaction was heated at reflux for 2.5 h. The reaction was allowed to cool, diluted with pentane and the organic fraction washed with sat. $NaHCO_3$ (3×) and H_2O (1×), dried ($MgSO_4$), filtered and evaporated to furnish silylenolether intermediate **2.54** (138 mg) as a yellow oil which was used without further purification.

^{1}H NMR ($CDCl_3$): δ 4.92 (1H, dd, *J* = 1.5, 2.0 Hz), 4.05 (1H, ddd, *J* = 3.4, 9.1, 12.2 Hz), 4.00 (1H, dd, *J* = 2.0, 9.1 Hz), 3.69 (3H, s), 3.23 (3H, s), 3.21 (3H, s), 2.06 (1H, dd, *J* = 12.2, 12.7 Hz), 1.97 (1H, ddd, *J* = 1.5, 3.4, 12.7 Hz), 1.30 (3H, s), 1.26 (3H, s), 0.20 (9H, s), 0.10 (9H, s).

^{13}C NMR ($CDCl_3$): δ 174.1, 152.0, 107.9, 100.3, 99.6, 75.2, 69.4, 65.3, 52.3, 47.6, 38.0, 17.7, 17.62, 1.9, 0.4.

Methyl (1*R*,3*S*,4S,6*S*)-3,4-dimethoxy-3,4-dimethyl-7-oxo-2,5-dioxabicyclo[4.4.0]dec-8-ene-9-carboxylate 2.56

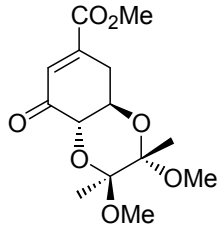

To a solution of protected dehydroquinate **2.12** (113 mg, 0.35 mmol) in dry toluene under Ar was added dry Et_3N (0.25 mL, 1.8 mmol), then trimethylsilyl trifluoromethanesufonate (0.39 mL, 2.12 mmol) and the reaction was heated at reflux for 2 h. The reaction was allowed to cool, diluted with pentane and the organic fraction washed with sat. $NaHCO_3$ (4×) and H_2O (1×), dried ($MgSO_4$), filtered and evaporated to give **2.56** as a yellow oil which crystallised on standing (100 mg, 94%).

^1H NMR ($CDCl_3$): δ 6.77 (1H, d, J = 3.2 Hz), 4.29 (1H, d, J = 11.7 Hz), 4.07 (1H, ddd, J = 5.4, 10.7, 11.7 Hz), 3.82 (3H, s), 3.28 (3H, s), 3.23 (3H, s), 3.05 (1H, dd, J = 5.4, 18.6 Hz), 2.62 (1H, ddd, J = 3.2, 10.7, 18.6 Hz), 1.39 (3H, s), 1.31 (3H, s).

^{13}C NMR ($CDCl_3$): δ 194.4, 165.8, 144.6, 132.6, 100.3, 99.3, 75.0, 67.0, 52.9, 48.4, 48.0, 30.4, 17.6, 17.5.

mp: 115-118 ºC (lit: 98-99 ºC)[1]

Methyl (1*R*,3*S*,4*S*,6*S*,8*S*,9*R*)-8-fluoro-3,4-dimethoxy-3,4-dimethyl-7-oxo-9-(trimethylsiloxy)-2,5-dioxabicyclo[4.4.0]decane-9-carboxylate 2.57

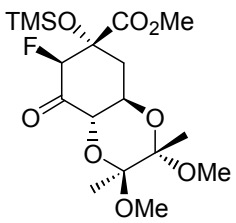

A mixture of silylenolether intermediate **2.54** and ketone **2.55** (5:2) (160 mg) was taken up in dry MeCN and Selectfluor® fluorinating reagent (131 mg, 0.37 mmol) added over 4 Å molecular sieves. The reaction was stirred at rt under Ar for 2.5 h. The reaction mixture was diluted with diethyl ether, washed with H_2O (3×), dried ($MgSO_4$), filtered and evaporated to give a 1:1 mixture of (2*S*)-2-fluoroketone **2.57** and unfluorinated ketone **2.55** as a yellow oil (210 mg). Flash chromatography on silica, eluting with 15% EtOAc/pet. ether furnished (2S)-2-fluoroketone **2.57** as a colourless oil (42 mg, 32% over 2 steps from **2.12**) and ketone **2.55** (58 mg, 31%).

^{1}H NMR ($CDCl_3$): δ 4.77 (1H, dd, *J* = 7.5, 10.0 Hz), 4.67 (1H, dd, *J* = 1.6, 48.8 Hz), 4.01 (1H, dddd, *J* = 1.0, 3.8, 10.0, 12.0 Hz), 3.78 (3H, s), 3.23 (3H, s), 3.21 (3H, s), 2.47 (1H, ddd, *J* = 4.7, 12.0, 14.3 Hz), 2.29 (1H, dddd, *J* = 1.6, 3.0, 3.8, 14.3 Hz), 1.37 (3H, s), 1.29 (3H, s), 0.08 (9H, s).

^{13}C NMR ($CDCl_3$): δ 196.2 (d, $J_{C\text{-}F}$ = 19.2 Hz), 169.7, 100.4, 99.6, 92.6 (d, $J_{C\text{-}F}$ = 186.3 Hz), 76.9 (d, $J_{C\text{-}F}$ = 26.5 Hz), 74.5 (d, $J_{C\text{-}F}$ = 2.1 Hz), 66.2, 52.8, 48.3, 48.0, 33.1, 18.0, 17.5, 1.0.

^{19}F NMR ($CDCl_3$, 282 MHz): δ -185.24 (1F, m, *J* = 48.8 Hz).

Methyl (1*R*,3*S*,4*S*,6*S*,8*R*,9*R*)-8-fluoro-9-hydroxy-3,4-dimethoxy-3,4-dimethyl-7-oxo-2,5-dioxabicyclo[4.4.0]decane-9-carboxylate 2.60

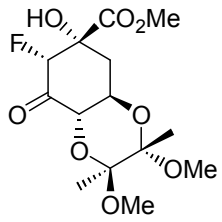

Unpurified silylenolether intermediate **2.54** (138 mg) was taken up in dry MeCN and Selectfluor® fluorinating reagent (118 mg, 0.33 mmol) added over 4 Å molecular sieves. The reaction was stirred at rt under Ar for 2.5 h. The reaction mixture was diluted with diethyl ether, washed with H_2O (3×), dried ($MgSO_4$), filtered and evaporated to give a 6:1 mixture of

(2*S*)-2-fluoroketone **2.57** and unfluorinated ketone **2.55** as a brown oil (90 mg). Flash chromatography on deactivated silica, eluting with 20-30% EtOAc/pet. ether, furnished (2*R*)-2-fluoroketone **2.60** (52 mg, 51% over 2 steps from **2.12**).

^{1}H NMR ($CDCl_3$): δ 5.23 (1H, dd, J = 1.5, 46.7 Hz), 4.43 (1H, dd, J = 1.5, 10.3 Hz), 4.22 (1H, ddd, J = 4.8, 10.3, 12.2 Hz), 3.88 (3H, s), 3.25 (3H, s), 3.21 (3H, s), 2.31 (1H, dd, J = 12.2, 13.5 Hz), 2.21 (1H, ddd, J = 4.8, 7.1, 13.5 Hz), 1.39 (3H, s), 1.29 (3H, s).

^{13}C NMR ($CDCl_3$): δ 193.97 (d, $J_{C\text{-}F}$ = 16.6 Hz), 171.22, 100.32, 99.75, 92.74 (d, $J_{C\text{-}F}$ = 199.2 Hz), 76.57 (d, $J_{C\text{-}F}$ = 18.2 Hz), 75.15 (d, $J_{C\text{-}F}$ = 2.6 Hz), 66.70, 53.97, 48.49, 48.09, 34.30 (d, $J_{C\text{-}F}$ = 4.2 Hz), 17.58, 17.36.

^{19}F NMR ($CDCl_3$, 282 MHz): -31.31 (1F, dd, J = 7.1, 46.7 Hz).

(1*R*,3*S*,4*S*,6*R*,7*R*,9*S*)-7,9-Dihydroxy-3,4-dimethoxy-3,4-dimethyl-2,5-dioxabicyclo[4.4.0]decane-9-carboxylic acid 2.61

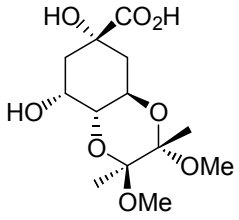

1.00 M $KOH_{(aq)}$ (1.5 mL, 1.5 mmol) was added to protected quinic acid **2.11** (201 mg, 0.63 mmol) and the reaction stirred over ice for 10 min. Amberlite IR 120 (H) ion exchange resin was added and the suspension stirred a further 5 min. The resin was removed by filtration and the filtrate freeze-dried to give the free acid intermediate **2.61** as a white solid (183 mg, 95%) which was used without further purification.

^{1}H NMR (D_2O): δ 4.21 (1H, ddd, J = 4.4, 10.7, 12.0Hz), 4.13 (1H, ddd, J = 2.9, 2.9, 2.9 Hz),3.59 (1H, dd, J = 2.9, 10.7 Hz), 3.21 (3H, s), 3.19 (3H, s), 1.99-2.07 (3H, m), 1.88 (1H, dd, J = 12.0, 12.7 Hz), 1.27 (3H, s), 1.23 (3H, s).

^{13}C NMR (D_2O): δ 178.2, 101.2, 101.0, 76.2, 73.3, 68.7, 63.7, 48.5, 48.4, 38.1, 17.7, 17.6.

Allyl (1*R*,3*S*,4*S*,6*R*,7*R*,9*S*)-7,9-dihydroxy-3,4-dimethoxy-3,4-dimethyl-2,5-dioxabicyclo[4.4.0]decane-9-carboxylate 2.62

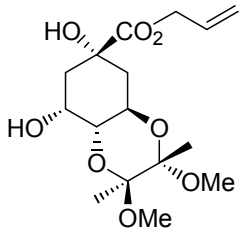

To a solution of acid intermediate **2.61** (438 mg, 1.43 mmol) in DMF (4 mL) was added $KHCO_3$ (329 mg, 3.28 mmol) and allyl bromide (2.0 mL, 23 mmol) and the suspension stirred at rt for 23 h. The reaction was diluted with diethyl ether and the organic phase washed with 1 M $KHSO_4$ (1×), sat. NaCl (1×) and H_2O (1×), dried ($MgSO_4$), filtered and evaporated. The residue was subjected to flash chromatography on silica gel, eluting with 50% pet. ether/EtOAc to give the desired allyl ester **2.62** as a colourless oil which crystallised on standing (322 mg, 65%).

^{1}H NMR ($CDCl_3$): *δ* 5.87 (1H, dddd, *J* = 5.7, 5.7, 10.5, 17.2 Hz), 5.30 (1H, dddd, *J* = 1.3, 1.3, 2.7, 17.2 Hz), 5.23 (1H, dddd, *J* = 1.3, 1.3, 2.7 10.5 Hz), 4.66 (1H, dddd, *J* = 1.3, 1.3, 5.7, 13.1 Hz), 4.61 (1H, dddd, *J* = 1.3, 1.3, 5.7, 13.1 Hz), 4.29 (1H, ddd, *J* = 4.6, 10.3, 11.9 Hz), 4.21 (1H, s), 4.16 (1H, m), 3.57 (1H, dd, *J* = 2.8, 10.3 Hz), 3.23 (3H, s), 3.23 (3H, s), 2.15 (1H, ddd, *J* = 3.0, 3.2, 14.9 Hz), 2.08 (1H, ddd, *J* = 3.0, 4.6, 12.7 Hz), 2.02 (1H, dd, *J* = 2.8, 14.9 Hz), 1.92 (1H, dd, *J* = 11.9, 12.7 Hz), 1.31 (3H, s), 1.27 (3H, s).

^{13}C NMR ($CDCl_3$): δ 173.6, 131.2, 119.1, 100.3, 99.7, 75.7, 72.8, 69.1, 66.4, 47.9, 38.6, 37.4, 17.8, 17.7.

mp: 82-84 ºC

Allyl (1*R*,3*S*,4*S*,6*S*,9*R*)-9-hydroxy-3,4-dimethoxy-3,4-dimethyl-7-oxo-2,5-dioxabicyclo[4.4.0]decane-9-carboxylate 2.63

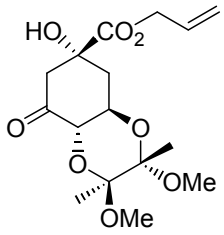

Alcohol **2.62** (838 mg, 2.42 mmol) in CH_2Cl_2 (10 mL) was added to a suspension of PCC (5.0 g, 23 mmol) in CH_2Cl_2 (15 mL) over 4 Å molecular sieves and the reaction stirred at rt for 20 h. The brown suspension was filtered through silica, rinsing with 10% MeOH/EtOAc (150 mL). The filtrate was concentrated, re-dissolved in EtOAc and heated at reflux with activated charcoal for 3 h. The suspension was filtered through silica, rinsing with 10% MeOH/EtOAc (150 mL). The filtrate was evaporated and the residue subjected to flash chromatography on silica, eluting with 40% EtOAc/pet. ether to give **2.63** as a colourless oil which slowly crystallised on cooling (589 mg, 71%).

^{1}H NMR ($CDCl_3$): δ 5.87 (1H, dddd, *J* = 5.8, 5.8, 10.5, 17.1 Hz), 5.32 (1H, ddd, *J* = 1.2, 1.4, 17.1 Hz), 5.27 (1H, ddd, *J* = 1.2, 1.4, 10.5 Hz), 4.71 (1H, dddd, *J* = 1.2, 1.4, 5.8, 13.1 Hz), 4.63 (1H, dddd, *J* = 1.2, 1.4, 5.8, 13.1 Hz), 4.40 (1H, dd, *J* = 1.1, 10.3 Hz), 4.23, (1H, ddd, *J* = 4.5, 10.3, 12.3 Hz), 3.31 (1H, s), 3.23 (3H, s), 3.20 (3H, s), 2.89 (1H, dd, *J* = 1.1, 14.3 Hz), 2.49 (1H, dd, *J* = 3.0, 14.3 Hz), 2.36 (1H, dd, *J* = 12.3, 12.9 Hz), 2.10 (1H, ddd, *J* = 3.0, 4.5, 12.9 Hz), 1.36 (3H, s), 1.27 (3H, s).

^{13}C NMR ($CDCl_3$): δ 199.4, 173.3, 130.7, 119.7, 100.5, 99.6, 77.2, 74.0, 67.1, 67.0, 49.0, 48.3, 48.0, 37.8, 17.6, 17.5.

mp: 143-145 ºC

TOF MS ES+: 345.1536; $C_{16}H_{25}O_8$ $[MH]^+$ requires 345.1549.

Allyl (1R,4S,5R)-1,4,5-trihydroxy-3-oxocyclohexane-1-carboxylate (Allyl 3-dehydroquinate) 2.64

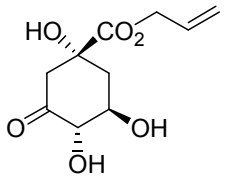

To ketone **2.63** (80 mg, 0.23 mmol) over ice was added H_2O (25 μL) and TFA (475 μL) and the reaction stirred over ice for 3 h. The solvent was removed by lyophilisation and the residue re-dissolved in MeOH and evaporated to give the free diol **2.64** as a colourless oil (52 mg, 96%).

^{1}H NMR (CD_3OD): δ 5.96 (1H, m), 5.35 (1H, d, J = 17.2 Hz), 5.23 (1H, d, J = 10.5 Hz), 4.67 (2H, d, J = 5.5 Hz), 4.40 (1H, d, J = 9.3 Hz), 3.90 (1H, ddd, J = 5.0, 9.6, 11.2 Hz), 3.05, (1H, d, J = 14.0 Hz), 2.54 (1H, dd, J = 3.0, 14.0 Hz), 2.28 (1H, ddd, J = 3.0, 5.0, 13.4 Hz), 2.22 (1H, dd, J = 11.2, 13.4 Hz).

^{13}C NMR (D_2O): δ 208.5, 174.5, 132.0, 119.5, 81.3, 74.8, 71.8, 67.7, 48.1, 40.1.

TOF MS ES+: 195.1147; $C_{10}H_{11}O_4$ $[MH\text{-}2H_2O]^+$ requires 195.0657.

Allyl (1*R*,3*S*,4S,6*S*,9*R*)-9-hydroxy-3,4-dimethoxy-3,4-dimethyl-7,9-bis(trimethylsiloxy)-2,5-dioxabicyclo[4.4.0]dec-7-ene-9-carboxylate 2.65

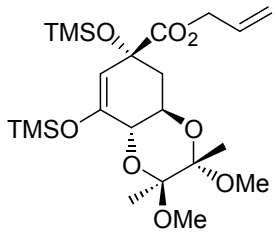

Ketone **2.63** (103 mg, 0.30 mmol), dry Et_3N (1.8 mL, 13 mmol), and TMSOTf (1.0 mL, 5.5 mmol) were heated at reflux in dry toluene (5 mL) for 2.5 h under Ar. The reaction was allowed to cool, then diluted with pentane and the organic fraction washed with sat. $NaHCO_3$ (5×), dried ($MgSO_4$) and filtered. The filtrate was evaporated to give silylenolether intermediate **2.65** as a yellow oil (137 mg) which was used without further purification.

^1H NMR ($CDCl_3$): δ 5.88 (1H, dddd, *J* = 5.7, 5.7, 10.4, 17.3 Hz), 5.30 (1H, dddd, *J* = 1.3, 1.3, 1.4, 17.3, Hz), 5.22 (1H, dddd, *J* = 1.3, 1.3, 1.4, 10.4 Hz), 4.95 (1H, dd, *J* = 1.6, 1.7 Hz), 4.61 (1H, dddd, *J* = 1.3, 1.3, 5.7, 13.3 Hz), 4.56 (1H, dddd, *J* = 1.3, 1.3, 5.7, 13.3 Hz), 4.07 (1H, ddd, *J* = 3.2, 9.2, 12.5 Hz), 4.03 (1H, dd, *J* = 1.7, 9.2 Hz), 3.25 (3H, s), 3.23 (3H, s), 2.11 (1H, dd, *J* = 12.5, 12.6 Hz), 2.00 (1H, ddd, *J* = 1.6, 3.2, 12.6 Hz), 1.32 (3H, s), 1.28 (3H, s), 0.21 (9H, s), 0.12 (9H, s).

Methyl (1*R*,3*S*,4*S*,6*S*,8*S*,9*R*)-8-fluoro-3,4-dimethoxy-3,4-dimethyl-7-oxo-9-(trimethylsiloxy)-2,5-dioxabicyclo[4.4.0]decane-9-carboxylate 2.66

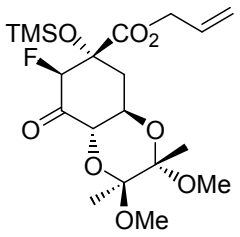

To a solution of silylenolether intermediate **2.65** (137 mg) in dry MeCN over 4 Å molecular sieves was added Selectfluor® fluorinating reagent (107 mg, 0.30 mmol) and the reaction stirred at rt for 20 h. The reaction mixture was diluted with diethyl ether and extracted with H_2O (3×). The organic phase was dried ($MgSO_4$), filtered and evaporated to give a brown oil containing a 3:1 mixture of **2.66** and **2.67**. The oil was subjected to flash chromatography on silica gel, eluting with 25% EtOAc/pet. ether to give the α-fluoroketone **2.66** as a colourless oil (46 mg, 37% over 2 steps from **2.63**).

^{1}H NMR ($CDCl_3$): δ 5.91 (1H, dddd, J = 5.7, 5.7, 10.5, 17.1 Hz), 5.36 (1H, dd, J = 1.3, 17.1, Hz), 5.29 (1H, dd, J = 1.3, 10.5 Hz), 4.80 (1H, dd, J = 7.4, 10.5 Hz), 4.70 (1H, dd, J = 1.3, 48.7 Hz), 4.67 (2H, m), 4.03 (1H, ddd, J = 4.3, 10.5, 12.0 Hz), 3.25 (3H, s), 3.22 (3H, s), 2.53 (1H, ddd, J = 4.7, 12.0, 16.8 Hz), 2.31 (1H, m), 1.39 (3H, s), 1.31 (3H, s), 0.11 (9H, s).

^{13}C NMR ($CDCl_3$): δ 196.2 (d, $J_{C\text{-}F}$ = 19.2 Hz), 169.1, 130.8, 119.4, 100.5, 99.7, 92.7 (d, $J_{C\text{-}F}$ = 186.8 Hz), 77.1 (d, $J_{C\text{-}F}$ = 26.5 Hz), 74.6 (d, $J_{C\text{-}F}$ = 2.6 Hz), 66.6, 66.4, 48.4, 48.1, 33.2, 17.7, 17.5, 1.2.

^{19}F NMR ($CDCl_3$, 282 MHz): -185.07 (1F, m, J = 48.7 Hz).

4-Methoxybenzyl (1*R*,3*S*,4*S*,6*R*,7*R*,9*S*)-7,9-dihydroxy-3,4-dimethoxy-3,4-dimethyl-2,5-dioxabicyclo[4.4.0]decane-9-carboxylate 2.68

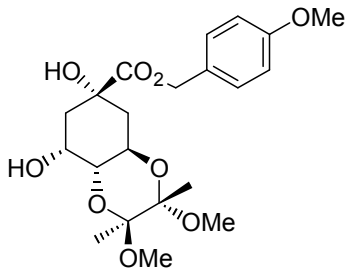

To protected quinic acid **2.11** (549 mg, 1.72 mmol) was added 1.00 M $KOH_{(aq)}$ (5.0 mL, 5.0 mmol) and the reaction stirred for 10 min over ice. Amberlite IR120 (H) ion exchange resin was added and the suspension stirred a further 5 min. The reaction was filtered and the filtrate freeze-dried. To the residue was added $KHCO_3$ (345 mg, 3.4 mmol), *p*-methoxybenzyl chloride (0.35 mL, 2.6 mmol) and dry DMF and the suspension stirred at rt under Ar for 45 h. The reaction was diluted with diethyl ether and washed with H_2O (2×) and sat. NaCl (2×), dried ($MgSO_4$), filtered and evaporated to give a yellow oil. The oil was subjected to flash chromatography on silica gel, eluting with 40% pet. ether/EtOAc to give the *p*-methoxybenzyl ester **2.68** as a colourless oil (304 mg, 41%).

^{1}H NMR ($CDCl_3$): δ 7.26 (2H, d, *J* = 8.7 Hz), 6.87 (2H, d, *J* = 8.7 Hz), 5.12 (1H, d, *J* = 11.7 Hz), 5.09 (1H, d, *J* = 11.7 Hz), 4.29 (1H, ddd, *J* = 4.8, 10.3, 12.5 Hz), 4.15 (2H, m), 3.80 (3H, s), 3.55 (1H, dd, *J* = 3.2, 10.3 Hz), 3.24 (3H, s), 3.23 (3H, s), 2.14 (1H, ddd, *J* = 2.8, 2.8, 15.1 Hz), 2.05 (1H, ddd, *J* = 2.8, 4.8, 12.7 Hz), 2.01 (1H, dd, *J* = 2.8, 15.1 Hz), 1.90 (1H, dd, *J* = 12.5, 12.7 Hz), 1.32 (3H, s), 1.28 (3H, s).

^{13}C NMR ($CDCl_3$): δ 173.8, 159.8, 130.1, 127.2, 114.0, 100.3, 99.7, 75.6, 72.8, 69.0, 67.5, 62.5, 55.3, 47.9, 38.5, 37.4, 17.8, 17.7.

TOF MS ES+: 395.1695; $C_{20}H_{27}O_8$ $[MH_2\text{-}H_2O\text{-}CH_3]^+$ requires 395.1706.

Methyl (1*R*, 3*S*, 4*S*, 6*S*, 9*R*)-3,4-dimethoxy-3,4-dimethyl-7-oxo-9-(trimethylsiloxy)-2,5-dioxabicyclo[4.4.0]decane-9-carboxylate 2.55

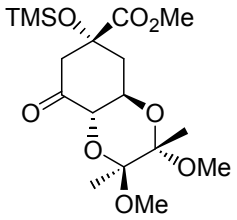

Protected dehydroquinate **2.12** (807 mg, 2.53 mmol), hexamethyldisilazane (2.0 mL, 9.5 mmol) and TMSCl (1.5 mL, 12 mmol) were stirred in pyridine at rt under Ar for 16 h. The reaction mixture was concentrated *in vacuo* and the residue partitioned between ether and water. The organic layer was washed with H_2O (1×), $CuSO_4$ (2×), H_2O (1×) and sat. $NaHCO_3$ (1×). The organic fraction was dried over $MgSO_4$, filtered and evaporated to give **2.55** as a cream coloured solid (948 mg, 96%) whose NMR data agreed with the literature[6] and which was used without further purification.

^{1}H NMR ($CDCl_3$): δ 4.34 (1H, dd, *J* = 1.5, 10.3 Hz), 4.11 (1H, ddd, *J* = 4.9, 10.3, 11.2 Hz), 3.75 (3H, s), 3.23 (3H, s), 3.21 (3H, s), 2.80 (1H, dd, *J* = 1.5, 14.7 Hz), 2.61 (1H, dd, *J* = 2.5, 14.7 Hz), 2.25 (1H, dd, *J* = 11.2, 13.2 Hz), 2.20 (1H, ddd, *J* = 2.5, 4.9, 13.2 Hz), 1.37 (3H, s), 1.27 (3H, s), 0.09 (9H, s).

^{13}C NMR ($CDCl_3$): δ 199.9, 172.8, 100.4, 77.1, 77.0, 67.1, 52.6, 49.9, 48.3, 47.9, 39.0, 17.7, 17.5, 1.6.

Methyl (1*R*, 3*S*, 4*S*, 6*R*, 9*S*)-3,4-dimethoxy-3,4-dimethyl-7-methylidene-9-(trimethylsiloxy)-2,5-dioxabicyclo[4.4.0]decane-9-carboxylate 2.70

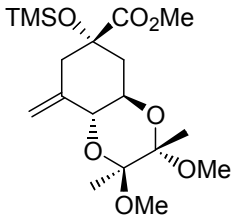

To a suspension of activated Zn dust (439 mg, 6.7 mmol) in anhydrous THF (2.5 mL) under Ar was added diiodomethane (220 µL, 2.73 mmol) and the suspension stirred at rt. for 45 min. The reaction vessel was cooled to 0 ºC and a 0.8 M solution of titanium (IV) chloride in CH_2Cl_2 was added slowly. The mixture was stirred at rt for a further 35 min, than a solution of ketone **2.55** (201 mg, 0.51 mmol) in THF (3.5 mL) was added over ice. The reaction was allowed to warm to room temperature and stirred for 3.5 h. The reaction mixture was diluted with diethyl ether and poured into ice cold 1 N HCl and the aqueous fraction extracted with diethyl ether (3×). The combined organic fractions were washed with sat. $NaHCO_3$, dried ($MgSO_4$) and evaporated. The residue was subjected to flash chromatography on silica gel, eluting with a gradient of 10 – 40% EtOAc/pet. ether to furnish the protected olefin **2.70** as a colorless oil (126 mg, 64%) (whose NMR data were consistent with the literature),[6] as well as the free alcohol **2.72** (16 mg, 10%).

^{1}H NMR ($CDCl_3$): *δ* 5.23 (1H, s), 4.85 (1H, s), 4.01 (1H, d, *J* = 9.8 Hz), 3.79 (1H, ddd, *J* = 5.9, 9.8, 10.3 Hz), 3.72 (3H, s), 3.23 (3H, s), 3.23 (3H, s), 2.47 (2H, s), 2.00-2.03 (2H, m), 1.35 (3H, s), 1.29 (3H, s), 0.09 (9H, s).

^{13}C NMR ($CDCl_3$): δ 174.4, 139.4, 109.5, 99.8, 99.4, 77.3, 72.7, 68.2, 52.2, 47.9, 43.8, 39.1, 17.9, 17.9, 1.7.

Methyl (1*R*, 3*S*, 4*S*, 6*R*, 9*S*)-9-hydroxy-3,4-dimethoxy-3,4-dimethyl-7-methylidene-2,5-dioxabicyclo[4.4.0]decane-9-carboxylate 2.72 and Methyl (1S,4R,5R)-1,4,5-trihydroxy-3-methylidenecyclohexane-1-carboxylate 2.73

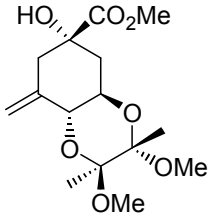

2.72

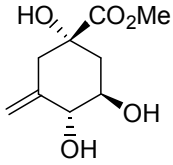

2.73

To a suspension of activated Zn dust (1.94 g, 29.6 mmol) in anhydrous THF (15 mL) was added CH_2I_2 (1.15 mL, 14.3 mmol). The suspension was stirred at rt under Ar for 1 h, then a 0.8 M solution of titanium (IV) chloride in CH_2Cl_2 (1.15 mL) added in portions over ice. After stirring a further 45 min at rt a solution of ketone **2.55** (1.13 g, 2.89 mmol) in THF (10 mL) was added over ice. The reaction was stirred at rt for 3.5 h under Ar, then diluted with diethyl ether and poured with stirring into ice-cold 1 N HCL. The aqueous layer was extracted with diethyl ether (3×) and the combined organic extracts washed with sat. $NaHCO_3$ (2×), dried ($MgSO_4$) and evaporated. The residue was subjected to flash chromatography on silica gel, eluting with pet. ether/EtOAc (3:1) to EtOAc/MeOH (19:1) to furnish protected olefin **2.72** as a pale yellow oil (459 mg, 50%) and the triol **2.73** as a colourless oil (147 mg, 25%).

Protected olefin 2.72

^1H NMR ($CDCl_3$): δ 5.28 (1H, m), 4.92 (1H, m), 4.06 (1H, d, J = 9.7 Hz), 3.87 (1H, ddd, J = 4.6, 9.7, 12.3 Hz), 3.78 (3H, s), 3.24 (3H, s), 3.21 (3H, s), 2.61 (1H, dd, J = 0.9, 13.9 Hz), 2.33 (1H, dd, J = 2.8, 13.9 Hz), 2.07 (1H, dd, J = 12.3, 12.7 Hz), 1.92 (1H, ddd, J = 2.8, 4.6, 12.7 Hz), 1.34 (3H, s), 1.29 (3H, s).

^{13}C NMR ($CDCl_3$): δ 175.4, 139.1, 109.9, 99.9, 99.5, 74.1, 72.4, 68.1, 53.0, 47.8, 47.8, 42.95, 37.9, 17.7, 17.7.

TOF MS ES+: 285.1350; $C_{14}H_{21}O_6$ $[MH_2\text{-}H_2O\text{-}CH_3]^+$ requires 285.1338.

Olefin Triol 2.73

^1H NMR ($CDCl_3$): δ 5.23 (1H, s), 4.94 (1H, s), 3.93 (1H, d, J = 9.1 Hz), 3.77 (3H, s), 3.73 (1H, ddd, J = 4.4, 9.1, 11.7 Hz), 2.59 (1H, d, J = 14.2 Hz), 2.38 (1H, dd, J = 3.4, 14.2 Hz), 2.11 (1H, ddd, J = 3.4, 4.4, 13.2 Hz), 1.95 (1H, dd, J = 11.7, 13.2 Hz).

^{13}C NMR ($CDCl_3$): δ 175.4, 142.5, 110.9, 76.9, 74.2, 71.8, 53.0, 42.6, 40.7.

TOF MS ES+: 203.0856; $C_9H_{15}O_5$ $[MH]^+$ requires 203.0919.

Methyl (1*R*, 3*S*, 4*S*, 6*R*, 9*R*)-7-(bromomethyl)-9-hydroxy-3,4-dimethoxy-3,4-dimethyl-2,5-dioxabicyclo[4.4.0]dec-7-ene-9-carboxylate 2.74

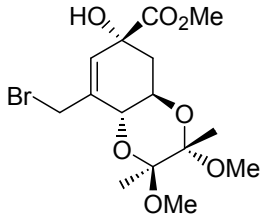

Na_2CO_3 (20 mg, 0.19 mmol) was added to a solution of phenylselenyl bromide (34 mg, 0.14 mmol) in dry CH_2Cl_2 (0.5 mL) under Ar. The mixture was cooled to -78 ºC and a solution of olefin **2.72** (39 mg, 0.12 mmol) in CH_2Cl_2 (0.75 mL) added. The reaction was stirred at -78 ºC for 23 h, then pyridine (23 µL, 0.29 mmol) was added, followed by a solution of *m*-CPBA (27 mg, 0.16 mmol) in CH_2Cl_2 (0.5 mL). The reaction was stirred a further 15 min at -78 ºC then at rt for 4.5 h. The reaction was partitioned between diethyl ether and H_2O and the organic phase washed with $Na_2S_2O_3$ (2×), $CuSO_4$ (2×), sat. $NaHCO_3$ (2×) and H_2O (2×), dried ($MgSO_4$) and evaporated. The resulting orange oil was subjected to flash chromatography on silica gel, eluting with 25% EtOAc/pet. ether to furnish allylic bromide **2.74** as a colourless oil (21 mg, 42%), whose NMR data was consistent with the literature.[6]

^{1}H NMR ($CDCl_3$): δ 5.60 (1H, s), 4.44 (1H, dd, *J* = 2.4, 9.3 Hz), 4.40 (1H, d, *J* = 9.8 Hz), 4.05 (1H, ddd, *J* = 3.9, 9.3, 13.2 Hz), 3.80 (4H, m), 3.41 (3H, s), 3.26 (3H, s), 2.19 (1H, dd, *J* = 13.2, 13.2 Hz), 1.94 (1H, ddd, *J* = 1.5, 3.9, 13.2 Hz), 1.34 (3H, s), 1.30 (3H, s).

^{13}C NMR ($CDCl_3$): δ 175.2, 139.2, 126.8, 100.5, 99.9, 73.1, 67.7, 65.4, 53.6, 48.7, 48.0, 37.0, 30.0, 17.8.

Methyl (1*R*,4*R*,5*R*)-3-(bromomethyl)-1,4,5-trihydroxycyclohex-2-ene-1-carboxylate 2.75

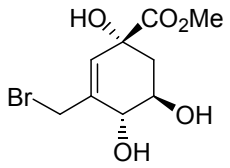

TFA (475 μL) and H_2O (25 μL) were added to protected allylic bromide **2.72** (5.9 mg, 0.01 mmol) and the reaction stirred over ice for 35 min. The solvent was removed by lyophilisation and the residue re-dissolved in MeOH and evaporated to furnish **2.75** as a colourless oil (4.9 mg, quant).

^{1}H NMR (CD_3OD): δ 5.88 (1H, s), 4.38 (1H, d, *J* = 9.8 Hz), 4.22 (1H, dd, *J* = 1.5, 7.8 Hz), 3.95 (1H, d, *J* = 9.8 Hz), 3.91 (1H, ddd, *J* = 5.4, 7.8, 10.3 Hz), 3.74 (3H, s), 2.00-2.02 (2H, m).

^{13}C NMR (CD_3OD): δ 176.1, 142.7, 128.9, 74.5, 73.3, 71.0, 53.5, 40.9, 33.4.

TOF MS ES+: 281.0056; $C_9H_{14}BrO_5$ $[MH]^+$ requires 281.0024.

Methyl (3*S*,4*S*,5*R*)-3-(bromomethyl)-4,5-dihydroxycyclohex-1-ene-1-carboxylate 2.79

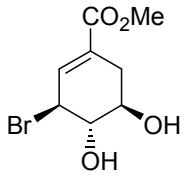

To allylic bromide **2.78** (86 mg, 0.24 mmol) in H_2O (25 μL) over ice was added TFA (475 μL) and the reaction stirred over ice for 1.75 h. The solvent was removed by lyophilisation and the residue re-dissolved in MeOH then evaporated. The product was purified by flash chromatography on silica gel, eluting with 33% pet. ether/EtOAc to furnish the free diol **2.79** as a colourless oil (55 mg, 91%).

^{1}H NMR (CD_3OD): δ 6.81 (1H, dd, *J* = 2.9, 2.9 Hz), 4.64 (1H, m), 3.75 (3H, s), 3.71 (1H, dd, *J* = 7.8, 9.8 Hz), 3.60 (1H, ddd, *J* = 5.4, 9.8, 9.8 Hz), 2.80 (1H, ddd, *J* = 1.5, 5.4, 17.6 Hz), 2.23 (1H, dddd, *J* = 2.9, 3.4, 9.8, 17.6 Hz).

^{13}C NMR (CD_3OD): δ 167.8, 138.9, 130.5, 80.0, 71.0, 53.2, 53.0, 50.2, 33.4.

Allyl (1*S*,4*R*,5*R*)-1,4,5-trihydroxy-3-methylidenecyclohexane-1-carboxylate 2.80

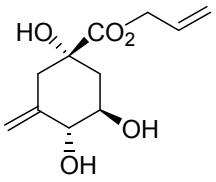

1.00 M $KOH_{(aq)}$ (0.75 mL, 0.75 mmol) was added to olefin **2.73** (59 mg, 0.29 mmol) and the reaction stirred over ice for 10 min. Amberlite IR 120 (H) ion exchange resin was added and the suspension stirred a further 5 min. The resin was removed by filtration and the filtrate freeze-dried. The free acid intermediate was obtained as a yellow glass (57 mg) which was used without further purification.

^{1}H NMR (D_2O): δ 5.07 (1H, d, J = 1.5 Hz), 4.91 (1H, d, J = 1.5 Hz), 3.91 (1H, d, J = 9.4 Hz), 3.54 (1H, ddd, J = 4.9, 9.4, 11.5 Hz), 2.60 (1H, dd, J = 0.9, 14.2 Hz), 2.41 (1H, dd, J = 3.2, 14.2 Hz), 2.07 (1H, ddd, J = 3.2, 4.9, 13.6 Hz), 1.93 (1H, dd, J = 11.5, 13.6 Hz).

To a solution of the free acid intermediate (54 mg, 0.29 mmol) in DMF (1 mL) was added $KHCO_3$ (62 mg, 0.62 mmol) and allyl bromide (0.40 mL, 4.6 mmol) and the reaction was stirred at rt for 24 h. The solvent was removed *in vacuo* and the residue taken up in EtOAc and washed with 1 M $KHSO_4$ (1×), sat. $NaHCO_3$ (1×), sat. NaCl (1×) and H_2O (1×). The organic phase was dried ($MgSO_4$), filtered and evaporated to give the crude product as a colourless oil (21 mg). The combined aqueous washings were extracted with CH_2Cl_2 (4×) and EtOAc (4×) and the organic fractions dried ($MgSO_4$) and evaporated to give a further 24 mg of the crude product. The two samples of product were combined and subjected to flash chromatography on silica, eluting with 30% pet. ether/EtOAc, to furnish the allyl ester **2.80** as a colourless oil (29 mg, 45% over 2 steps from **2.73**).

^{1}H NMR ($CDCl_3$): δ 5.65 (1H, dddd, J = 5.7, 5.7, 10.4, 17.3 Hz), 5.33 (1H, dd, J = 1.3, 17.3 Hz), 5.25 (1H, dd, J = 1.3, 10.4 Hz), 5.24 (1H, d, J = 1.4 Hz), 4.96 (1H, d, J = 1.4 Hz), 4.67 (2H, d, J = 5.7 Hz), 3.95 (1H, d, J = 9.3 Hz), 3.75 (1H, ddd, J = 4.8, 9.3, 11.5 Hz), 3.63 (1H, br s), 3.44 (2H, br s), 2.63 (1H, d, J = 13.9 Hz), 2.39 (1H, dd, J = 3.0, 13.9 Hz), 2.12 (1H, ddd, J = 3.0, 4.8, 13.5 Hz), 1.99 (1H, dd, J = 11.5, 13.5 Hz).

Allyl (4*S*,5*R*,7*R*)-4,5,7-trihydroxy-1-oxaspiro[2.5]octane-7-carboxylate 2.81

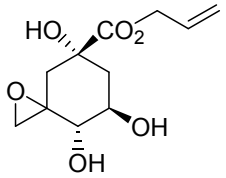

To a solution of alkene **2.80** (21 mg, 0.09 mmol) in CH_2Cl_2 (1.5 mL) was added 70% *m*-CPBA (24 mg, 0.10 mmol) and the reaction stirred at rt for 1.5 h. The solvent was evaporated to give the crude product as a 4:1 ratio of isomers. Two repetitions of flash chromatography on silica, eluting with 10% pet. ether/EtOAc furnished the major isomer of epoxide **2.81** as a

colourless oil containing 11% residual *m*-CPBA (15 mg, 60% yield by ^{1}H NMR). The minor isomer was also obtained, contaminated with 15% *m*-CPBA (3 mg, 13% by ^{1}H NMR).

^{1}H NMR ($CDCl_3$): δ (major isomer, containing 11% *m*-CPBA) 5.88 (1H, dddd, *J* = 5.7, 5.7, 10.5, 17.1 Hz), 5.31 (1H, dd, *J* = 1.3, 17.1 Hz), 5.24 (1H, d, *J* = 10.5 Hz), 4.63 (2H, d, *J* = 5.7 Hz), 4.06 (1H, ddd, *J* = 4.0, 9.3, 11.5 Hz), 3.96 (3H, br s), 3.70 (1H, d, *J* = 9.3 Hz), 3.01 (1H, d, *J* = 4.8 Hz), 2.52 (1H, d *J* = 14.7 Hz), 2.46 (1H, d, *J* = 4.8 Hz), 2.25 (1H, ddd, *J* = 3.4, 4.0, 13.1 Hz), 1.92 (1H, dd, *J* = 11.5, 13.1 Hz), 1.58 (1H, dd, *J* = 3.4, 14.7 Hz).

^{13}C NMR ($CDCl_3$): δ (major isomer, containing 11% *m*-CPBA) 174.1, 131.3, 119.1, 74.5, 72.6, 69.4, 66.4, 58.1, 46.3, 40.5, 39.7.

TOF MS ES+: 245.0985; $C_{11}H_{17}O_6$ $[MH]^+$ requires 245.1025.

(4*S*,5*R*,7*R*)-4,5,7-Trihydroxy-1-oxaspiro[2.5]octane-7-carboxylic acid 2.4

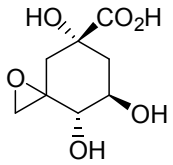

To a solution of the major isomer of epoxide **2.81** (contaminated with 11% *m*-CPBA) (10 mg, 0.036 mmol) in dry THF (0.75 mL) was added Pd(0)(PPh_3)$_4$ (5 mg, 4.1 μmol) and dimedone (61 mg, 0.44 mmol) and the reaction was stirred at rt under Ar for 1 h. The solvent was evaporated and the residue partitioned between CH_2Cl_2 and H_2O. The aqueous phase was extracted with CH_2Cl_2 (3×) and EtOAc (5×), then freeze-dried to furnish the free acid **2.4** as a colourless glass (5 mg, 72%).

^{1}H NMR (CD_3OD): δ 3.93 (1H, ddd, *J* = 3.9, 9.3, 11.5 Hz), 3.61 (1H, d, *J* = 9.3 Hz), 2.89 (1H, d, *J* = 5.2 Hz), 2.51 (1H, d, *J* = 14.4 Hz), 2.42 (1H, d *J* = 5.2 Hz), 2.16 (1H, m), 1.93 (1H, dd, *J* = 11.5, 12.2 Hz), 1.57 (1H, d, *J* = 14.4 Hz).

^{13}C NMR (CD_3OD): δ 174.1, 74.2, 70.6, 59.4, 47.2, 42.3, 41.0.

TOF MS ES-: 203.0660; $C_8H_{11}O_6$ $[M-H]^-$ requires 203.0556.

6.3 ASSAY DETAILS

Biological studies on type I DHQase were carried out in phosphate buffer. Studies on type II DHQase were carried out in Tris·HCl buffer. Buffer concentrations employed in individual experiments are detailed in Table 6.2.

Stock solutions of enzymes were stored in 1:1 glycerol:0.05M buffer at -4 ºC. Stock enzyme solution concentrations were 9.1 $mgmL^{-1}$ (*S. typhi* DHQase), 5.1 $mgmL^{-1}$ (*S. coelicolor* DHQase) and 1 $mgmL^{-1}$ (*M. tuberculosis* DHQase). Enzyme samples for assay were prepared by dilution of the stock solution into a buffer solution of the concentration to be employed in the assay (Table 6.2), and stored over ice while in use.

The concentration of substrate solutions for assay was determined spectrophotometrically at 234 nm. A 20 μL aliquot of substrate solution in 50 mM buffer was reacted with 2 μL of enzyme stock solution until equilibrium. The change in absorbance was measured and the initial substrate concentration in the sample calculated using Beer's Law and an equilibrium constant for the conversion of DHQ to DHS of 15 (Equation 6.1).

$$[\text{DHQ}](\mu\text{M}) = \frac{\Delta\text{Abs}}{\varepsilon l} \times \frac{16}{15} \times 10^6 \qquad (6.1)$$

The concentration of inhibitor samples was determined by ^1H NMR. A sample was prepared from a known volume of the inhibitor solution and a known volume of the DMF reference solution in H_2O, or 50 mM tris·HCl buffer, and a proton NMR spectrum acquired with solvent suppression and with the relaxation delay (d1) set to 60 s to account for discrepancies in relaxation times between the various proton signals. The integrals of the reference signal and an inhibitor signal were measured and the inhibitor concentration in the sample calculated according to Equation 6.2.

$$[\text{inhibitor}] = \frac{\text{inhib integral}}{\text{ref integral}} \times \frac{V_{ref}\,[\text{ref}]}{V_{inhib}} \qquad (6.2)$$

6.3.1 Spectrophotometric Assays

Assays of inhibitors were carried out at ambient temperature. Data for Michaelis-Menten curves was obtained in a temperature controlled room at 25 ºC.

Assay samples were prepared in 3 mL, 1 cm path-length quartz cuvettes. Stock solutions of substrate, inhibitor, buffer and water were pipetted directly into the cuvette. The concentrations of substrate, inhibitor, buffer and enzyme employed in the individual assays are detailed in Table 6.2. The reaction was initiated by addition of enzyme solution (10 or 20 μL) to make a final volume of 2000 μL. Enzyme solutions were 5.1 μgmL^{-1} for *S. coelicolor* DHQase, 50 μgmL^{-1} for *M. tuberculosis* DHQase and 9.1 μgmL^{-1} for *S. typhi* DHQase. The absorbance at 234 nm was recorded for 60-120 s. A straight line was fitted to the data using MS Excel. Beer's Law was used to calculate the rate of the reaction from the slope of the Abs *vs*. t curve. The rates of reaction were plotted against inverse inhibitor concentration in a Dixon plot to determine K_i as described in Chapter 3.

Irreversible inhibition studies

Samples of *S. typhi* DHQase were incubated with epoxide **2.4** at rt (Table 6.1).

In order to study the progress of the inhibition by UV/vis spectroscopy, aliquots of enzyme incubation **A** (Table 6.1) were taken at intervals over a period of 3 h and diluted into a solution containing substrate (31 μM) and buffer (368 mM) with a total volume of 2000 μL. The reaction progress was monitored at 234 nm.

Sample **B** (Table 6.1) was prepared in order to study the irreversible binding of **2.4** by LCMS. Prior to LCMS the extent of inactivation after 93 h was determined by UV/vis by carrying out a 10-fold dilution of a 2 μL aliquot of sample **B**, and then adding a 1 μL aliquot of the diluted sample into a 123 μM substrate solution in 100 mM buffer in a quartz cuvette (total volume 2000 μL). The reaction progress was monitored at 234 nm. The steady state rate was

compared to that of a control sample prepared under identical conditions except for the absence of inhibitor.

Table 6.1 Experimental details for time-dependent inhibition of *S. typhi* DHQase by **2.4**.

	Irreversible Inhibition Assay of 2.4 *S. typhi* DHQase	
	UV/vis study (Sample **A**)	LCMS study (Sample **B**)
[Buffer]	368 mM (Phosphate)	100 mM (Phosphate)
[Enzyme]	4.6 μgmL^{-1}	1.37 $mgmL^{-1}$ (50 μM)
[Inhibitor]	400 μM	9413 μM
Time	0-3 h	93 h

6.3.2 ^{1}H NMR Assays

^{1}H NMR spectra were acquired at 500 MHz on a Varian Inova 500 spectrometer. All ^{1}H NMR data for the purpose of determining reaction rates was acquired at 25 ºC. NMR spectra were measured using a 5 mm NMR tube with an insert containing D_2O. Spectra were acquired with suppression of the water signal.

Solutions of the enzymatic product DHS were prepared enzymatically and their concentrations determined spectrophotometrically at 234 nm using Beer's Law.

Assay samples were prepared by pipetting milli-Q water, substrate, inhibitor and reference solutions into 2 mL vials. The concentrations employed in the individual assays are detailed in Table 6.3. The reaction was initiated by addition of *S. coelicolor* DHQase solution (8 μL of a 2.55 μgmL^{-1} solution, or 16 μL of a 1.28 μgmL^{-1} solution) to make a final volume of 550 μL. The solution was transferred to an NMR tube and the sample inserted into the spectrometer.

The experiment was set up for a ^{1}H NMR in D_2O, with lock power and lock gain set to 28 and 38 respectively. After locking and shimming, one transient was acquired with nt=1, pw=2, gain=2. The spectrum was autophased and the cursor set on the solvent signal, the decoupler set by entering sd, and the suppression pulse sequence selected (suppr). Data acquisition was initiated with gain=30, d1=5 and pad=0,5,5,5,5,5,5,5,5,5,5. This meant that a series of 10 spectra would be acquired with a 5 s delay between each, with 8 transients (the default value) per spectrum and a relaxation delay of 5 s between each transient. The spectra were processed with fn=128k and lb=2. The product concentration was calculated for each spectrum as described in Chapter 4, and the rate of reaction determined by fitting a straight line to the [DHS] *vs*. time data.

Table 6.2 Experimental details for reversible competitive inhibition spectrophotometric assays.

Inhibitor	Enzyme		
	S. typhi DHQase	*M. tuberculosis* DHQase	*S. coelicolor* DHQase
1.36			[B] = 50 mM (Tris·HCl) [E] =26 ngmL^{-1} [S] = 207, 311, 415 μM [I] = 0-500 μM
2.4	[B] = 396 mM (Phosphate) [E] = 91 ngmL^{-1} [S] = 12, 31 μM [I] = 0-210 μM	[B] = 297 mM (Tris·HCl) [E] = 0.99 μgmL^{-1} [S] = 12, 30 μM [I] = 0-208 μM Vtot = 2020 μL	
2.5		[B] = 50 mM (Tris·HCl) [E] = 0.50 μgmL^{-1} [S] = 8, 15, 30, 63 μM [I] = 0-330 μM	[B] = 50 mM (Tris·HCl) [E] = 51 ngmL^{-1} [S] = 25, 63, 125, 250 μM [I] = 0-998 μM
2.15		[B] = 50 mM (Tris·HCl) [E] = 0.50 μgmL^{-1} [S] = 20, 40, 100 μM [I] = 0-257 μM	
2.16		[B] = 50 mM (Tris·HCl) [E] = 0.50 μgmL^{-1} [S] = 10, 20, 35, 60 μM [I] = 0-171 μM	[B] = 50 mM (Tris·HCl) [E] = 51 ngmL^{-1} [S] = 25, 50, 100, 200 μM [I] = 0-662 μM
2.17		[B] = 50 mM (Tris·HCl) [E] = 0.25 μgmL^{-1} [S] = 10, 20, 30 μM [I] = 0-256 μM	[B] = 50 mM (Tris·HCl) [E] = 51 ngmL^{-1} [S] = 25, 50, 100, 200 μM [I] = 0-1075 μM* * 2:1 **2.17**:**2.16**
2.18		[B] = 50 mM (Tris·HCl) [E] = 0.50 μgmL^{-1} [S] = 15, 25, 50 μM [I] = 0-1128 μM	[B] = 50 mM (Tris·HCl) [E] = 51 ngmL^{-1} [S] = 25, 50, 100, 200 μM [I] = 0-1128 μM
2.27		[B] = 50 mM (Tris·HCl) [E] = 0.50 μgmL^{-1} [S] = 20, 30, 50, 100 μM [I] = 0-396 μM Vtot = 2010 μL	
2.28		[B] = 50 mM (Tris·HCl)	[B] = 50 mM (Tris·HCl)

Inhibitor	Enzyme		
	S. typhi DHQase	*M. tuberculosis* DHQase	*S. coelicolor* DHQase
		[E] = 0.50 μgmL^{-1} [S] = 24, 33, 49, 82 μM [I] = 0-516 μM	[E] = 51 ngmL^{-1} [S] = 52, 78, 104 μM [I] = 0-1960 μM
2.29		[B] = 50 mM (Tris·HCl) [E] = 0.50 μgmL^{-1} [S] = 10, 21, 31, 52 μM [I] = 0-502 μM	[B] = 50 mM (Tris·HCl) [E] = 26 ngmL^{-1} [S] = 78, 104, 130 μM [I] = 0-1675 μM
2.38 20:1 *E*:*Z*		[B] = 50 mM (Tris·HCl) [E] = 0.50 μgmL^{-1} [S] = 12, 25, 37, 61 μM [I] = 0-84 μM	
2.42 *E* only		[B] = 50 mM (Tris·HCl) [E] = 0.05 μgmL^{-1} [S] = 33, 49, 82 μM [I] = 0-77 μM	
2.44 9:1 *E*:*Z*		[B] = 50 mM (Tris·HCl) [E] = 0.50 μgmL^{-1} [S] = 6, 12, 25, 61 μM [I (*E*)] = 0-72 μM	
2.46 3:2 *E*:*Z*		[B] = 50 mM (Tris·HCl) [E] = 0.50 μgmL^{-1} [S] =12, 25, 62 μM [I (*E*+*Z*)] = 0-130 μM*	
3.1		[B] = 50 mM (Tris·HCl) [E] = 0.05 μgmL^{-1} [S] = 20, 40, 60 μM [I] = 0-502 μM	
3.2		[B] = 50 mM (Tris·HCl) [E] = 0.50 μgmL^{-1} [S] = 20, 40, 60, 100 μM [I] = 0-185 μM	

Key: B = buffer, E = enzyme, S = substrate, I = inhibitor, R = reference. *E*/*Z* refers to the *E*/*Z* isomers of the inhibitor.

Table 6.3 Experimental details for ^{1}H NMR assays against *S. coelicolor* DHQase.

Inhibitor	***S. coelicolor* DHQase**	
	Dose-response curve	% Inhibition study
1.32	[B] = 50 mM (Tris·HCl) [E] = 37 ngmL^{-1} [S] = 812 μM [I] = 0.84-27000 μM [R] = 364 μM	
2.15		[B] = 50 mM (Tris·HCl) [E] = 37 ngmL^{-1} [S] = 823 μM [I] = 5611 μM [R] = 364 μM
2.27	[B] = 50 mM (Tris·HCl) [E] = 46 ngmL^{-1} [S] = 1000 μM [I] = 9.7x10^{-5} - 3.2x10^{4} μM [R] = 364 μM	
2.38 20:1 *E*:*Z*		[B] = 50 mM (Tris·HCl) [E] = 37 ngmL^{-1} [S] = 800 μM [I (*E*)] = 5000 μM [R] = 436 μM
2.44 9:1 *E*:*Z*	[B] = 50 mM (Tris·HCl) [E] = 37 ngmL-1 [S] = 800 μM [I (*E*)] = 0.1-20800 μM [R] = 436 μM	[B] = 50 mM (Tris·HCl) [E] = 37 ngmL-1 [S] = 800 μM [I (*E*)] = 4500 μM [R] = 430 μM total concn = 558 μL
2.46 3:2 *E*:*Z*		[B] = 50 mM (Tris·HCl) [E] = 37 ngmL^{-1} [S] = 800 μM [I (*E*+*Z*)] = 1100 μM [R] = 436 μM
3.1	[B] = 50 mM (Tris·HCl) [E] = 37 ngmL^{-1} [S] = 823 μM [I] = 0.7-5000 μM [R] = 364 μM	[B] = 50 mM (Tris·HCl) [E] = 37 ngmL^{-1} [S] = 823 μM [I] = 5000 μM [R] = 364 μM

Key: B = buffer, E = enzyme, S = substrate, I = inhibitor, R = reference. *E*/*Z* refers to the *E*/*Z* isomers of the inhibitor.

6.4 REFERENCES FOR CHAPTER 6

(1) Alves, C.; Barros, M. T.; Maycock, C. D.; Ventura, M. R. *Tetrahedron* **1999**, *55*, 8443-8456.

(2) Le Sann, C.; Abell, C.; Abell, A. D. *Synthetic Communications* **2003**, *33*, 527-533.

(3) Delfourne, E.; Despeyroux, P.; Gorrichon, L.; Veronique, J. *J. Chem. Res. (M)* **1991**, 0532-0544.

(4) Tian, F.; Montchamp, J.-L.; Frost, J. W. *J. Org. Chem.* **1996**, *61*, 7373.

(5) Le Sann, C.; Abell, C.; Abell, A. D. *J. Chem. Soc., Perkin Trans. 1* **2002**, 2065-2068.

(6) Montchamp, J.-L.; Frost, J. W. *J. Am. Chem. Soc.* **1997**, *119*, 7645-7653.

List of Abbreviations

ADP	adenosine diphosphate
Arg	arginine
ATP	adenosine triphosphate
BBA	butane-2,3-bisacetal
CSA	camphorsulphonic acid
DAHP	deoxy-D-*arabino*-heptulosonate 7-phosphate
DAST	diethylaminosulphur trifluoride
DCM	dichloromethane
DHQ	dehydroquinate, dehydroquinic acid
DHQase	dehydroquinase
DHS	dehydroshikimate, dehydroshikimic acid
DMAP	4-(dimethylamino)pyridine
DME	1,2-dimethoxyethane
DMF	*N,N*-dimethylformamide
EPSP	5-enolpyruvylshikimate 3-phosphate
His	histidine
HMDS	1,1,1,3,3,3-hexamethyldisilazane
Lys	lysine
m-CPBA	*m*-chloroperbenzoic acid
MDR-TB	multi-drug resistant *Mycobacterium tuberculosis*
MOM	methoxymethyl
MRSA	methicillin resistant *Staphylococcus aureus*
$NADP^+$	nicotinamide adenine dinucleotide phosphate
NADPH	reduced nicotinamide adenine dinucleotide phosphate
NMR	nuclear magnetic resonance spectroscopy
PCC	pyridinium chlorochromate
PDC	pyridinium dichromate
PEP	phosphoenol pyruvate
PMB	*p*-methoxybenzyl
TBDMSCl	tert-butyldimethylsilyl chloride
TFA	trifluoroacetic acid
TMB	2,2,3,3-tetramethoxybutane
TMS	trimethylsilyl
TMSOTf	trimethylsilyl trifluoromethanesuphonate
Tyr	tyrosine
VRE	vancomycin resistant enterococci